

Durham E-Theses

Mechanistic investigations of the S-nitrosothiol, peroxy-nitrous acid and thiol system

Coupe, Paul J.

How to cite:

Coupe, Paul J. (2001) *Mechanistic investigations of the S-nitrosothiol, peroxy-nitrous acid and thiol system*, Durham theses, Durham University. Available at Durham E-Theses Online:
<http://etheses.dur.ac.uk/4211/>

Use policy

The full-text may be used and/or reproduced, and given to third parties in any format or medium, without prior permission or charge, for personal research or study, educational, or not-for-profit purposes provided that:

- a full bibliographic reference is made to the original source
- a [link](#) is made to the metadata record in Durham E-Theses
- the full-text is not changed in any way

The full-text must not be sold in any format or medium without the formal permission of the copyright holders.

Please consult the [full Durham E-Theses policy](#) for further details.

Mechanistic Investigations of the *S*-Nitrosothiol, Peroxynitrous acid and Thiol System

Paul J. Coupe B. Sc. (Hons.)

(Graduate Society)

The copyright of this thesis rests with the author. No quotation from it should be published in any form, including Electronic and the Internet, without the author's prior written consent. All information derived from this thesis must be acknowledged appropriately.

A thesis submitted for the degree of Doctor of Philosophy in the
Department of Chemistry, University of Durham

October 2001



22 MAR 2002

Mechanistic Investigations of the *S*-Nitrosothiol, Peroxynitrous Acid and Thiol System

Abstract

S-Nitrosothiols have been found to undergo nucleophilic attack by the hydroperoxide anion to effect electrophilic nitrosation of the nucleophile. Peroxynitrite anion is formed in almost quantitative yields and the kinetics of the reaction examined, confirming attack through the deprotonated form of hydrogen peroxide.

Conversely, under slightly acidic conditions peroxynitrous acid, the neutral form of peroxynitrite, has been shown to nitrosate an excess of thiol in an indirect pathway. Initially two moles of thiol are oxidised to the corresponding disulfide with the concomitant production of nitrite. Under mildly acidic conditions nitrous acid is formed which can then nitrosate excess thiol present. The reaction of a 2:1 excess of thiol over peroxynitrous acid has been shown to generate nitrous acid, which remains relatively stable, as there is no thiol remaining due to its oxidation to the disulfide. At higher acidities an additional source of nitrosation is uncovered which is explained in the terms of the formation of a protonated form of peroxynitrous acid with analogies toward the nitrous acidium ion.

A comparison of the antioxidant potential of *S*-nitrosothiols versus thiols has also been examined using the powerful oxidant potassium bromate. Complex kinetic traces were generated but evidence was obtained which showed that *S*-nitrosothiols have enhanced antioxidant potential over thiols due to the nitroso moiety.

The alkaline hydrolysis of *S*-nitrosothiols was also investigated with attack of the hydroxide ion postulated to proceed *via* nucleophilic attack on the sulfur atom of *S*-nitrosothiols. Also the reaction between *S*-nitrosothiols and phenolic compounds was found to proceed through different mechanisms depending on the ring substituents on the phenol.



Declaration

The material in this thesis is the result of research carried out in the Chemistry Department at the University of Durham between October 1998 and September 2001. It has not been submitted for any other degree and is the author's own work, except where acknowledged by reference.

Statement of Copyright

The copyright of this thesis rests with the author. No quotation from it should be published without his prior written consent and information derived from it should be acknowledged. No part of this thesis may be reproduced, stored in a retrieval system or transmitted in any form or by any means without the written consent of the author.

Acknowledgements

I would like to thank my supervisor Lyn Williams for his support and friendship over the past three years. Also in Durham University I would like to thank Colin Greenhalgh for his expertise on the technical side of the lab. My gratitude can never be underestimated for the time Doctor's Holmes and Munro have spent reading this "story" of my research at the University of Durham. I must also thank the ESPRC for their funding and the scholarships generously donated to me by the University of Durham and ICI.

On to the fun part! The social side of the past three years in Durham leaves me with the impossibility of naming everybody who has made my time here more than worthwhile, however I will attempt to acknowledge them all. Even whilst writing these acknowledgements I am fuelled by the liquefied wonders of the New Inn and is therefore the reason why this is the final piece of text prepared for this thesis. I must accordingly acknowledge the staff of the New Inn for being such a wondrous social relaxant and the staff of Klute who took on their mantle after closing time! Thanks especially to Andy and the doormen and also to those bar staff to which I became very close friends. The people that I have met over the last three years are what make my time here so special.

In the lab I am indebted to the daily banter provided by the likes of Dr. Andy "sensei" Munro, Dr Tony "one beer after work" Holmes, Dr. "I'm driving in three days" Noble and the Crampton doctors (Ne ladies). Thanks also to the current crop of "pro" doctors Dave "I thought she was alright" Parkin and Ian "wonky neck" Smith, trust me it is a marathon not a sprint. Gratitude also to the members of Grad. Soc Hockey.

Although the last three years were spent in Durham, weekends always belonged to Middlesbrough and the athletes of Marton Furness Hockey Club who hold up the testicular fortitude of the club. Thanks to Chris, Geoff, Ian, Leigh, Kidda, Reg, Marco, Foggy, Big Aidy, Gibbo, Cuffy, Richie, Dodge, Chubbs and my apologies to those I have omitted.

Finally I would like to thank my very best friend Nicky for always being there.

To all of my family, past and present, who I know are proud.

	Page
Abstract	1
Declaration / Statement of Copyright	2
Acknowledgements	3
Dedication	4
Contents pages	5
1 Introduction	16
1.1 Nitric Oxide	16
1.1.1 Physical Properties	17
1.1.2 Applications	17
1.1.3 The Biochemistry of NO	19
1.1.3.1 Pre 1980	19
1.1.3.2 The NO Story	19
1.1.3.3 NO Biosynthesis	22
1.1.3.4 NO Pathway to Smooth Muscle Relaxation	23
1.1.4 Other <i>in vivo</i> applications of NO	24
1.1.4.1 Vasodilation	24
1.1.4.2 NO in neurotransmission	24
1.1.4.3 Immune system NO	25
1.1.4.4 NO in platelet aggregation	26

1.1.4.5 NO in erectile dysfunction	27
1.1.5 Conclusion	27
1.2 S-Nitrosothiols	28
1.2.1 Introduction	28
1.2.2 Physical Properties	28
1.2.3 Synthesis	29
1.2.4 Reactions of RSNOs	29
1.2.4.1 Thermal and Photochemical Decomposition	29
1.2.4.2 Copper catalysed decomposition	30
1.2.4.3 Other Metals	32
1.2.4.4 Ascorbate mediated decomposition	32
1.2.4.5 The effect of the presence of thiol	33
1.2.4.6 Nucleophiles	34
1.2.4.7 RSNO decomposition by superoxide	36
1.2.4.8 RSNO decomposition by selenocystamine	36
1.2.4.9 RSNO decomposition by iron (II) complexes	37
1.2.4.10 Acid hydrolysis of RSNOs	38
1.2.5 RSNOs <i>in vivo</i>	39
1.3 Peroxynitrite	41
1.3.1 Introduction	41
1.3.2 Physical Properties	41
1.3.3 <i>In vitro</i> formation of peroxynitrite	43
1.3.3.1 Nitrosation of hydrogen peroxide	43
1.3.3.2 Peroxynitrite from alkyl nitrites	44
1.3.3.3 Peroxynitrite generators	44
1.3.3.4 Peroxynitrite from other sources	45

1.3.4	Peroxynitrite formation <i>in vivo</i>	46
1.3.5	Peroxynitrite decomposition pathways	46
1.3.5.1	Rearrangement to nitrate	47
1.3.5.2	Decomposition to nitrite	48
1.3.5.3	Decomposition <i>via</i> free radicals	48
1.3.5.4	Other reactions of peroxynitrite	49
1.3.6	Conclusion	49
1.4	S-Nitrosation of thiols	50
1.4.1	Introduction	50
1.4.2	S-Nitrosation by nitrous acid	50
1.4.3	S-Nitrosation by dinitrogen trioxide	51
1.4.4	S-Nitrosation by alkyl nitrites	52
1.4.5	Conclusion	53
1.5	References	54
 Results and Discussion		
2	Reaction of hydrogen peroxide with S-nitrosothiols	61
2.1	Introduction	61
2.2	Hydrogen peroxide and S-nitrosoglutathione	62
2.3	Hydrogen peroxide and S-nitrosocysteine	63
2.3.1	Addition of a metal ion chelator	63
2.4	Evidence of H ₂ O ₂ reaction with thiolate anion	64
2.4.1	Cu ⁺ , thiolate and peroxide reactions	65

2.5	Kinetics of the reaction between H_2O_2 and RSNOs	66
2.5.1	Determining k_2 for the H_2O_2 mediated decomposition of GSNO	67
2.5.2	Determining k_2 for the H_2O_2 mediated decomposition of SNCys	68
2.5.3	<i>S</i> -Nitrosopenicillamine (SNP)	69
2.5.4	Results summary	69
2.6	Proposed reaction scheme	70
2.7	Product study of the reaction between RSNOs and hydrogen peroxide	71
2.7.1	Detection of peroxynitrite	71
2.7.2	Reaction at physiological pH	71
2.7.3	Reaction at pH 9.9	72
2.7.4	Reaction at pH 11.6	73
2.7.5	Reaction at pH 13.1	73
2.8	pH dependence	75
2.8.1	Reaction <i>via</i> the hydroperoxide anion	76
2.8.2	Determination of k_D and $\text{p}K_a$ by Scientist [®]	77
2.8.3	Determination of k_D and $\text{p}K_a$ by the reciprocal plot	77
2.8.4	k_2 value at physiological pH	79
2.8.5	Factors responsible for RSNO decomposition at pH 7.4 – 11	79
2.8.6	Anomalies at pH \approx 9.8 and 10.8	81
2.9	Investigations on the nitrogen product, peroxynitrite	82
2.9.1	Peroxyntirite decomposition	82

2.9.2	Peroxynitrite yield is not quantitative	85
2.9.3	Peroxynitrite reaction with thiolate anions	85
2.10	Fate of the sulfur product	87
2.10.1	Oxidation of disulfides	87
2.10.2	Organic product from SNCys and H_2O_2	88
2.11	Conclusions	88
2.11.1	Biological considerations	88
2.11.2	Chemical considerations	90
2.12	References	91
3	Direct and indirect nitrosation by peroxynitrous acid	94
3.1	Introduction	94
3.2	Initial investigation of the reaction between peroxynitrous acid and thiols	96
3.2.1	Reaction of equimolar peroxynitrite and thiols	96
3.2.2	Reaction of excess thiol with peroxynitrous acid	97
3.3	Effect of thiol concentration on final RSNO yield	98
3.4	Reaction of a 2:1 excess of thiol over peroxynitrous acid	100
3.4.1	Detection of nitrous acid	102
3.5	Quantification of the disulfide product	102

3.5.1	Determining the stability of the disulfide product	104
3.6	Indirect nitrosation mechanism	104
3.6.1	Nitrosation of cysteine ethyl ester	104
3.6.2	Nitrosation of glutathione	108
3.6.3	Nitrosation of cysteine	108
3.6.4	Summary	109
3.6.5	The effect of increasing pH on the final RSNO yield	110
3.7	Direct nitrosation	112
3.7.1	Diode array study	113
3.7.2	Kinetic analysis of the formation curves	114
3.7.3	The effect of bromide catalysis	117
3.7.4	Predicting the high acidity pathway	118
3.8	Conclusions	120
3.9	References	123
4	The antioxidant properties of <i>S</i> -nitrosothiols	126
4.1	Introduction	126
4.1.1	Properties of bromate	127
4.1.2	Use of bromates	128
4.1.3	Oxidation of cysteine by acidified potassium bromate	128
4.2	Oxidation of <i>S</i> -nitrosocysteine	130
4.2.1	Initial study with excess bromate	130

4.2.2	Reaction with equimolar bromate	133
4.3	Determination of the sulfur product	134
4.3.1	Detection of sulfate	134
4.3.2	¹ H NMR determination of products	135
4.3.2.1	Experimental Procedure	136
4.3.2.2	Spectra obtained	136
4.3.3	Sulfur product at equimolar concentrations	139
4.4	Determination of the nitrogen product	140
4.4.1	Quantification of the nitrogen product	142
4.4.2	Experimental procedure	142
4.5	Reaction stoichiometry	144
4.5.1	Overall Reaction stoichiometry	146
4.6	Varying the concentration of bromate	146
4.6.1	Experimental procedure	147
4.6.2	Utilising the pre bromine time period	148
4.6.3	Bromine formation	149
4.6.4	Bromine formation with a two-fold excess of bromate over SNCys	150
4.7	Varying the acid concentration	151
4.8	Bromine oxidation of SNCys	152
4.9	Reaction of bromate and SNCys at physiological pH	153

4.10	Other RSNOs	153
4.11	Mechanistic summary	154
4.11.1	At equimolar concentrations	156
4.11.2	Key points of the mechanism	156
4.12	Biological considerations	158
4.13	Conclusion	159
4.14	References	160
5	Further reactions of <i>S</i> -nitrosothiols	163
5.1	Introduction	163
5.2	Reaction of <i>S</i> -nitrosopenicillamine with the hydroxide anion	164
5.2.1	Results of the SNP and hydroxide anion reaction	165
5.2.2	Nitrogen product	169
5.2.3	Attempts to detect nitroxyl	169
5.2.4	Trapping by tetracyanonickelate, TCN	170
5.2.5	Trapping by nitrosobenzene, NB	171
5.2.6	Detection of the sulfenic acid	174
5.3	Reactions of other RSNOs with the hydroxide anion	175
5.3.1	Discussion of the reactivity of RSNOs with hydroxide	177
5.3.1.1	Sulfenic acids	178

5.3.2	Structural comparisons	180
5.4	Reaction of GSNO with the hydroxide anion	183
5.4.1	Repeat scan spectra for the reaction between NaOH and GSNO	184
5.4.2	Identity of the yellow species	186
5.4.3	The reaction of hydroxide and GSNO	188
5.4.4	Conclusions on the reaction of hydroxide and GSNO	190
5.5	Overall conclusions in the reaction of NaOH and RSNOs	191
5.6	Reactions of <i>S</i> -nitrosothiols with phenol	193
5.6.1	Reaction of <i>S</i> -nitrosopenicillamine, SNP, and phenol at pH 7.4	194
5.6.1.1	Reaction of SNP and phenol at pH 7.4 with EDTA	197
5.6.1.2	Stoichiometric calculation of <i>p</i> -nitrosophenol formed	199
5.6.2	Reaction of SNP and phenol at pH 10 with and without EDTA	200
5.6.3	Reaction of SNP and phenol at pH 13 with and without EDTA	201
5.6.4	Reaction of SNP and 2, 4, 6- trichlorophenol, TCP	201
5.6.4.1	Reaction of SNP and 2, 4, 6- trichlorophenol, TCP at pH 12	202
5.6.5	Conclusion	205
5.7	References	207
6	Experimental Details	210

6.1	Reagents used	210
6.1.1	Preparation of <i>S</i> -nitrosothiols, RSNOs	210
6.1.2	Preparation of peroxynitrite	211
6.1.2	Buffer preparation	211
6.2	Equipment	212
6.2.1	Spectrophotometers	212
6.2.2	Stopped-flow spectrophotometer	212
6.2.2.1	Diode array attachment	213
6.2.3	pH meter	213
6.2.4	Nitric Oxide probe	213
6.2.5	¹ H NMR	214
6.2.6	Scientist®	214
6.3	Analytical methods	214
6.3.1	Griess Test	214
6.3.2	Ellman's Test	215
6.3.3	Ammonia Test	216
6.4	Derivations	217
6.4.1	Spectrophotometric determination of k_{obs}	217
6.4.2	Chapter 2, Equation 2.6	219
6.5	Data Fitting	221
6.6	References	222
	Appendices	224
	Abbreviations	226

Chapter 1

1 Introduction

1.1 Nitric Oxide

Exactly 220 years after its discovery by Joseph Priestley,¹ nitric oxide, NO, was voted as molecule of the year by *Science*² in 1992. For such a simple and well-known molecule to achieve this is indicative of the revival of research into NO.

The five years preceding this award witnessed NO being attributed to the control of numerous bioprocesses from literally head to toe, including smooth muscle relaxation,³ immune regulation,⁴ neurotransmission⁵ and inhibition of platelet aggregation.⁶

Since 1992 research has continued to expand, see Figure 1.1, with almost ten thousand publications on NO in the year 2000.

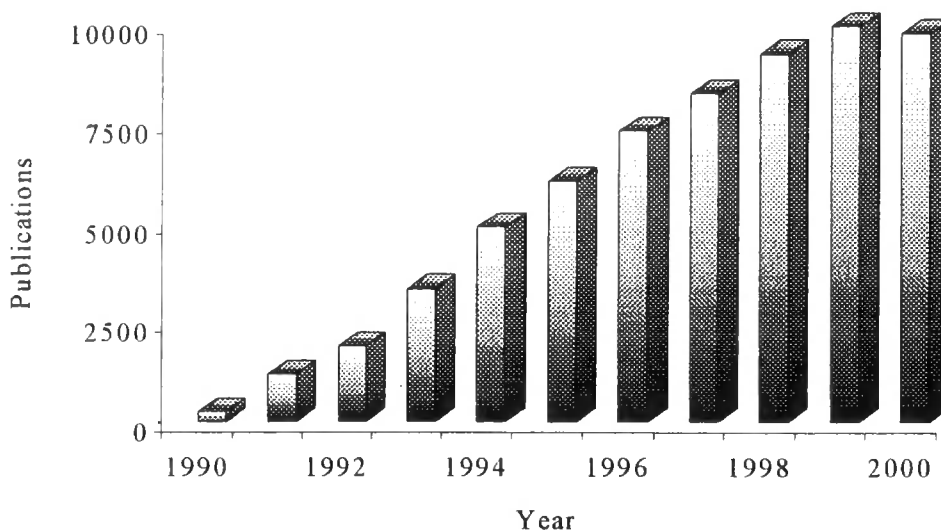


Figure 1.1 Increase in NO related publications over the ten years to 2000

The topic of NO has gained prominence recently through appearances on the covers of *Cosmopolitan* and *The Times*; the most famous drug of its generation, *Viagra*, acts on the NO pathway to blood flow enhancement and in 1998 Furchgott, Ignarro and Murad were awarded the Nobel Prize for medicine, for their work on the role of NO in the body.

1.1.1 Physical Properties

At room temperature and pressure NO is a colourless, diatomic gas, boiling and melting at $-151.8\text{ }^{\circ}\text{C}$ and $-163.6\text{ }^{\circ}\text{C}$ respectively. It is classed as a neutral radical due to an unpaired electron delocalised in the π^* orbital which also affords paramagnetism.

The delocalisation of the single π^* electron, Figure 1.2, may explain the low tendency of NO to dimerise in solution.

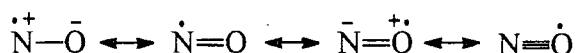


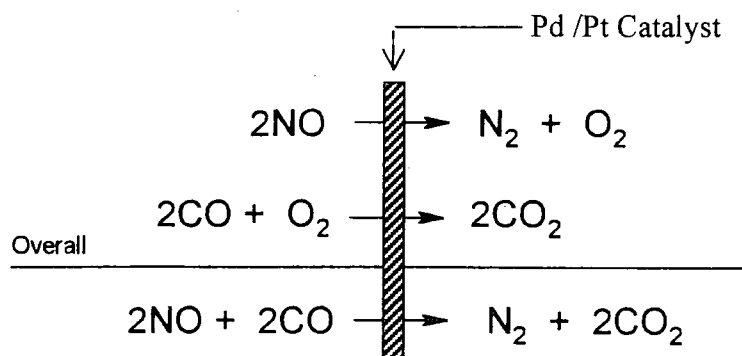
Figure 1.2 Canonical forms of NO molecule

NO reaches saturation in water at millimolar concentrations (1.9 mmol dm^{-3} at $25\text{ }^{\circ}\text{C}$)⁷ but never reaches this concentration physiologically.

NO may lose a π^* electron to form the nitrosonium ion, NO^+ . As the electron removed is from an anti-bonding orbital the bond strengthens with a bond length decrease of 0.95 \AA . Addition of an electron to NO forms the nitroxyl anion NO^- with a bond length increase of 0.50 \AA .⁸ Bond orders of 2 and 3 for NO^- and NO^+ respectively are averaged for the NO molecule resulting in a bond order of 2.5.

1.1.2 Applications

Before the realisation of the importance of NO *in vivo*, NO had few applications and was regarded as a cause of pollution and a toxin. NO is a by-product of the internal combustion engine due to the high temperatures generated in the presence of nitrogen and oxygen. At ground level it is oxidised to NO_x (NO/NO_2 mixture), a constituent of photochemical smog. Catalytic converters are therefore used to break down NO_x and carbon monoxide to relatively harmless nitrogen, oxygen and carbon dioxide, Scheme 1.1, although carbon dioxide is regarded as a pollutant contributing to the greenhouse effect.

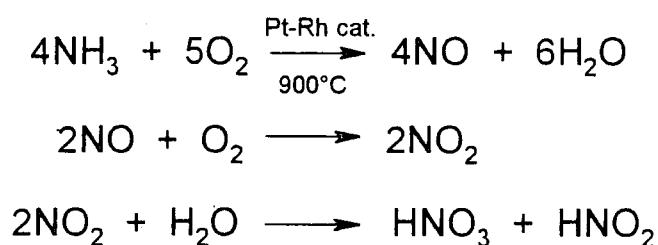


Scheme 1.1 Catalytically converted pollutants

Emission of NO in the stratosphere by aircraft engines causes depletion of the ozone layer *via* free radical reactions.

NO is analogous to carbon monoxide with respect to its actions upon inhalation. Toxicity arises from binding to haemoglobin and myoglobin with a much greater affinity than dioxygen causing, in effect, suffocation.

From an industrial stance NO is an intermediate in the Ostwald process, a three stage route from ammonia to nitric acid which earned Ostwald the Nobel prize in 1909. NO is produced in the efficient primary stage, the platinum / rhodium based catalytic oxidation of ammonia, Scheme 1.2.



Scheme 1.2 The Ostwald process

Subsequently NO is exposed to air and the resulting NO₂ is dissolved in water to form a mixture of nitrous and nitric acid. On the labscale NO may be produced from the reduction of nitric acid by metallic copper and other reducing agents, equation 1.1, and also through the reduction of nitrous acid with a variety of reagents.



Equation 1.1 Labscale generation of NO from nitric acid

1.1.3 The Biochemistry of NO

1.1.3.1 Pre 1980

As early as 1916 Mitchell, Shole and Grindley⁹ concluded, “more nitrate is excreted in the urine of man than is ingested” thus suggesting the formation of inorganic nitrogen oxides *in vivo*. By 1970 evidence suggested that NO might be a protein bound intermediate in the reduction of nitrite to ammonia, in plants.⁸

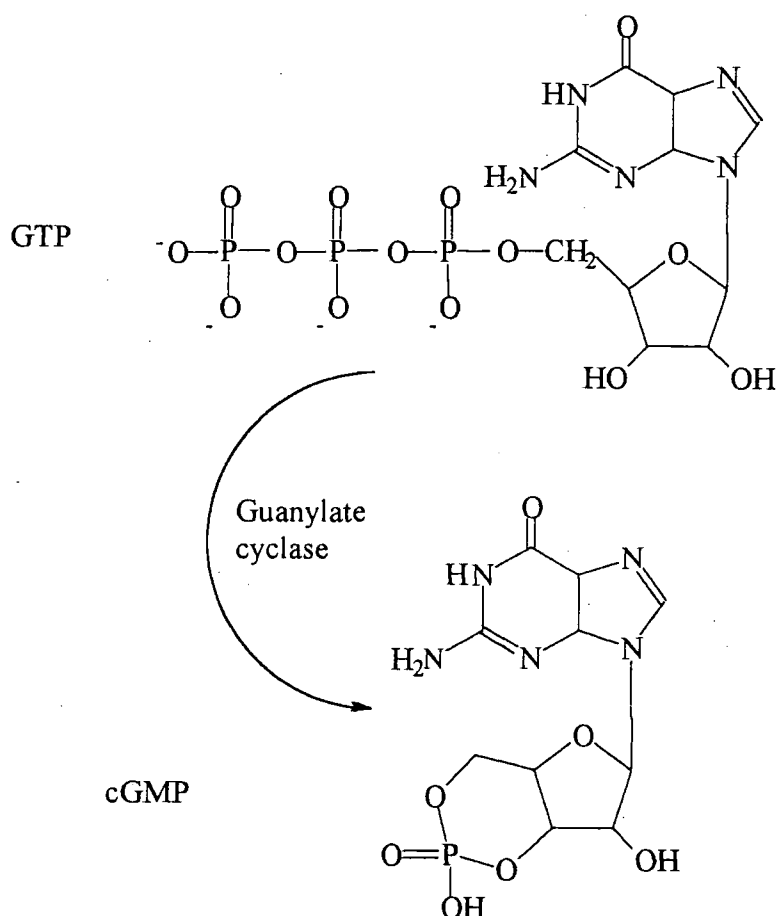
Up until 1980 biochemical research into NO was limited to its involvement in atmospheric pollution,¹⁰ food preservatives (via nitrites),¹¹ the microbial nitrogen cycle,¹² the actions of nitrogen based carcinogens¹⁰ and as a stimulator of guanylate cyclase.¹³

As an analytical tool, particularly in bioinorganic chemistry, NO was used in the study of metalloproteins due to its similarities with dioxygen. NOs almost identical binding to Fe^{2+} in heme prosthetic groups allowed the complexes to be studied by EPR spectroscopy (Electron Paramagnetic Resonance) due to the induced paramagnetism. This lead to the elucidation of the heme ligand binding environment and information on the structure of many heme based proteins.

1.1.3.2 The NO Story

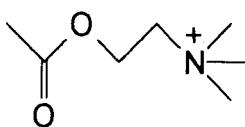
The precursor to the discovery of NOs bio-importance came in 1980 during Furchgott and Zawadzki's study of blood vessels. Blood vessels consist of three layers, the endothelium, smooth muscle and the outer protective collagen layer. The smooth muscle layer enforces contraction and dilation of a blood vessel, where dilation is caused by relaxation.

Smooth muscle relaxation is activated by the enzyme guanylate cyclase which catalyses the conversion of guanosine triphosphate, GTP, to 3', 5-cyclic guanosine monophosphate, cGMP, an intracellular messenger, Scheme 1.3.



Scheme 1.3 Enzyme catalysed conversion of GTP to cGMP

cGMP stimulates protein phosphorylation by cGMP-dependent protein kinase causing smooth muscle relaxation. Substances such as acetylcholine, ACh, and bradykinin (a 9 unit polypeptide) initiate this relaxation and it was presumed to be via activation of guanylate cyclase.



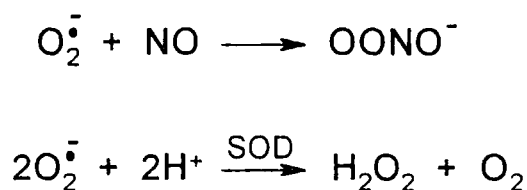
Acetylcholine

Furchgott and Zawadski disposed of this theory through their studies of the effects of ACh on isolated strips/rings of rabbit aorta. They discovered that the vasodilating action of ACh was greatly reduced in samples where the endothelium was removed or damaged.

Therefore ACh did not act directly on the smooth muscle but rather the endothelium which subsequently produced a "second messenger" to diffuse into the smooth muscle cells and activate guanylate cyclase. The identity of this "second messenger" was unknown but was termed the endothelium derived relaxation factor, EDRF.

The next several years witnessed a race to determine the identity of the EDRF. Many groups searched the body's more complex molecules such as amines, peptides, fatty acids etc. as it was presumed that such an important molecule would have a complex structure.

In 1987 two research groups^{15, 16} independently determined that the EDRF was in fact a very simple molecule, NO. The scientific community found it difficult to believe that a toxic gas could be synthesised *in vivo* and have such biological relevance. However, sufficient evidence was already available. Vasodilation was suppressed by haemoglobin and increased by superoxide dismutase, SOD. Haemoglobin strongly binds NO and SOD eliminates superoxide *in vivo*, which is known to react with NO at rates approaching the diffusion controlled limit, Scheme 1.4.

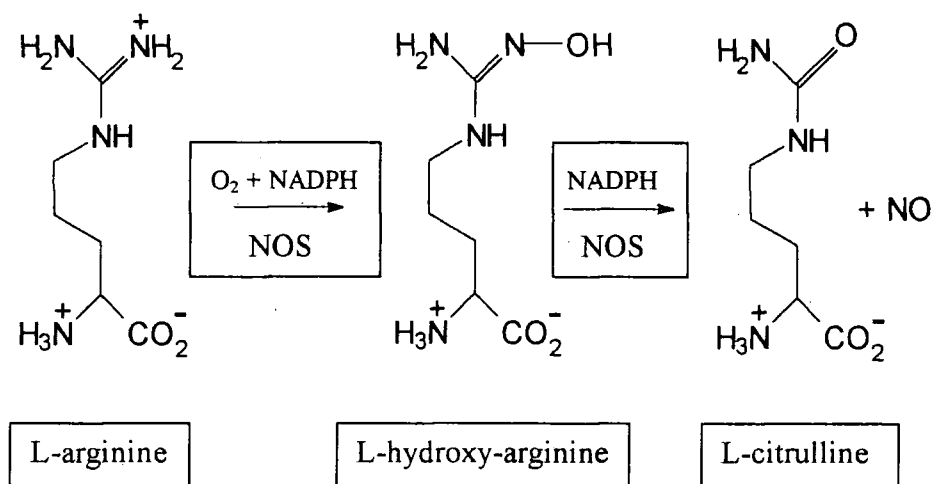


Scheme 1.4 Protection of NO through elimination of superoxide

Any doubts over NO as the EDRF subsided a year later when the biosynthetic production of NO from L-arginine was determined through isotopically labelled reactions.¹⁷

1.1.3.3 NO Biosynthesis

NO is synthesised *in vivo* by the enzyme nitric oxide synthase, NOS, which catalyses the reaction of L-arginine with O_2 to yield NO and L-citrulline. Isotopically labelled nitrogen and oxygen were used to elucidate the reaction pathway, Scheme 1.5.^{17, 18}



Scheme 1.5 Biosynthetic route to NO through the NOS enzyme

Investigations into the structure and functions of NOS led to the discovery of three types of NOS : endothelial NOS (eNOS), neuronal or brain NOS (bNOS) and macrophage NOS (iNOS). eNOS and bNOS are constitutive enzymes that is, they are permanently present ready for a quick response upon activation. They are activated by calcium ions through their interaction with Ca^{2+} -calmodulin, a protein that binds Ca^{2+} ions. They produce picomolar quantities of NO in quick bursts.

iNOS is an inducible enzyme therefore only released from the macrophage when required. It is Ca^{2+} /calmodulin independent but can release nanomolar quantities of NO over a long period of time. With the discovery of three types of NOS came the realisation that NO had many more biological applications than first thought.

1.1.3.4 NO Pathway to Smooth Muscle Relaxation

The full pathway was now elucidated, see Figure 1.3.

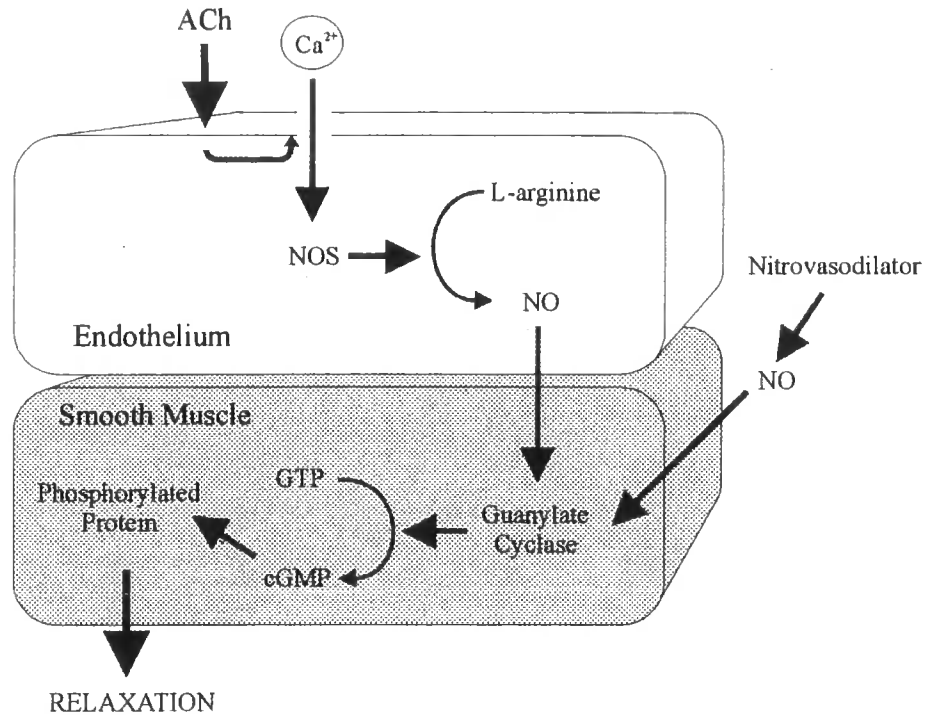


Figure 1.3 NO pathway to vasodilation

The scheme can be summarised in six steps :

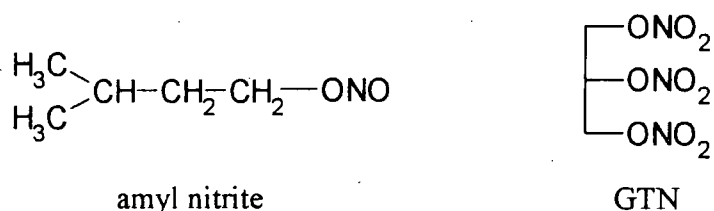
- 1) ACh acts on the endothelium resulting in an influx of Ca^{2+} ions.
- 2) Ca^{2+} ions activate NOS via interaction with Ca^{2+} -calmodulin.
- 3) NOS catalyses the reaction of L-arginine with dioxygen to yield NO.
- 4) NO diffuses across the endothelium / smooth muscle interface and activates guanylate cyclase.
- 5) Guanylate cyclase catalyses the conversion of GTP to cGMP.
- 6) cGMP stimulates protein phosphorylation by cGMP-dependent protein kinase causing smooth muscle relaxation.

NO donors or nitrovasodilators produce NO that is not endothelium derived and may act directly on the smooth muscle.

1.1.4 Other *in vivo* applications of NO

1.1.4.1 Vasodilation

NO has been used to relieve the pain of angina pectoris, caused by insufficient blood flow to the heart, for over 100 years. Victorian physicians knew that the alkyl nitrite, amyl nitrite relieved the pain of angina and World War I doctors noticed that ammunition factory workers responsible for the packing of nitro-glycerine, GTN, into shells had very low blood pressure.



Both were used effectively without the slightest notion that once *in vivo* their vasodilating action was a result of NO release. Nitrovasodilators bypass the endothelium and release NO to act directly on the enzyme guanylate cyclase in the smooth muscle, see Figure 1.3.

There is currently much interest in the development of NO donor compounds such as *S*-nitrosothiols, alkyl nitrites and metal nitrosyl complexes as nitrovasodilating drugs.

1.1.4.2 NO in neurotransmission

Neurotransmitters are chemical messengers that move across the synapses, the gaps between nerve cells. Garthwaite *et al.*¹⁹ noted that an EDRF like substance was produced by brain cells upon excitation. It was already known that excitation within the central nervous system led to an increase of cGMP and that the precursor to activation was L-arginine, strongly suggesting NO as a neurotransmitter. Further evidence surfaced, as an isoform of NOS was isolated from rat forebrain.²⁰

Neuronal NOS is 55% identical to endothelial NOS and produces NO to function in a number of ways. NO is believed to be a retrograde messenger in the development of memory, it is produced in the postsynaptic nerve and diffuses to act on the presynaptic nerve strengthening the connection across the synapse.

Other functions include action as a true neurotransmitter on other nerve cells, in regulation of cerebral blood supply and in the peripheral nervous system in NANC (Non-Adrenergic Non-Cholinergic) nerves.^{21, 22}

1.1.4.3 Immune system NO

The immune system is the body's defence to invading micro-organisms, parasites etc. Macrophages are a class of cells that are an essential part of this system. They are found in almost all organs and tissues and act as the garbage disposal units of the immune system. Once activated, macrophages attack foreign matter engulfing or killing it, a process called phagocytosis.

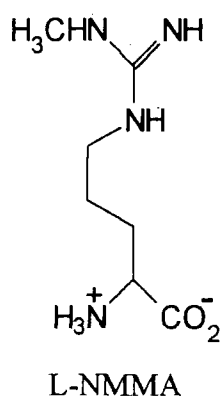
It was known that activation of the immune system resulted in increased levels of nitrate in urine and the killing process was discovered to involve NO.²³ Macrophages also produce superoxide and in the diffusion controlled reaction with NO produce peroxynitrite, Scheme 1.4. Peroxynitrite is a very powerful bio-oxidant and is believed to be the driving force for phagocytosis.

The requirement for NO was confirmed by experimental evidence showing macrophage cytotoxicity required L-arginine.²⁴ Accordingly a third type of NOS, iNOS, was discovered, an inducible Ca^{2+} /calmodulin independent enzyme present in macrophages and neutrophils, white blood cells which kill bacteria.

Being Ca^{2+} /calmodulin independent perhaps explains why it takes several hours after activation for NO to be produced. Once activated NO production may last for many hours in large quantities, unlike the constitutive NOS.

Over-reaction to bacterial infection can lead to the production of excessive amounts of NO. This results in an extreme and potentially fatal lowering of the blood pressure known as septic or endotoxic shock. The loss of blood flow can cause tissue damage, which may result in an increased production of NO, lowering the blood pressure even further.

This vicious circle can be stopped by introduction of an inhibitor of NOS. One such compound N-monomethyl-L-arginine, (L-NMMA), competitively inhibits NOS thus halting NO production.



1.1.4.4 NO in platelet aggregation

Blood contains platelets that possess the ability to aggregate and plug blood vessel ruptures thus protecting against blood loss. However, myocardial infarction, heart attacks, are primarily caused by abnormal clotting of the blood in blood vessels, usually as a result of high cholesterol levels.

NO is known to prevent platelet aggregation and promote disaggregation.⁶ Platelets (and the endothelial cells that they bind to), contain NOS and can produce NO, preventing over aggregation through a cGMP regulated mechanism. They can therefore self-regulate themselves as well as prevent platelet aggregation from alternative sources.

1.1.4.5 NO in erectile dysfunction

Erection is a result of vasodilation in the corpus cavernosum. The cGMP dependent process is hydrolysed by the cGMP specific enzyme, phosphodiesterase type 5, PDE5. Viagra, sildenafil citrate, inhibits PDE5 and allows a build up of cGMP thus increasing the blood supply to the penis.²⁵

1.1.5 Conclusion

There continues to be much research into NO and countless numbers of new applications *in vivo* are being discovered. A recent review highlights the ongoing research.²⁵

- NO in memory and learning processes
- NO inhibition as a neurotransmitter to prevent pain and depression
- NO as a mediator of inflammation and rheumatism
- NO involvement in stroke, Alzheimer's and Parkinson's disease
- NO in vision, as the retina contains guanylate cyclase
- NO as an anti-tumour agent, inhibiting aconitase and ribonucleotase reductase

Doubts over NO production *in vivo* have now subsided with endless amounts of evidence produce annually. Many sceptics were not convinced that the identity of the EDRF could be a toxic gas in solution, but in fact it is perfect for the task as it is small, mobile, soluble in water and lipid, stable in isolation and yet highly reactive as a radical.

Research in this field is both exciting and highly rewarding and there can be no doubt that many more important discoveries will be made involving the biochemistry of NO.

1.2 S-Nitrosothiols

1.2.1 Introduction

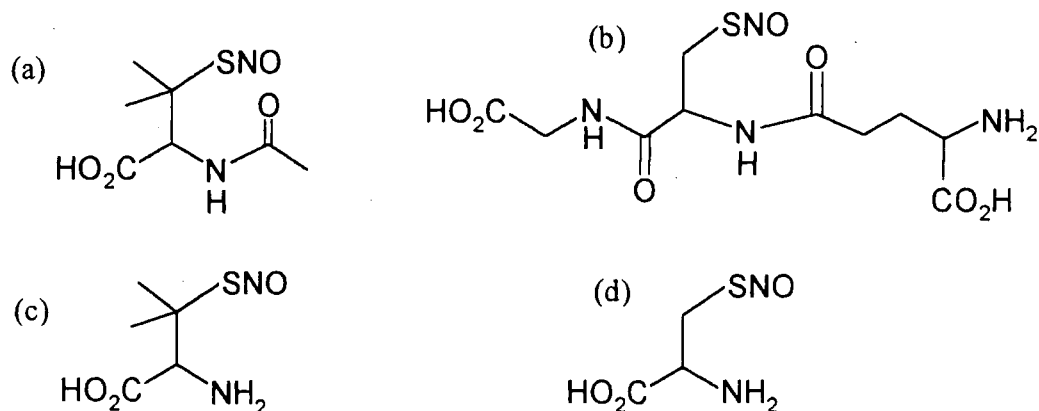
In the search for the identity of the EDRF, *S*-nitrosothiols were considered. Even though NO is favoured²⁶ controversy still existed with suggestions of *S*-nitrosothiols as,^{27, 28} or as mediators of, the EDRF.

S-Nitrosothiols or thionitrites are more generally abbreviated to RSNOs. There are strong similarities between RSNOs and their oxygen analogues the alkyl nitrites, RONO. However, instability has left RSNOs to be the lesser studied of the two.

Studies on RSNOs have been reviewed up until 1983²⁹ and more recently by Williams.³⁰ Interest has been revived recently following the amazing NO story and the discovery of RSNOs *in vivo*.³¹

1.2.2 Physical Properties

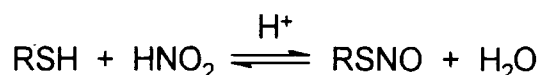
RSNOs physical and chemical properties are less well studied than their oxygen analogues, the alkyl nitrites, RONO. The instability is due to the sulfur-nitrogen bond, which is weak in comparison to the oxygen-nitrogen bond in RONO. A few RSNOs however, have been isolated and characterised, particularly, *S*-nitroso-N-acetyl penicillamine, SNAP (a), and *S*-nitrosogluthathione, GSNO (b). Most research is carried out upon RSNOs synthesised *in situ* such as *S*-nitrosopenicillamine, SNP (c), and *S*-nitrosocysteine, SNCys (d).



Primary and secondary RSNOs are red / pink in colour and tertiary RSNOs are green allowing convenient analysis in solution by UV / Visible spectrophotometry. Two bands are present, the 330-350 nm region ($\epsilon \approx 10^3 \text{ dm}^3 \text{ mol}^{-1} \text{ cm}^{-1}$) has been assigned to $n_{\text{O}} \rightarrow \pi^*$ transition and the 550-600 nm ($\epsilon \approx 20 \text{ dm}^3 \text{ mol}^{-1} \text{ cm}^{-1}$) region is due to $n_{\text{N}} \rightarrow \pi^*$ transition.³²

1.2.3 Synthesis

The oldest and simplest route to RSNOs is by the *S*-nitrosation of thiols. Any NO^+ donor may be used and the easiest method for water soluble thiols is the reaction with nitrous acid, equation 1.5, in an essentially irreversible reaction, $K = 10^5 - 10^6 \text{ dm}^3 \text{ mol}^{-1}$ ³³



Equation 1.5 Nitrosation of thiols by nitrous acid

Although reported,³⁴ NO alone will not nitrosate thiols but will in the presence of oxygen, presumably *via* the reactive nitrosation species N_2O_3 .³⁵

S-Nitrosation of thiols will be expanded upon in Section 1.4.

1.2.4 Reactions of RSNOs

1.2.4.1 Thermal and Photochemical Decomposition

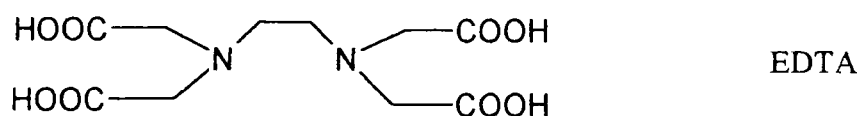
RSNOs undergo similar reactions in thermal and photochemical decomposition, through homolysis of the S-N bond. The process³⁶ yields the corresponding disulfide and NO , which is subsequently oxidised to NO_2 in the presence of oxygen. The mechanism has been well studied and shown to proceed through the homolytically generated thiyl radicals' reaction with GSNO, yielding GSSG and more NO , equations 1.6 and 1.7.



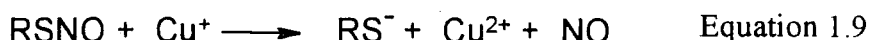
In the presence of oxygen the peroxy radical is generated which subsequently reacts further with GSNO to yield disulfide and NO.

1.2.4.2 Copper catalysed decomposition

One of the most important reactions of RSNOs is their decomposition at physiological pH. Work performed prior to 1993 showed kinetic inconsistencies between many research groups yet the same products, RSSR and NO, as in thermal and photochemical decomposition. Justification arrived in 1993 when Williams *et al.*³⁷ determined that the reaction was copper catalysed and the irregularities were due to varying concentrations of copper in buffers, distilled water etc. Addition of Cu^{2+} increased the reaction rate whereas addition of a metal chelator, ethylenediaminetetraacetic acid, EDTA, reduced the reaction rate to that of the thermal reaction.

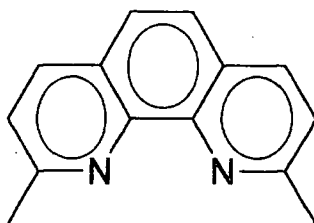


The true reagent emerged as the cuprous³⁸ ion Cu^+ , formed through reduction of Cu^{2+} by thiolate anions present through incomplete nitrosation, equations 1.8 and 1.9.



Cu^{2+} is regenerated after reaction of Cu^+ and RSNO and is therefore only required in catalytic concentrations.

Addition of neocuproine, a specific Cu^+ chelator, halted the reaction and the UV/Vis spectrum of the Cu^+ -neocuproine complex was recorded.

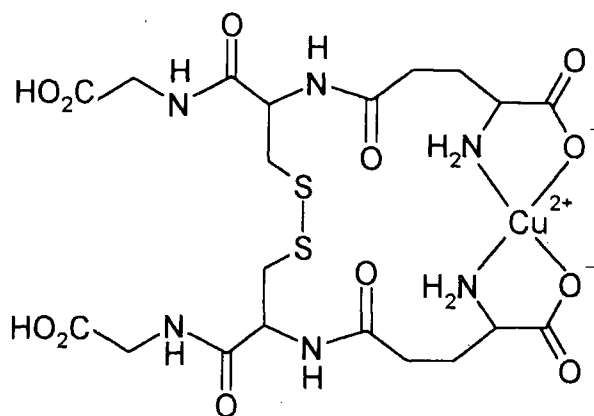


Neocuproine

Although the products are the same as thermal / photochemical decomposition, the mechanism is proposed to be radical free as no thiyl radicals were detected in the copper catalysed decomposition of RSNOs.³⁹

The concentration of free copper in the body is low but protein bound copper also acts to decompose RSNOs to RSSR and NO.⁴⁰

Structural differences between the R groups of RSNOs results in vast differences in stability with regard to the copper mediated decay mechanism, when reactions were followed spectrophotometrically at millimolar concentrations. The second order rate constant for the reaction of SNP and Cu^{2+} was determined as $67\,000\text{ dm}^3\text{ mol}^{-1}\text{ s}^{-1}$, whereas GSNO and Cu^{2+} is comparatively stable.³⁸ The kinetic traces for Cu^{2+} mediated GSNO decay display partial decay followed by gradual cessation resulting in incomplete decomposition. The reactivity difference is a result of the formation of glutathione disulfide, GSSG, as the end product. GSSG is known to bind Cu^{2+} in a 1:1 complex,⁴¹ hence upon its formation copper is chelated from the reaction solution halting the decomposition, see Figure 1.4.

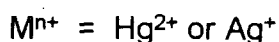
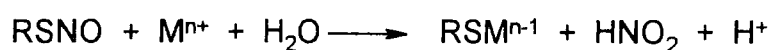
Figure 1.4 Glutathione disulfide: Cu^{2+} , 1:1 complex

The detection of NO release from RSNOs can be analysed down to micromolar concentrations with the use of an NO electrode. At micromolar concentrations of GSNO the complexation of copper by formed GSSG does not stop the reaction because the copper concentration is higher than the GSSG produced.⁴² At these concentrations GSNO is found to have comparable reactivity to SNCys.

Other RSNOs which show similar features are the *S*-nitroso thiosugars which have been generated, isolated and fully characterised.⁴³ Complexation occurs by the disulfide sulfur product but they are more susceptible to thermal and photochemical decomposition therefore decomposition continues, but at a much slower rate than the initial copper mediated pathway. It was noted that the bound copper could continue to play a part in *S*-nitroso thiosugar decay in a similar mode to the way protein bound copper can still decompose RSNOs.⁴⁰

1.2.4.3 Other Metals

Many other metals were tested but it seems that Cu^{2+} is catalytically unique. However mercury (II),⁴⁴ Hg^{2+} , and silver (I)⁴⁵, Ag^+ , have been shown to react stoichiometrically with RSNOs (equation 1.10), generating nitrous acid and the thiol.

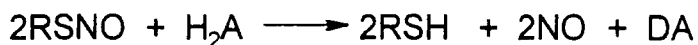


Equation 1.10 Silver and mercury induced decomposition of RSNOs

1.2.4.4 Ascorbate mediated decomposition

Catalytic amounts of thiolate anion are sufficient to reduce Cu^{2+} . The addition of any reducing agent, in principle, will initiate RSNO decomposition, if Cu^{2+} is present. Ascorbate (Vitamin C) in low concentrations, 10^{-5} - 10^{-6} mol dm⁻³ achieves similar results to the thiolate anion, when the thiolate anion is absent or negligibly low.⁴⁶

However at higher ascorbate concentrations, 10^{-2} - 10^{-3} mol dm⁻³, NO is still released even in the presence of a metal ion chelator.⁴⁶ The reaction occurs *via* nucleophilic attack on the nitroso nitrogen and hence electrophilic nitrosation by RSNO. The products are NO and the thiol, not the disulfide, equation 1.11.



Equation 1.11 Ascorbate acting as a nucleophile in the decomposition of RSNOs

H₂A = ascorbate, DA = dehydroascorbic acid

1.2.4.5 The effect of the presence of thiol

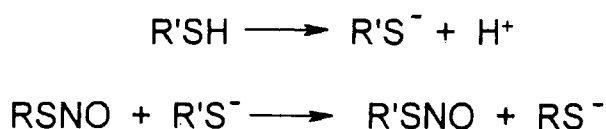
Thiols can affect the decomposition of RSNOs in one of three ways.

- ❖ At low catalytic amounts of thiol, small increases in concentration increase the rate of decomposition of RSNOs. The rate enhancement is due to manipulation of the copper mediated decomposition where more thiolate anion will reduce more of the Cu²⁺ producing more of the active reagent, Cu⁺, thus speeding up the decomposition of RSNOs, see equation 1.8 and 1.9.

Rates increase with increased thiol concentration until a point where structurally appropriate thiols begin to complex copper ions. This occurs with SNAP where complexation is attributed to the carboxylate groups.³⁸

- ❖ The addition of a structurally different thiol, R'SH to RSNO results in transnitrosation reactions. Oae *et al.*⁴⁷ noted the decomposition of RSNOs with added thiols, R'SH releases NO and a mixture of disulfides, notably RSSR R'SSR' and a mixed disulfide, RSSR' indicating nitroso group transfer. The work by Oae *et al.* was carried out prior to discovery of the copper catalysed decay mechanism.

More recently Williams *et al.*⁴⁸ discovered that the thiolate anion is the reactive species in a copper independent reaction, that consists of direct NO^+ transfer from RSNO to $\text{R}'\text{SH}$. The newly formed $\text{R}'\text{SNO}$ may then decompose if copper is not excluded, Scheme 1.6.



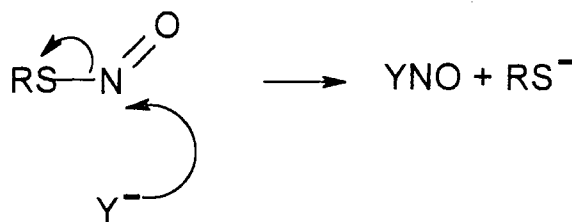
Scheme 1.6 Transnitrosation to a structurally different thiol

Transnitrosation reactions also occur between low molecular weight RSNOs and thiol groups of proteins⁴⁹ and *vice versa*,⁵⁰ adding weight to the speculation that NO is stored and transported by *S*-nitroso compounds *in vivo*.³¹

- ❖ The addition of a large excess of the parent thiol, RSH , to RSNO causes copper independent decay of the RSNO. These high thiol reactions have been reported by a number of groups^{51, 52} where the disulfide is the major sulfur product but the yield of NO is diminished and replaced by ammonia and N_2O . The pH rate profile indicates that the thiolate anion is the active species and a complex reaction scheme has been suggested⁵¹ and confirmed.⁵³

1.2.4.6 Nucleophiles

Nucleophilic attack at the nitroso nitrogen atom seems to be quite general for RSNOs and strongly resembles the corresponding reaction of RONO. The nucleophile, Y^- , undergoes electrophilic nitrosation to generate YNO , which may react further, Scheme 1.7. The reactions do not involve Cu^+ and NO^+ seems to be transferred to the nucleophile without liberation, any NO release is the result of further reactions of YNO .



Scheme 1.7 Electrophilic nitrosation of the nucleophile Y^-

As well as thiols an extensive range of sulfur-centred nucleophiles have been investigated such as sulfite ion, thiourea, thiocyanate ion, thiosulfate ion, thiomethoxide ion and sulfide ion.⁵⁴ They all undergo rapid electrophilic nitrosation with SNP in a reaction that is pseudo first order in SNP and nucleophile except for sulfide.

The reaction between SNP and sulfide was also rapid but produced kinetically complex absorbance time data. A relatively stable yellow species was formed which was believed to be the nitrosodisulfide ion, SSNO^- . Quantitative studies were performed leading to the suggestion of sulfide as a quantitative test reagent for RSNOs using the yellow species formed at 410 nm ($\epsilon_{410 \text{ nm}} = 773 \text{ dm}^3 \text{ mol}^{-1} \text{ cm}^{-1}$).⁵⁴

Nitrogen nucleophiles have also been extensively studied with particular interest in the formation of the carcinogenic nitrosamines from secondary amines and RSNOs.⁵⁵ The reactions are slow but first order in both reactant and substrate and shown to proceed through the electrophilic nitrosation of the free base form of the amine.

For ammonia and primary amines plots of observed rate constant versus [nucleophile] level out at high [nucleophile]. This was explained in the terms of the reversible formation of an inactive RSNO-amine complex, Figure 1.5, in parallel with the main reaction.

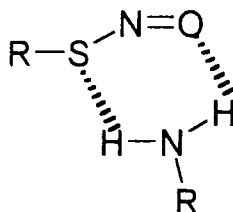


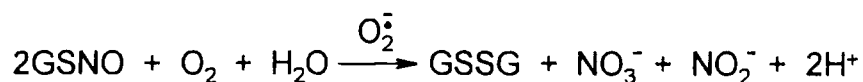
Figure 1.5 Proposed structure for the complex between a primary amine or ammonia, $\text{R} = \text{H}$, and a RSNO

Spectral evidence for the complex formation was observed.

1.2.4.7 RSNO decomposition by superoxide

Superoxide is an oxygen metabolite produced by a reaction between xanthine and xanthine oxidase. It has been shown by a number of groups to decompose GSNO and SNCys at physiological pH.^{56, 57}

A complex mechanism was suggested by Jourdeuil *et al.* involving the formation of a GSNO superoxide intermediate which is broken down to give the glutathione disulfide radical and either dinitrogen tetroxide or peroxynitrite. In each case superoxide is regenerated, hence only a catalytic amount is required and the overall products are the same, equation 1.12.⁵⁶

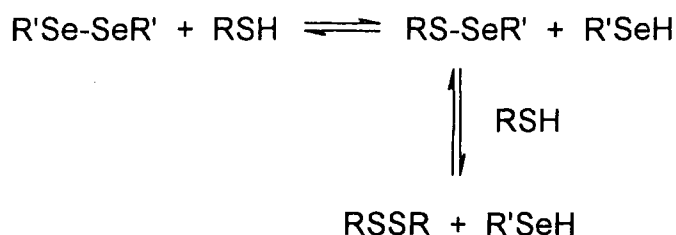


Equation 1.12 Superoxide catalysed decay of GSNO

GSNO bound NO is less reactive to superoxide than free NO. Hence, RSNOs are suggested as protectors of NO from superoxide *in vivo* allowing them to serve as transport or storage molecules.⁵⁷

1.2.4.8 RSNO decomposition by selenocystamine

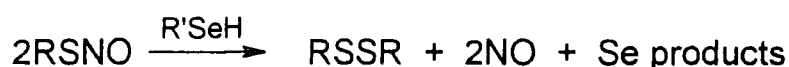
Selenols, R'SeH, are the selenium based analogues of thiols and are produced from exchange reactions between diselenides and thiols to produce transient selenosulfides and eventually R'SeH, Scheme 1.8.⁵⁸



Scheme 1.8 Formation of selenols from diselenides and thiols

Selenium is essential to mammalian life and deficiencies have been shown to result in heart disease. Glutathione peroxidase is a selenium containing enzyme which is believed to linked to NO pathway.⁵⁸

Selenols have been suggested to help invoke NO release from RSNOs at physiological pH in the presence of EDTA and thiols.⁵⁸ The mechanistic details are undefined but disulfide and NO have been characterised as the major products, equation 1.13.



Equation 1.13 Selenol based decomposition of RSNOs

1.2.4.9 RSNO decomposition by iron (II) complexes

Many of the processes involving NO *in vivo* are understood to proceed through activation of the enzyme guanylate cyclase. The NO binding site in the enzyme is a heme iron centre, which is known to possess a great affinity for NO.

RSNOs have been shown to react rapidly with simpler iron complexes and transfer NO and NO⁺ depending on the complex used.⁵⁹ The iron complexes were derived from 2, 3- dimercaptopropane-1-sulfonate, DMPS (a), and *N*-methyl-D-glucamine dithiocarbamate, MGD (b), Figure 1.6.

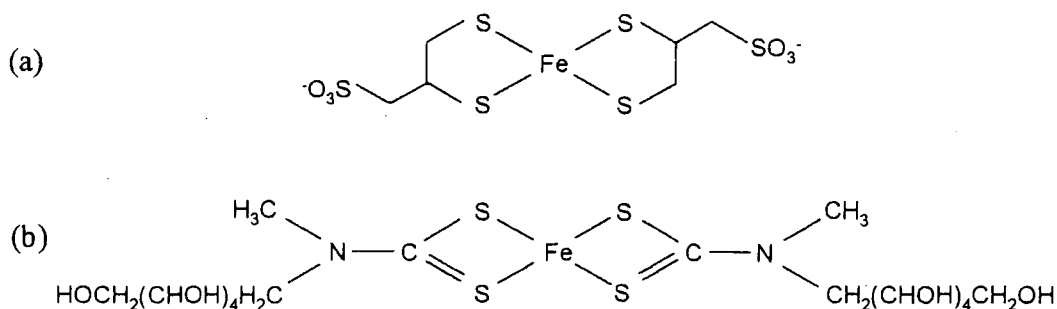


Figure 1.6 Iron complexes derived from (a) DMPS and (b) MGD

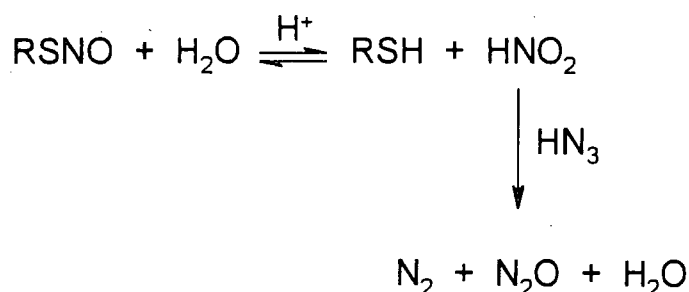
Complex (a) has been shown to undergo direct transfer of NO^+ as indicated by the thiol product. The iron nitrosyl product has identical spectral properties to that formed from the complex and free NO therefore an oxidation stage is anticipated during the process.

Complex (b) undergoes NO transfer but the reaction is faster than the spontaneous release of NO from the RSNO hence direct NO transfer is inferred.

In conclusion the possibilities of NO and NO^+ transfer from RSNOs to iron complexes *in vivo* is implied.⁵⁹

1.2.4.10 Acid hydrolysis of RSNOs

All of the above reactions are concerned with RSNO decomposition at physiological pH or above. However, RSNOs may decay through acid hydrolysis. The reaction is slow and requires a nitrous acid trap, such as azide, to avoid renitrosation of the thiol back to the starting RSNO, Scheme 1.9.⁶⁰



Scheme 1.9 Acid hydrolysis of RSNOs with the inclusion of azide as a nitrous acid trap

1.2.5 RSNOs *in vivo*

A variety of RSNOs have been detected *in vivo* and an *in vivo* concentration of $<1 \mu\text{mol dm}^{-3}$ is quoted.⁶¹ However, a biosynthetic route has yet to be established. Suggestions of thiol nitrosation by NO ⁶² and peroxynitrite⁶³ have been criticised.

The majority of RSNOs *in vivo* are present as the *S*-nitroso derivative of serum albumin.⁶⁴ It has been proposed that due to the reactivity of NO with oxygen, a carrier system is required for transport to the required site of action.⁵⁵

Evidence indicates that NO is transported *in vivo* by *S*-nitroso serum albumin and delivered to the required target by transnitrosation to a more reactive thiol such as cysteine.⁶⁶ SNCys is present in plasma in concentrations as high as $0.3 \mu\text{M}$ but detected levels vary greatly, due its the reactivity.⁶⁷

The *S*-nitroso derivative of hemoglobin, with nitrosation of a cysteine residue in the β -chain, has been identified *in vivo*.⁶⁸ From this, the theory that interconversion between the *S*- NO and Fe-NO forms instigates vasodilation, has been derived.

RSNOs show biological effects similar to NO. They are vasodilatory⁶⁹ and not subject to tolerance, unlike GTN.⁷⁰ They are also inhibitors of platelet aggregation with GSNO currently undergoing medical trials to prevent blood clotting during surgery. A lack of RSNOs in airways is thought to bring on asthmatic respiratory failure.⁷¹

Deleterious effects have also been noted with evidence that RSNOs may cleave DNA in the presence of H₂O₂.⁷²

There is agreement that RSNO decomposition *in vitro* is not comparable to that *in vivo*,⁷³ but some research needs to be reassessed to account for copper catalysed decomposition, which has been confirmed, to occur *in vivo*. Neocuproine chelation of Cu⁺ affects the bio-activity of RSNOs in platelet aggregation inhibition⁷⁴ and vasodilation.⁷⁵

It seems that RSNOs are very closely linked to the NO pathway and research continues to determine their exact actions *in vivo* and ways to utilise them as NO donor drugs.⁷⁶

1.3 Peroxynitrite

1.3.1 Introduction

The free radical nature of NO allows reaction with other free radicals. Beckman *et al.*⁷⁷ created an explosion of research in 1990 after suggesting that peroxynitrite could be formed *in vivo* through the direct combination of two endogenous free radicals NO and superoxide, O₂^{•-}, equation 1.14.



Subsequent research displayed peroxynitrite's cytotoxic diversity in reactions with many biomolecules including thiols,⁷⁸ lipids,⁷⁹ cytochrome *c*,⁸⁰ DNA,⁸¹ zinc fingers⁸² and Fe/S clusters.⁸³ Hence peroxynitrite has been described as “the ugly side” of NO⁸⁴ and many of the toxic effects exhibited by NO have now been attributed to peroxynitrite.

1.3.2 Physical Properties

Peroxynitrous acid is a highly unstable inorganic peroxy acid, however its conjugate base peroxynitrite anion is relatively stable and may be kept for days in alkaline solutions in the presence of a metal chelator and for months in a freezer. The term peroxynitrite is generally assumed to refer to the sum of the anion and the protonated acid. A pK_a of 6.8^{78,85} means that at physiological pH approximately 20% of peroxynitrite is in the protonated form.

Pure peroxynitrite is yellow in colour and may be studied spectrophotometrically. The anion has a λ_{max} centred on 301 nm. Since the first spectrophotometric study in 1941⁸⁶ the accepted value for the extinction coefficient has increased due to instrument improvements and currently stands at 1700 dm³ mol⁻¹ cm⁻¹.⁸⁷ The acid is less well studied due to its instability, however a λ_{max} of 240 nm has been detected by pulse radiolysis with an extinction coefficient of 770 dm³ mol⁻¹ cm⁻¹.⁸⁸

Structurally peroxyxynitrite can exist as two geometrical isomers, *cis* and *trans*. The negative charge is delocalised across the entire peroxyxynitrite anion and the *cis* conformer has a weak partial bond between the terminal oxygen atoms. This results in a 21-24 kcal mol⁻¹ barrier preventing isomerisation to the *trans* form. The terminal oxygen of the *trans* isomer may directly attack the nitrogen allowing internal rearrangement to nitrate, Figure 1.7.⁸⁹

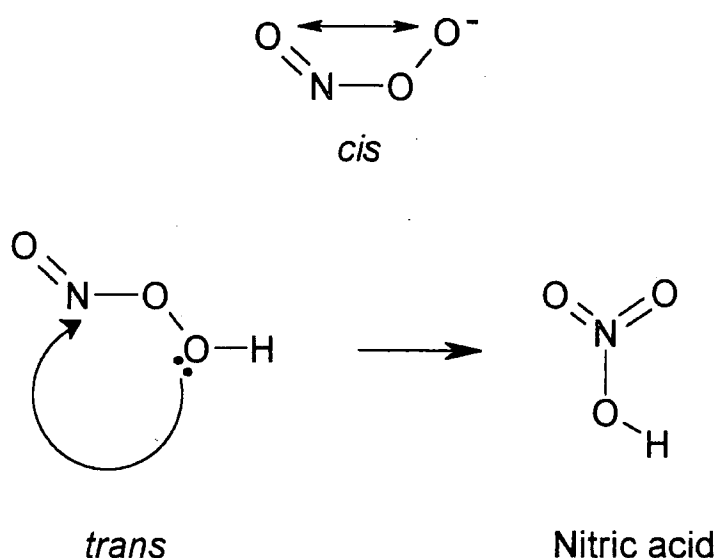


Figure 1.7 Geometrical isomers of peroxyxynitrite anion and peroxyxynitrous acid

Protonation to peroxyxynitrous acid halves the isomerisation barrier thus facilitating *cis-trans* isomerisation and the subsequent decay to nitrate.⁸⁹

Literature values for the $\text{p}K_{\text{a}}$ of peroxyxynitrous acid have varied depending on the method of calculation and crucially the type of substrate used.⁹⁰ Evidence is now available that peroxyxynitrite may react via the *cis* or *trans* isomers depending on buffer concentrations, pH, the concentrations of reagents and the presence of metal ions.⁹¹

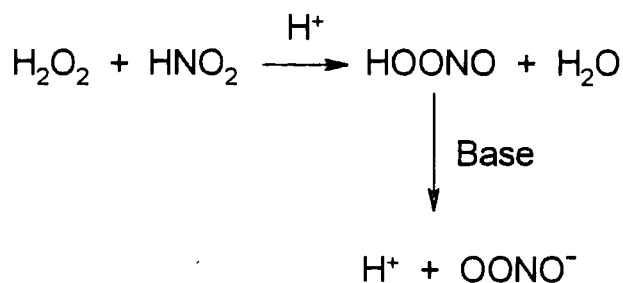
Consequently this has led to assignment of two $\text{p}K_{\text{a}}$ values of 6.8 and 8.0 for the *cis* and *trans* isomers respectively.⁹⁰

1.3.3 *In vitro* formation of peroxynitrite

1.3.3.1 Nitrosation of hydrogen peroxide

There are many procedures quoted in the literature for the generation of peroxynitrite, each with its own pitfalls.⁹² However, the vast variety of methods allows selection of an appropriate technique for a specific reaction requirement.

The cheapest and simplest route to peroxynitrite is the nitrosation of hydrogen peroxide, H_2O_2 , by nitrous acid, equation 1.15.⁹³



Scheme 1.10 Nitrosation of H_2O_2 by nitrous acid with subsequent quenching by base

The highly reactive peroxynitrous acid rearranges to nitrate under the initially acidic conditions and must be quenched quickly with base affording the stable anion in approximately 50% yield.

Using nitrosating conditions featuring an excess of H_2O_2 results in nitrite-free peroxynitrite. Conversely, the use of excess nitrite allows the generation of H_2O_2 -free peroxynitrite.

This technique may be modified with the use of a quenched flow reactor where the reagents are drawn from two wells and combined at a mixing point before quenching with the solution of NaOH drawn from the third well. All solutions are drawn along the tubing by vacuum to a product collection flask. The technique allows peroxynitrite yields of ~90 %, Figure 1.8.⁹⁴

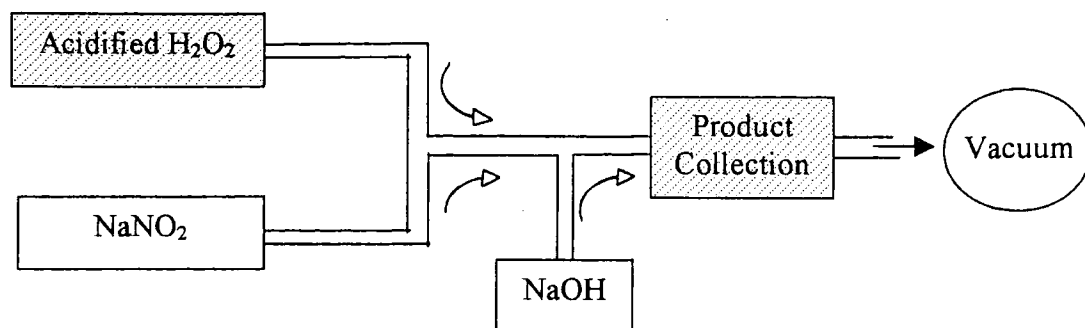
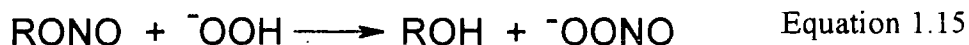


Figure 1.8 Quenched flow reactor for the generation of peroxynitrite

1.3.3.2 Peroxynitrite from alkyl nitrites

A very high yielding method is available from the reaction of alkyl nitrites with the hydroperoxide anion in basic solution, equation 1.15.⁹⁵

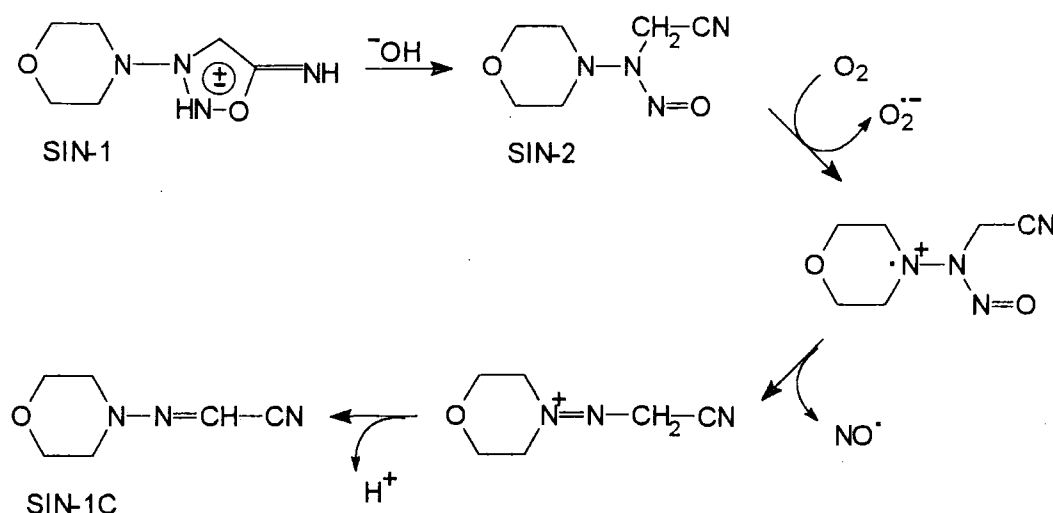


97% yield is attainable but the final solution is contaminated with equimolar concentrations of alcohol, which is then susceptible to oxidation by peroxide.

This procedure has been adapted with the synthesis occurring in a two-phase system incorporating isoamyl nitrite as the nitrosating agent in the organic phase and alkaline H_2O_2 in the aqueous phase.⁹⁶ Peroxynitrite is formed upon agitation over 1 hour and settles in the aqueous layer, stabilised by the alkaline conditions. Although this technique is free from organic contaminants and produces high concentrations of peroxynitrite it suffers from nitrite contamination.

1.3.3.3 Peroxynitrite generators

SIN-1 (3, -morpholino-sydnomimine-hydrochloride) is a potent vasorelaxant and antiplatelet agent that generates superoxide and NO simultaneously, Scheme 1.11.⁹⁷



Scheme 1.11 SIN-1 production of NO and superoxide

As described earlier superoxide and NO combine to yield peroxynitrite, equation 1.14. SIN-1 is widely used in the studies of the biological effects of peroxynitrite as it can produce a sustained release upon reaction with base.

1.3.3.4 Peroxynitrite from other sources

There are many other techniques to produce peroxynitrite however some have little preparative value.⁹²

The most recently reported routes to peroxynitrite are the reactions of NO with solid potassium superoxide⁹⁸ and NO with tetramethylammonium superoxide in liquid ammonia.⁹⁹ The latter yields the first pure peroxynitrite salt.

1.3.4 Peroxynitrite formation *in vivo*

The precursor to the Beckman *et al.* paper was the discovery of the reaction between superoxide and NO by Blough and Zafiriou in 1985.¹⁰⁰ The extremely fast reaction ($k = 4.3 - 6.7 \times 10^9 \text{ dm}^3 \text{ mol}^{-1} \text{ s}^{-1}$)^{101, 102} is near to the diffusion controlled limit which is characteristic of free radical termination reactions. NO is the only known biological molecule that is produced in high enough concentrations to out-compete SOD for superoxide. The reaction between NO and superoxide is 2-3 times faster than SOD and superoxide ($k = 2 \times 10^9 \text{ dm}^3 \text{ mol}^{-1} \text{ s}^{-1}$).¹⁰³

There is much research involving the *in vitro* reactions of peroxynitrite but questions have been raised as to their relevance *in vivo*, due to the relative concentrations of NO and superoxide in cells.¹⁰⁴ *In vivo* concentrations of NO and superoxide are between 10-100 nmol dm⁻³ and 0.1-1 nmol dm⁻³ respectively. However under conditions of pathological stress the concentrations of superoxide increase and therefore peroxynitrite levels increase inducing further oxidative stress.¹⁰⁵

Initially the reaction with superoxide was believed to be a detoxification mechanism for NO but this has been queried, as the destruction of a weak oxidant to give a stronger oxidant seems unlikely.¹⁰⁶

1.3.5 Peroxynitrite decomposition pathways

The decomposition mechanisms of peroxynitrite have been the subject of a large amount of research recently after the realisation that peroxynitrite was formed *in vivo*. Various groups have suggested a wide range of mechanisms but the general consensus categorises peroxynitrite decomposition into three possible routes: internal rearrangement to nitrate, decomposition to nitrite and a free radical type pathway.

1.3.5.1 Rearrangement to nitrate

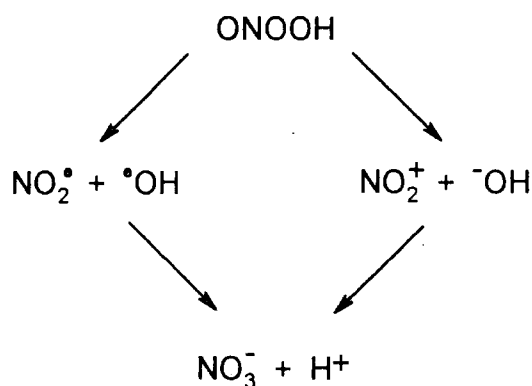
In acidic solutions, peroxynitrite is present as the protonated form, peroxynitrous acid. Its decay is *via* internal rearrangement to nitrate through migration of the distal peroxynitrite oxygen to nitrogen, Figure 1.7. The reaction is believed to be quantitative under acidic conditions and product testing has found no nitrite in the final solution.¹⁰⁷

The rate equation for the rearrangement to nitrate has been interpreted using the assumption that the peroxynitrite anion is stable and therefore the peroxynitrous acid decays through a first order process.⁸⁸ This gives an observed first order rate constant of:

$$k_{\text{obs}} = k \left(\frac{[\text{H}^+]}{[\text{H}^+] + K_a} \right)$$

Where $k = 1.0 \pm 0.2 \text{ s}^{-1}$ and $K_a = (1.0 \pm 0.3) \times 10^{-7}$.

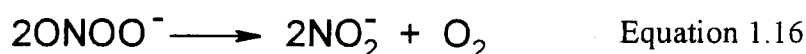
There is some contention that isomerisation to nitrite may occur by heterolytic or homolytic pathways rather than through internal rearrangement, but still yielding the nitrate ion as the quantitative product, Scheme 1.12.¹⁰⁸ There is much discussion as to the true mechanism but as yet no conclusive evidence in favour of any single pathway. The arguments for and against each pathway are discussed in references 92 and 108.



Scheme 1.12 Homolysis and heterolysis of peroxynitrous acid

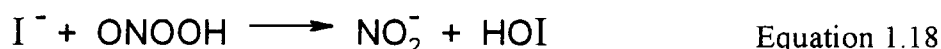
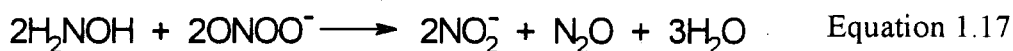
1.3.5.2 Decomposition to nitrite

In basic solutions ($\text{pH} > 10$) an alternative decay pathway is available. The rearrangement to nitrate pathway becomes very slow and decomposition occurs *via* the peroxynitrite anion to yield nitrite and oxygen, equation 1.16.⁹²



At $\text{pH} > 10$ deviations from the rate law occur and this is attributed to the anionic decomposition pathway, which is catalysed by Cu^{2+} ions.⁹²

Nitrite is also formed when peroxynitrite and peroxynitrous acid act as oxidising agents. The oxidations of hydroxylamine (equation 1.17),⁹³ and iodide (equation 1.18),¹⁰⁹ are examples of this.



1.3.5.3 Decomposition *via* free radicals

The major area for debate in the decomposition of peroxynitrite is whether free radicals, notably hydroxy radicals, are formed or not. Hydroxy radicals may be detected by free radical traps or through reaction product studies that suggest their presence. It is difficult to determine whether peroxynitrite actually generates free hydroxy radicals or whether it behaves as a hydroxy radical donor, without ever generating the free HO^\bullet species. The conclusions are diverse and contradictory however, the general consensus is that the formation of free radicals, if any, is due to a minor pathway and the majority of peroxynitrite decays by the nitrite or nitrate routes.^{92, 108}

1.3.5.4 Other reactions of peroxynitrite

As mentioned peroxynitrite is known to react with many bio-molecules, predominantly by oxidation but also by nitration and nitrosation and is reviewed comprehensively in reference 108.

Oxidation by peroxynitrite yields nitrite as the nitrogen product and some nitrate depending on pH and the substrate. A measure of the oxidising ability of peroxynitrite is made through comparison to H_2O_2 in the oxidation of thiols to disulfides. The oxidation by peroxynitrite is measured at over 1000 times faster than H_2O_2 at physiological pH.¹¹⁰ The reaction yields quantitative disulfide and presumably nitrite, although this has not been quantified.^{110, 111}

Some reports suggest RSNOs are formed in the oxidation of thiols by peroxynitrite but the quantities are small, between 1–2 %.^{112, 113}

1.3.6 Conclusion

With reference to peroxynitrite, Edwards and Plumb conclude “a comprehensive understanding of this chemistry has not been achieved”.⁹² That was in 1993 and although progress has been made, their statement still holds.

Doubts over the existence of peroxynitrite *in vivo* have now declined with confirmation of peroxynitrite production from activated macrophages¹¹⁴ and endothelial cells.¹¹⁵ However, the exact role of peroxynitrite *in vivo* is still not clear and extrapolation of *in vitro* findings towards *in vivo* situations still remains tenuous.

1.4 *S*-Nitrosation of thiols

1.4.1 Introduction

In Section 1.3 the formation of RSNOs from nitrous acid was briefly introduced and in the latter section the formation of RSNOs during the oxidation of thiols by peroxynitrite reported.

In this final section of the introduction these reactions will be looked at in more depth and categorised into a class of nitrosating agents with the potential to invoke *S*-nitrosation.

1.4.2 *S*-Nitrosation by nitrous acid

The classical route to RSNOs is through nitrosation of thiols with nitrous acid, a process that has been known since the mid 1800s.

Kinetic investigations revealed that *S*-nitrosation resembles *O*- and *N*-nitrosation mechanistically, but the reaction is much less reversible.³³ Accordingly the reaction of nitrous acid with thiols is acid catalysed and the rate equation has been determined to be:

$$\text{Rate} = k_3[\text{RSH}][\text{HNO}_2][\text{H}^+]$$

Equation 1.19 Third order rate equation for nitrosation of thiols by nitrous acid

Third order rate constants, k_3 , vary with the thiol substrate. Thiols that can form a 5 or 6 membered ring in the transition state for nitrosation have higher k_3 values. An example being that *N*-acetylation of cysteine allows electrostatic interactions which stabilise the charge distribution and enhance nitrosation at the sulfur atom, Figure 1.9.¹¹⁶ Consequently an increase in the third order rate constant is achieved, $k_3 = 456$ and $1590 \text{ dm}^6 \text{ mol}^{-2} \text{ s}^{-1}$ for cysteine and *N*-acetyl cysteine respectively.⁶⁰

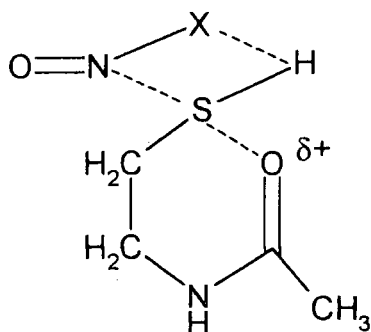


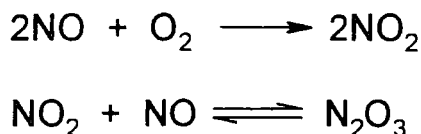
Figure 1.9 Proposed intermediate structure between HNO_2 and some thiols, where X is OH/OH_2

As depicted in Figure 1.9 it is quite common to treat a nitrosating agent as NOX where X is a suitable leaving group. In the case of nitrous acid the suggested nitrosating species is the nitrous acidium ion, H_2NO_2^+ , resulting in water as the leaving group.¹¹⁷

The treatment of nitrosating species as NOX helps in the understanding of why peroxynitrite may not be a particularly good nitrosating agent. Nitrosation by peroxynitrite and peroxynitrous acid would require O_2^{2-} and HO_2^- as the respective leaving groups.¹¹⁸

1.4.3 S-Nitrosation by dinitrogen trioxide

The formation of dinitrogen trioxide, N_2O_3 , from NO in aerobic aqueous solutions has led to many reports of direct nitrosation by NO , Scheme 1.13.

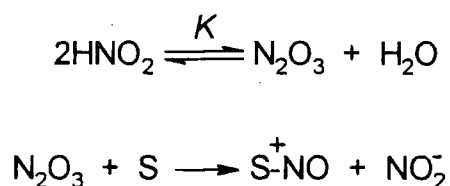


Scheme 1.13 Key steps to the formation of N_2O_3 from NO in oxygenated solutions

N_2O_3 exists in aqueous solution in equilibrium with nitrous acid, equation 1.20.



Hence during acidified nitrous acid nitrosation reactions, and depending on the conditions and the substrate, nitrosation may pass through N_2O_3 . Kinetically this is observed as a second order dependence on nitrous acid interpreted in terms of Scheme 1.14.

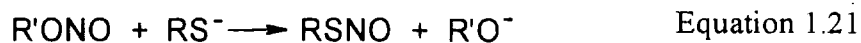


Scheme 1.14 Nitrous acid nitrosation where N_2O_3 becomes the active nitrosating agent

Overall, NO in aerated solutions can nitrosate substrates through the N_2O_3 pathway even at physiological pH.¹¹⁷

1.4.4 S-Nitrosation by alkyl nitrites

Alkyl nitrites, RONO , can also nitrosate thiols in the XNO sense. The leaving group in this case is the alcohol and the reaction is interpreted as thiolate anion attack on the RONO nitroso group, giving electrophilic nitrosation of sulfur, equation 1.21.¹¹⁹



1.4.5 Conclusion

The nitrosation of thiols is well documented¹²⁰ and is physiologically important given the perceived activity of RSNOs *in vivo*. Although most *S*-nitrosations require acidic pH, some, especially through N_2O_3 and RONO, can occur at physiological pH. This has an enormous bearing on the NO pathway given that RSNOs are expected to be the transport and storage molecules of NO *in vivo*.

1.5 References

- 1 E. W. Ainscough and A. M. Brodie, *J. Chem. Ed.*, 1995, **71**, 26.
- 2 E. Culotta and D. E. Koshland Jr., *Science*, 1992, **258**, 1862.
- 3 L. J. Ignarro, *Semin. Hematol.*, 1989, **26**, 63.
- 4 M. A. Marletta, P. S. Yoon, R. Iyengar, C. D. Leaf and J. S. Wishnok, *Biochemistry*, 1988, **27**, 8706.
- 5 J. Garthwaite, *Trends Neurosci.*, 1991, **14**, 60.
- 6 M. W. Radomski, R. M. Palmer and S. Moncada, *Br. J. Pharmacol.*, 1987, **92**, 639.
- 7 M. Feelisch, *J. Cardiovasc. Pharmacol.*, 1991, **17**, S25.
- 8 F. A. Cotton and G. Wilkinson, "*Advanced Inorganic Chemistry*", p. 356, 3rd ed., John Wiley & Sons Ltd, 1972.
- 9 H. H. Mitchell, H. A. Shonle and H. S. Grindley, *J. Biol. Chem.*, 1916, **24**, 461.
- 10 "*The Health Effects of Nitrate, Nitrite and N-Nitroso Compounds*", National Academy Press, 1981.
- 11 R. G. Cassens, M. L. Greaser, T. Ito and M. Lee, *Food Technol.*, 1979, **33**, 46.
- 12 J. I. Sprent, "*The Ecology of the Nitrogen Cycle*", Cambridge University Press, 1987.
- 13 F. Murad, C. K. Mittal, W. P. Arnold, S. Katsuki and H. Kimura, *Adv. Cyclic Nucl. Res.*, 1978, **9**, 145.
- 14 R. F. Furchgott and J. V. Zawadzki, *Nature*, 1980, **288**, 373.
- 15 R. M. J. Palmer, A. G. Ferrige and S. Moncada, *ibid*, 1987, **327**, 524.
- 16 L. J. Ignarro, G. M. Buga, K.S. Wood, R. E. Byrns and G. Chaudui, *Proc. Natl. Acad. Sci. USA*, 1987, **84**, 9265.
- 17 R. M. J. Palmer, D. S. Ashton and S. Moncada, *Nature*, 1988, **333**, 664.
- 18 A. M. Leone, R. M. J. Palmer, R. G. Knowles, P. L. Francis, D. S. Ashton and S. Moncada, *J. Biol. Chem.*, 1991, **226**, 2379.
- 19 J. Garthwaite, S. L. Charles and R. Chess-Williams, *Nature*, 1988, **336**, 385.
- 20 R. G. Knowles, M. Palacios, R. M. J. Palmer and S. Moncada, *Proc. Natl. Acad. Sci. USA*, 1989, **86**, 5159.

- 21 H. Bult, G. E. Boeckxstaens, P. A. Pelckmans, F. H. Jordaens, Y. M. Van Maercke and A. G. Herman, *Nature*, 1990, **345**, 346.
- 22 F. Holmquist, H. Hedlund and K.-E. Andersson, *Acta Physiol. Scand.*, 1991, **141**, 441.
- 23 J. B. Hibbs, R. R. Taintor, Z. Vavrin and E. M. Rachlin, *Biochem. Biophys. Res. Commun.*, 1988, **157**, 87.
- 24 J. B. Hibbs, Z. Vavrin and R. R. Taintor, *J. Immunol.*, 1987, **138**, 550.
- 25 M. Aranda and R. G. Pearl, *Respiratory Care*, 1999, **44**, 156.
- 26 M. Feelisch, M. te Poel, R. Zamora, A. Deussen and S. Moncada, *Nature*, 1994, **368**, 62.
- 27 P. R. Myers, R. L. Minor Jr., R. Geurra Jr., J. Bates and D. G. Harrison, *ibid.*, 1990, **345**, 161.
- 28 G. M. Rubanyi, A. Johns, D. Harrison and D. Wilcox, *Circulation*, 1988, **80**, 281.
- 29 S. Oae and K. Shinham, *Org. Prep. Proc. Int.*, 1983, **15**, 165.
- 30 D. L. H. Williams, *Acc. Chem. Res.*, 1999, **32**, 870.
- 31 J. S. Stamler, O. Jaraki, J. Osborne, D. I. Simon, J. Keaney, J. Vita, D. Singel, C. R. Valeri and J. Loscalzo, *Proc. Natl. Acad. Sci. USA*, 1992, **89**, 7674.
- 32 D. J. Barret, D. F. Debenham and J. Glauser, *J. Chem. Soc., Chem. Commun.*, 1965, **12**, 248.
- 33 P. H. Beloso and D. L. H. Williams, *Chem. Commun.*, 1997, 89.
- 34 L. J. Ignarro, B. K. Barry, D. Y. Gruetter, J. C. Edwards, E. H. Ohlstein, C. A. Gruetter, and W. H. Barricos, *Biochem. Biophys. Res. Commun.*, 1980, **94**, 93.
- 35 V. G. Kharitonov, A. R. Sunquist and V. S. Sharma, *J. Biol. Chem.*, 1995, **270**, 2815; S. Goldstein and G. J. Czapski, *J. Am. Chem. Soc.*, 1996, **118**, 3419.
- 36 D. J. Sexton, A. Muruganandam, D. J. McKenny and B. Mutus, *Photochem. Photobiol.*, 1994, **59**, 463.
- 37 J. McAninly, D. L. H. Williams, S. C. Askew, A. R. Butler and C. Russell, *J. Chem. Soc., Chem. Commun.*, 1993, **23**, 1758.
- 38 S. C. Askew, J. Barnett, J. McAninly and D. L. H. Williams, *J. Chem. Soc., Perkin Trans. 2*, 1995, 741; A. P. Dicks, H. R. Swift, D. L. H. Williams, A. R. Butler, H. H. Al-Sadoni and B. G. Cox, *J. Chem. Soc., Perkin Trans. 2*, 1996, 481.

- 39 R. J. Singh, N. Hogg, J. Joseph and B. Kalyanaraman, *J. Biol. Chem.*, 1994, **271**, 18596.
- 40 A. P. Dicks and D. L. H. Williams, *Chem. Biol.*, 1996, **3**, 655.
- 41 K. Varnagy, I. Sovago and H. Kozlowski, *Inorg. Chim. Acta.*, 1988, **151**, 117.
- 42 D. R. Noble and D. L. H. Williams, *Nitric Oxide: Biology and Chemistry*, 2000, **4**, 392.
- 43 A. P. Munro and D. L. H. Williams, *Can. J. Chem.*, 1999, **77**, 550.
- 44 B. Saville, *Analyst*, 1958, **83**, 670.
- 45 H. R. Swift and D. L. H. Williams, *J. Chem. Soc., Perkin Trans. 2*, 1997, 1933.
- 46 A. J. Holmes and D. L. H. Williams, *J. Chem. Soc., Perkin Trans. 2*, 2000, 1639.
- 47 S. Oae, Y. H. Kim, D. Fukushima and K. Shinham, *J. Chem. Soc., Perkin Trans. 1*, 1978, 913.
- 48 D. J. Barnett, A. Rios and D. L. H. Williams, *J. Chem. Soc., Perkin Trans. 2*, 1995, 1279.
- 49 J.-W. Park, *Biochem. Biophys. Res. Commun.*, 1988, **152**, 916.
- 50 D. R. Noble and D. L. H. Williams, *J. Chem. Soc., Perkin Trans. 2*, 2001, 13.
- 51 S. P. Singh, J. S. Wishnok, M. Keshive, W. M. Deen and S. R. Tannenbaum, *Proc. Natl. Acad. Sci. USA*, 1996, **93**, 14428.
- 52 P. S.-Y. Wong, J. Hyun, J. M. Fukuto, F. Shirota, E. G. DeMaster, D. W. Shoeman and H. T. Nagasawa, *Biochemistry*, 1998, **37**, 5362.
- 53 A. P. Dicks, E. Li, A. P. Munro, H. R. Swift and D. L. H. Williams, *Canad. J. Chem.*, 1998, **76**, 789.
- 54 A. P. Munro and D. L. H. Williams, *J. Chem. Soc., Perkin Trans. 2*, 2000, 1794.
- 55 A. P. Munro and D. L. H. Williams, *ibid.*, 1999, 1989.
- 56 D. Jourdeuil, C. T. Mau, F. S. Laroux, D. A. Wink and M. B. Grisham, *Biochem. Biophys. Res. Commun.*, 1988, **244**, 525.
- 57 S. Aleryani, E. Milo, Y. Rose and P. Kostka, *J. Biol. Chem.*, 1998, **273**, 6041.
- 58 Y. Hou, Z. Guo, J. Li and P. G. Wang, *Biochem. Biophys. Res. Commun.*, 1996, **228**, 88.
- 59 A. R. Butler, S. Elkins-Daukes, D. Parkin and D. L. H. Williams, *Chem. Commun.*, 2001, 1732.
- 60 D. L. H. Williams, "Nitrosation", Ch. 7, Cambridge University Press, Cambridge, 1988.

- 61 J. S. Stamler, O. Jaraki, J. A. Osbourne, D. I. Simon, J. Keaney, J. Vita, D. Singel, C. R. Valeri and J. Loscalzo, *Proc. Natl. Acad. Sci. USA*, 1992, **89**, 7674.
- 62 A. J. Gow, D. G. Buerk and H. Ischiropoulos, *J. Biol. Chem.*, 1997, **272**, 2841.
- 63 M. Balazy, P. M. Kaminski, K. Mao, J. Tan and M. S. Wolin, *ibid.*, 1998, **273**, 32009; A. van der Vliet, P. A. Chr. 't Hoen, P. S.-Y. Wong, A. Bast and C. E. Cross, *ibid.*, 1998, **273**, 30255.
- 64 J. S. Stamler, D. I. Simon, J. A. Osbourne, M. E. Mullins, O. Jaraki, T. Michel, D. J. Singel and J. Loscalzo, *Proc. Natl. Acad. Sci. USA*, 1992, **89**, 444.
- 65 D. Pietraforte, C. Mallozzi, G. Scorza and M. Minetti, *Biochemistry*, 1995, **34**, 7177.
- 66 M. P. Gordge, J. S. Hothersall, G. H. Neild and A. A. Noronha-Dutra, *Br. J. Pharmacol.*, 1996, **119**, 533.
- 67 A. R. Butler and P. Rhodes, *Anal. Biochem.*, 1997, **249**, 1.
- 68 L. Jia, C. Bonaventura, J. Bonaventura and J. S. Stamler, *Nature*, 1996, **380**, 221.
- 69 B. T. Mellion, L. J. Ignarro, C. B. Meyers, E. H. Ohlstein, B. A. Ballot, A. L. Hyman and P. J. Kadowitz, *Mol. Pharmacol.*, 1983, **23**, 653; H. A. Moynihan and S. M. Roberts, *J. Chem. Soc., Perkin Trans. 1*, 1994, 797.
- 70 J. A. Bauer and H.-L. Fung, *J. Pharmacol. Exp. Ther.*, 1991, **256**, 249; J. D. Horowitz, E. N. Antman, B. H. Lorell, W. H. Barry and T. W. Smith, *Circulation*, 1993, **68**, 1247.
- 71 B. Gaston, S. Sears, J. Woods, J. Hunt, M. Ponaman, T. McMahon and J. S. Stamler, *Lancet*, 1998, **351**, 1317.
- 72 J.-W. Park, P. Kopi and H. K. Kim, *Biochem. Biophys. Res. Commun.*, 1994, **200**, 966.
- 73 W. R. Mathews and S. W. Kerr, *J. Pharmacol. Exp. Ther.*, 1993, **267**, 1529; B. Gaston, J. M. Drazen, A. Jansen, D. A. Sugarbaker, J. Loscalzo, W. Richards and J. S. Stamler, *ibid.*, **268**, 978.
- 74 M. P. Gordge, D. Meyer, J. S. Hothersall, G. H. Neild, N. N. Payne and A. A. Noronha-Dutra, *Br. J. Pharmacol.*, 1995, **114**, 1083.
- 75 H. H. Al-Sadoni, I. L. Megson, S. Bisland, A. R. Butler and F. W. Flitney, *Br. J. Pharmacol.*, 1997, **121**, 1047.
- 76 H. Al-Sa'Doni and A. Ferro, *Clinical Sc.*, 2000, **98**, 507.

- 77 J. S. Beckman, T. W. Beckman, J. Chen, P. A. Marshall and B. A. Freeman, *Proc. Natl. Acad. Sci. USA*, 1990, **87**, 1620.
- 78 R. Radi, J. S. Beckman, K. M. Bush and B. A. Freeman, *J. Biol. Chem.*, 1991, **266**, 4244.
- 79 R. Radi, J. S. Beckman, K. M. Bush and B. A. Freeman, *Arch. Biochem. Biophys.*, 1991, **288**, 481.
- 80 L. Thompson, M. Trujillo, R. Telleri and R. Radi, *ibid.*, 1995, **319**, 491.
- 81 P. A. King, V. E. Anderson, J. O. Edwards, G. Gustafson, R. C. Plumb and J. W. Suggs, *J. Am. Chem. Soc.*, 1992, **114**, 5430.
- 82 J. P. Crow, J. S. Beckman and J. M. McCord, *Biochemistry*, 1995, **34**, 3544.
- 83 L. Castro, M. Rodriguez and R. Radi, *J. Biol. Chem.*, 1994, **269**, 29409.
- 84 J. S. Beckman and W. H. Koppenol, *Am. J. Physiol. (Cell Physiol. 40)*, 1996, **271**, 1424.
- 85 W. H. Koppenol, W. A. Pryor, J. J. Moreno, H. Ischiropoulos and J. S. Beckman, *Chem. Res. Toxicol.*, 1992, **5**, 834.
- 86 G. Kortum and B. Finckh, *Z. physik. Chemie*, 1941, **48B**, 32.
- 87 D. S. Bohle, B. Hansert, S. C. Paulson and B. D. Smith, *J. Am. Chem. Soc.*, 1994, **116**, 7423.
- 88 T. Logager and K. Sehested, *J. Phys. Chem.*, 1993, **97**, 6664.
- 89 J-H. M. Tsai, J. G. Harrison, J. C. Martin, T. P. Hamilton, M. van der Woerd, M. J. Jablonsky and J. S. Beckman, *J. Am. Chem. Soc.*, 1994, **116**, 4115.
- 90 J. P. Crow, P. C. Spruell, J. Chen, C. Gunn, H. Ischiropoulos, M. Tsai, C. D. Smith, R. Radi, W. H. Koppenol and J. S. Beckman, *Free Radical Biol. Med.*, 1994, **15**, 331.
- 91 R. Kissner, J. S. Beckman and W. H. Koppenol, *Methods Enzymol.*, 1999, **301**, 342.
- 92 J. O. Edwards and R. C. Plumb, *Prog. Inorg. Chem.*, 1993, **41**, 599.
- 93 M. N. Hughes and H. G. Nicklin, *J. Chem. Soc. A.*, 1970, 925.
- 94 "Methods in Nitric Oxide Research", p. 67, Ed. M. Feelisch and J. S. Stamler, John Wiley & Sons Ltd, Chichester, 1996
- 95 J. R. Leis, M. E. Pena and A. Rios, *Chem. Commun.*, 1993, 1298.
- 96 R. M. Uppu and W. A. Pryor, *Anal. Biochem.*, 1996, **236**, 242.
- 97 Reference 93, p. 94.
- 98 W. H. Koppenol, R. Kissner and J. S. Beckman, *ibid.*, 1996, **269**, 296.

- 99 D. S. Bohle, P. A. Glassbrenner and B. Hansert, *ibid.*, 1994, **116**, 7423.
- 100 N. V. Blough and O. C. Zafiriou, *Inorg. Chem.*, 1985, **24**, 3502.
- 101 R. E. Huie and S. Padmaja, *Free Radical Res. Commun.*, 1993, **18**, 195.
- 102 H. M. Hassan, *Free Radical Biol. Med.*, 1988, **5**, 377.
- 103 S. Goldstein and G. Czapski, *Free Radical Biol. Med.*, 1995, **117**, 12078.
- 104 D. Jourdeuil, F. L. Jourdeuil, P. S. Kutchukian, R. A. Musah, D. A. Wink and M. B. Grisham, *J. Biol. Chem.*, 2001, **276**, 28799.
- 105 J. T. Groves, *Curr. Opin. Chem. Biol.*, 1999, **3**, 226.
- 106 J. M. Fukuto and L. J. Ignarro, *Acc. Chem. Res.*, 1997, **30**, 149.
- 107 R. C. Plumb, J. O. Edwards and M. Herman, *The Analyst*, 1992, **117**, 1639.
- 108 W. H. Koppenol, *Metal Ions Biol. Syst.*, 1999, **36**, 597.
- 109 M. N. Hughes, H. G. Nicklin and W. A. C. Sackrile, *J. Chem. Soc. A.*, 1971, 3722.
- 110 R. Radi, J. S. Beckman, K. M. Bush and B. A. Freeman, *J. Biol. Chem.*, 1991, **266**, 4244.
- 111 C. Quijano, B. Alvarez, R. M. Gatti, O. Augusto and R. Radi, *Biochem. J.*, 1997, **322**, 167.
- 112 A. van der Vliet, P. A. Chr. 't Hoen, Patrick S.-Y. Wong, A. Bast and C. E. Cross, *J. Biol. Chem.*, 1998, **273**, 30255.
- 113 "Methods in Nitric Oxide Research", p. 104, Ed. M. Feelisch and J. S. Stamler, John Wiley & Sons Ltd, Chichester, 1996.
- 114 H. Ischiropoulos, Z. Zhu and J. S. Beckman, *Arch. Biochem. Biophys.*, 1992, **298**, 446.
- 115 N. W. Kooy and J. A. Royall, *ibid.* 1994, **310**, 352.
- 116 P. A. Morris and D. L. H. Williams, *J. Chem. Soc., Perkin Trans. 2*, 1988, 513.
- 117 Reference 60, Ch. 1.
- 118 D. L. H. Williams, *Nitric Oxide: Biology and Chemistry*, 1997, **1**, 522.
- 119 H. M. S. Patel and D. L. H. Williams, *J. Chem. Soc., Perkin Trans. 2*, 1990, 37.
- 120 D. L. H. Williams, *Chem. Soc. Rev.*, 1985, **14**, 171.

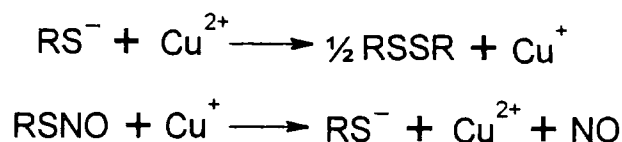
Chapter 2

2 Reaction of hydrogen peroxide with *S*-nitrosothiols

The discovery that the decomposition of RSNOs in aqueous solution was copper catalysed¹ explained the kinetic inconsistencies between many research groups, through varied amounts of copper in distilled water/buffers. Further work revealed the intricate redox system involving copper and the thiolate anion.² The addition of a reducing agent increases reaction rate³ by increasing the concentration of the active catalyst Cu^+ . It is now of interest to study the effect of an oxidising agent, hydrogen peroxide, on the copper catalysed decomposition of RSNOs.

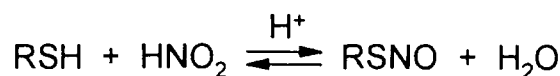
2.1 Introduction

As discussed in Chapter 1.2.4.2, the copper catalysed decomposition of RSNOs is highly dependent on a reducing species, usually the thiolate anion. This is present from the reversibility of the RSNO nitrosation and generates the active catalyst Cu^+ , Scheme 2.1.



Scheme 2.1 Copper catalysed decomposition of RSNOs

The reaction may be slowed or even stopped when an excess of the nitrosating species is used during the formation of the RSNO,⁴ thus driving the equilibrium to the right and leaving insufficient amounts of thiol to produce a high enough $[\text{Cu}^+]$, equation 2.1.



Equation 2.1 Nitrosation of thiols

The addition of an oxidising agent should have a similar result, stopping the reaction through oxidation of the thiolate anion to the disulfide and Cu^+ to Cu^{2+} . In fact, the reaction of RSNOs under anaerobic aqueous conditions is faster than aerobic aqueous conditions, due to oxidation of the Cu^+ ions, equation 2.2.²



Equation 2.2 Aerobic aqueous oxidation of copper (I) ions by oxygen

2.2 Hydrogen peroxide and *S*-nitrosglutathione

The addition of varying amounts of hydrogen peroxide, H_2O_2 , to *S*-nitrosglutathione, GSNO, did not stop or slow the reaction as predicted. Conversely, increased overall reaction rate was observed in a concentration dependent manner, see Figure 2.1.

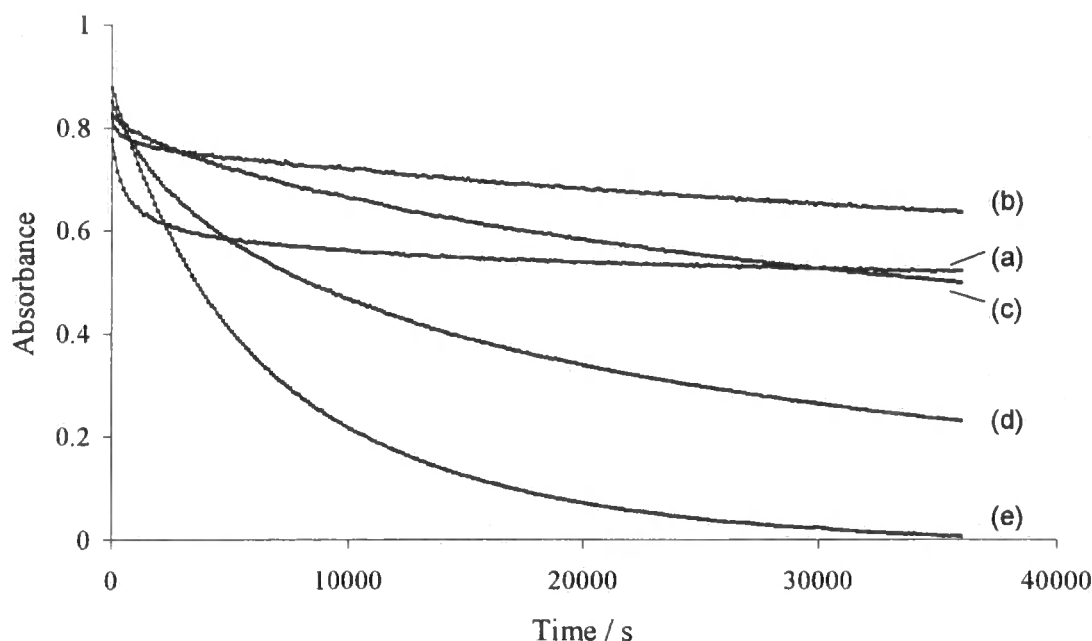


Figure 2.1 Addition of varying $[\text{H}_2\text{O}_2]$ to 1 mM GSNO with $10 \mu\text{M Cu}^{2+}$ at pH 7.4.
 (a) 0 M H_2O_2 (b) 1 mM H_2O_2 (c) 10 mM H_2O_2 (d) 0.1 M H_2O_2
 (e) 1 M H_2O_2

With no added H_2O_2 the general Cu^+ catalysed decay ensued. The initial fast decay was followed by a prompt cessation of the reaction. This is due to the known complexation of copper by glutathione disulfide, GSSG,⁵ which occurs when the initial GSNO concentration is greater than Cu^{2+} concentration.⁶ With added H_2O_2 an alternative route for GSNO decomposition became available and was unaffected by formation of the disulfide, if any.

2.3 Hydrogen peroxide and *S*-nitrosocysteine

The Cu^+ catalysed decomposition of *S*-nitrosocysteine, SNCys, is much faster than GSNO, due to the GSSG complexation of copper.⁷ The addition of H_2O_2 to SNCys had no visible effect on the Cu^+ catalysed decomposition, with complete decomposition occurring within seconds (results not shown). Unlike GSSG, cysteine disulfide does not complex copper ions therefore the reaction proceeds to completion. The SNCys reaction with H_2O_2 was therefore slower than the Cu^+ pathway. By adding a metal ion chelator any reaction observed would be solely due to the H_2O_2 mediated decomposition.

2.3.1 Addition of a metal ion chelator

The reactions of SNCys with varying concentrations of H_2O_2 were repeated, this time in the presence of the metal ion chelator, EDTA (ethylenediaminetetraacetic acid). As in Figure 2.1 decomposition occurred in a H_2O_2 concentration dependent manner, see Figure 2.2.

With no added H_2O_2 and in the presence of EDTA only the thermal/photochemical reaction was visible. At high concentrations of H_2O_2 good first order decay was observed.

The presence of EDTA in the H_2O_2 /GSNO reaction had little effect, thus confirming the excellent copper chelation ability of GSSG.

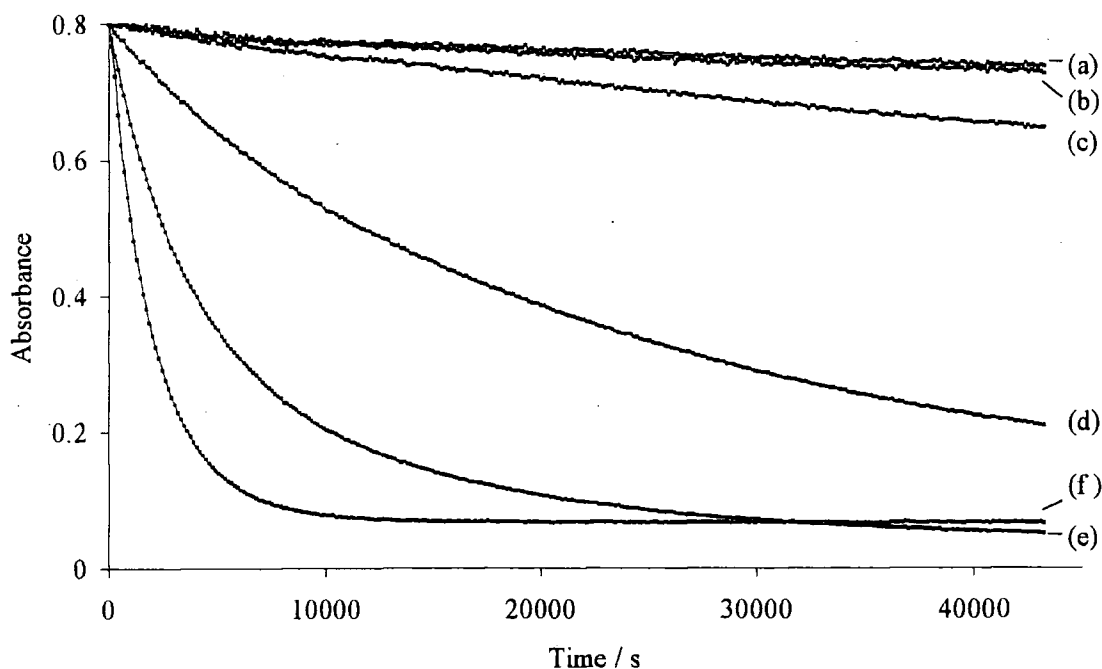


Figure 2.2 Addition of varying $[H_2O_2]$ to 1 mM SNCys with 0.1 mM EDTA at pH 7.4. (a) 0 M H_2O_2 (b) 0.1 mM H_2O_2 (c) 1 mM H_2O_2 (d) 10 mM H_2O_2 (e) 0.1 M H_2O_2 (f) 1 M H_2O_2

2.4 Evidence of H_2O_2 reaction with thiolate anion

The reaction of GSNO with copper, Figure 2.1 (a), reveals the initially rapid copper mediated decay followed by the slow photochemical/thermal reaction, the Cu^+ process being halted as a result of copper chelation by GSSG. Upon closer inspection of the 1 mM H_2O_2 reaction, Figure 2.1 (b), expanded in Figure 2.3, there is an initial copper catalysed decay which is also followed by the slow photochemical/thermal reaction. The copper reaction was curtailed sooner when H_2O_2 was present.

This suggests that the thiolate anion or thiol is quickly oxidised to disulfide preventing further Cu^+ formation. The reaction of RSNOs with Cu^+ was unaffected by H_2O_2 because no inhibition of SNCys copper mediated decay was observed, Section 2.3.

The subsequent reaction profiles are indistinguishable indicating photochemical/thermal reaction only. With higher concentrations of H_2O_2 , Figure 2.1, the initial copper reaction is immediately inhibited due to the large excess of H_2O_2 over the thiolate anion.

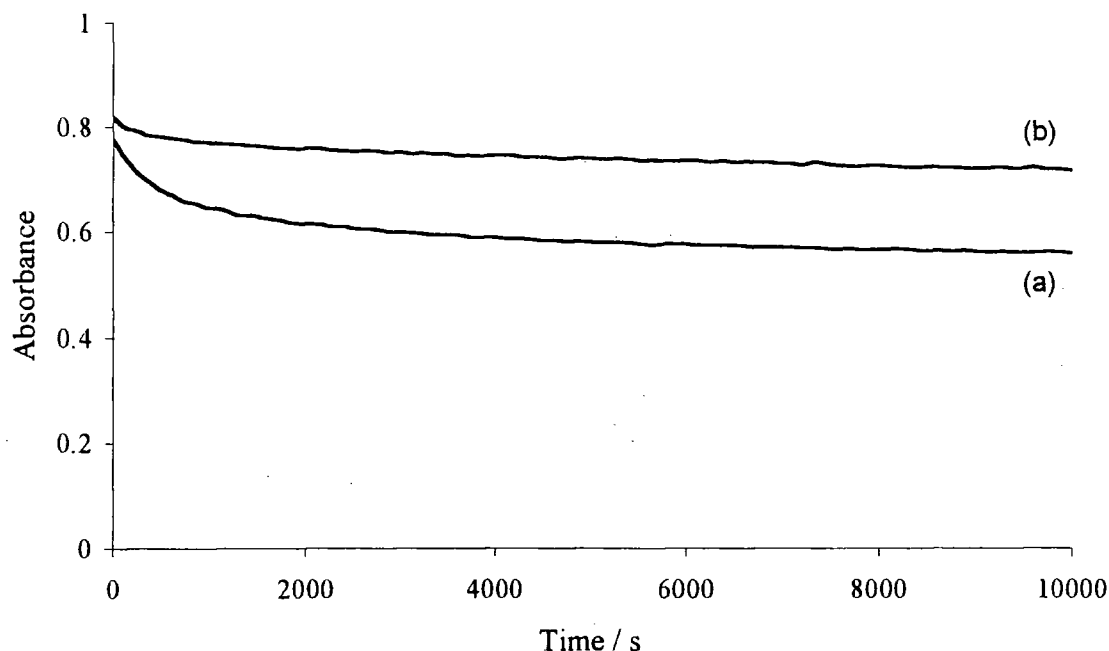


Figure 2.3 Comparison of a) 0 M H_2O_2 (b) 1 mM H_2O_2 with 1 mM GSNO and 10 μM Cu^{2+} at pH 7.4

2.4.1 Cu^+ , thiolate and peroxide reactions

The reduction of Cu^{2+} by the thiolate anion is a well-known reaction⁸ and subsequent oxidation of Cu^+ by H_2O_2 has been studied by Gilbert *et al.*⁹ The initial reaction in Scheme 2.1 is much faster than the re-oxidation of Cu^+ by H_2O_2 . Second order rate constants for the re-oxidation step have been determined as $k(\text{H}_2\text{O}_2) = 9.38 \text{ mol}^{-1} \text{ dm}^3 \text{ s}^{-1}$ at 25°C.

With SNCys, the possible reactions of H_2O_2 with Cu^+ and thiolate anion are too slow and the Cu^+ mediated decay occurs. For GSNO the formation of the disulfide halts the copper reaction, Figure 2.3(a). This occurs sooner in the presence of H_2O_2 , Figure

2.3(b), presumably due to oxidation of the thiolate anion from both the adventitious thiol and from RSNO decay.

2.5 Kinetics of the reaction between H_2O_2 and RSNOs

All reactions were carried out in pH 7.4 phosphate buffer (0.15 M) at 298 K following the decrease in absorbance at 340 nm over time. Experiments were carried out with $[\text{H}_2\text{O}_2]_0 \gg [\text{RSNO}]_0$ and good first order behaviour was observed in each run for a variety of RSNOs, for example Figure 2.4.

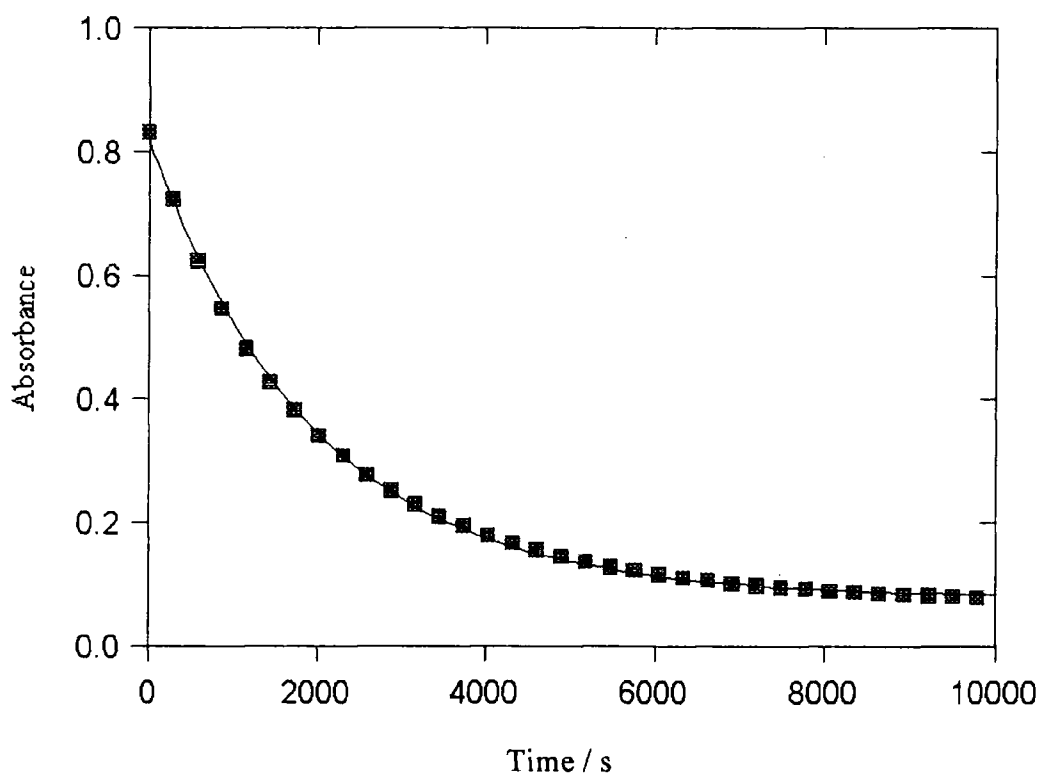


Figure 2.4 Reaction of 1 M H_2O_2 and 1 mM SNCys with 0.1 mM EDTA at pH 7.4, squares. Curve fitted using Scientist^{® 10}

The reaction was studied over a range of H_2O_2 concentrations and reproducible ($\pm 3\%$) observed rate constants, k_{obs} , were obtained using the computer package Scientist[®]. Plots of mean k_{obs} (mean determined from at least three repetitions) against H_2O_2 concentration were linear, hence there is a first order dependence on H_2O_2

concentration. The second order rate constants, k_2 , were determined from the slope of the fitted lines. An intercept was observed due to RSNO decomposition by an alternative route with a rate constant k' .

Therefore,

$$\frac{-d[\text{RSNO}]}{dt} = k_2[\text{RSNO}][\text{H}_2\text{O}_2] + k'[\text{RSNO}] \quad \text{Equation 2.3}$$

When $[\text{H}_2\text{O}_2] \gg [\text{RSNO}]$, H_2O_2 concentration is effectively constant, thus,

$$\frac{-d[\text{RSNO}]}{dt} = k_{\text{obs}}[\text{RSNO}]$$

Where,

$$k_{\text{obs}} = k_2[\text{H}_2\text{O}_2] + k' \quad \text{Equation 2.4}$$

2.5.1 Determining k_2 for the H_2O_2 mediated decomposition of GSNO

As in Figure 2.4, good first order behaviour was observed for a range of H_2O_2 concentrations, Table 2.1, enabling k_2 to be determined, Figure 2.5.

$[\text{H}_2\text{O}_2] / \text{M}$	$k_{\text{obs}} / 10^{-5} \text{ s}^{-1}$
0.20	6.70 ± 0.17
0.40	7.78 ± 0.19
0.60	8.65 ± 0.26
0.80	9.44 ± 0.29
1.00	10.1 ± 0.30

Table 2.1 Rate constants determined from the reaction of H_2O_2 with 1 mM GSNO in the presence of 0.1 mM EDTA at pH 7.4

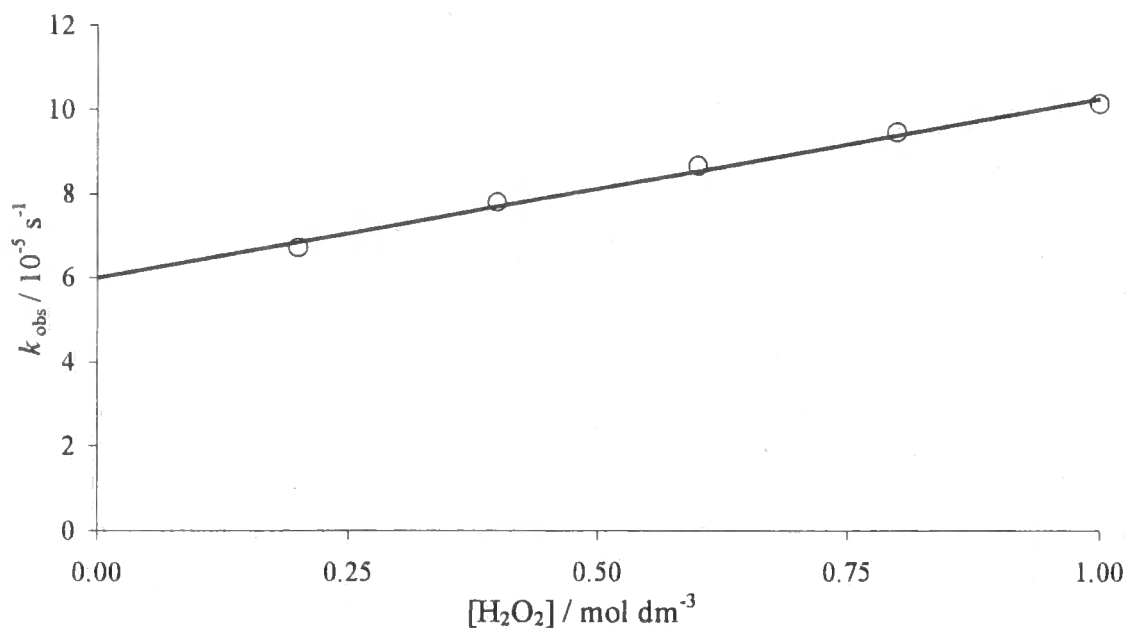


Figure 2.5 Plot of data in Table 2.1

k_2 and k' were then determined from equation 2.4

$$k_2 = (4.23 \pm 0.23) \times 10^{-5} \text{ dm}^3 \text{ mol}^{-1} \text{ s}^{-1}$$

$$k' = (6.00 \pm 0.60) \times 10^{-5} \text{ s}^{-1}$$

2.5.2 Determining k_2 for the H_2O_2 mediated decomposition of SNCys

$[\text{H}_2\text{O}_2] / \text{M}$	$k_{\text{obs}} / 10^{-4} \text{ s}^{-1}$
0.20	1.35 ± 0.03
0.40	1.76 ± 0.02
0.60	2.13 ± 0.02
0.80	2.46 ± 0.01
1.00	2.75 ± 0.01

$$k_2 = (1.75 \pm 0.07) \times 10^{-4} \text{ dm}^3 \text{ mol}^{-1} \text{ s}^{-1}$$

$$k' = (1.04 \pm 0.05) \times 10^{-4} \text{ s}^{-1}$$

Table 2.2 Rate data for the reaction of H_2O_2 with SNCys (1 mM) in the presence of 0.1 mM EDTA at pH 7.4

2.5.3 Determining k_2 for the H_2O_2 mediated decomposition of *S*-Nitrosopenicillamine (SNP)

$[\text{H}_2\text{O}_2] / \text{M}$	$k_{\text{obs}} / 10^{-3} \text{s}^{-1}$
0.20	0.69 ± 0.01
0.40	0.96 ± 0.01
0.60	1.22 ± 0.02
0.80	1.45 ± 0.04
1.00	1.60 ± 0.04

Table 2.3 Rate data for the reaction of H_2O_2 with SNP (1 mM) in the presence of 0.1 mM EDTA at pH 7.4

$$k_2 = (1.15 \pm 0.07) \times 10^{-3} \text{ dm}^3 \text{ mol}^{-1} \text{ s}^{-1}$$

$$k' = (4.92 \pm 0.45) \times 10^{-4} \text{ s}^{-1}$$

2.5.4 Results summary

Equation 2.4 holds for the range of RSNOs tested. The result are summarised in Table 2.4.

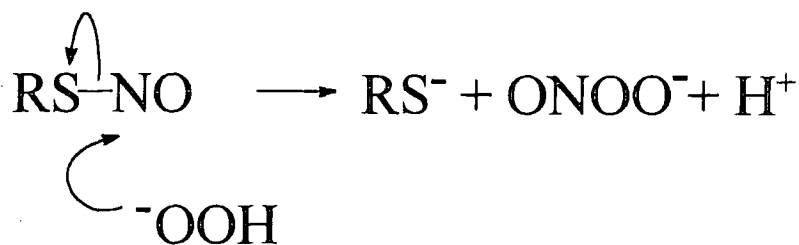
	$k_2 / 10^{-5} \text{ dm}^3 \text{ mol}^{-1} \text{ s}^{-1}$	$k' / 10^{-4} \text{ s}^{-1}$
GSNO	4.23 ± 0.2	0.60 ± 0.1
SNCys	17.5 ± 0.7	1.04 ± 0.1
SNP	115 ± 6	4.92 ± 0.5

Table 2.4 Second order rate constants for the H_2O_2 induced decomposition of RSNOs

The intercept, k' , also increases with more reactive RSNOs and is attributed to the thermal or photochemical reaction. The copper reaction is far too fast to be influenced by the thermal or photochemical decomposition pathway, but on the timescales of the reaction with H_2O_2 these alternative reactions become significant. SNP is known to be highly susceptible to thermal and photochemical decomposition, at pH 7.4,¹¹ and has the highest intercept in the experimental values, Table 2.4.

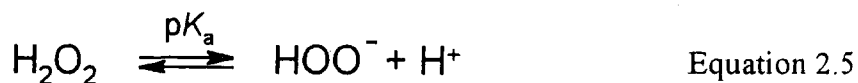
2.6 Proposed reaction scheme

k_2 values are substrate dependent, with an order of reactivity identical to RSNO reactions with other nucleophiles.^{12,13,14} This evidence supports nucleophilic attack of H_2O_2 or its anion, at the nitroso nitrogen atom, Scheme 2.2.



Scheme 2.2 Proposed mechanism of reaction

The reaction rate would therefore be dependent on the concentration of the anion, which is governed by the pH of the solution and the acid dissociation constant K_a . The $\text{p}K_a$ for H_2O_2 is 11.6.¹⁵



If this were the case, rate-limiting nucleophilic attack would require the peroxyxynitrite anion and the rate be pH dependent.

2.7 Product study of the reaction between RSNOs and hydrogen peroxide

RSNOs have been shown² to release NO from the reaction with Cu^+ and they can also act as direct electrophilic nitrosating species with a variety of nucleophiles.

The nucleophilic attack of H_2O_2 on RSNOs is predicted to produce peroxynitrite. If so, this reaction might have biological significance. It is therefore important to study the reaction further and determine the products.

2.7.1 Detection of peroxynitrite

Peroxynitrite has a distinct λ_{max} at 301 nm with an extinction co-efficient of $1\,700\text{ dm}^3\text{ mol}^{-1}\text{ cm}^{-1}$.¹⁶ If peroxynitrite is formed from the reaction of H_2O_2 and RSNOs then it may be conveniently detected through UV/Vis spectrophotometry. All repeat scan spectra in this chapter were recorded over a wavelength range of 250-450 nm, with varying time intervals. Reactions were carried out with $[\text{H}_2\text{O}_2]_0 \gg [\text{RSNO}]_0$ in the presence of 0.1 mM EDTA.

2.7.2 Reaction at physiological pH

The reaction of SNCys with H_2O_2 and EDTA in potassium dihydrogen phosphate buffer (pH 7.4, 0.15 M) was followed by repeat-scan spectroscopy at 20 minute intervals. There was no visible evidence of peroxynitrite formation. Only the decreasing RSNO absorbance at 340 nm was observed, due to the H_2O_2 promoted decomposition of SNCys, Figure 2.6.

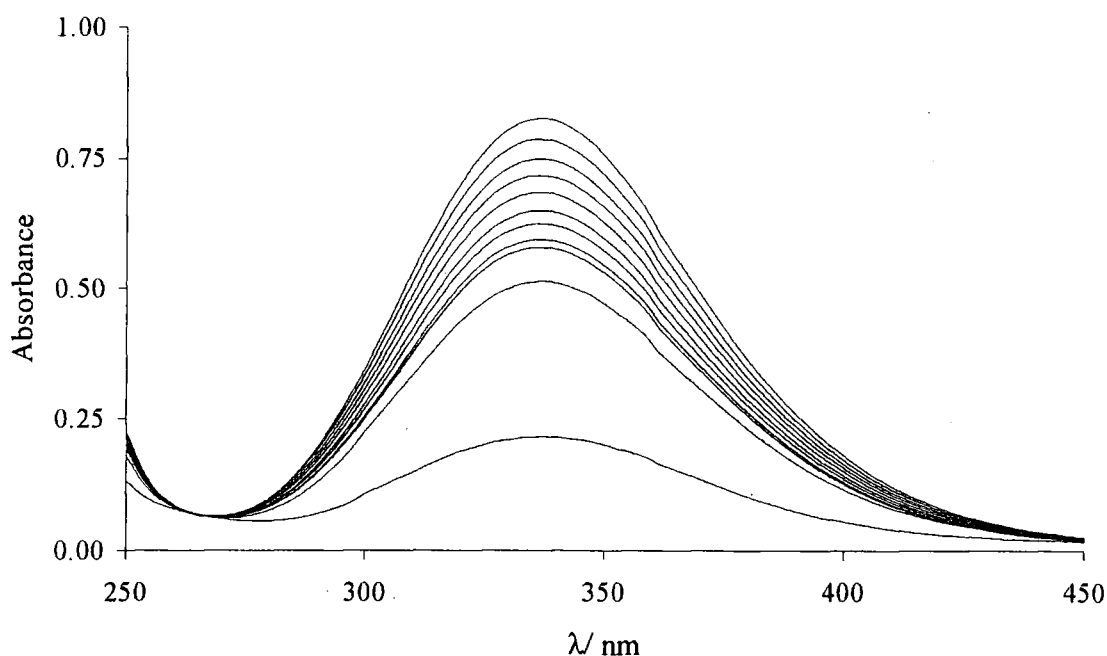


Figure 2.6 SNCys (1 mM) and H₂O₂ (10 mM) with EDTA (0.1 mM) at pH 7.4. Repeat scans every 20 min showing the decomposition at 340 nm. The last two scans are taken after 4 and 24 hours

As discussed in the introductory chapters, peroxynitrite is extremely unstable at acidic and physiological pH, with a half-life for decomposition of approximately one second. The reaction between H₂O₂ and RSNOs is slow at pH 7.4 therefore peroxynitrite is unobserved under these conditions and time scale.

2.7.3 Reaction at pH 9.9

The reaction was repeated at higher pH in borax buffer (pH 9.9, 0.025 M) as the peroxynitrite anion is stabilised by alkaline conditions. There was still no visible evidence of peroxynitrite formation (spectra not shown). However the decreasing absorbance at 340 nm due to the H₂O₂ promoted decay of SNCys was markedly quicker than at physiological pH.

2.7.4 Reaction at pH 11.6

The decomposition of SNCys due to H_2O_2 was much quicker at pH 11.6 (disodium hydrogen phosphate buffer, 0.05 M) and required repeat-scan time intervals of one minute. As before, decomposition of SNCys occurred at 340 nm, but at this pH the simultaneous formation of peroxynitrite was detected by the increase of its characteristic absorbance at 301 nm, see Figure 2.7.

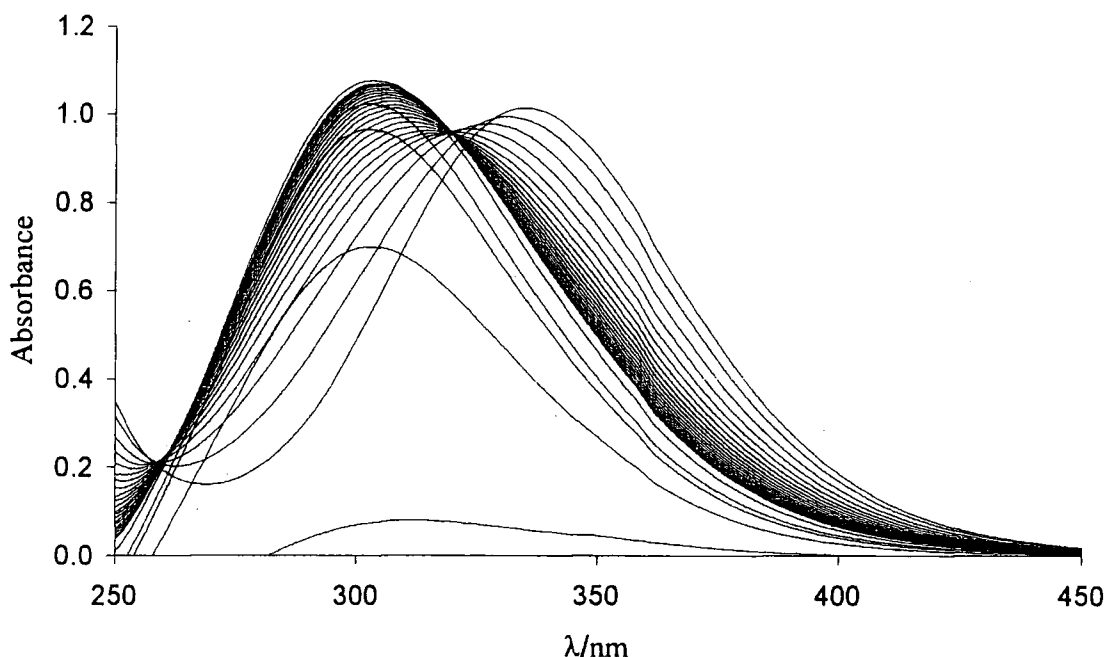


Figure 2.7 SNCys (1 mM) and H_2O_2 (10 mM) with EDTA (0.1 mM) at pH 11.6. 20 repeat scans at 1 minute intervals followed by 3 x 30 minute intervals with the last two scans after 3½ and 18 hours

2.7.5 Reaction at pH 13.1

At higher pH (potassium chloride buffer, 0.2 M) the reaction yielded a final peroxynitrite absorbance that was relatively constant on the time scale studied, Figure 2.8.

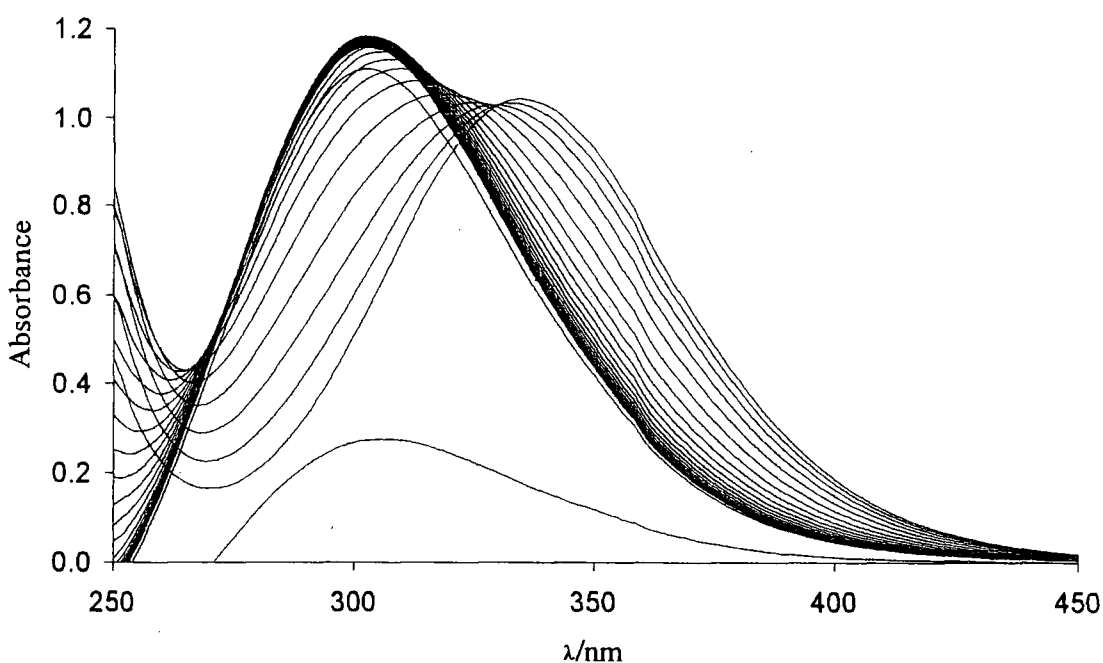


Figure 2.8 SNCys (1 mM) and H_2O_2 (10 mM) with EDTA (0.1 mM) at pH 13.1. 35 repeat scans at 1 minute intervals with the last two scans after 1½ and 18 hours.

The rate of H_2O_2 promoted decomposition of SNCys increases with pH, which is consistent with the proposed reaction scheme. The scheme predicts the formation of peroxyxynitrite, which has also been confirmed. However the reaction is not quantitative and even at high pH, where peroxyxynitrite is relatively stable, the yield does not exceed 80% (determined using the extinction coefficient of $1\,700\text{ dm}^3\text{ mol}^{-1}\text{ cm}^{-1}$ at 301 nm).. Possible reasons for this will be discussed later, Section 2.9.2.

2.8 pH dependence

The production of peroxynitrite at higher pH confirms that the reaction occurs via nucleophilic attack of the hydroperoxide anion. In order to observe the formation of peroxynitrite it was necessary to increase the reaction pH. The rate of decay of SNCys increased with pH, which suggests that reaction occurs through the hydroperoxide anion and not H₂O₂.

To establish this more quantitatively, rate constants were determined over the pH range 9.8-13.5 by monitoring the disappearance of the lower intensity RSNO absorbance at 545 nm ($\epsilon_{545 \text{ nm}} \approx 20 \text{ dm}^3 \text{ mol}^{-1} \text{ cm}^{-1}$).¹² This wavelength was used to avoid complications arising from peroxynitrite formation overlapping with the RSNO decay in the 300-340 nm spectral region.

Due to the small extinction coefficient, higher concentrations of SNCys (5 mM) and H₂O₂ (0.1 M) were used, hence with $[\text{H}_2\text{O}_2]_0 \gg [\text{SNCys}]_0$. Good first order behaviour was observed. Replicates could not be accurately achieved due to slightly variations in final pH of each run, as determined by a pH meter, therefore a large number of data points were generated; see Table 2.5 for a selection of them.

pH	$k_{\text{obs}} / 10^{-3} \text{ s}^{-1}$
9.8	1.68 ± 0.05
10.8	2.55 ± 0.02
11.2	3.61 ± 0.05
11.4	5.61 ± 0.07
11.5	5.81 ± 0.09
11.7	7.11 ± 0.03
11.9	8.60 ± 0.11
12.0	9.49 ± 0.09
12.2	11.7 ± 0.1
12.5	14.5 ± 0.2
12.9	15.9 ± 0.5
13.5	17.5 ± 0.8

Table 2.5 Selection of first order rate constants for the reaction of SNCys (5 mM) and H₂O₂ (0.1 M) at various pH values.

As predicted, the rate of H_2O_2 mediated decomposition of SNCys increased with pH.

2.8.1 Reaction *via* the hydroperoxide anion

A plot of k_{obs} versus pH, incorporating the results in Table 2.5, gave a sigmoidal curve, Figure 2.9.

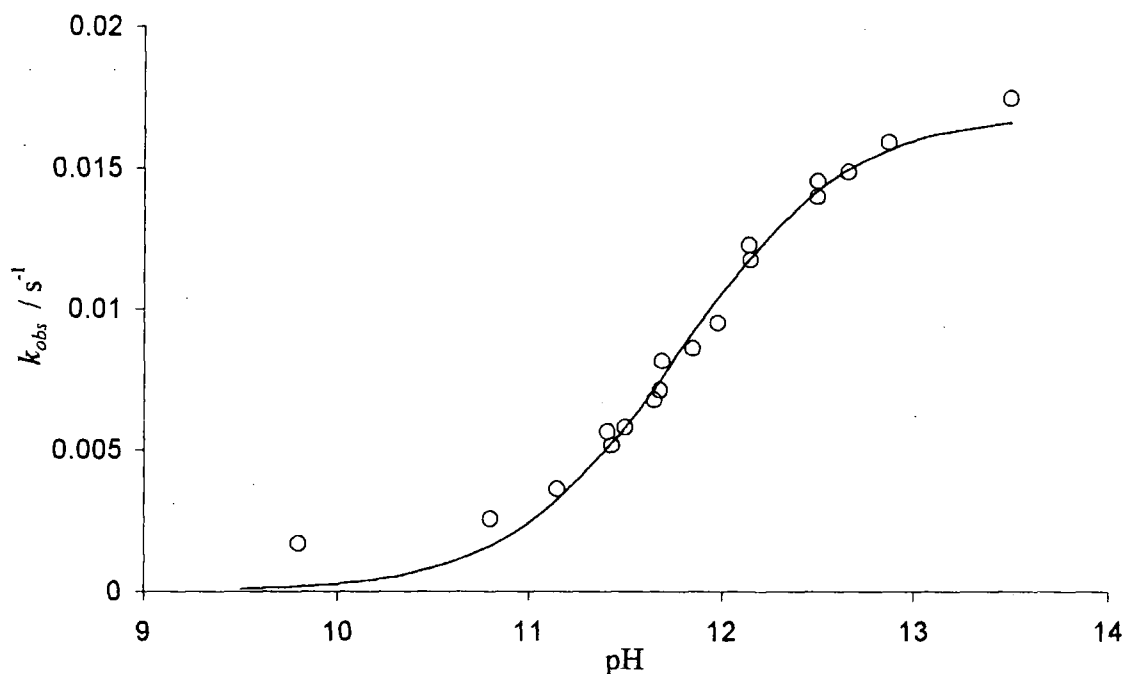


Figure 2.9 Plot of k_{obs} versus pH for the reaction of SNCys (5 mM) and H_2O_2 (0.1 M)

A point of inflexion is observed around the locality of the $\text{p}K_{\text{a}}$ value of H_2O_2 ,¹⁵ 11.6, which is consistent with attack through the hydroperoxide anion.

If the reactive species is the basic form of hydrogen peroxide (hydroperoxide anion), then expression for k_{obs} is given by equation 2.6, derived in Section 6.4.2

$$k_{\text{obs}} = \frac{k_{\text{D}} K_{\text{a}} [\text{H}_2\text{O}_2]_{\text{t}}}{K_{\text{a}} + [\text{H}^+]} \quad \text{Equation 2.6}$$

k_D is the second order rate constant for the reaction between SNCys and the dissociated form of H_2O_2 , the hydroperoxide anion, $[H^+]$ is the acid concentration, and $[H_2O_2]_t$ is the total stoichiometric concentration of H_2O_2 . K_a is the acid dissociation constant of H_2O_2 , equation 2.5.

Equation 2.6 takes into account the proportion of H_2O_2 in the anionic form at a given pH.

2.8.2 Determination of k_D and pK_a by Scientist[®]

The curve fitted to the data in Figure 2.9 is derived from the curve fitting function of Scientist[®]. This fits the data to equation 2.6 and calculates the values of k_D and the K_a of H_2O_2 to be $0.169 \pm 5 \times 10^{-3} \text{ dm}^3 \text{ mol}^{-1} \text{ s}^{-1}$ and $2.04 \times 10^{-12} \pm 1 \times 10^{-13}$ respectively.

2.8.3 Determination of k_D and pK_a by the reciprocal plot

The reciprocal form of equation 2.6 gives equation 2.7:

$$\frac{1}{k_{\text{obs}}} = \frac{1}{k_D[H_2O_2]_t} + \frac{[H^+]}{k_D K_a [H_2O_2]_t} \quad \text{Equation 2.7}$$

Therefore by plotting $1/k_{\text{obs}}$ versus $[H^+]$ (Figure 2.10), the gradient, m , and intercept, c , are given by:

$$m = \frac{1}{k_D K_a [H_2O_2]_t} \quad c = \frac{1}{k_D [H_2O_2]_t}$$

$$\therefore \frac{c}{m} = K_a$$

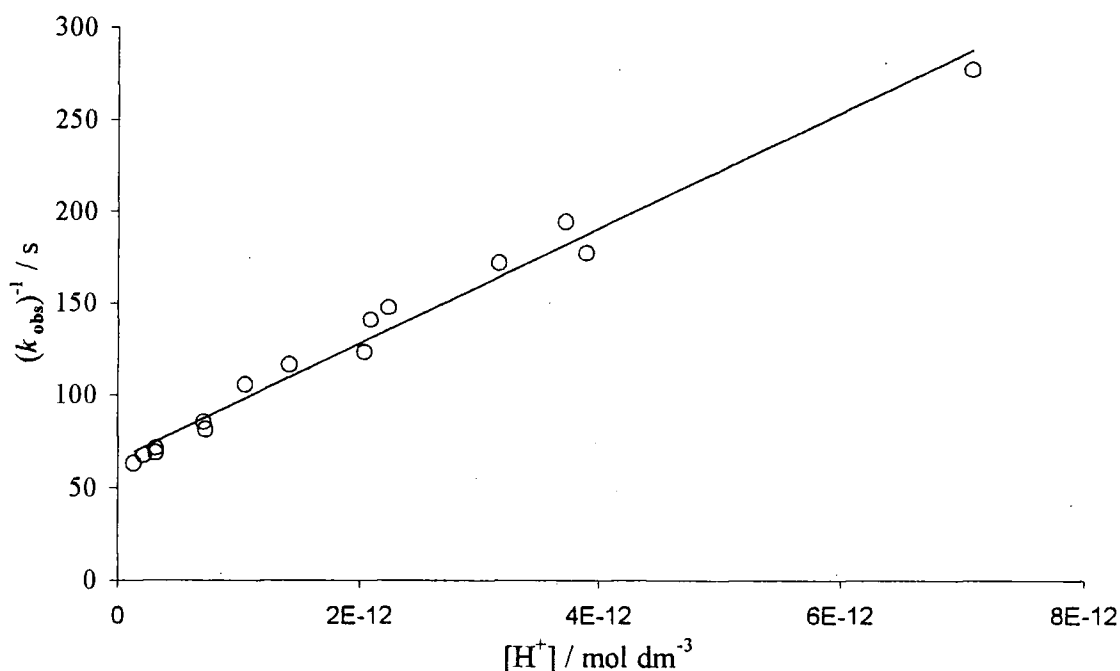


Figure 2.10 Plot of $1/k_{\text{obs}}$ versus $[\text{H}^+]$ for the reaction of SNCys (5 mM) and H_2O_2 (0.1 M)

From Figure 2.10 :

$$m = 2.98 \times 10^{13} \pm 9 \times 10^{11} \text{ mol dm}^{-3} \text{ s}$$

$$c = 68 \pm 2 \text{ s}$$

$$\therefore K_a = 2.28 \times 10^{-12} \pm 1 \times 10^{-13} \text{ mol dm}^{-3}$$

$$\text{p}K_a = 11.64 \pm 0.02$$

From the intercept, k_D is calculated as $0.147 \pm 5 \times 10^{-3} \text{ dm}^3 \text{ mol}^{-1} \text{ s}^{-1}$.

The data obtained confirm that the reactive species is the hydroperoxide anion. The calculated values of $\text{p}K_a$ for H_2O_2 (summarised in Table 2.6) are in excellent agreement with each other and with the literature value of 11.6.¹⁵

Method	$k_D / \text{dm}^3 \text{mol}^{-1} \text{s}^{-1}$	$\text{p}K_a$
Scientist [®]	$0.169 \pm 5 \times 10^{-3}$	11.69 ± 0.03
Graphical	$0.147 \pm 5 \times 10^{-3}$	11.64 ± 0.02

Table 2.6 Summary of values obtained using both methods of analysis

2.8.4 k_2 value at physiological pH

Equation 2.6 has been confirmed. The reaction occurs *via* the hydroperoxide anion and the value of k_2 obtained previously at pH 7.4 may now be corrected to account for this.

The gradient of the line plotted from Table 2.2 is now equal to equation 2.8.

$$m = \frac{k_D K_a}{K_a + [\text{H}^+]} \quad \text{Equation 2.8}$$

Therefore the k_2 value calculated at physiological pH is becomes a k_D value of $3.06 \text{ dm}^3 \text{mol}^{-1} \text{s}^{-1}$.

This value is a factor of 20 greater than that calculated by the pH dependence method (Table 2.6). It is indicative of some other factor affecting the decomposition of RSNO at lower pH and is consistent with the anomalies observed below pH 11 in Figure 2.9.

2.8.5 Factors responsible for RSNO decomposition at pH 7.4 - 11

Equation 2.6 does not hold in the pH range 7.4 – 11. However, there are a number of plausible reasons for this.

H_2O_2 may react through the neutral form. Equation 2.6 was modified to account for this, yielding equation 2.9, where k_N is the rate constant for the reaction of the neutral H_2O_2 with SNCys and k_D is the rate constant for the reaction of the dissociated form of H_2O_2 with SNCys.

$$k_{\text{obs}} = \frac{k_D K_a [\text{H}_2\text{O}_2]_t}{K_a + [\text{H}^+]} + \frac{k_N [\text{H}_2\text{O}_2]_t [\text{H}^+]}{K_a + [\text{H}^+]} \quad \text{Equation 2.9}$$

Scientist[®] was used to fit equation 2.9 to the data in Figure 2.9 and generated the fitted line shown in Figure 2.11.

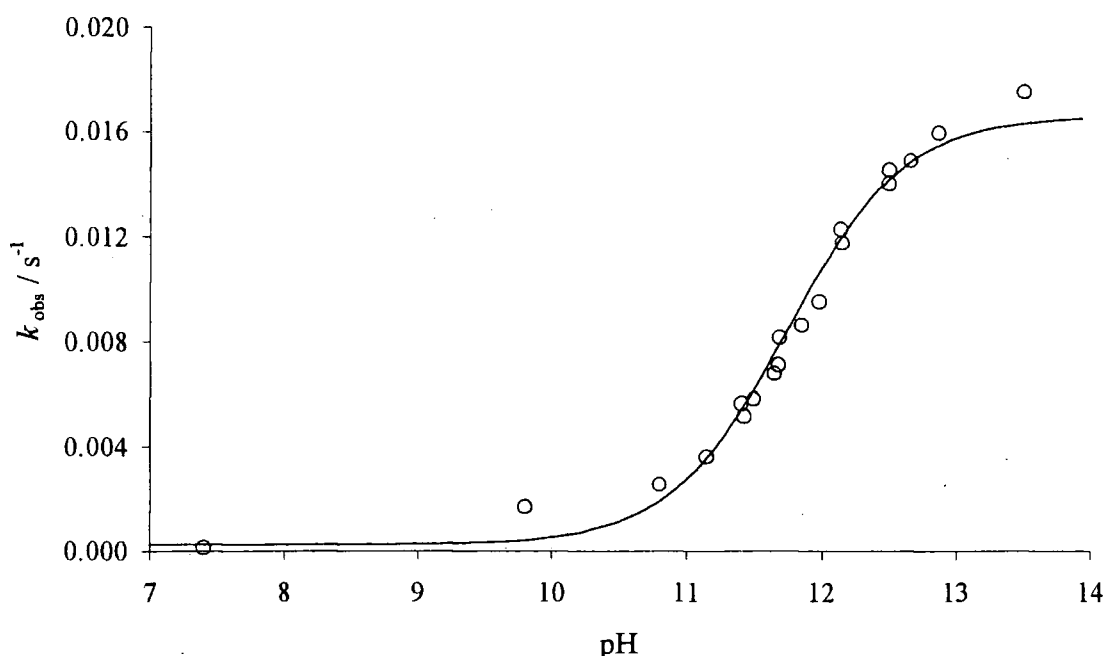


Figure 2.11 Plot with the addition of the k_{obs} value obtained at pH 7.4 to the data in Figure 2.9, with a fit line generated using Scientist[®] allowing for reaction of H_2O_2 through the neutral form

Equation 2.9 gives a good fit and yields $\text{p}K_a$ and k_D values within error of those determined previously. This is to be expected as reaction through the neutral form at $\text{pH} > 11$ becomes increasingly negligible.

Equation 2.9 simplifies to equation 2.4 at pH 7.4, therefore k_N becomes equal to k_2 , $1.75 \times 10^{-4} \text{ dm}^3 \text{ mol}^{-1} \text{ s}^{-1}$. This is not the case and suggests that k_N is inaccurate, probably due to the value being strongly affected by the data at pH ≈ 9.8 and 10.8.

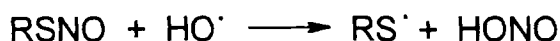
Overall the values for the pK_a of H_2O_2 and the rate constant k_D , for the reaction of RSNO and the hydroperoxide anion, are consistent throughout. It also seems wise to trust the value of k_N , determined as k_2 , using the varied $[\text{H}_2\text{O}_2]$ method at pH 7.4 i.e $1.75 \times 10^{-4} \text{ dm}^3 \text{ mol}^{-1} \text{ s}^{-1}$.

2.8.6 Anomalies at pH ≈ 9.8 and 10.8

The unexpected increase in reactivity between pH 9.5 and pH 11 may be a result of free radical formation and subsequent attack on the RSNO. RSNOs are known to react very rapidly with radicals.^{17, 18} It is feasible that during longer time scale reactions, such as those at pH < 11 , substantial free radical formation may occur. The nature of free radical propagation means that a small initial concentration may result in a large effect on the reaction.

The classical free radical generator is the Fenton reaction, which consists of catalytic amounts of iron (II) and an excess of H_2O_2 . Iron (II) EDTA complexes are catalysts for the decomposition of H_2O_2 and generate radicals like the Fenton reaction.^{19, 20} It has been determined that the rate of decomposition and the concomitant release of hydroxyl radicals is maximal at pH 9.5, over a pH range of 6.5 – 12.

The iron (II) present in this work from the water/buffer source will be low, but the probability of some free radical generation is high especially over longer time scales. Hence, it can be envisaged that at the peak of the free radical generation, around pH 9.5, Scheme 2.3 could occur thus resulting in higher than expected rates of decomposition of RSNOs.



Scheme 2.3 Selection of possible free radical decomposition pathways for RSNOs

2.9 Investigations concerning the nitrogen product, peroxynitrite

2.9.1 Peroxynitrite decomposition

The stability of the peroxynitrite species formed was dependent on the pH of the reaction solution. At sufficiently basic conditions it was possible to measure the rate of decay of peroxynitrite spectrophotometrically at 301 nm. The relatively fast formation is also observed but is overlapped with the decay of the RSNO, which also absorbs in this region, see Figure 2.12.

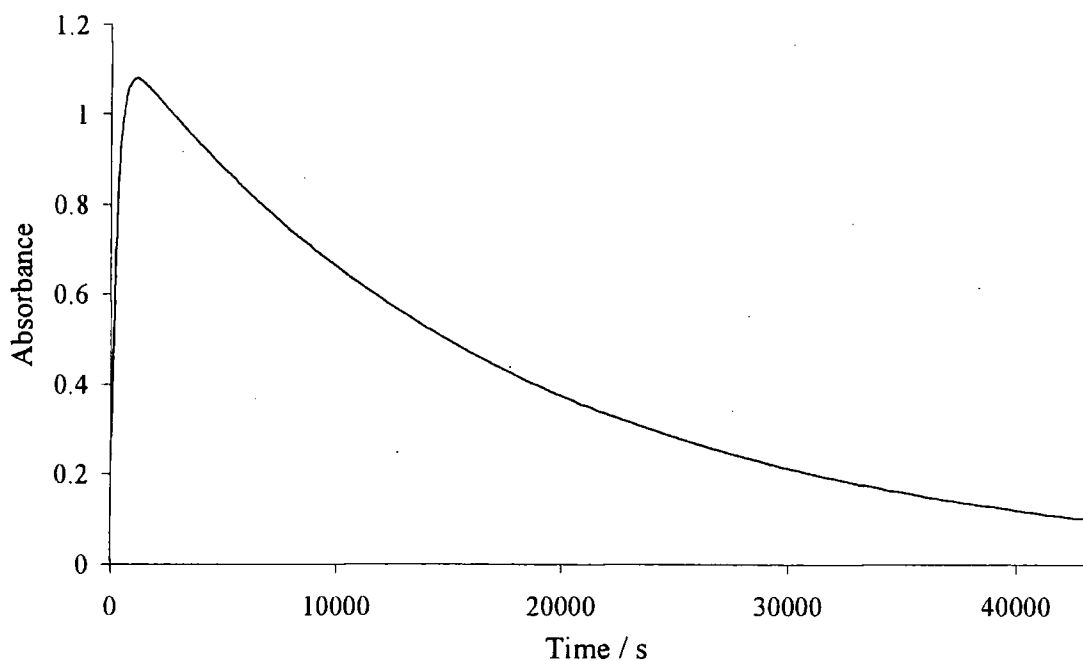


Figure 2.12 Formation and decay of peroxynitrite at 301 nm from the reaction of SNCys (1 mM) and H_2O_2 (0.1 M) at pH 11.1

The reaction in Figure 2.12 was repeated at varying pH and rate measurements were made once all the SNCys had decayed, i.e. when the absorbance due to peroxynitrite had peaked and begun to decay. Good first order behaviour was observed showing increasing stability with increasing pH, Table 2.7.

pH	$k_{\text{obs}} / 10^{-5} \text{ s}^{-1}$
10.39	27.2 ± 0.5
11.14	5.88 ± 0.19
11.46	4.46 ± 0.05
12.14	3.08 ± 0.07
12.78	2.20 ± 0.03
12.96	2.32 ± 0.05

Table 2.7 First order rate constants for the decomposition of peroxynitrite with increasing pH

Logager and Sehested²¹ derived the rate equation for the spontaneous decomposition of peroxynitrite as a function of pH. K_a is the acid dissociation constant of peroxynitrite (determined in reference 21 as $(1.0 \pm 0.3) \times 10^{-7}$) and k_{18} is first order rate of isomerisation of peroxynitrous acid to nitrate.

$$k_{\text{obs}} = \frac{k_{18}[\text{H}^+]}{[\text{H}^+] + K_a}$$

Equation 2.10 Rate equation for the decay of peroxynitrous acid as a function of pH.

The data in Table 2.7 are plotted (as circles) in Figure 2.13. They show good agreement with equation 2.10 (depicted by a solid line) until \approx pH 11.5.

Above pH 11.5 the experimental points deviate in a way consistent with the incursion of an alternative mechanism. The equation only accounts for peroxynitrite decomposition *via* internal rearrangement to nitrate. Logager and Sehested²² noted similar results above pH 11 along with a number of other authors. These earlier results are summarised in reference 22.

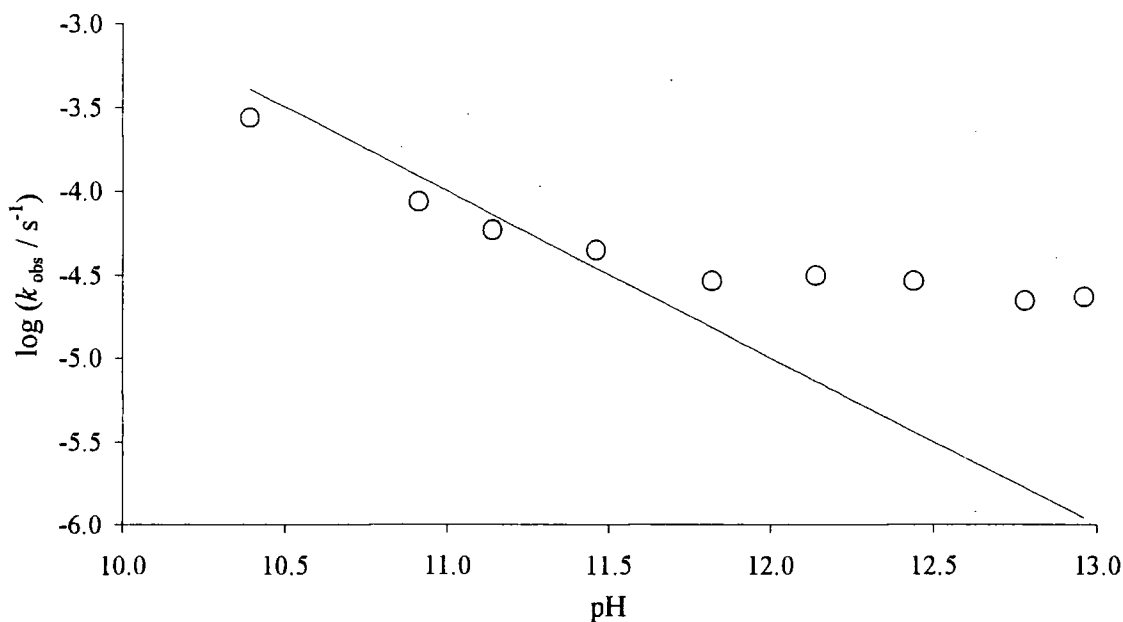
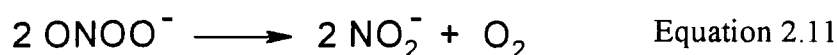


Figure 2.13 Logarithms of the first order rate constants for the decomposition of peroxynitrite with increasing pH (circles). The solid line is the expected trend calculated using equation 2.10

The slower reaction is believed to be decomposition to nitrite and other products.²²



The spontaneous decomposition of peroxynitrite formed in the systems studied here, results in clean first order decay at rates comparable to the decay of pure peroxynitrite. This suggests that either all the other products of the H₂O₂ mediated decomposition of RSNOs are unreactive towards peroxynitrite, or they have reacted quickly and no longer affect its decay.

2.9.2 Peroxynitrite yield is not quantitative

The measured yields of peroxynitrite reach $\approx 80\%$ when H_2O_2 is in a large excess over RSNO and the pH of the reaction medium is >13 . At lower pH the non-quantitative nature is attributed to the facile decay of peroxynitrite. Quantitative yields should be generated at $\text{pH} > 13$ where peroxynitrite is extremely stable. This is in direct analogy to the yield of peroxynitrite from the reaction of alkyl nitrites (RONOs) and H_2O_2 , which nears 100% .²³

It is likely that the diminished peroxynitrite yield in the RSNO reaction is due to oxidation of the thiol by peroxynitrite. This does not occur with RONO as they yield the stable alcohol, which may only be oxidised further with very powerful oxidants and under specific conditions.

2.9.3 Peroxynitrite reaction with thiolate anions

Peroxynitrite has a particular affinity towards thiol groups. Rate constants for the reaction are known to be over 1000 times that of the corresponding rate constants for the reaction of thiols and H_2O_2 , at physiological pH.²⁴ Freeman *et al.* concluded that peroxynitrite reacts with the free thiol form, RSH, as opposed to the thiolate anion, RS^- , equation 2.12. However, data within reference 25 clearly show maximum oxidation yields at alkaline pH.



In this work, thiolate anions are formed after the reaction of SNCys with H_2O_2 , Scheme 2.2, and will be subsequently oxidised by H_2O_2 or catalysed by hydroxide ions. The reaction of peroxynitrite with thiols is dependent on the rate of thiolate oxidation by other oxidants, but may be insignificant due to lack of free thiol, RSH, at high pH.

To test this, peroxynitrite was formed by the usual method (1 mM SNCys + 10 mM H_2O_2) at pH 13 and left to decay for 10^4 seconds after which 10mM cysteine was added, Figure 2.14.

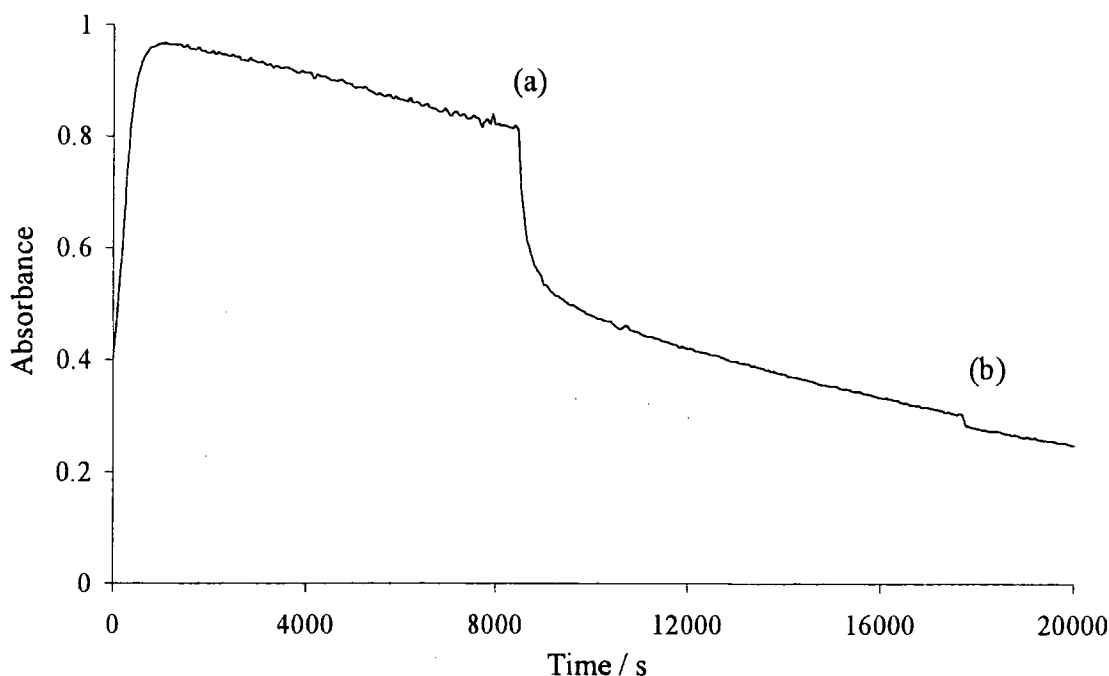


Figure 2.14 Peroxynitrite reaction with cysteine at pH 13 followed at 301nm.

(a) Addition of 10 mM cysteine in 0.1 ml water

(b) Dilution effect of 0.1ml water

The added cysteine had a dramatic effect on the decomposition of peroxynitrite indicating that even at high pH the loss of peroxynitrite by reaction with thiolate anion is a valid pathway and explanation for the non-quantitative nature of the reaction.

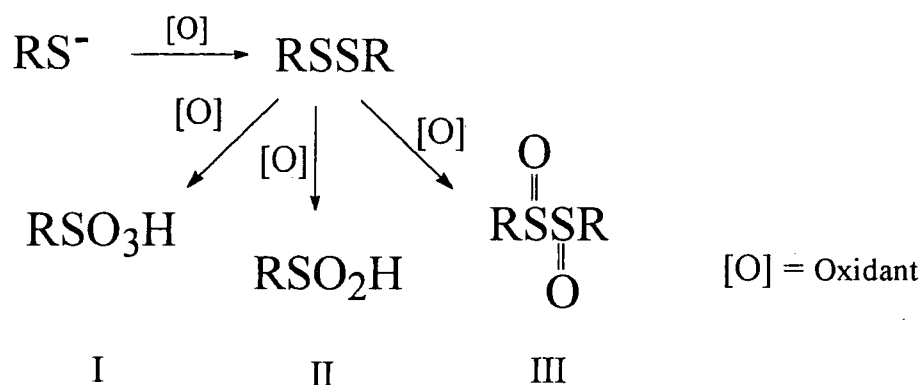
The added cysteine was in 10-fold excess, so complete decomposition of peroxynitrite should be expected. This does not occur due to simultaneous oxidation of cysteine by the excess H_2O_2 present from the initial formation of peroxynitrite. Although peroxynitrite is 1000 times more potent than H_2O_2 in the oxidation of free thiol, RSH , it is clearly evident that reaction of peroxynitrite with thiolate, RS^- , is slower.²⁴ This is revealed by the ability of H_2O_2 to compete with the peroxynitrite – thiolate reaction.

2.10 Fate of the sulfur product

The proposed mechanism for the reaction of RSNOs with H_2O_2 predicts the organic product to be the thiolate anion. However, due to reaction with the excess H_2O_2 , further oxidation occurs. Reaction of the thiol with peroxynitrite is well documented to yield the disulfide, however under alkaline conditions H_2O_2 can oxidise the disulfide further to a wide range of products.²⁶

2.10.1 Oxidation of disulfides

The oxidation of thiols and disulfides has been well studied and reference 26 provides an excellent review. With a very large excess of H_2O_2 and base, the principal product is the sulfonic acid, (I). It is extremely stable though under very harsh conditions may desulfurise to give an aldehyde and sulfate. With less than excess H_2O_2 , the sulfinic acid (II) and disulfide dioxide (III) are also produced, Scheme 2.4, along with other products. The amount and nature of the oxidant present determines the quantities of I, II and III.



Scheme 2.4 Possible final oxidation products of the H_2O_2 mediated decomposition of RSNOs

If the disulfide is not the primary product, then a mixture of I, II, III and others is expected.

2.10.2 Organic product from SNCys and H_2O_2

Negligible amounts of thiol were detected using Ellmans test, see chapter 6.3.2 for procedure.

The disulfide of cysteine, cystine, is particularly insoluble in water. Reactions on a larger scale, 1 M H₂O₂ and 0.1 M SNCys, were performed to detect the insoluble disulfide, which should precipitate from solution at neutral pH. After reaction at pH 13 the reaction solution was neutralised with 1 M HCl. Even after 24 hours no cystine was evident.

¹H NMR analysis proved inconclusive.

Therefore the final organic products are probably mixed higher oxidised species.

2.11 Conclusions

2.11.1 Biological considerations

The reaction of H₂O₂ and SNCys is a new preparative method for peroxynitrite and may have important biological implications. With doubts over the relevance of peroxynitrite *in vivo*,²⁵ an alternative route from two endogenous species provides a further angle to the discussion. The argument against peroxynitrite as a cytotoxic species revolves around its formation and action. Activated macrophages kill invading parasites, bacteria, etc. through phagocytosis. Peroxynitrite has been identified as the species responsible for the "killing" and has been detected in activated macrophages.²⁷

It is not understood how peroxynitrite created by macrophages does not cause oxidative damage to its source site and how it can travel to the site of action without being destroyed.

Excess NO or superoxide can react with peroxynitrite. This implies that NO and superoxide must be synthesised simultaneously.

Peroxynitrite does not react with SNCys or H_2O_2 and may, in fact, be stabilised by H_2O_2 .²⁸

When peroxynitrite is formed by activated macrophages they must have a self-defence mechanism to prevent “killing” themselves, as the point of formation will have the greatest concentration of peroxynitrite. The organic product of the reaction of SNCys and H_2O_2 is the thiol, which can be oxidised to the disulfide in the presence of an oxidising species. Peroxynitrite is known to have a particular affinity for thiols, therefore an elegant hypothesis would be self-preservation by the thiol by-product.

A puzzling piece of research by Nathan *et al.*²⁹ found that macrophage cytotoxicity was enhanced by SOD and attenuated by catalase, this can be explained by peroxynitrite formation from SNCys and H_2O_2 . SOD reacts with superoxide to yield H_2O_2 , therefore enhancement would be due to increased concentrations of H_2O_2 . Catalase scavenges H_2O_2 and so attenuation could be due to decreased concentrations of H_2O_2 .

Although the biological considerations are speculative, they may explain away some of reasons clouding the acceptance of peroxynitrite's role *in vivo*.

Even though experiments *in vitro* show that the reaction of RSNOs and H_2O_2 is probably too slow to have any physiological relevance, conditions *in vivo* may prove more favourable.

The reactions of peroxynitrite, H_2O_2 , NO and RSNOs are of great interest in relation to their modes of action *in vivo*. There is no doubt that peroxynitrite formation from two key-players in this cycle will add further argument to an already fierce debate.

2.11.2 Chemical considerations

The addition of H_2O_2 to RSNOs could in theory halt the copper catalysed decay mechanism. H_2O_2 could oxidise the thiolate anion to the disulfide and Cu^+ to Cu^{2+} , however, this is not the case. The results in this chapter show that the nucleophilic nature of the hydroperoxide anion allows RSNO decomposition by an alternative path.

The slow copper reaction with GSNO, in comparison to SNCys, and subsequent copper chelation by the disulfide, conveniently highlights the H_2O_2 mediated decay. However in the same reaction with SNCys, decomposition is complete within seconds where H_2O_2 oxidation of Cu^+ is out-competed by SNCys.

The reaction of H_2O_2 with the thiolate anion is evident for GSNO and indeed may occur in SNCys. However in the latter case the Cu^+ mediated decay is too fast requiring only a catalytic amount of Cu^+ .

The addition of a metal ion chelator removes the Cu^+ catalysed decomposition pathway revealing a copper independent decay due to H_2O_2 . The reaction occurs predominantly via nucleophilic attack of the hydroperoxide anion and yields peroxynitrite.

2.12 References

- 1 J. McAninly, D. L. H. Williams, S. C. Askew, A. R. Butler and C. Russell, *J. Chem. Soc., Chem. Commun.*, 1993, **23**, 1758.
- 2 A. P. Dicks, H. R. Swift, D. L. H. Williams, A. R. Butler, H. H. Al -Sa'doni and B. G. Cox, *J. Chem. Soc., Perkin Trans. 2*, 1996, 481.
- 3 A. J. Holmes and D. L. H. Williams, *J. Chem. Soc., Chem. Commun.*, 1998, 1711.
- 4 A. P. Dicks, P. H. Beloso and D. L. H. Williams, *J. Chem. Soc., Perkin Trans. 2*, 1997, 1429.
- 5 K. Varnagy, I. Sovago and H. Kozlowski, *Inorg. Chim. Acta*, 1988, **151**, 117.
- 6 D. R. Noble, H. R. Swift and D. L. H. Williams, *Chem. Commun.*, 1999, 2317.
- 7 S. C. Askew, J. Barnett, J. McAninly and D. L. H. Williams, *J. Chem. Soc., Perkin Trans. 2*, 1995, 741.
- 8 B. C. Gilbert, G. Scrivens and T. C. P. Lee, *J. Chem. Soc., Perkin Trans. 2*, 1995, 995.
- 9 B. C. Gilbert, S. Silvester and P. H. Walton, *J. Chem. Soc., Perkin Trans. 2*, 1999, 1115.
- 10 Micromath[®] Scientist[®] for Windows[®], Version 2.02.
- 11 Unpublished group findings.
- 12 A. J. Holmes and D. L. H. Williams, *J. Chem. Soc., Perkin Trans. 2*, 2000, 1639.
- 13 A. P. Munro and D. L. H. Williams, *J. Chem. Soc., Perkin Trans. 2*, 1999, 1989.
- 14 A. P. Munro and D. L. H. Williams, *J. Chem. Soc., Perkin Trans. 2*, 2000, 1794.
- 15 R. M. Smith and A. E. Martell, *Critical Stability Constants*, Plenum Press, New York, vol. 6, 1989.
- 16 D. S. Bohle, B. Hansert, S. C. Paulson and B. D. Smith, *J. Am. Chem. Soc.*, 1994, **116**, 7423.
- 17 D. J. Sexton, A. Muruganandam, D. J. McKenny and B. Mutus, *Photochem. Photobiol.*, 1994, **59**, 463.
- 18 M. Trujillo, M. N. Alvarez, G. Peluffo, B. A. Freeman and R. Radi, *J. Biol. Chem.*, 1998, **273**, 7828.
- 19 C. Walling, M. Kurz and H. J. Schugar, *Inorg. Chem.*, 1970, **9**, 931.

- 20 K. C. Francis, D. Cummins and J. Oakes, *J. Chem. Soc., Dalton Trans.*, 1985, 493.
- 21 T. Logager and K. Sehested, *J. Phys. Chem.*, 1993, **97**, 6664.
- 22 J. O. Edwards and R. C. Plumb, *Prog. Inorg. Chem.*, 1993, **41**, 599.
- 23 J. R. Leis, M. E. Peña and A. M. Ríos, *J. Chem. Soc., Perkin Trans. 2*, 1995, 587.
- 24 R. Radi, J. S. Beckman, K. M. Bush and B. A. Freeman, *J. Biol. Chem.*, 1991, **266**, 4244.
- 25 J. M. Fukuto and L. J. Ignarro, *Acc. Chem. Res.*, 1997, **30**, 149.
- 26 P. C. Jocelyn, "Biochemistry of the SH group", Chapter 4, Academic Press Inc., London, 1972; N. Kharasch and C. Y. Meyers, "The chemistry of organic sulfur compounds", p. 367-402, Pergamon Press, Oxford, vol. 2, 1966.
- 27 H. Ischiropoulos, Z. Zhu and J. S. Beckman, *Arch. Biochem. Biophys.*, 1992, **298**, 446.
- 28 B. Alvarez, A. Denicola and R. Radi, *Chem. Res. Toxicol.*, 1995, **8**, 859.
- 29 C. F. Nathan, S. C. Silverstein, L. H. Brukner and Z. A. Cohn, *J. Exp. Med.*, 1979, **149**, 100.

Chapter 3

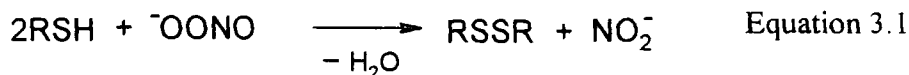
3 Direct and indirect nitrosation by peroxynitrous acid

Peroxynitrite^a is a very potent oxidising agent as discussed in the introductory chapter. Its particular affinity for thiols has resulted in much study of their oxidation at physiological and alkaline pH. Some reports indicate that peroxynitrite can nitrosate thiols at physiological pH^{1, 2} and suggest this as a possible route for the *in vivo* generation of *S*-nitrosothiols, the mechanism of which is unknown. This chapter investigates the reaction of peroxynitrite and thiols below physiological pH in an attempt to clarify these findings and suggest a mechanistic explanation.

3.1 Introduction

The discovery and quantification of RSNOs *in vivo* led naturally to the question of how they are generated. Suggestions of the direct reaction between NO and thiols³, N₂O₃ and thiols⁴ and peroxynitrite and thiols¹ are just some of the proposed mechanisms discussed in the literature, the latter two are feasible but direct reaction of NO and thiols is unlikely and probably proceeds through N₂O₃.

The reaction between peroxynitrite and thiols has been studied at and above physiological pH.^{5, 6, 7} Under these conditions peroxynitrite is in its stable anionic form and the main thiol derived product is the disulfide. The nitrogen product is nitrite, which is characteristic of all peroxynitrite mediated oxidations,⁸ see equation 3.1.



During studies of thiol oxidation by peroxynitrite, very low yields of RSNOs were detected at physiological pH, typically between one and two percent,^{1, 2} the remaining thiol was oxidised to the disulfide.

^a The term peroxynitrite implies the sum of the peroxynitrite anion and peroxynitrous acid therefore irrespective of pH.

It is therefore conceivable that these very low yields of RSNOs could arise through indirect nitrosation pathways, rather than from a direct reaction between peroxynitrite and thiol.

For example, the nitrite ion may be formed from the reaction in equation 3.1 or by the decomposition of peroxynitrite at pHs above its pK_a , which is known to yield nitrite⁸. The nitrite ion could then generate (a) low concentrations of NO/NO₂ which could then form N₂O₃, and/or (b) small amounts of nitrous acid. Both scenarios could then effect thiol nitrosation.

Most literature studies have not investigated the reactions at lower pH due to the instability of peroxynitrite. Below its pK_a of ~ 6.8 the peroxynitrous acid is the predominant species, and this quickly isomerises to nitrate with a half-life of ~ 1 s.⁸

With decreasing pH, trends indicated that the disulfide was the quantitative product and this was extrapolated through to low pH.⁶

It has been argued⁹ that both the peroxynitrite anion and peroxynitrous acid are unlikely to act as nitrosating species due to their very poor leaving groups, O₂²⁻ and HO₂⁻ respectively. However, some reports indicate small amounts of RSNOs form from reactions involving peroxynitrite and thiols at physiological pH.^{1,2}

Grossi *et al.*⁵ indicated that at high acidities *ca.* 1 mol dm⁻³, RSNOs were generated in good yield. This involved a two phase system (water/acetonitrile) and suggested peroxynitrous acid could act as a conventional electrophilic nitrosating agent.

With this in mind a thorough investigation of the acidic pH range was undertaken for the reaction between peroxynitrous acid and thiols.

3.2 Initial investigation of the reaction between peroxynitrous acid and thiols

Peroxynitrite was prepared as detailed in Section 6.1.2 and stored at $-10\text{ }^{\circ}\text{C}$ in pH ~ 13.5 NaOH. This method ensured that no adventitious nitrite would be present which, under acidic conditions, would nitrosate thiols through nitrous acid.¹⁰

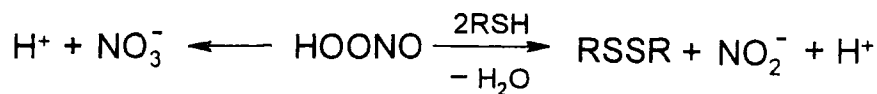
3.2.1 Reaction of equimolar peroxynitrite and thiols

Peroxynitrite (final concentration = 2 mmol dm^{-3}) was added to an acidified solution of cysteine (2 mmol dm^{-3} in 1 mol dm^{-3} HClO_4). Initial tests were performed using an equimolar amount of peroxynitrous acid and thiol as performed by Grossi *et al.*⁵ However, there was no visible formation of the characteristic red colour of *S*-nitrosocysteine, SNCys, merely the instantaneous decolouration of the yellow peroxynitrite anion upon its addition to acid.

Accounting for the thiol concentration used, a large absorbance was expected in the UV / Visible spectrum with a peak at 340 nm, according to the extinction co-efficient for SNCys, ($\epsilon_{340\text{ nm}} = 855\text{ dm}^3\text{ mol}^{-1}\text{ cm}^{-1}$).¹¹ The product UV / Visible spectrum displayed no evidence of RSNO formation. Grossi *et al.*⁵ noted up to 70 % yield, hence it was evident that the modifications of the procedure described by Grossi *et al.* resulted in no observable RSNO generation.

The major change in procedure was the shift to completely aqueous conditions compared to the two-phase water / acetonitrile system adopted by Grossi *et al.*

The lack of RSNO formation suggests that the two alternative pathways for peroxynitrite decay prevail rather than nitrosation of thiol. The spontaneous decomposition of peroxynitrous acid, through isomerisation to nitrate anion,⁸ and / or the oxidation of the thiol to the corresponding disulfide, with the concomitant reduction of peroxynitrous acid to nitrite, Scheme 3.1.



Scheme 3.1 Possible decomposition pathways for peroxynitrous acid.

If the reaction of peroxynitrite and thiols under acidic conditions is analogous to the reaction under alkaline conditions,^{5, 6} then nitrite is the expected product. Under sufficiently acidic conditions the nitrite ion would be protonated, generating nitrous acid which could nitrosate any thiol present.

Under equimolar conditions this seems unlikely as the competition from spontaneous isomerisation to nitrate anion and the oxidation of the thiol to disulfide would leave insufficient nitrite and thiol.

It was envisaged that a reaction in which there was a large excess of thiol over peroxynitrous acid would be more likely to yield detectable amounts of RSNO.

3.2.2 Reaction of excess thiol with peroxynitrous acid

To test the reaction of an excess of thiol with peroxynitrous acid, 1 mmol dm⁻³ peroxynitrous acid was added to a large excess of thiol (25 mmol dm⁻³) in 0.5 mol dm⁻³ HClO₄. Upon mixing, the distinctive red of SNCys promptly replaced the yellow colouration of peroxynitrite.

The UV / Visible spectrum of the product revealed the characteristic peaks at 340 and 545 nm associated with SNCys, Figure 3.1. From the extinction co-efficient of SNCys the product yield was calculated to be 85 %.

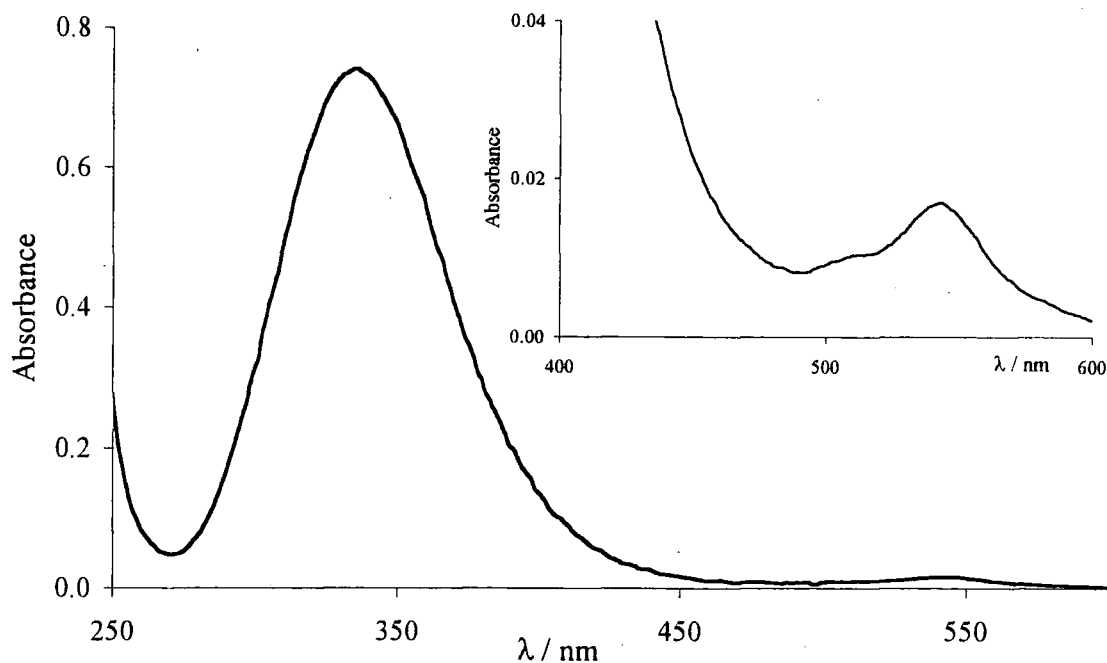


Figure 3.1 Product spectrum of the reaction between 1 mM and 25 mM cysteine in 0.5 M HClO_4 . Inset displays expansion of 545 nm peak

It was therefore confirmed that peroxynitrous acid could nitrosate thiols and produce the respective RSNO. However, a large excess of thiol and, in this case, high acidities were required to produce almost quantitative conversion. Further investigations were then initiated to examine the reaction further.

3.3 Effect of thiol concentration on final RSNO yield

In the previous sections, two extremes of thiol concentration were investigated; hence it was considered prudent to fill in the blanks. A range of initial thiol concentrations was used to check the dependency of the final RSNO yield upon the initial thiol concentration. In this section the thiol used was the tri-peptide glutathione hence the product was *S*-nitrosoglutathione, GSNO.

A constant acid concentration of 0.5 mol dm^{-3} was maintained and thiol concentrations of 0.5 to 50 mmol dm^{-3} were systematically reacted with 0.5 mmol dm^{-3} peroxynitrous acid.

The final product yield, with respect to peroxynitrous acid (the limiting reagent), was calculated from the extinction co-efficient for GSNO at 340 nm ($\epsilon_{340\text{ nm}} = 895\text{ dm}^3\text{ mol}^{-1}\text{ cm}^{-1}$).¹¹ As expected it was revealed that the product yield was dependent on initial thiol concentration, Table 3.1.

[GSH] / mM	% GSNO	[GSH] / mM	% GSNO
0.50	0	5.0	53
0.75	0	10	72
1.0	0	15	82
1.5	13	20	88
2.0	20	30	92
2.5	28	50	96
3.0	36	-	-

Table 3.1 Yield of GSNO from the reaction of varying [GSH] with 0.5 mmol dm^{-3} peroxynitrite in $0.5\text{ mol dm}^{-3}\text{ HClO}_4$.

To achieve quantitative GSNO formation a large molar excess of thiol over peroxynitrous acid was required, depicted graphically in Figure 3.2.

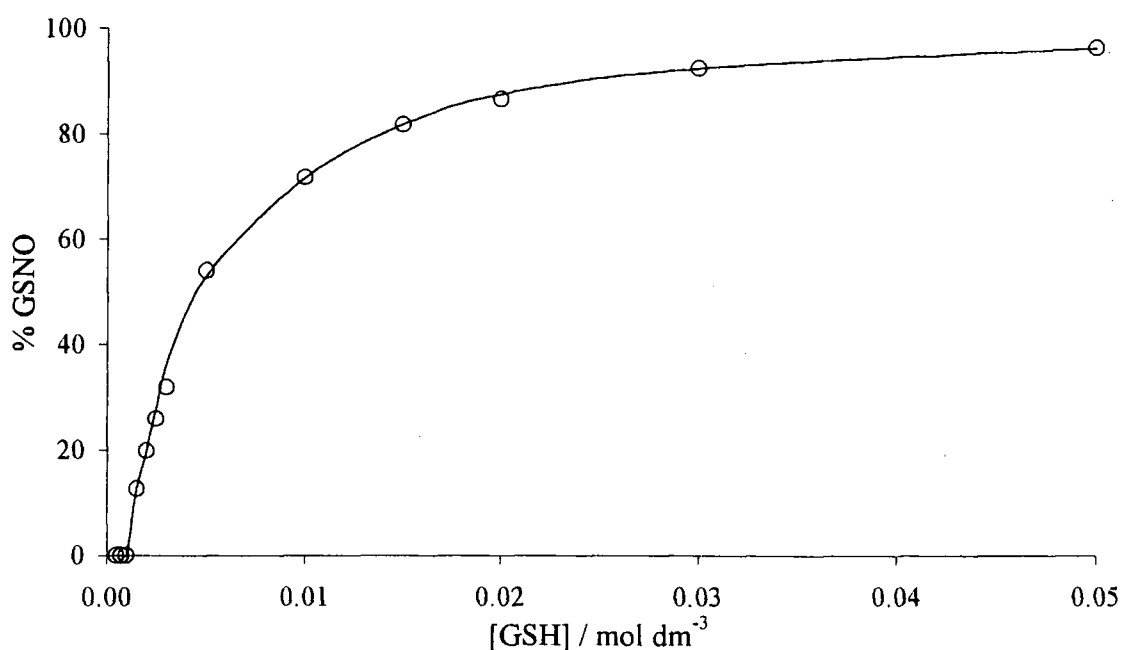


Figure 3.2 The % GSNO yield as a function of [GSH] from the data in Table 3.1

As indicated earlier, equimolar amounts of thiol and peroxynitrous acid do not yield detectable amounts of RSNOs. Figure 3.2 indicates this, as the line does not pass through the origin, thus indicating an approximate stoichiometric point. This is approximate, as the losses of peroxynitrous acid to nitrate need to be considered.

From Scheme 3.1 it can be assumed that greater than a two-fold excess of thiol over peroxynitrous acid should start to produce RSNOs providing no peroxynitrous acid is lost to nitrate. Any nitrite produced through the oxidation of thiol to disulfide would be protonated to form nitrous acid at this acidity ($0.5 \text{ mol dm}^{-3} [\text{H}^+]$). Nitrosation of thiols is anticipated to be quick under these conditions; hence any excess thiol present would undoubtedly be nitrosated yielding the RSNO.

For Scheme 3.1 to be correct we should expect to observe nitrous acid formation when the thiol is in a two-fold excess over peroxynitrous acid, providing that the oxidation of thiol by peroxynitrous acid is faster than its decomposition to nitrate.

3.4 Reaction of a 2:1 excess of thiol over peroxynitrous acid

3.4.1 Detection of nitrous acid

Working at the same concentrations as the previous sections would result in nitrous acid absorptions too small to detect. Therefore the thiol content, in this case GSH, was kept at 25 mmol dm^{-3} but the peroxynitrous acid concentration was increased 25-fold to $12.5 \text{ mmol dm}^{-3}$, resulting in a two fold excess of thiol over peroxynitrite. The acid concentration was kept at $0.5 \text{ mol dm}^{-3} \text{ HClO}_4$.

The reaction was performed on a stopped flow spectrophotometer with a diode array attachment allowing the reaction to be followed through repeat scan spectra over small time intervals. The resultant spectra displayed part of the characteristic five-fingered nitrous acid peak within one millisecond although parts of the spectra were obscured by other absorbances in the UV region, see Figure 3.3.

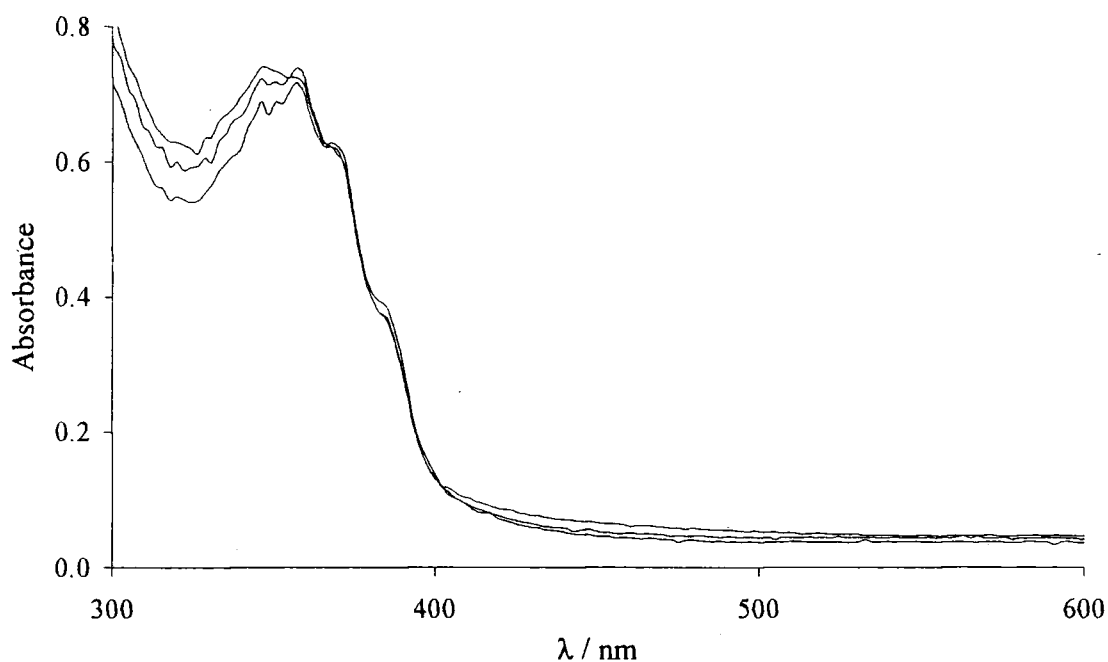
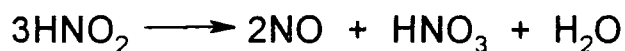


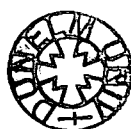
Figure 3.3 Reaction of 25 mmol dm^{-3} GSH with $12.5 \text{ mmol dm}^{-3}$ peroxynitrous acid in 0.5 mol dm^{-3} HClO_4 . Scans recorded at 1.3, 9 and 20 ms

The nitrous acid peak displayed no further reaction for the next second. The spectra recorded after those shown in Figure 3.3 suffered from a uniform increase of absorbance across the studied spectral region, not shown. This is characteristic of bubbles forming in the observation cell of the stopped flow. The bubble formation is attributed to nitrous acid decay, which is well known to generate gaseous NO on standing, equation 3.2.¹⁰



Equation 3.2 Acidic decomposition of nitrous acid

The formation of nitrous acid may be quantified by using the known extinction coefficients. Table 3.2 shows the calculation of the nitrous acid concentration by two of the four extinction coefficients determined by Markovits *et al.*¹²



λ / nm	Abs	ϵ^a / dm ³ mol ⁻¹ cm ⁻¹	[HNO ₂] ^b / M
371	0.60	49.4	1.21E-02
386	0.35	28.6	1.22E-02

Table 3.2 Calculation of [HNO₂] from the extinction co-efficients

^a From reference 12

^b Calculated [HNO₂] / mol dm⁻³

Only two of the four extinction coefficients of nitrous acid were used as the lower wavelength peaks suffer from an overlap from absorbing species in the UV region.

Nitrous acid was calculated to form in almost quantitative yield (~ 95 %) from the reaction of thiols and peroxynitrous acid, when the thiol is in a two-fold excess. This appears to be the first time that thiol oxidation by peroxynitrous acid in acid solution has been demonstrated. It clearly forms nitrous acid and presumably the disulfide as described for thiol oxidation at physiological and alkaline pH, where the deprotonated form of nitrous acid, nitrite ion, is the quantitative nitrogen product.

3.5 Quantification of the disulfide product

The disulfide of glutathione, GSSG has no distinguishing UV / Visible absorptions. However, upon binding to copper (II) ions it forms a blue 1:1 complex in acidic and neutral solutions. The complex is stable and can be quantified by its UV / Visible spectrum ($\epsilon_{620} = 61 \text{ dm}^3 \text{ mol}^{-1} \text{ cm}^{-1}$).^{13, 14}

Varnagy *et al.*¹⁴ proposed a structure for the GSSG:Cu²⁺ complex with square planar geometry surrounding the metal ion and co-ordination from the amine and glutamyl carboxylic groups, Figure 3.4.

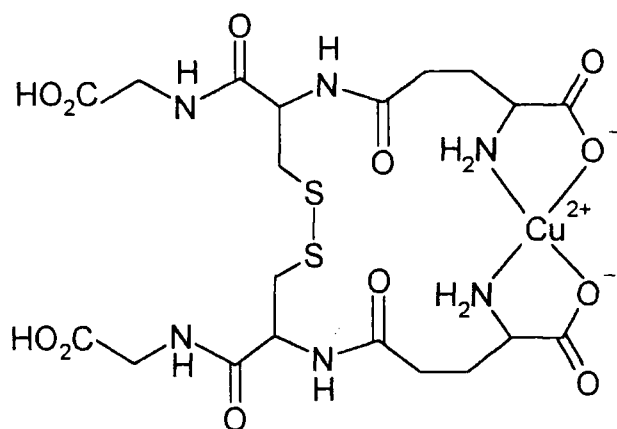


Figure 3.4 Glutathione disulfide copper complex.

The absorbance at 620 nm is a result of the Cu^{2+} d-d transitions. A larger peak is present at 250 nm and is tentatively assigned to the $\text{N}_\sigma \rightarrow \text{Cu}$ charge transfer transition.¹⁵

To quantify the GSSG, 20 mmol dm^{-3} GSH was reacted with 5 mmol dm^{-3} peroxynitrous acid in 0.5 mol dm^{-3} acid. The resulting absorbance was the GSNO peak. The solution was then treated with sufficient NaOH to neutralise the acid, an excess of CuSO_4 was added, and the peak at 620 nm formed. This confirmed two facts, that the product was GSNO by its copper catalysed decomposition and that the resulting product was disulfide, Figure 3.5.

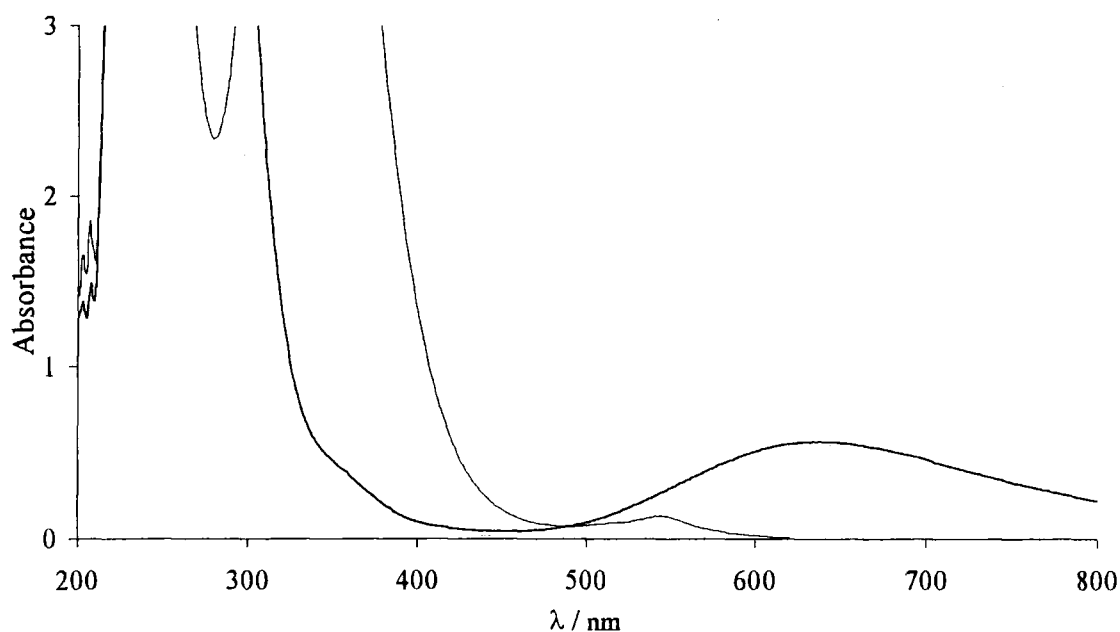


Figure 3.5 The reaction product from 20 mmol dm^{-3} GSH and 5 mmol dm^{-3} peroxynitrous acid in 0.5 mol dm^{-3} acid and the effect of neutralisation and treatment with excess CuSO_4

The GSSG yield was quantitative as calculated from the GSSG:Cu²⁺ extinction coefficient. The product from the 2:1 GSH:peroxynitrous acid reaction also yielded quantitatively GSSG which confirms for the first time equation 3.1 in acidic solution.

3.5.1 Determining the stability of the disulfide product

As observed in the previous section the formation of disulfide from the reaction of a 2:1 excess of thiol over peroxynitrous acid is quantitative. It was therefore necessary to determine the disulfide stability with a view to the overall mechanism of the reaction. An experiment was performed to check the stability of disulfide in reaction with peroxynitrous acid and nitrous acid. In both cases no species were detectable in the UV / Visible spectrum and therefore disulfides can be suggested to be unreactive to nitrosation.

3.6 Indirect nitrosation mechanism

3.6.1 Nitrosation of cysteine ethyl ester

Under sufficiently acidic conditions the formation of nitrous acid should initiate nitrosation of any excess thiol. The nitrosation of thiols by nitrous acid has been studied for many different thiols as outlined in Section 1.4.2. As with many nitrosations by nitrous acid they obey the following rate equation:

$$\text{Rate} = k_3[\text{RSH}][\text{HNO}_2][\text{H}^+]$$

Equation 3.3 Third order rate equation for nitrosation of thiols by nitrous acid

Third order rate constants, k_3 , have been determined accordingly for the many thiols investigated.

Under the conditions utilised so far the concentrations of acid and thiol were in a large excess over peroxynitrous acid. Therefore any nitrous acid formed should nitrosate the thiol under pseudo first order conditions.

The reaction of 0.5 mmol dm^{-3} peroxynitrous acid with excess thiol, in this case 25 mmol dm^{-3} cysteine ethyl ester, was studied spectrophotometrically by the formation of the characteristic RSNO peak at 340 nm under varied concentrations of acid. Good first order formation traces were observed over a range of acid concentrations, Figure 3.6.

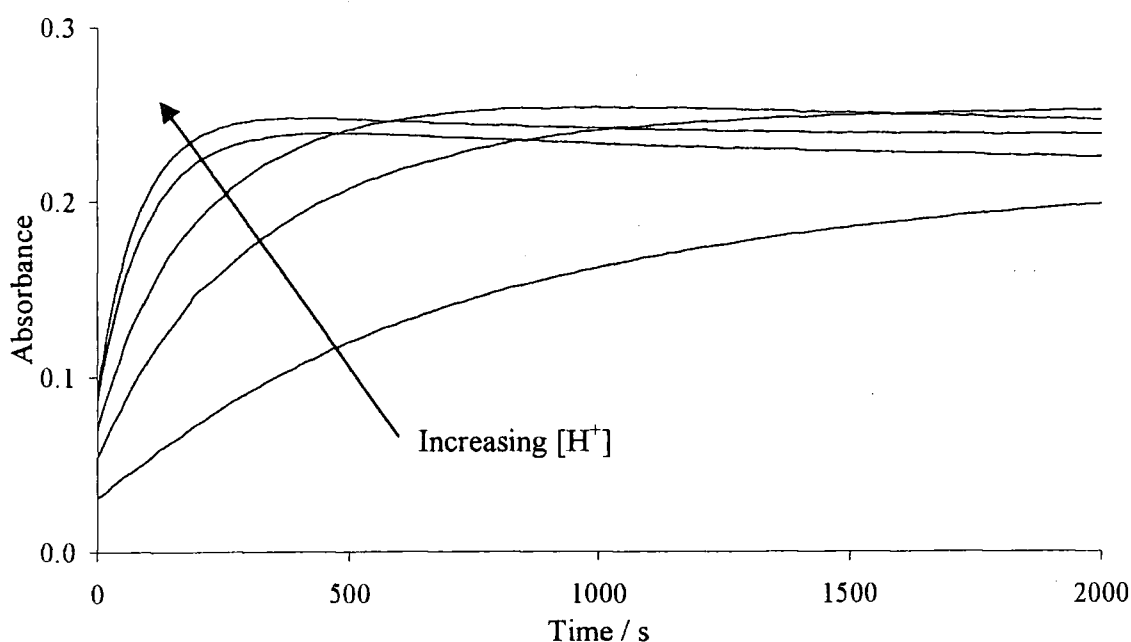


Figure 3.6 0.5 mmol dm^{-3} peroxynitrous acid with 25 mmol dm^{-3} cysteine ethyl ester in $0.22, 0.50, 0.93, 2.00$ and $2.40 \text{ mmol dm}^{-3} [\text{HClO}_4]$

First order rate constants were obtained from the traces in Figure 3.6 using the Scientist[®] computer program¹⁶ and the results displayed in Table 3.3.

$[\text{H}^+] / \text{mM}$	$10^3 k_{\text{obs}} / \text{s}^{-1}$
2.40	13.1 ± 0.06
2.00	11.0 ± 0.04
0.93	5.22 ± 0.03
0.50	2.98 ± 0.02
0.22	1.34 ± 0.01

Table 3.3 First order rate constants calculated using Scientist[®] from the traces in Figure 3.6

An example of the fit line generated by Scientist® is displayed in Figure 3.7.

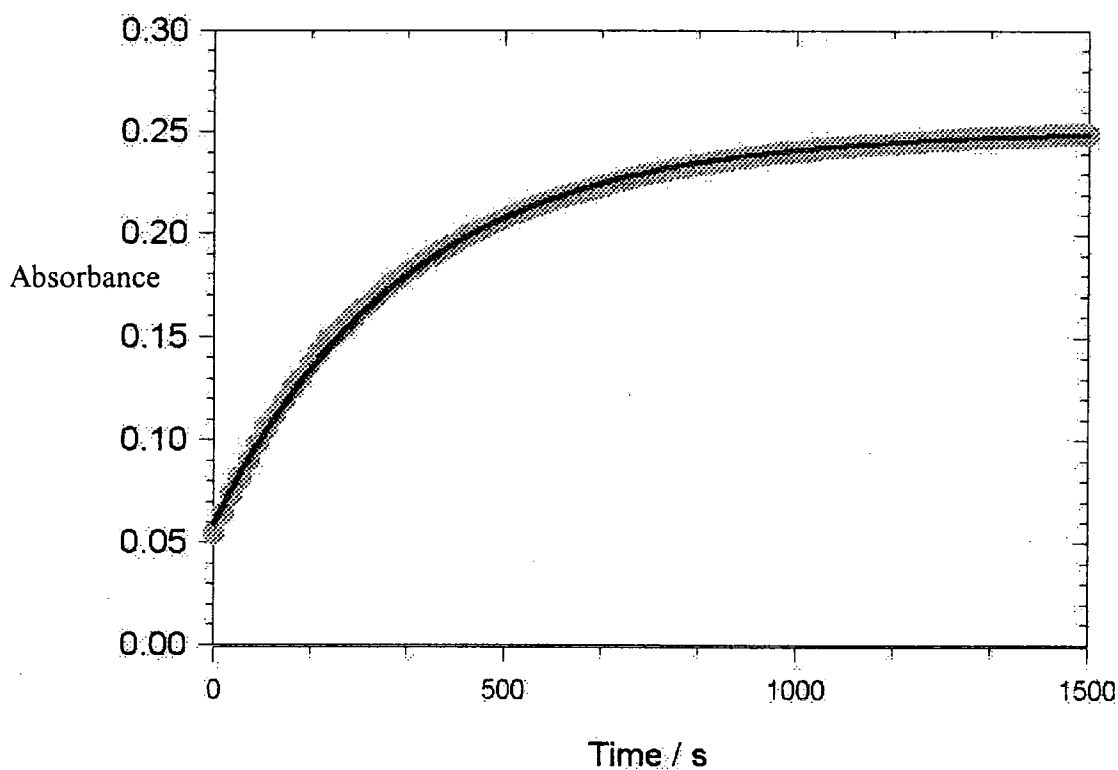


Figure 3.7 Fit line (black line) generated by Scientist® from data obtained (grey circles) in the reaction of 0.5 mmol dm^{-3} peroxynitrous acid with 25 mmol dm^{-3} cysteine ethyl ester in $0.50 \text{ mmol dm}^{-3} [\text{HClO}_4]$

A linear relationship was observed between k_{obs} and $[\text{H}^+]$, plotted from the values in Table 3.3, see Figure 3.8. From this the third order rate constant for the reaction of peroxynitrous acid and thiols could be determined according to the rate equation :-

$$\text{Rate} = k_3[\text{RSH}][\text{ONOOH}][\text{H}^+]$$

Equation 3.4 Third order rate equation for nitrosation of thiols by peroxynitrous acid

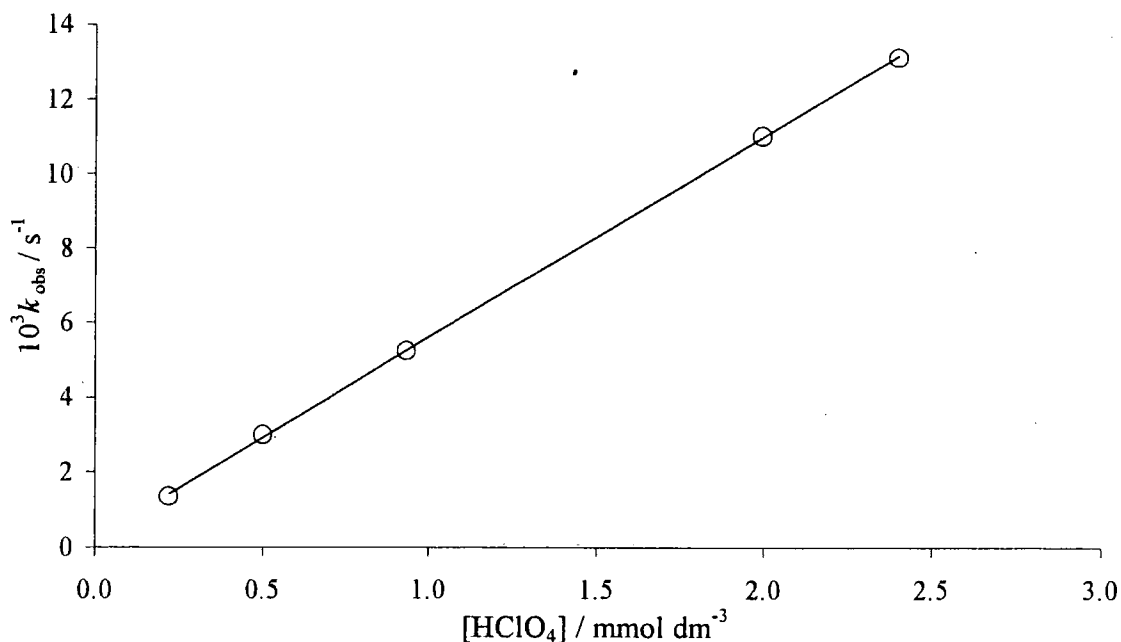


Figure 3.8 Plot of the values in Table 3.3 obtained from the traces displayed in Figure 3.6

As the concentrations of thiol was in large excess and the acid is catalytic, equation 3.4 simplifies to:

$$\text{Rate} = k_{\text{obs}}[\text{ONOOH}]$$

Where,

$$k_{\text{obs}} = k_3[\text{RSH}][\text{H}^+]$$

Therefore a plot of k_{obs} versus acid concentration allows the calculation of the third order rate constant from the gradient.

From Figure 3.8 the third order rate constant was calculated as :

$$k_3 = 215 \pm 1 \text{ dm}^6 \text{ mol}^{-2} \text{ s}^{-1}$$

The value obtained is in excellent agreement with that obtained for the nitrosation of cysteine ethyl ester by authentic nitrous acid, $k_3 = 213 \text{ dm}^6 \text{ mol}^{-2} \text{ s}^{-1}$.¹⁷

3.6.2 Nitrosation of glutathione

To obtain further understanding of the indirect nitrosation mechanism, alternative thiols were used. The procedure utilised in the previous section was repeated using glutathione as the thiol. Again almost quantitatively RSNO was generated and excellent first order plots were obtained from which the observed rate constants were generated, Table 3.4.

$[H^+] / \text{mM}$	$10^3 k_{\text{obs}} / \text{s}^{-1}$
0.45	11.0 ± 0.09
0.25	6.28 ± 0.09
0.14	2.80 ± 0.02
0.05	0.94 ± 0.01

Table 3.4 Observed rate constants calculated from the reaction of 25 mmol dm^{-3} glutathione and 0.5 mmol dm^{-3} peroxynitrous acid under varying $[\text{HClO}_4]$

From the values in Table 3.4 the third order rate constant was calculated as :

$$k_3 = 1\,077 \pm 41 \text{ dm}^6 \text{ mol}^{-2} \text{ s}^{-1}$$

As previously, the value obtained was in very good agreement with that obtained for the nitrosation of glutathione by authentic nitrous acid, $k_3 = 1\,080 \text{ dm}^6 \text{ mol}^{-2} \text{ s}^{-1}$.¹⁷

3.6.3 Nitrosation of cysteine

The procedure was repeated once more using cysteine as the thiol. The results obtained followed a similar trend, Table 3.5.

$[H^+]/\text{mM}$	$10^3 k_{\text{obs}}/\text{s}^{-1}$
1.58	21.0 ± 0.12
0.78	10.5 ± 0.10
0.45	5.50 ± 0.09
0.38	5.00 ± 0.04
0.18	2.61 ± 0.03

Table 3.5 Observed rate constants calculated from the reaction of 25 mmol dm⁻³ cysteine and 0.5 mmol dm⁻³ peroxynitrous acid under varying [HClO₄]

From the values in Table 3.4 the third order rate constant was calculated as :

$$k_3 = 529 \pm 14 \text{ dm}^6 \text{ mol}^{-2} \text{ s}^{-1}$$

Again the value obtained agreed with that obtained for the nitrosation of cysteine by authentic nitrous acid, $k_3 = 514^{18} (456)^{19} \text{ dm}^6 \text{ mol}^{-2} \text{ s}^{-1}$.

3.6.4 Summary

The summary of the third order rate constants obtained from the peroxynitrous acid nitrosation of thiols shows excellent correlation to those obtained from the thiol and authentic nitrous acid, Table 3.6.

	Experimental	Literature
Thiol	$k_3 / \text{dm}^6 \text{ mol}^{-2} \text{ s}^{-2}$	$k_3 / \text{dm}^6 \text{ mol}^{-2} \text{ s}^{-3}$
Cysteine ethyl ester	215	213^{17}
Cysteine	529	$514^{18} (456)^{19}$
Glutathione	1 077	$1\ 080^{17}$

Table 3.6 Third order rate constants determined from the nitrosation of thiols with peroxynitrous acid versus those obtained from nitrous acid

It is clear that the formation of RSNO species from thiol and peroxynitrous acid, in the acidity range studied, occurs by rapid oxidation of two equivalents of thiol which generates one equivalent of nitrite / nitrous acid, as shown in section 3.4.1. The nitrous acid then nitrosates the excess thiol in a conventional electrophilic *S*-nitrosation.

3.6.5 The effect of increasing pH on the final RSNO yield

The reaction of 25 mmol dm⁻³ glutathione and 0.5 mmol dm⁻³ peroxynitrous acid under varying pH was followed spectrophotometrically at 340 nm over time with the final yield calculated using the extinction coefficient of GSNO ($\epsilon_{340\text{ nm}} = 895\text{ dm}^3\text{ mol}^{-1}\text{ cm}^{-1}$),¹¹ see Figure 3.9.

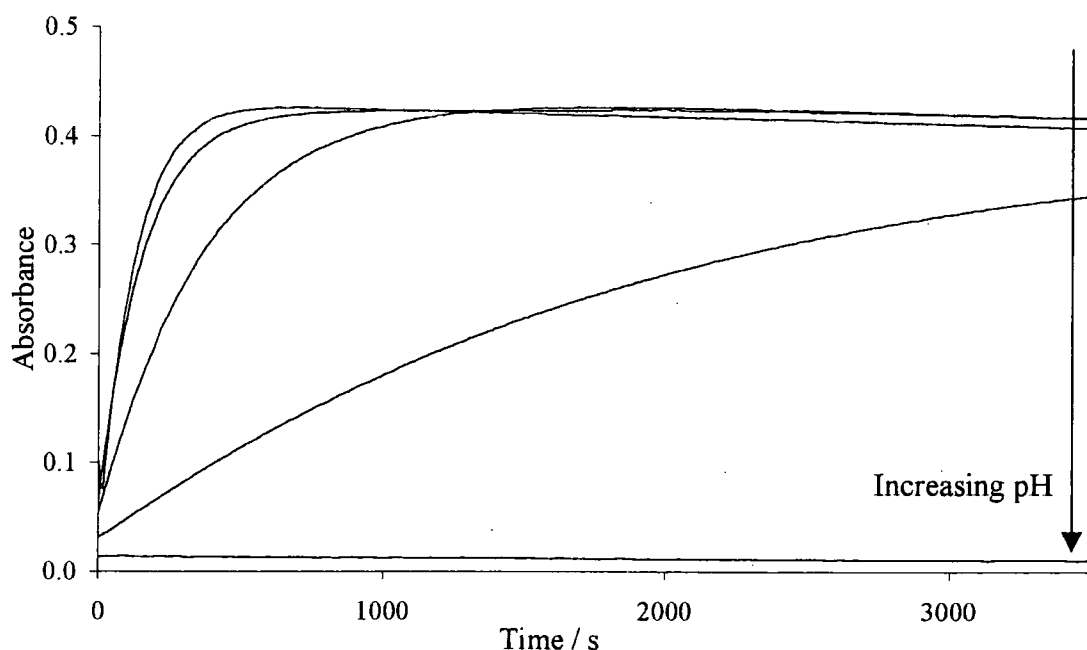


Figure 3.9 Reaction of 25 mmol dm⁻³ glutathione with 0.5 mmol dm⁻³ peroxynitrous acid at pH a) 3.3, b) 3.6, c) 3.8, d) 4.3, and e) 7

At the acidities studied in the previous sections almost quantitative yields of RSNOs are generated. However with a wider range of pH as the solution pH is increased a decrease in the final GSNO yield is observed. EDTA, 0.5 mmol dm⁻³, was added in all reactions to suppress the copper mediated decomposition pathway.

The yield of GSNO dropped progressively as the pH increased and at pH 7 no spectrophotometrically detectable GSNO was formed. However at pH 5, 25% GSNO was formed and at pH 6, 5% GSNO was obtained (both not shown). Hence the few % of RSNO detected (by HPLC) in the reaction of peroxynitrite at physiological pH^{1, 2} can easily be attributed to the indirect nitrosation mechanism proposed.

3.7 Direct nitrosation

The initial studies were carried out at high acidity *ca.* 0.5 mol dm^{-3} and with thiol in large excess over peroxynitrous acid. The very rapid formation of the corresponding RSNO was observed. At higher acidity the absorbance time data accrued were more complicated, in that they were not simple first order formations but appeared to show two reactions. A range of acid concentrations was used between 0.3 and 1 mol dm^{-3} in the reaction of 25 mmol dm^{-3} glutathione with 0.5 mmol dm^{-3} peroxynitrous acid. The reactions were followed by their absorbance increases at 340 nm using a stopped-flow spectrophotometer, Figure 3.10.

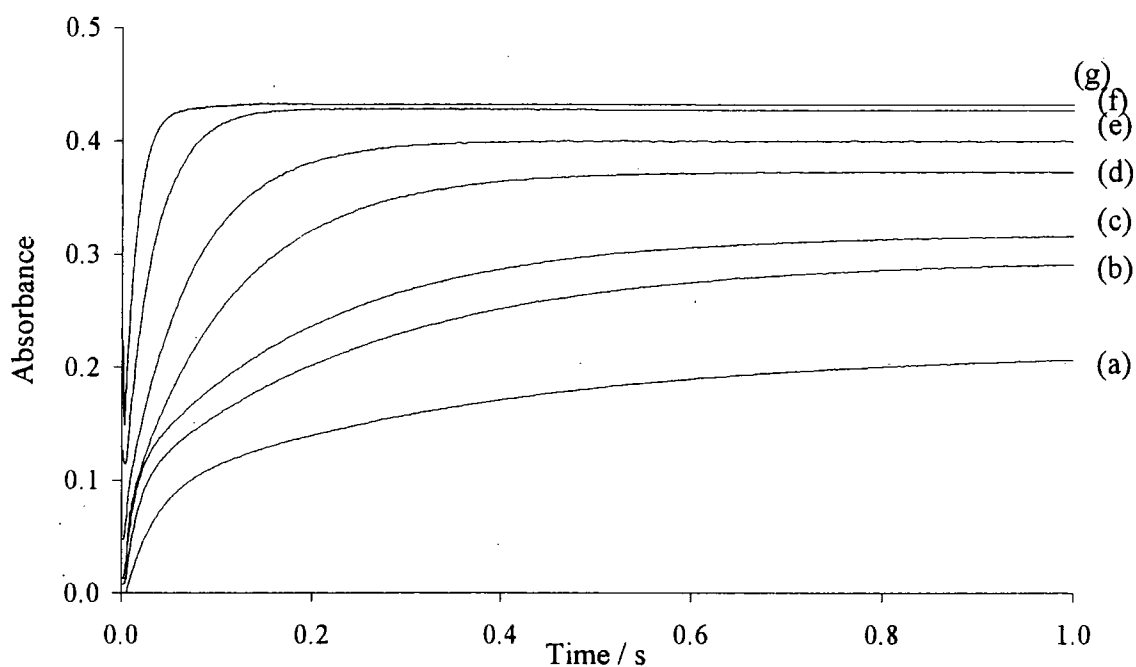


Figure 3.10 The reaction of 25 mmol dm^{-3} glutathione with 0.5 mmol dm^{-3} peroxynitrous acid in (a) 0.3 , (b) 0.5 , (c) 0.6 (d) 0.7 , (e) 0.8 , (f) 0.9 and (g) $1.0 \text{ mol dm}^{-3} [\text{H}^+]$.

The increase in acidity from the pH range studied in the previous section resulted in a double exponential formation of RSNO. Further increase in acid concentration returned the absorbance time traces to single exponential first order formation. This implies that RSNO formation is occurring from an alternative source under the higher concentrations of acid.

3.7.1 Diode array study

The diode array attachment of the stopped flow spectrophotometer was utilised to confirm that the complex nature of the absorbance time traces displayed in Figure 3.10 were not the result of additional absorbance increases or decreases around 340 nm. The reaction of 25 mmol dm^{-3} glutathione with 1.0 mmol dm^{-3} peroxynitrous acid in $0.7 \text{ mol dm}^{-3} [\text{H}^+]$ was followed by the diode array equipment. A higher concentration of peroxynitrous acid was used to generate a larger absorbance so that the reaction may be more easily observed, Figure 3.11.

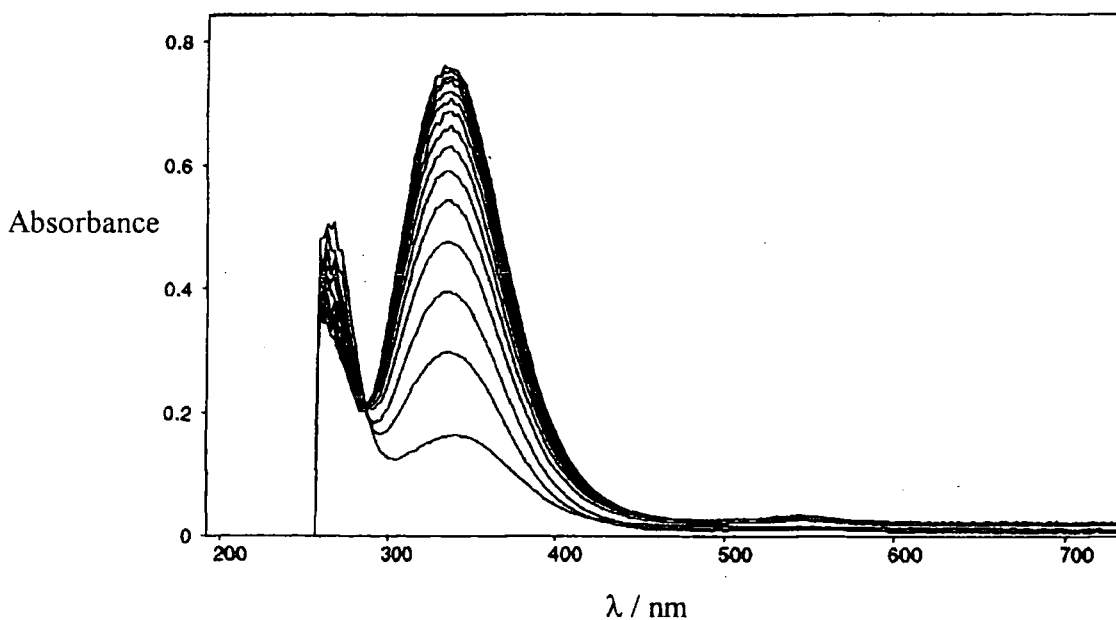


Figure 3.11 The reaction of 25 mmol dm^{-3} glutathione with 1.0 mmol dm^{-3} peroxynitrous acid in $0.7 \text{ mol dm}^{-3} [\text{H}^+]$, scans taken every 0.07 s showing the absorbance increase at 340 nm due to RSNO

As can be seen in Figure 3.11 no additional absorbing species were detected, hence it could be confirmed that the absorbance time traces obtained are a result of RSNO formation by two pathways.

3.7.2 Kinetic analysis of the formation curves

The Scientist[®] computer program¹⁶ allowed the determination of the observed first order rate constants for both processes. The rate constants obtained were designated k_{slow} and k_{fast} and are given in Table 3.7, the errors in the values were less than 1%.

$[\text{H}^+] / \text{mol dm}^{-3}$	$k_{\text{fast}} / \text{s}^{-1}$	$k_{\text{slow}} / \text{s}^{-1}$
4.0	-	57.4
3.0	-	31.2
2.5	100	22.3
2.0	68.3	15.0
1.5	48.4	11.2
1.0	27.9	6.87
0.90	23.9	6.20
0.70	18.0	5.40
0.50	11.2	4.23
0.40	8.98	3.56
0.30	6.70	-
0.07	0.14	-

Table 3.7 Rate constants obtained using Scientist[®] for the reaction of 25 mmol dm^{-3} glutathione with 0.5 mmol dm^{-3} peroxynitrous acid in varying $[\text{H}^+]$

A plot of the values in Table 3.7 resulted in non-linear relationships between rate constant and acid concentration, Figure 3.12.

Initially the relationship appeared linear but increasing acid concentrations resulted in increased curvature of the plots. This has been observed before in a study of the nitrosation of a number of species²⁰ and the curvature attributed to the acidity of acid solutions increasing more rapidly than the molar concentration.²¹

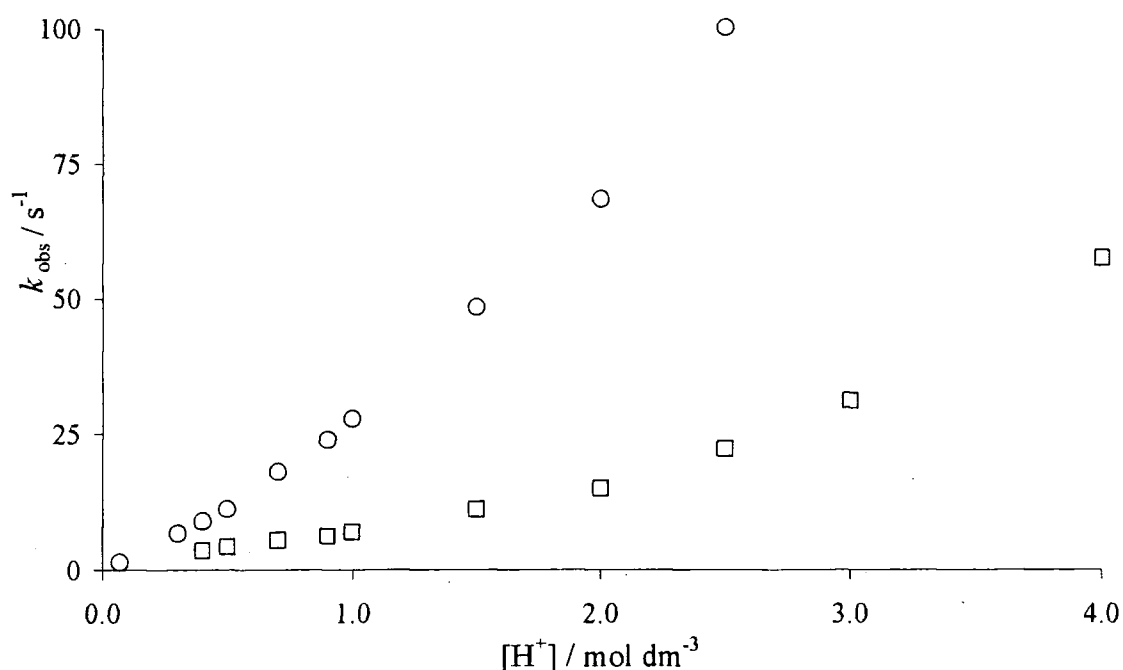


Figure 3.12 Plot of the values displayed in Table 3.7, circles and squares indicate k_{fast} and k_{slow} respectively

Assuming that the reaction follows the rate equations set out previously in section 3.6.1 the initial linear sections of the plots in Figure 3.12 could be used to determine the third order rate constants, k_3 , for both reactions. The data for both k_{fast} and k_{slow} were analysed and generated the k_3 values displayed in Table 3.8.

	$k_{3 \text{ fast}} / \text{dm}^6 \text{ mol}^{-2} \text{ s}^{-2}$	$k_{3 \text{ slow}} / \text{dm}^6 \text{ mol}^{-2} \text{ s}^{-2}$
k_3	$\sim 1\,150 \pm 48$	$\sim 287 \pm 13$

Table 3.8 k_3 values determined from the linear sections of the plots in Figure 3.12

$k_{3 \text{ fast}}$ is comparable to the k_3 value of $1\,077 \text{ dm}^6 \text{ mol}^{-2} \text{ s}^{-1}$ obtained in section 3.6.2 at lower acidity and is therefore attributed to the indirect nitrosation pathway. The other value, $k_{3 \text{ slow}}$, is a result of an alternative mechanism of RSNO formation. It was presumed that $k_{3 \text{ slow}}$ followed a similar mechanism to $k_{3 \text{ fast}}$ in order to allow comparisons however this may not be appropriate depending on the actual mechanism.

It was noticeable that at extremely high acid concentrations, only single exponential formation was observed, see Table 3.7. Also, the observed rate constants were less than that of the highest measurable value of k_{fast} , thus assigning them as k_{slow} . This is highly indicative that at very high acid concentrations the indirect nitrosation pathway is arrested. In order for this to happen the reaction of peroxynitrous acid must be through an alternative preferred pathway at high acidity, that does not produce nitrite through the oxidation of thiol.

From the rate constant determinations with Scientist[®] the percentage RSNO formation from each pathway could be calculated, as a percentage of the overall RSNO produced, Table 3.9.

$[\text{H}^+] / \text{mol dm}^{-3}$	% RSNO	
	k_{fast}	k_{slow}
2.0	3	97
1.5	6	94
1.0	11	89
0.75	16	84
0.50	22	78
0.33	37	63
0.27	44	56
0.05	100	0

Table 3.9 Percentage RSNO formation from each pathway calculated as a percentage of the overall RSNO produced using Scientist[®]

The percentage of RSNO produced tends toward the k_{slow} pathway with increasing concentrations of acid. Again this is indicative of the cessation of the indirect nitrosation pathway. This mechanistic swing seems unfeasible as the fastest pathway should always dominate.

A plot of the values in Table 3.9 displays the switch of the dominant RSNO formation pathway more clearly.

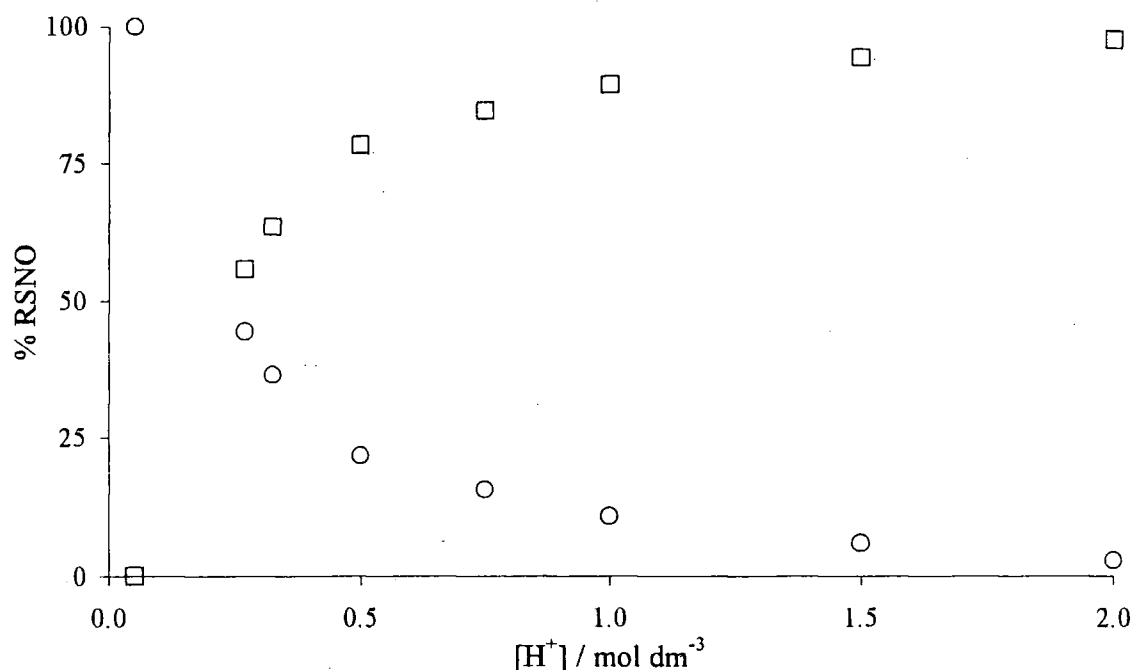


Figure 3.13 A plot of the values in Table 3.9 circles and squares indicate k_{fast} and k_{slow} respectively

3.7.3 The effect of added bromide

Nitrous acid nitrosation of thiols is catalysed by added nucleophiles, such as bromide, chloride and thiocyanide.²² As one of the pathways has been shown to proceed *via* nitrous acid and both reaction pathways are acid catalysed the effect of halide catalysis was briefly investigated.

The reaction of 1.5 mmol dm⁻³ peroxynitrous acid with 50 mmol dm⁻³ glutathione in 0.6 mol dm⁻³ acid was followed using stopped flow spectrophotometry with and without the addition of 50 mmol dm⁻³ NaBr, see Figure 3.14.

Reaction rate enhancement was observed with both pathways and in approximately the same proportion, Table 3.10, suggesting nucleophilic catalysis in both pathways, presumably through the formation of nitrosyl bromide.²²

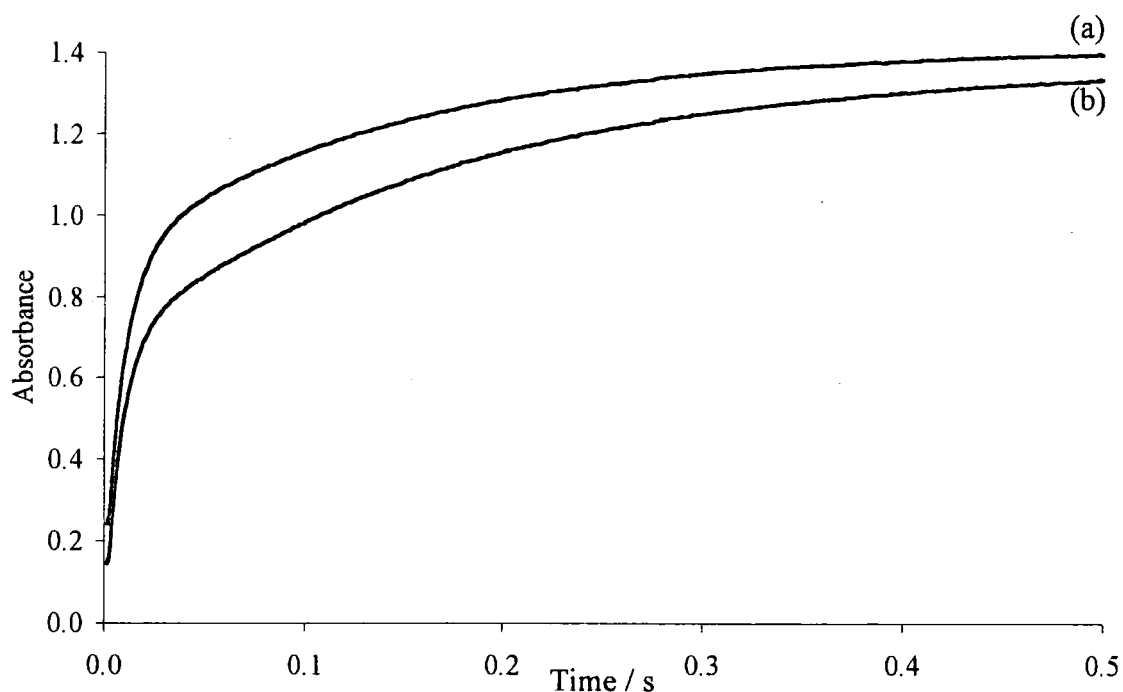


Figure 3.14 Reaction of 1.5 mmol dm^{-3} peroxynitrous acid with 50 mmol dm^{-3} glutathione in 0.6 mol dm^{-3} acid (a) with and (b) without the addition of 50 mmol dm^{-3} NaBr

NaBr	$k_{\text{fast}} / \text{s}^{-1}$	$k_{\text{slow}} / \text{s}^{-1}$
Without	71.9	5.79
With	105	7.16

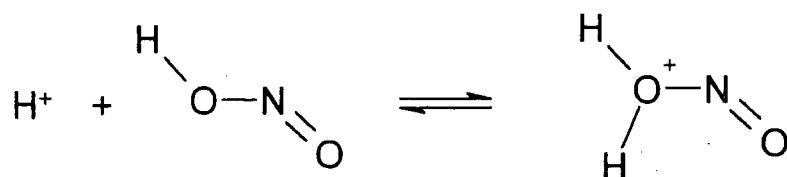
Table 3.10 Rate constants calculated using Scientist[®] from the absorbance time plots in Figure 3.14

3.7.4 Predicting the high acidity pathway

The high acidity pathway, k_{slow} , is suggested as a separate reaction mechanism but has similarities to the nitrosation of thiols by nitrous acid. Both pathways are acid catalysed, undergo bromide catalysis and produce a nitrosated product.

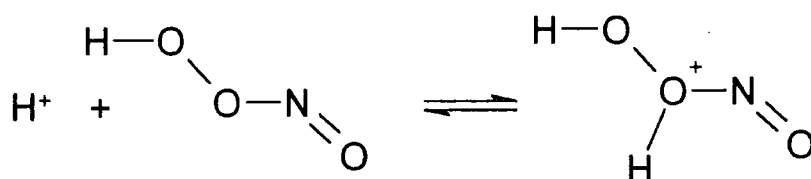
Therefore the prediction of a species similar to that proposed to be the active species in nitrosations by nitrous acid, seems plausible.

The proposed nitrosating agent in nitrosation by nitrous acid, is a protonated form of nitrous acid, Scheme 3.2, where water is the leaving group.²³



Scheme 3.2 Proposed species for nitrosation derived from nitrous acid

In a direct analogy to Scheme 3.2 a protonated form of peroxyxynitrous acid is suggested as the species responsible for direct electrophilic nitrosation of the thiol, Scheme 3.3.



Scheme 3.3 Proposed species for nitrosation derived from peroxyxynitrous acid

In the case of protonated peroxyxynitrous acid, H_2O_2 becomes the leaving group. Although this species has not been characterised it has been suggested as a possible reagent for the nitrosation of thiols in acetonitrile.⁵ Proton affinity studies on protonated peroxyxynitrous acid suggest protonation on the oxygen depicted in Scheme 3.3 to be the preferred site.²⁴

3.8 Conclusions

In slightly acidic solutions peroxynitrous acid has been shown to nitrosate thiols through an indirect pathway involving the oxidation of two thiol molecules to the corresponding disulfide, with concomitant reduction of peroxynitrous acid to nitrite. Under sufficiently acidic conditions nitrite forms nitrous acid, which may then nitrosate any remaining thiol to form RSNOs.

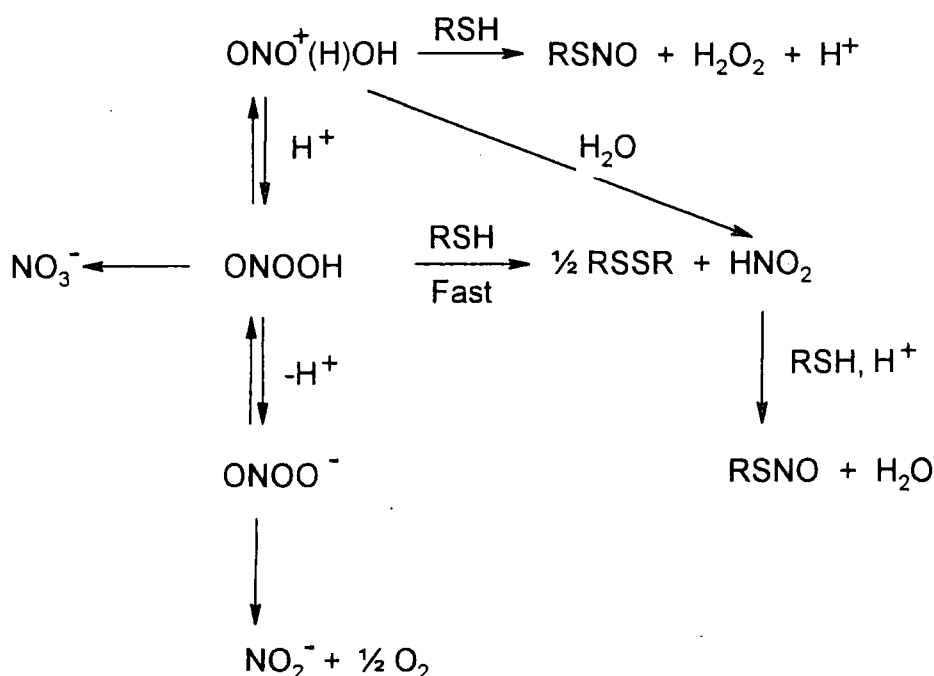
The formation of nitrous acid was confirmed when a two-fold excess of thiol was reacted with peroxynitrous acid. The characteristic five-fingered UV / Visible spectra of nitrous acid was observed which remained relatively stable due to the lack of any residual nitrosatable substrates, thus confirming the predicted stoichiometry.

The formation of RSNOs was quantitative when a large excess of thiol was used and was sufficiently rapid to out-compete the spontaneous decomposition of peroxynitrous acid to nitrate anion.

At higher acidities, $> 0.3 \text{ mol dm}^{-3}$, there was evidence that an alternative pathway was involved which also generated RSNOs. Both pathways were acid catalysed and an attempt was made to kinetically quantify both. Eventually at very high acid concentrations it seems that the slower rate of RSNO formation predominates but this could be a combination effect caused by the two observed rate constants becoming comparable. This does seem unlikely as the plots of k_{fast} and k_{slow} versus $[\text{H}^+]$ in Figure 3.12 do not seem to be tending toward one another. Also, given that the proportion of RSNO from each pathway has a dramatic switch from one to another it seems likely that the k_{slow} pathway predominates at higher acidity. This makes sense when considering the formation of protonated peroxynitrous acid as depicted in Scheme 3.3. If direct electrophilic nitrosation occurred then the oxidation of thiols to disulfide yielding nitrite would not be necessary.

A check for the absence of disulfide would confirm this but thiol oxidation occurs through the presence of H_2O_2 . A large excess was used in the generation of peroxynitrous acid and it would be the by-product of nitrosation by protonated peroxynitrous acid.

An overall scheme can therefore be predicted that accommodates both pathways and the possible decomposition pathways of peroxynitrite, Scheme 3.4.



Scheme 3.4 Reaction summary of the nitrosation of thiols by peroxynitrous acid

The possibility of nitrosation of water has been included in Scheme 3.4 as an alternative route to nitrous acid which may then nitrosate excess thiol.

Examination of Scheme 3.4 indicates the reasons for the switch from k_{fast} to k_{slow} i.e. the change from the indirect to the direct nitrosation pathway. Upon protonation peroxynitrous acid is proposed to form $\text{ONO}^+(\text{H})\text{OH}$ which in turn effects nitrosation, rather than oxidation, of the excess thiol. This crucial protonation step is the key to the entire scheme on which the rate of reaction and final product ratios from each pathway are dependent.

The direct nitrosation by protonated peroxynitrous acid has little physiological relevance, however the indirect nitrosation pathway may hold some significance. At physiological pH the small percentage yield of RSNOs reported^{1, 2} may be attributed to the indirect nitrosation pathway and at lower pH found in the stomach these reactions may have greater biological consequences.

3.9 References

- 1 A. van der Vliet, P. A. Chr. 't Hoen, Patrick S.-Y. Wong, A. Bast and C. E. Cross, *J. Biol. Chem.*, 1998, **273**, 30255.
- 2 "Methods in Nitric Oxide Research", p. 104, Ed. M. Feelisch and J. S. Stamler, John Wiley & Sons Ltd, Chichester, 1996.
- 3 F. S. Sheu, W. Zhu and P. C. W. Fung, *Biophys. Journal*, 2000, **78**, 1216; L. Rossig, B. Fichtlscherer, K. Breitschopf, J. Haendeler, A. M. Zeiher, A. Mulsch, S. Dimmeler, *J. Biol. Chem.*, 1999, **274**, 6823.
- 4 D. A. Wink, J. F. Darbyshire, R. W. Nims, J. E. Saavedra and P. C. Ford, *Chem. Res. Toxicol.*, 1994, **6**, 23; V. G. Kharitov, A. R. Sundquist and V. S. Sharma, *J. Biol. Chem.*, 1995, **270**, 28158.
- 5 L. Grossi, P. C. Montecvecchi and S. Strazzari, *Eur. J. Org. Chem.*, 2001, 131.
- 6 R. Radi, J. S. Beckman, K. M. Bush and B. A. Freeman, *J. Biol. Chem.*, 1991, **266**, 4244.
- 7 C. Quijano, B. Alvarez, R. M. Gatti, O. Augusto and R. Radi, *Biochem. J.*, 1997, **322**, 167.
- 8 J. O. Edwards and R. C. Plumb, *Prog. Inorg. Chem.*, 1994, **41**, 599.
- 9 D. L. H. Williams, *Nitric Oxide: Biology and Chemistry*, 1997, **1**, 522.
- 10 D. L. H. Williams, "Nitrosation", Ch. 7, Cambridge University Press, Cambridge, 1988.
- 11 D. J. Barnett, Ph. D. Thesis, University of Durham, 1994.
- 12 G. Y. Markovits, S. E. Schwartz and L. Newman, *Inorg. Chem.*, 1981, **20**, 445.
- 13 J. M. White, R. A. Manning and N. C. Li, *J. Am. Chem. Soc.*, 1956, **78**, 2367.
- 14 K. Varnagy, I. Sovago and H. Kozlowski, *Inorg. Chim. Acta.*, 1988, **151**, 117.
- 15 A. R. Amundsen, J. Whelan and B. Bosnich, *J. Am. Chem. Soc.*, 1977, **99**, 6730.
- 16 Micromath[®] Scientist[®] for Windows[®], Version 2.02.
- 17 P. A. Morris and D. L. H. Williams, *J. Chem. Soc., Perkin Trans. 2*, 1988, 513.
- 18 J. Casado, A. Castro, J. R. Leis, M. Mosquera and M. E. Pena, *ibid.*, 1985, 1859.
- 19 K. Al-Mallah, P. Collings and G. Stedman, *J. Chem. Soc., Dalton Trans.*, 1974, 2469.
- 20 J. Fitzpatrick, T. A. Meyer, M. E. O'Neill and D. L. H. Williams *J. Chem. Soc., Perkin Trans. 2*, 1984, 927.

- 21 C. H. Rochester, *Chem. Rev.*, 1957, 57, 1.
- 22 D. L. H. Williams, "Nitrosation", Ch. 7, Cambridge University Press, Cambridge, 1988.
- 23 Reference 22, Ch 1.
- 24 S. Kazazic, S. Kazazic, L. Klasinc, S. P. McGlynn and W. A. Pryor, *Croatica Chemica Acta*, 2001, 74, 271.

Chapter 4

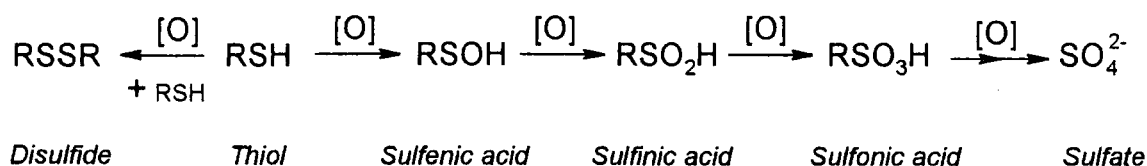
4 The antioxidant properties of *S*-nitrosothiols

The ability of *S*-nitrosothiols, RSNOs, to behave as antioxidants has been hypothesised in the biological literature¹ but with very little chemical evidence. In order to further the understanding of the chemistry of RSNOs *in vitro*, this chapter investigates their antioxidant properties, using the oxidation of thiols as a benchmark.

4.1 Introduction

A prerequisite for antioxidant capability is that the substrate is easily oxidised to a relatively stable species. The well-documented oxidation of thiols² shows that they are particularly good antioxidants as they may be oxidised as far as the stable sulfonic acid in a sequence of steps. The final oxidation product depends on the oxidation potential of the oxidant and also that of the substrate.

Oxidations generally proceed through the same successive stages of oxidation of the thiol, forming the sulfenic, sulfinic and sulfonic acids and in some cases sulfate ion, see Scheme 4.1.



Scheme 4.1 Thiol oxidation sequence [O] = Oxidant

Most sulfur oxidations result in non-linear kinetics such as oligooscillatory³ and clock-type reactions⁴ due to the multiple oxidation states available to sulfur atoms.

Thiol groups are prevalent in many biological functions utilising the thiol-disulfide couple, e.g. structure, catalysis and protection.⁵

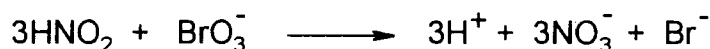
Particular interest has been shown in the protection of DNA⁶ and of thiols in cells⁷ by lower molecular weight thiols such as cysteine and glutathione. Their ability to be oxidised in place of the protein thiols lead them to be extremely potent antioxidants.

Many *in vivo* studies investigating the effects of antioxidants use potassium bromate, KBrO₃, to induce oxidative stress.

*Darkwa et al.*⁸ have recently studied the oxidation of cysteine with acidified bromate. The complex reaction proceeds through the sequential oxidations as in Scheme 4.1 but stops at the sulfonic acid stage and suffers no oxidation of the amino moiety. The reaction shows clock-type features with bromine formation after an induction period.

4.1.1 Properties of bromate

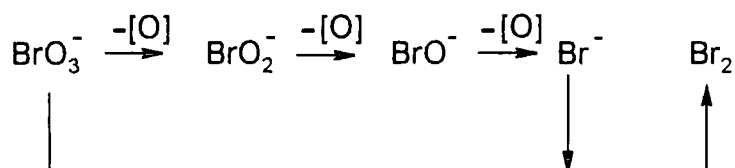
Bromates are strong oxidising agents ($E_0 = 1.52$ V). They rapidly oxidise sulfur based compounds potentially as far as sulfate (see Scheme 4.1) and nitrous acid to nitrate.⁹



Equation 4.1 Oxidation of nitrous acid by bromate

Even dry mixtures of bromates and sulfur will detonate on percussion. *Darkwa et al.*⁸ have shown that a powdered mixture of cysteine and potassium bromate will explode upon the addition of one drop of water, releasing bromine.

Bromates are extremely powerful oxidants due to their ability to transfer successively oxygen atoms to the substrate. The reduced species produced after oxygen transfer are even more potent oxidants than bromate itself, see Scheme 4.2.



Scheme 4.2 Sequential reduction of bromate producing even more potent oxidising species

Once bromide is formed it can react with any excess bromate present to yield bromine. This leads to autocatalytic behaviour in the oxidation of many substrates by bromate.

4.1.2 Use of bromates

Bromates, in particular potassium and sodium bromate, have found use in the baking, brewing, food, hair care and textile industries mainly due to their ability to modify thiol groups.¹⁰

In 1992, the World Health Organisation indicated that potassium bromate was “an inappropriate substance” for use as a food additive due to its mutagenicity and carcinogenicity.^{6, 11} The ability to mutate DNA is highlighted by the wide use of bromate as a renal oxidant in biological research.⁶ This is reflected by the latest EC drinking water directives, which contain for the first time a maximum limit for bromate present in drinking water, set at $10 \mu\text{g}/\text{dm}^3$.^{6, 11} Much of the bromate contamination of drinking water arises from the use of bromate as an industrial cleaning agent.

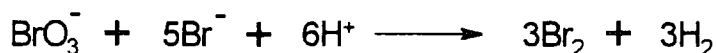
4.1.3 Oxidation of cysteine by acidified potassium bromate

In acidic aqueous solution, bromate sequentially oxidises cysteine to the sulfonic acid, cysteic acid, and is itself reduced to bromide. The oxidation reaction occurs exclusively at the sulfur centre and no cleavage of the C-S bond is observed, equation 4.2.



Equation 4.2 Oxidation of cysteine by bromate

If the concentration of bromate is in excess over the concentration of cysteine, the bromide produced will react with bromate to yield bromine, which may be detected spectrophotometrically at 390 nm, equation 4.3.



Equation 4.3 Pure oxyhalogen generation of bromine

If equation 4.3 occurs before the sulfur atom is completely oxidised, bromine will react with the sulfur species at diffusion controlled rates.⁸ Hence, the formation of bromine will only be spectrophotometrically detected once all of the cysteine has been oxidatively saturated.

The formation of bromine is a useful “marker” for the completion of cysteine oxidation. Usually it is difficult to measure and compare rates of thiol oxidation directly due to thiols being undetectable in the visible region of the electromagnetic spectrum. The use of bromate allows the determination of a definite end-point. The end-point has been utilised in this chapter to compare the antioxidant capability of RSNOs with that of thiols.

4.2 Oxidation of *S*-nitrosocysteine

4.2.1 Initial study with excess bromate

S-Nitrosocysteine, SNCys, was prepared as in, chapter 6.1.1 and used *in situ*.

The addition of SNCys to an acidified solution of potassium bromate, in a 2-fold excess over SNCys, facilitated rapid decay of SNCys and the slower formation of bromine once all of the SNCys had decomposed. This was conveniently observed using a stopped flow spectrophotometer equipped with diode array detector, see Figure 4.1.

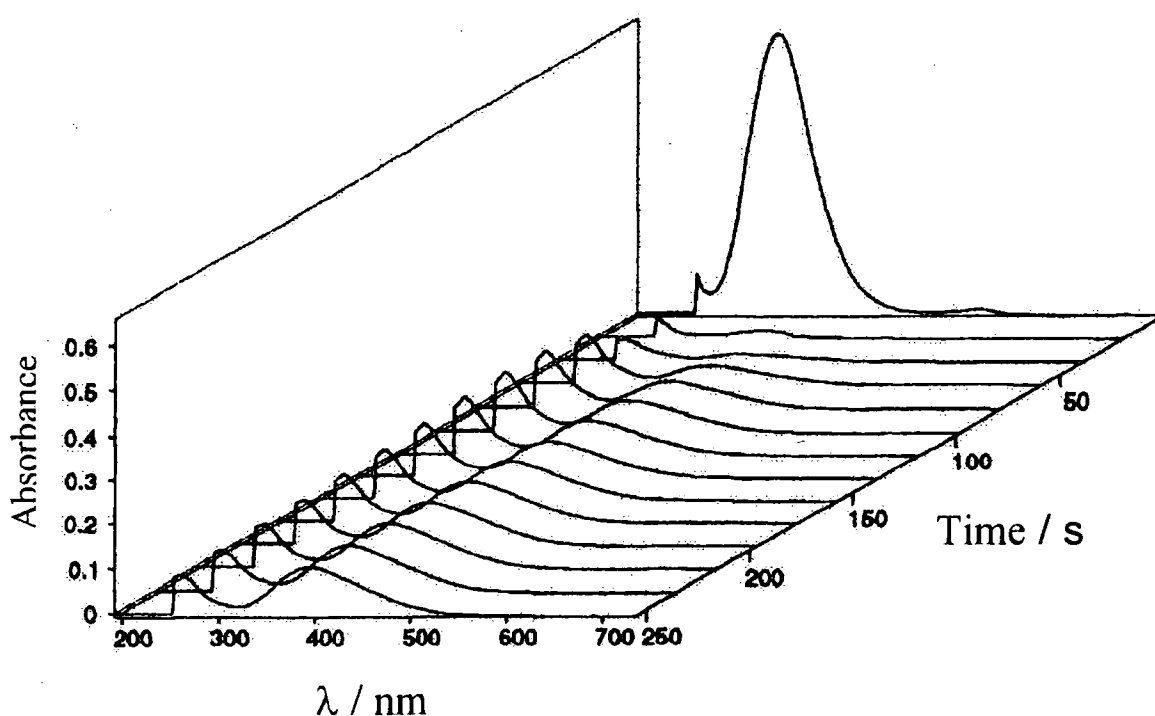


Figure 4.1 Diode array spectra (0 – 250 seconds) of the reaction between KBrO_3 ($2 \times 10^{-3} \text{ M}$) and SNCys ($1 \times 10^{-3} \text{ M}$) in 0.4 M HClO_4

Figure 4.2 shows the initial decay of SNCys over 0 – 15 seconds, displaying the rapidity of the reaction.

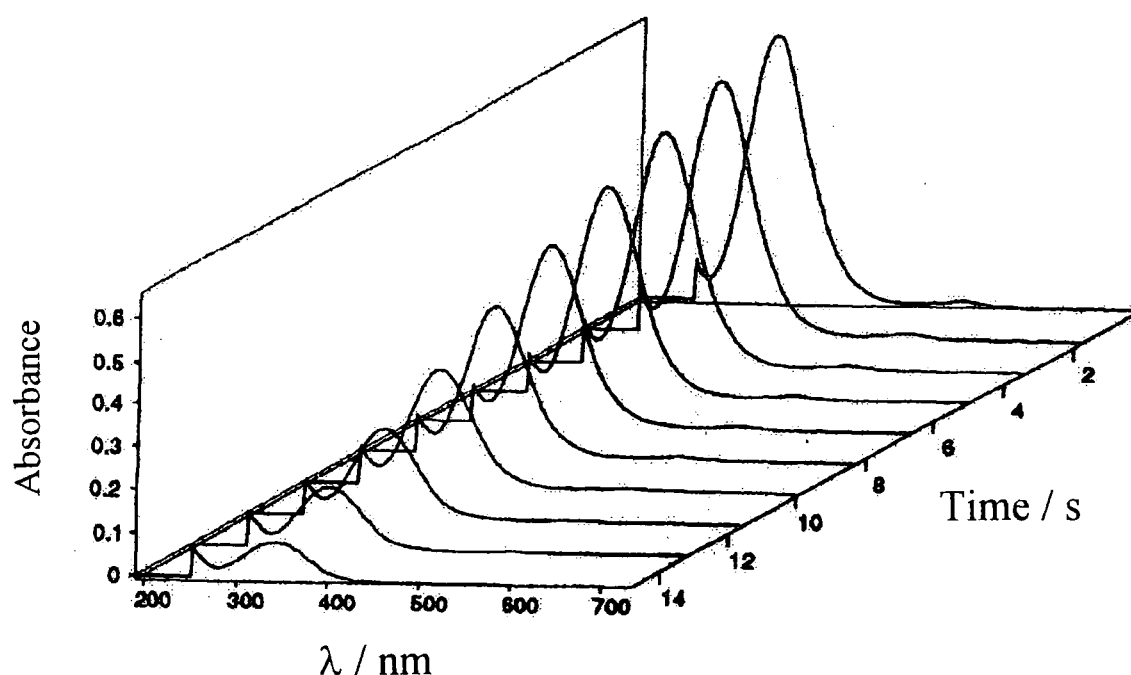


Figure 4.2 Expansion of the first phase of decomposition in Figure 4.1

Once it was established that acidified bromate could decompose SNCys the reaction was subjected to further study in order to allow comparisons with the analogous reaction involving cysteine.

The reaction was observed spectrophotometrically at 390 nm allowing convenient observation of the bromine formation and also the decay of SNCys, which also absorbs at 390 nm, on the tail of its characteristic peak at 340 nm, see Figure 4.3.

The initial section of trace (a) in Figure 4.3, shows the decay profile of SNCys, which is suggestive of an autocatalytic mechanism. This was postulated by Darkwa *et al.*⁸ for thiols but never proven due to the inability to follow cysteine decay, as it is undetectable in the visible region of the electromagnetic spectrum.

SNCys clearly displayed a shorter pre bromine time period than cysteine, i.e. the time taken for free bromine to develop. This indicates that SNCys is completely oxidised 5 times faster than its un-nitrosated analogue.

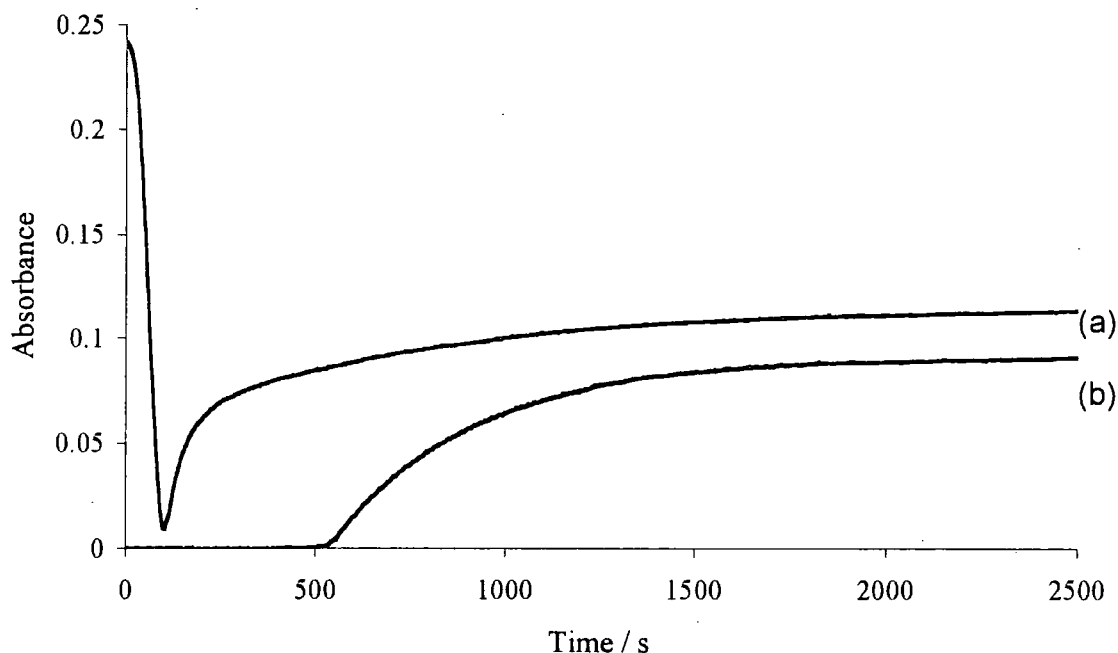


Figure 4.3 Reaction of substrate (1×10^{-3} M) with KBrO_3 (2×10^{-3} M) in 0.4 M HClO_4 , (a) SNCys (b) Cysteine

The percentage yield of bromine at the end of the reaction was calculated from Figure 4.3 by its extinction co-efficient at 390 nm ($\epsilon_{390} = 142 \text{ dm}^3 \text{ mol}^{-1} \text{ cm}^{-1}$)¹² (Table 4.1). Over 15% more bromine is produced with SNCys. The bromine formation curves are distinctly different and this will be discussed later in this chapter.

	Cysteine ^a	Cysteine ^b	SNCys ^a
Pre bromine time Period / s	540	~500 ^c	102
% Yield Br_2 (w.r.t. bromate)	64	63	80

^a This work. ^b Values taken from ref 8. ^c Estimated value from plots in ref 8.

Table 4.1 Comparisons between the reaction of acidified potassium bromate with SNCys and cysteine

4.2.2 Reaction with equimolar bromate

The formation of bromine signifies the complete reaction of the substrate and the subsequent onset of the pure oxyhalogen reaction, see equation 4.3. If equimolar amounts of the substrate and bromate are used, there should be no bromine formation. Figure 4.4 shows this to be true, displaying the rapid decay of SNCys. As hypothesised, no bromine is formed at the end of the reaction.

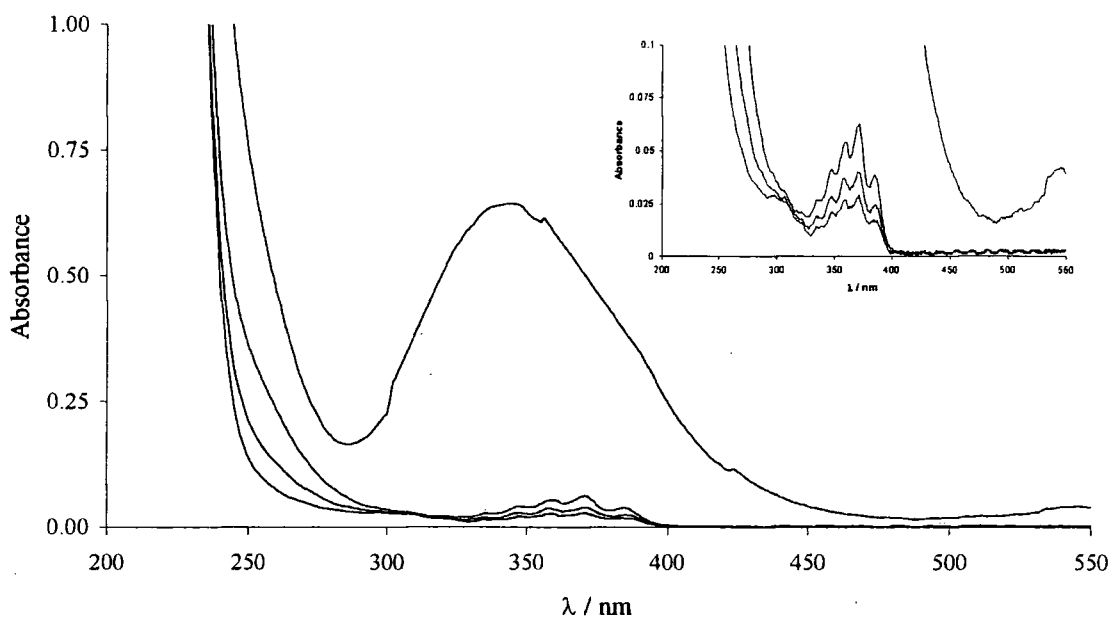


Figure 4.4 Repeat spectra scans (every 30 s) of the reaction between SNCys ($1 \times 10^{-3} \text{ M}$) and an equimolar amount of KBrO_3 in 0.4 M HClO_4

Inset : Expansion of nitrous acid peak

It has therefore been established that the reaction is analogous to bromate induced thiol oxidation in that one equivalent of bromate will oxidise one equivalent of SNCys. Additionally, the characteristic five-fingered spectrum of nitrous acid is observed and expanded in the inset of Figure 4.4. This gives further evidence of the involvement of the nitroso moiety in the reaction and that it too has been oxidised.

4.3 Determination of the sulfur product

In order to establish the stoichiometry of the reaction the end products must first be identified.

4.3.1 Detection of sulfate

Sulfate is classically determined gravimetrically through the precipitation of BaSO_4 after the addition of BaCl_2 .¹³ Solutions were analysed for sulfate 24 hours after initial reaction to guarantee that the reaction had reached completion. This also assured complete decomposition of bromate, as $\text{Ba}(\text{BrO}_3)_2$ is slightly insoluble in aqueous solutions. $\text{Ba}(\text{NO}_3)_2$ is soluble in water.

	BaSO_4	$\text{Ba}(\text{BrO}_3)_2$	$\text{Ba}(\text{NO}_3)_2$
Solubility g/dm^3	0.0022	3.0	87

Table 4.2 Solubility of barium salts in water at 25°C ¹⁴

The addition of barium chloride to the reaction solutions produced no precipitate implying that the highest possible oxidation state of the sulfur product is the sulfonic acid derivative of cysteine, cysteic acid (Figure 4.5).

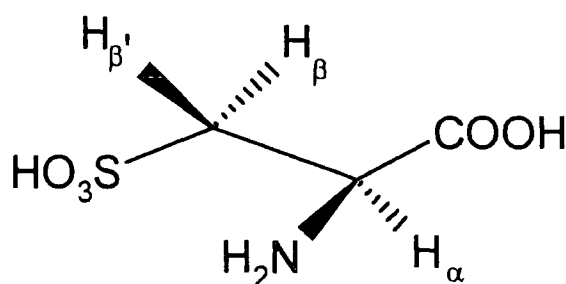


Figure 4.5 Cysteic acid (3-sulfo-alanine)

4.3.2 ^1H NMR determination of products

^1H NMR was used to characterise the organic products. Cysteine and its sulfur oxidised derivatives display classic ABX patterns in ^1H NMR. The geminal protons, H_β and $\text{H}_{\beta'}$, in Figure 4.5 are diastereotopic. This chemical shift inequivalence is a result of the adjacent chiral centre. The Newman projection, Figure 4.6, for the possible sulfur products clearly illustrates that the environment of the two methylene protons, H_β and $\text{H}_{\beta'}$, is never the same. Even upon rotation the chirality of the adjacent carbon atom ensures that the protons are not magnetically equivalent.¹⁵

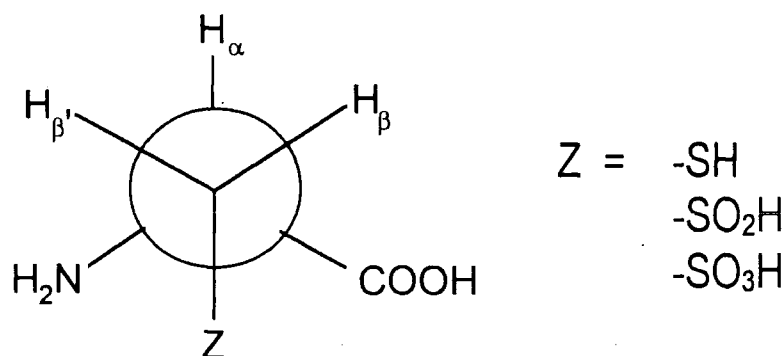


Figure 4.6 Newman projection for the potential sulfur products

The ABX system produces a distinct ^1H NMR spectrum as the proton on the chiral carbon, H_α , couples to each of the geminal protons, which in turn couple to each other. This produces a characteristic twelve line spectrum consisting of a double doublet for the X component and two double doublets for the AB component.

The chemical shift and coupling constants vary depending on the nature of the Z-substituent and are therefore useful tools to distinguish between RSH , RSNO , RSO_2H and RSO_3H . The reaction products were characterised by comparison of their ^1H NMR spectra with those obtained from authentic samples.

4.3.2.1 Experimental Procedure

^1H NMR spectra were obtained using a Varian Unity 300MHz spectrometer at ambient temperature. Authentic samples were dissolved in D_2O and acidified with HClO_4 (final acid concentration of 0.4 M) before transfer to an NMR tube. Spectra were then obtained for the authentic samples.

For the analysis of the products, the reactions were performed *in situ* by the addition of a little solid bromate followed by shaking to aid dissolution. Efficient mixing was necessary to facilitate the exchange of any labile protons for deuterons and thus remove any spectral complications arising from amine, carboxylic or thiol protons.

The effect of the shaking and the addition of HClO_4 caused an increase in the intensity of the HDO peak centred approximately about 4.7 ppm. However, the characteristic spectral region studied is well away from the HDO peak.

4.3.2.2 Spectra obtained

It was anticipated that with the absence of sulfate in the reaction products, the highest oxidised thiol derived species would be the sulfonic acid. The authentic sample displayed the hallmark twelve line spectrum expected from an ABX system, in addition to the large HDO peak, see Figure 4.7. Expansion of the spectra allowed the observation of the fine structure and determination of the coupling constants, Figure 4.8.

This was repeated for all authentic samples and SNCys, which was prepared and used *in situ*, by the procedure mentioned earlier.

Various reactions were performed and the product spectra taken in order to understand the possible oxidation products. Spectra of the reaction product solutions were obtained for cysteine with bromate, cysteine sulfonic acid with bromate and SNCys with bromate.

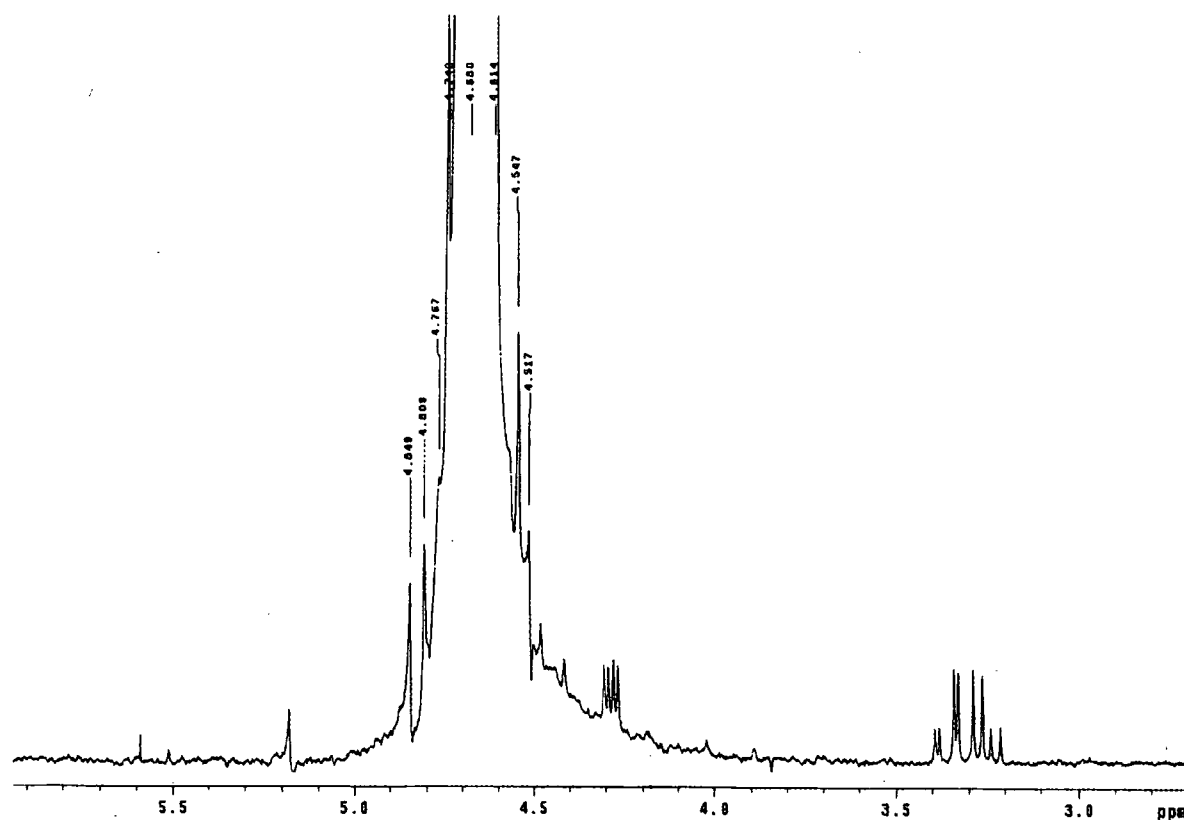


Figure 4.7 ^1H NMR spectra of authentic cysteic acid in 0.4 M HClO_4 / D_2O

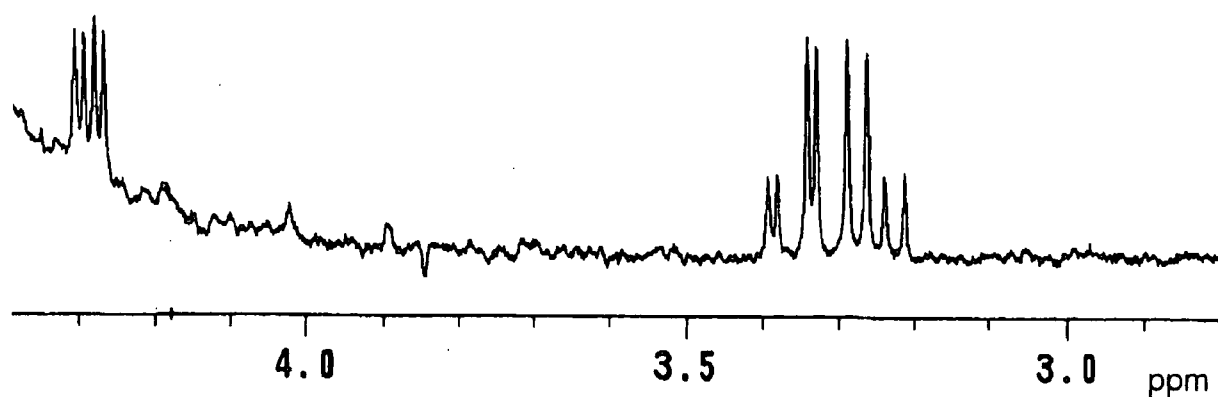


Figure 4.8 Enlarged section of Figure 4.8 displaying ABX splitting

All spectra obtained displayed this type of splitting except SNCys. The nitrosation of thiols results in a strong downfield chemical shift of around 1 ppm for the methylene protons, H_β and $H_{\beta'}$, and a small shift of 0.1 ppm for H_α .¹⁶ The splitting is not as pronounced and the coupling constants could not be determined.

The chemical shift and coupling constants were calculated for the other spectra and are displayed in Tables 4.3 to 4.5.

	δ/ppm				J/Hz		
	H_α	H_β	$H_{\beta'}$	$H_\beta - H_{\beta'}$	$J_{\alpha\beta}$	$J_{\alpha\beta'}$	$J_{\beta\beta'}$
CYS	4.16	3.03	2.94	0.09	4.5	5.5	15
CYSO ₂ H	4.38	3.05	2.89	0.16	4.2	8.4	14
CYSO ₃ H	4.29	3.36	3.25	0.11	3.6	7.8	15

Table 4.3 Chemical shift and coupling constants from authentic samples

The authentic samples, although displaying almost identical ABX spectra have some key differences in their coupling constants and their chemical shifts. $H_{\beta'}$ is at the highest field and is affected most by oxidative modification of the sulfur atom.

	δ/ppm				J/Hz		
	H_α	H_β	$H_{\beta'}$	$H_\beta - H_{\beta'}$	$J_{\alpha\beta}$	$J_{\alpha\beta'}$	$J_{\beta\beta'}$
CYSO ₂ H + KBrO ₃ (1 hour)	4.29	3.36	3.25	0.11	3.6	7.8	15
CYS + KBrO ₃	4.29	3.36	3.25	0.11	3.6	7.8	15

Table 4.4 Chemical shift and coupling constants from authentic samples after reaction with KBrO₃

The reaction of bromate with cysteine or cysteine sulfinic acid developed products that were identical in chemical shift and coupling constants, see Table 4.4, thus confirming that the oxidation of thiols and sulfinic acids by bromate produced the sulfonic acid in both cases. It was noticeable that the final sulfonic acid spectra took longer to generate from the sulfinic acid than from cysteine.

The reaction of SNCys with bromate, gave a product with identical spectra to the authentic cysteic acid after ten minutes, see Table 4.5

	δ /ppm				J / Hz		
	H α	H β	H β'	H β – H β'	J $\alpha\beta$	J $\alpha\beta'$	J $\beta\beta'$
SNCYS	4.26	4.10	4.09	0.01	-	-	-
SNCYS + KBrO ₃ (10 min)	4.32	3.40	3.29	0.11	3.6	7.8	15
SNCYS + KBrO ₃ (2 hour)	4.32	3.40	3.29	0.11	3.3	8.1	15

Table 4.5 Chemical shift and coupling constants from SNCys before and after reaction with KBrO₃

There were minor differences in chemical shift between the authentic and SNCys derived cysteic acid. This was due to slight differences in solution acidity. However, it was possible to use the difference between the chemical shift of the geminal protons, H β – H β' , rather than the shift itself. As the acidity of the medium affects both the protons, the difference between them is always constant and is therefore a useful tool.

H β – H β' for cysteic acid was shown to be 0.11 ppm and this was found in the reaction product spectra also. Therefore, the end sulfur product was shown to be the sulfonic acid, as with the analogous reaction with thiols.

4.3.3 Sulfur product at equimolar concentrations

The procedure was repeated as in 4.3.2.1 but with equimolar concentrations of SNCys and bromate. The ¹H NMR product spectra proved the sulfur product to be the sulfonic acid which has implications on the equimolar reaction equation which will be discussed later.

4.4 Determination of the nitrogen product

The reaction between equimolar concentrations of bromate and SNCys did not yield bromine. The repeat scan spectra in Figure 4.4 showed that nitrous acid was formed. The reaction of nitrous acid and bromate is well known,⁹ equation 4.1, and yields bromide. Therefore, an excess of bromate would react with bromide developing bromine. The ultimate nitrogen product was anticipated to be nitrate.

This hypothesis was tested initially by the reaction of nitrous acid with excess bromate. Figure 4.9 shows the initial nitrous acid peak and the final bromine peak. There is a small increase in absorbance at 300 nm, which is due to the formation of nitric acid.

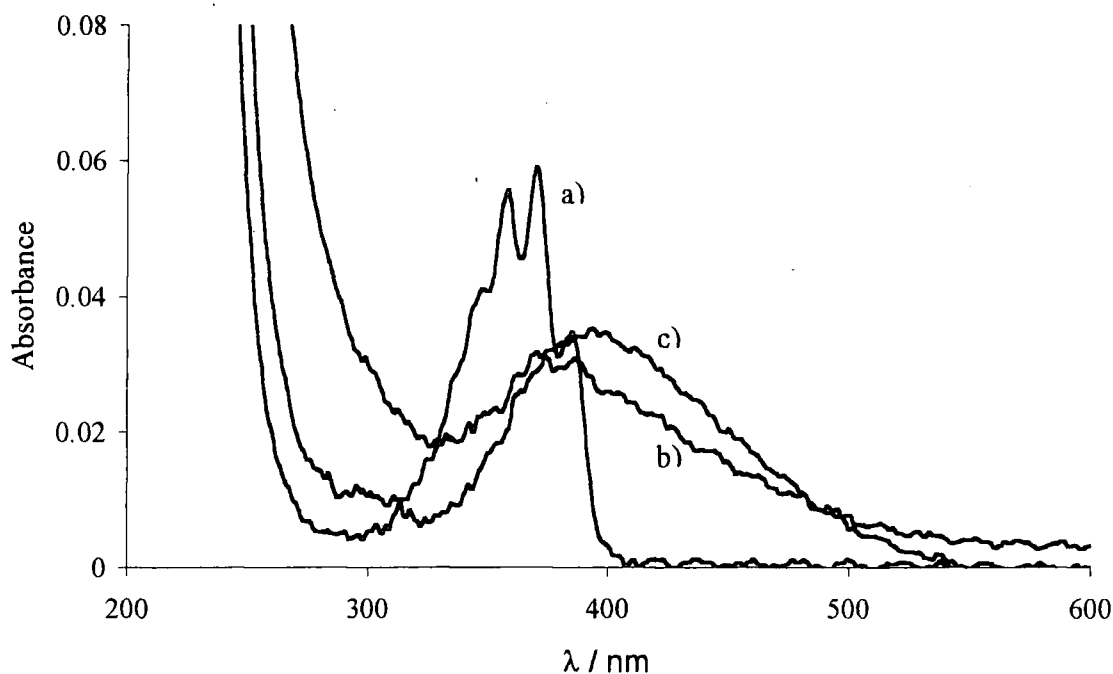
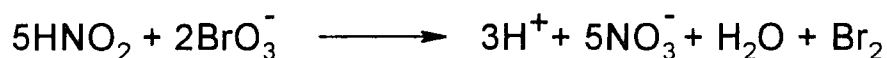


Figure 4.9 Spectral scan of HNO₂ (1.2 mM) in HClO₄ (0.4 M) with the addition of 25 mM KBrO₃, a) HNO₂ alone before addition, b) 30 s after addition, c) End of reaction, constant after 60 s

With excess KBrO₃, equation 4.1 is modified to include the bromine formation component and becomes equation 4.4.



Equation 4.4 Reaction of nitrous acid with excess bromate

The stoichiometry of the reaction states that five equivalents of nitrous acid will yield one equivalent of bromine.

The concentration of each reagent and product was determined using its extinction coefficient. Table 4.6 shows the calculation of the nitrous acid concentration by the four extinction co-efficients determined by Markovits *et al.*¹⁷

λ / nm	Abs	$\epsilon^a / \text{dm}^3 \text{mol}^{-1} \text{cm}^{-1}$	$[\text{HNO}_2]^b / \text{M}$
347	0.041	32.8	1.25E-03
358	0.055	47.7	1.15E-03
371	0.059	49.4	1.19E-03
386	0.034	28.6	1.19E-03

Table 4.6 Calculation of $[\text{HNO}_2]$ from the extinction co-efficients

- a From reference 17
b Calculated $[\text{HNO}_2] / \text{M}$

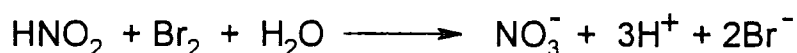
For equation 4.4 to hold, one would expect a final bromine concentration of 2.4×10^{-4} M and an absorbance of 0.034 at 390 nm ($\epsilon_{390} = 142 \text{ dm}^3 \text{mol}^{-1} \text{cm}^{-1}$)¹². This was experimentally achieved.

The time scale of the reaction is such that, in the reaction of SNCys with bromate the nitrous acid developed can easily produce bromine itself, hence creating two possible routes to the bromine product. Closer examination of the initial time drive work reveals this to be the case and will be discussed later.

4.4.1 Quantification of the nitrogen product

The characteristic UV/Vis absorbance of nitrate was used to quantify the nitrogen product. This could not be achieved using Figure 4.9, as the concentrations used were insufficient to accurately quantify nitrate due to its small extinction co-efficient. Nitrate absorbs at 302 nm with extinction co-efficient of $7 \text{ dm}^3 \text{ mol}^{-1} \text{ cm}^{-1}$.¹⁸

At higher concentrations, direct UV/Vis quantification of nitrate became further complicated by the large absorbance of the bromine product overlapping the nitric acid peak. However bromine can be conveniently reduced to bromide, which does not interfere spectrally with the nitrate absorbance, using nitrous acid which itself is oxidised to nitrate.



Equation 4.5 Reduction of bromine by nitrous acid

Therefore a known amount of nitrous acid may be used and the extra absorbance at 302 nm is then attributed to the original concentration of nitrate.

Equation 4.5 may be deemed as quantitative and irreversible as defined by the equilibrium constant of $1.6 \times 10^{-6} \text{ M}^{-3}$ for the nitric acid-bromide reaction.¹⁹

4.4.2 Experimental procedure

SNCys (0.05 M) was reacted with an excess amount of bromate (0.1 M) in 0.4 M HClO_4 and left to react completely. The solution was then treated with 0.1 M sodium nitrite to reduce the bromine and any excess bromate to bromide. The sodium nitrite added was quantitatively oxidised to nitrate.

It was anticipated that the concentration of nitrate could then be calculated from the absorbance at 302nm. Unfortunately this could not be achieved due to the residual absorbance present from the sulfur products, see Figure 4.10.

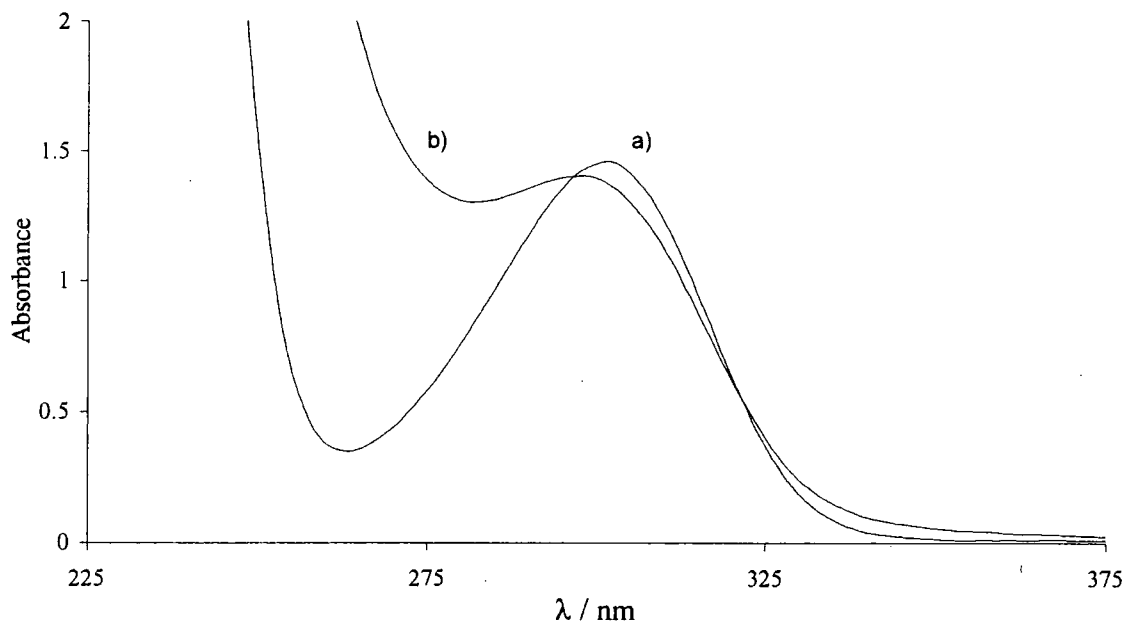


Figure 4.10 a) 0.2 M NaNO_3 in 0.4 M HClO_4
b) End product scan after NaNO_2 treatment

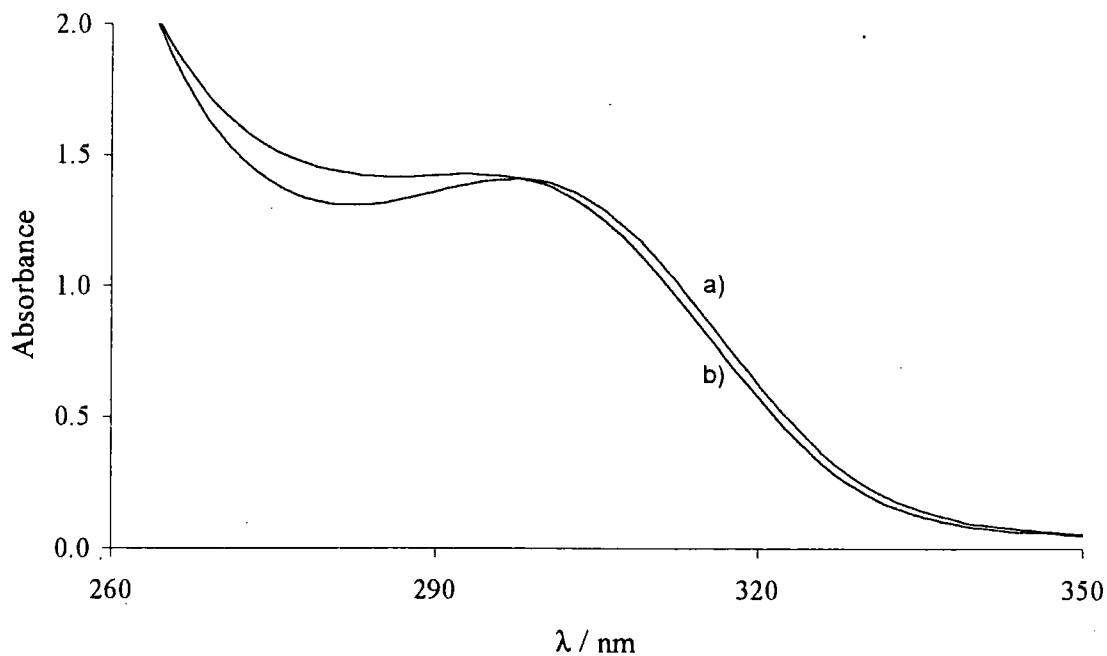


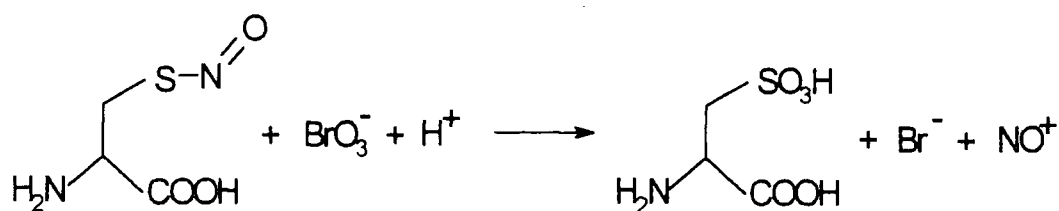
Figure 4.11 a) Cysteine product after NaNO_2 treatment with added NaNO_3
b) SNCys product after NaNO_2 treatment

To compensate for this, the experiment was repeated using cysteine in place of SNCys and a balance amount of nitrate was added (0.05M) to simulate the conditions with SNCys. The resultant product spectra displayed identical absorbances in the wavelength region investigated, Figure 4.11.

It was therefore assumed that nitrate was the quantitative nitrogen product.

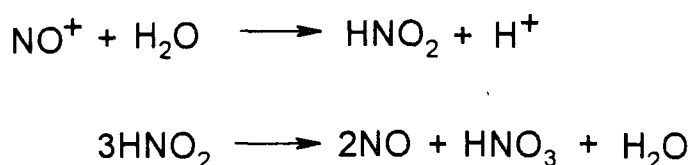
4.5 Reaction stoichiometry

The products of the reaction between SNCys and excess acidified bromate have been determined as cysteic acid and nitrate. The products of the reaction at equimolar concentrations were cysteic acid and nitrous acid. The equimolar reaction must also yield bromide because with excess bromate, bromine is developed. Therefore the stoichiometry of the reaction must follow equation 4.6.



Equation 4.6 Stoichiometry of the reaction at equimolar concentrations of SNCys and KBrO₃

The nitrosonium ion, NO⁺, will immediately react with water to yield nitrous acid, see Scheme 4.3, which will then decay in acidic media to nitrate and nitric oxide²⁰ as observed in Figure 4.5.



Scheme 4.3 Nitrogen products at equimolar concentrations of SNCys and KBrO₃.

The reaction that forms bromine is an extraneous pure oxyhalogen reaction that will only occur when bromate is in stoichiometric excess. It was therefore possible to use this to determine the overall equation by varying the [SNCys]:[bromate] ratio.

As the amount of SNCys is increased the percentage yield of bromine formed also increases, see Figure 4.12, as measured by the absorbance at 390nm. All measurements were taken two hours after the reaction was initiated, ensuring complete conversion.

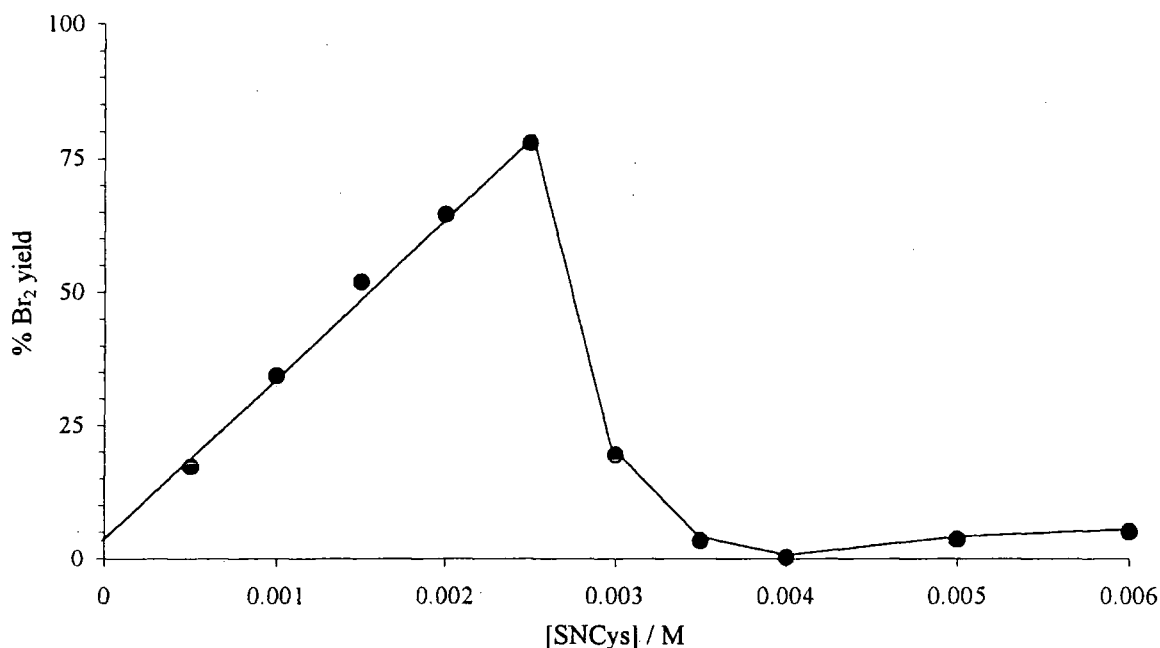


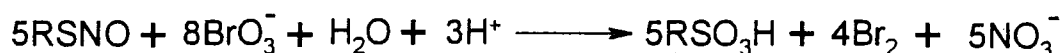
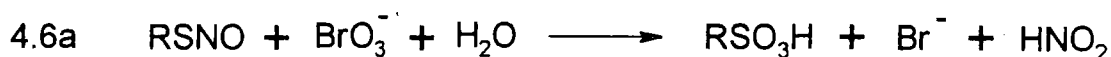
Figure 4.12 Determining the stoichiometric point. Varied [SNCys] with 4 mM bromate in 0.4 M HClO₄. The points are an average of 3 replicates

The plot reaches a maximum value, as more bromide ions are made available to react with the excess bromate. The maximum equates to 78% conversion to bromine with respect to bromate. Further increasing the concentration of SNCys results in a decrease in the yield of bromine. As the bromate is progressively used up there can be no production of bromine from the bromide produced.

Therefore, the stoichiometry obtained at the formation of the maximum amount of bromine equates to a SNCys:bromate ratio of 5:8.

4.5.1 Overall Reaction stoichiometry

The overall reaction can therefore be defined using a combination of the following equations.



Equation 4.7 Overall stoichiometry when bromate is in excess

Equation 4.6a is a modified version of equation 4.6 to include the nitrosation of water.

The RSNO to bromate ratio of 5:8 is as predicted by Figure 4.12 and the maximum bromine yield of 80% equates to the 5:4 RSNO:bromine ratio.

Once the overall equation was determined it became possible to look at the effects of varying acid and bromate concentrations.

4.6 Varying the concentration of bromate

The aim of this study was to compare qualitatively the antioxidant capability of RSNOs and thiols, as a quantitative approach would be extremely complex given the species involved. The primary reason for the use of bromate is its ability to determine the end-point of the thiol oxidation.

It was not possible to obtain clean first order kinetics even with a large excess of bromate and acid. However, it was possible to gain important confirmation of the reaction stoichiometry by varying the concentration of bromate.

4.6.1 Experimental procedure

Varying concentrations of bromate were reacted with 1 mM SNCys in 0.4 M HClO₄. The reaction was followed spectrophotometrically at 390nm, as previously, where the decomposition of SNCys could be monitored along with any formation of bromine, see Figure 4.13.

The traces produced were initially sigmoidal, which is characteristic of an autocatalytic mechanism, displaying the decomposition of SNCys. With an equimolar amount of bromate, the peripheral oxyhalogen reaction was not observed. This was expected, as all of the bromate would be reduced to bromide leaving none for the pure oxyhalogen reaction.

As the amount of bromate increases, the time taken for bromine to develop and the initial plateau decrease. The rate of formation of bromine also increases and takes on a single exponential profile as the bromate concentration increases.

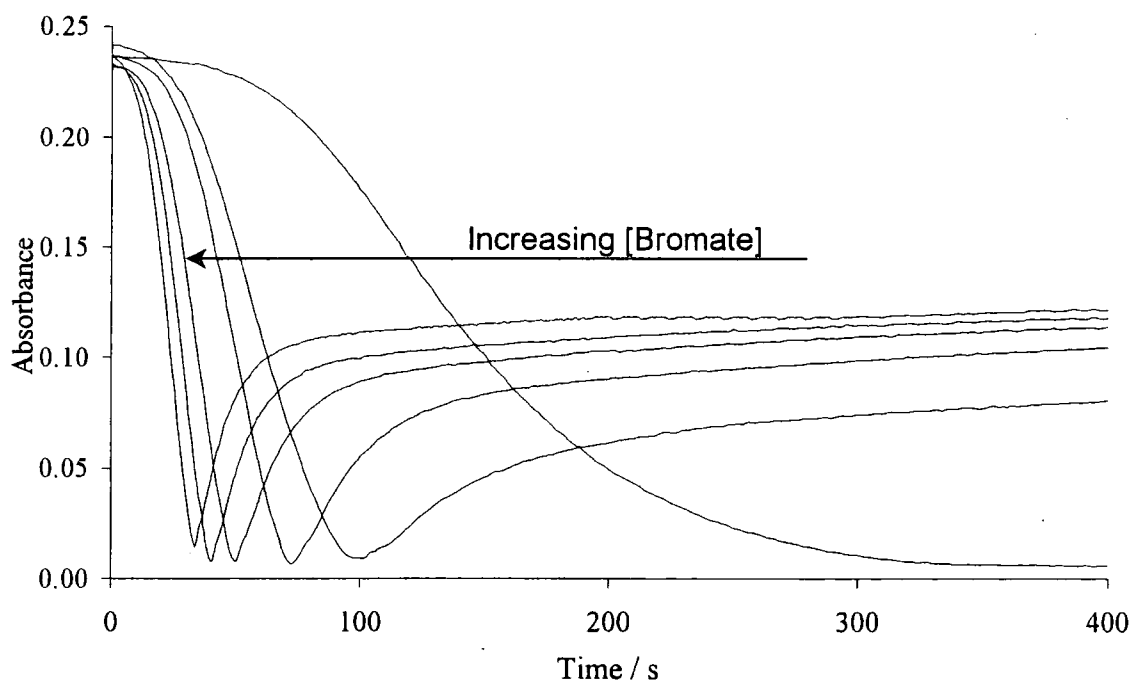


Figure 4.13 Varying concentrations of bromate (1 mM, 2 mM, 3 mM, 4 mM, 5 mM, 6 mM) with 1 mM SNCys in 0.4 M HClO₄

As expected, it was impossible to determine any rate constants for the decay of SNCys due to the complexity of sulfur oxidation. However, the time period prior to bromine formation could be used as a guide for the speed of the reaction and the dependence on bromate concentration.

4.6.2 Utilising the pre-bromine time period

The pre-bromine time period is taken to imply the time when all of the SNCys has decayed and the onset of bromine formation occurs. As we increase the concentration of bromate, the period shortens. This is due to more oxidant being present; hence the reaction proceeds more quickly.

$[\text{KBrO}_3]/\text{M}$	t_{ind}/s	$(1/t_{\text{ind}})/\text{s}^{-1}$
0.002	98	0.010
0.003	56	0.019
0.004	38	0.028
0.005	30	0.037
0.006	24	0.048

Table 4.7 Variation in pre bromine time periods with increasing $[\text{KBrO}_3]$ plotted in Figure 4.14

The pre bromine time period displays an inverse dependence on the initial concentration of bromate.

Figure 4.14 shows the relationship as a plot of the inverse of the pre bromine time period versus bromate concentration. The fit line displays a negative intercept, and crosses the x-axis at 1mM bromate. This gives valuable confirmation of equation 4.6a, whereby no bromine is produced at equimolar SNCys:bromate. This is the limiting bromate concentration before bromine is formed and, as predicted, when we have an excess over the required stoichiometry of equation 4.6a, bromine formation results.

Once the bromate is in sufficient excess the stoichiometry of the reaction follows equation 4.7.

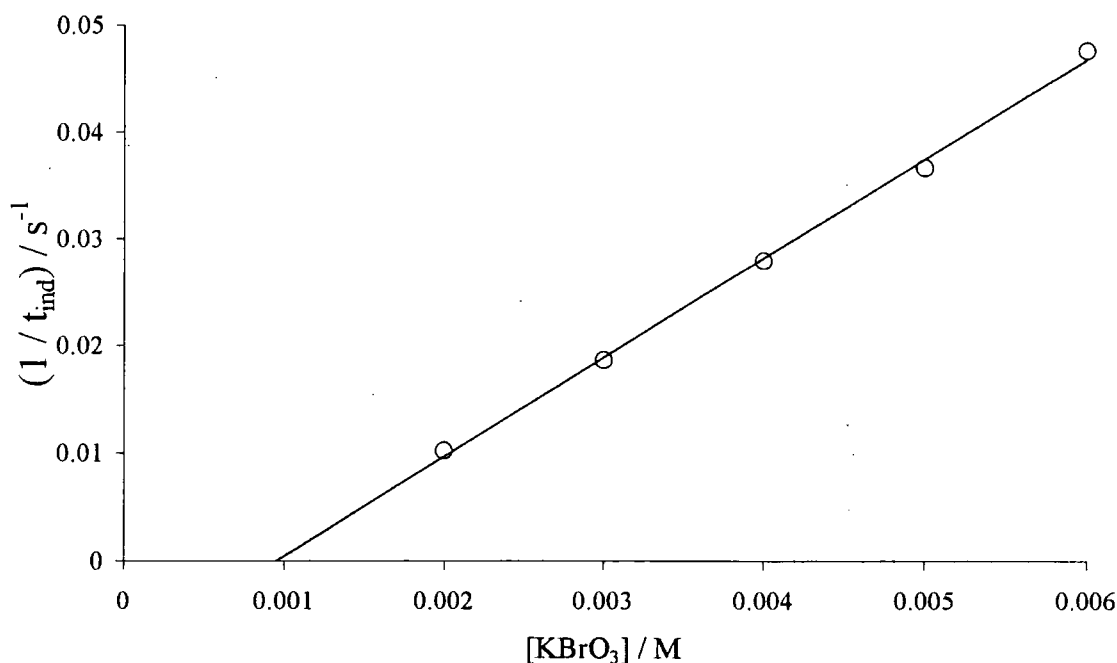


Figure 4.15 Plot of the inverse pre bromine time period versus bromate concentration

4.6.3 Bromine formation

The rate of formation of bromine is dependent on the concentration of bromate present.

In the reaction between cysteine and bromate, Figure 4.3 (b), the only route to bromine is the extraneous oxyhalogen reaction, equation 4.3. This cannot occur until bromide is ultimately formed and there is sufficient bromate present to react. It was anticipated that any bromine formed, before all of the sulfur and nitrogen species were oxidatively saturated, would react with them at extremely fast rates. Hence bromine is removed faster than it is produced until the nitrogen and sulfur species are oxidised to nitrate and sulfonic acid, respectively. From this point bromine is free to form.

In the reaction between SNCys and bromate, nitrous acid is formed rapidly upon the decay of SNCys and will react with bromate, equation 4.4, to yield bromine rapidly, Figure 4.9. The formation of bromine from the “nitrogen source” must occur more rapidly than the “sulfur source”, as determined by inspection of Figure 4.3. The

bromine produced will react extremely quickly with the SNCys still present and its oxidised analogues. The halogen product is bromide, which is then free to react with excess bromate and produce more bromine, thus beginning the autocatalytic stage of the reaction.

4.6.4 Bromine formation with a two-fold excess of bromate over SNCys

A two-fold excess of bromate over SNCys results in two-stage formation, an initial fast period followed by a slower formation phase, see Figure 4.3 (a). This is due to a decrease in the rate of the bromine forming oxyhalogen reaction as the concentration of bromate is reduced through its reaction with SNCys.

The initial fast phase is due to formation of bromine from the reaction of nitrous acid with bromate, the “nitrogen source”. This is followed by a slower formation resulting from the pure oxyhalogen reaction, equation 4.3.

With a larger excess of bromate over SNCys, the bromine formation was faster and of exponential nature because the oxyhalogen reaction (equation 4.3) yields bromine at a comparable rate to the nitrogen source.

The kinetics of the bromate-bromide reaction are complex but have been well studied.²¹ As the RSNO has reacted completely, the kinetics of the formation of bromine are inconsequential to this study.

4.7 Varying the acid concentration

Most oxyhalogen oxidations are strongly catalysed by acid.²² Bromate oxidation of thiols displays a linear relationship between the inverse of the pre bromine time period and the concentration of the acid squared.⁸ The acid concentration did not affect the final bromine yield.

With SNCys the decay traces show the expected decrease in the pre bromine time period with increasing acid concentration, Figure 4.16.

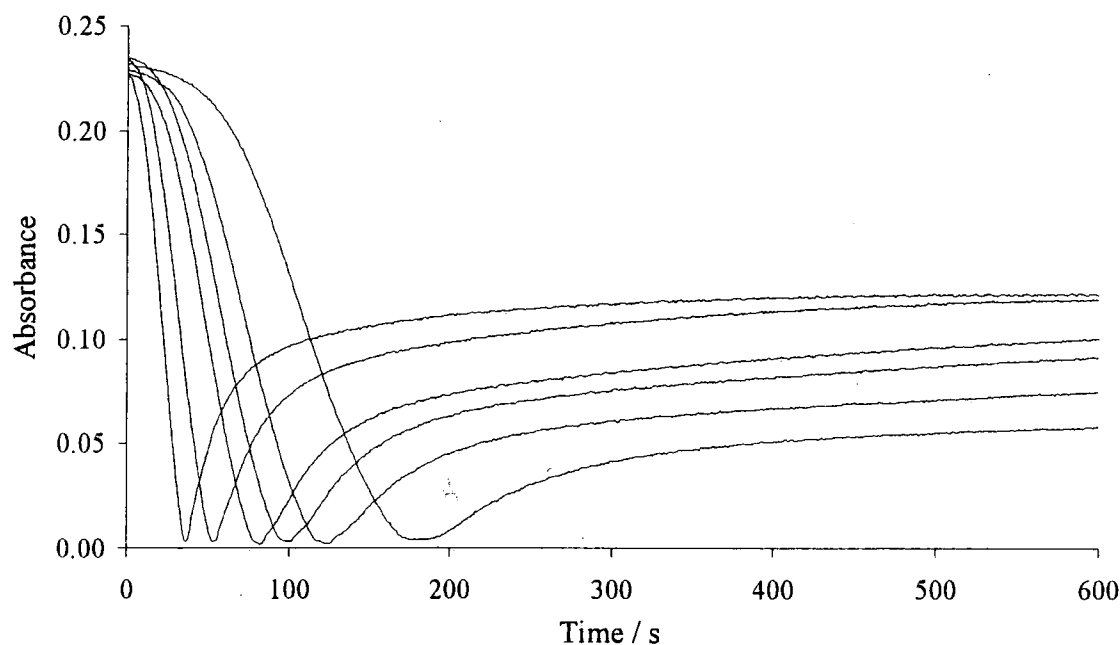


Figure 4.16 Decomposition of SNCys (1 mM) by bromate (2 mM) in varying $[\text{HClO}_4]$:- 0.3 M, 0.4 M, 0.5 M, 0.7 M, 0.9 M and 1 M

The traces also show that the inverse of the pre bromine time period is linearly proportional to the square of the acid concentration, Figure 4.17.

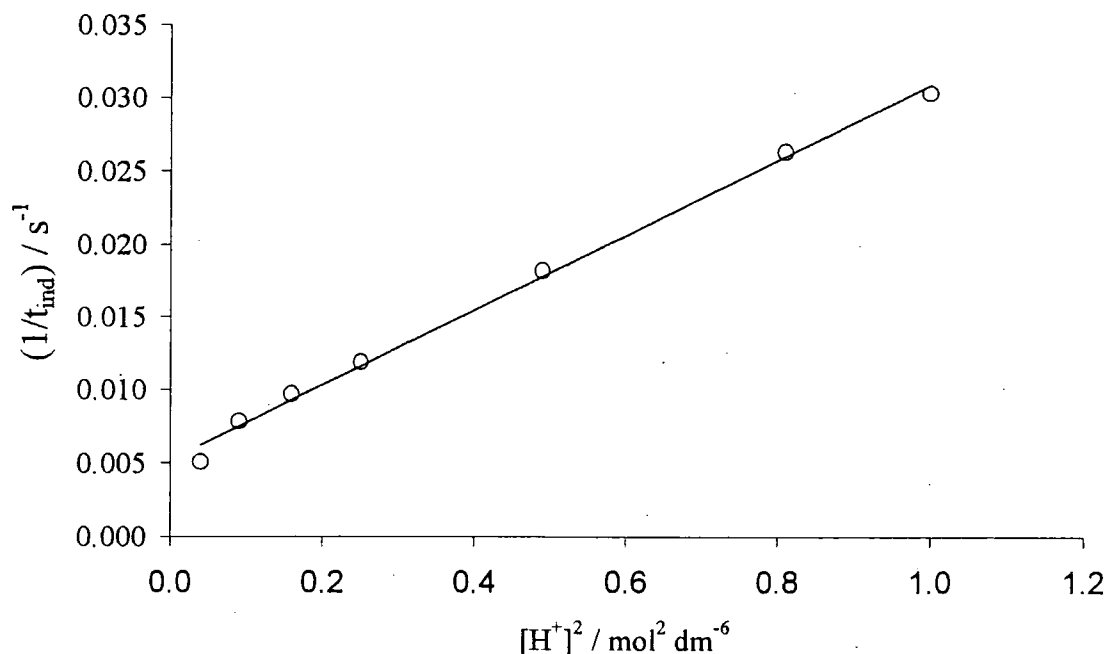


Figure 4.17 Plot of the inverse pre bromine time period versus the square of $[\text{HClO}_4]$ from Figure 4.16.

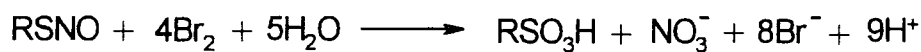
This indicates that the reaction prior to bromine formation is strongly catalysed by acid. It is impossible to claim that it is second order in acid, although, this has been implied by some groups studying the oxidation of other substrates by acidified bromate.²³

The slight intercept in Figure 4.17 may be attributed to complexities arising from the introduction of the nitroso moiety, as this is not evident in the reaction with thiols. The reasons for the intercept are currently unknown.

4.8 Bromine oxidation of SNCys

The reactions of bromine with many sulfur-based molecules such as cysteine⁸ and thiocyanate²⁴ are diffusion controlled. The reaction of bromine with SNCys was difficult to measure as relatively large quantities of RSNO were needed to gain a measurable absorbance, therefore the rate of decay was very fast. An attempt was made to follow the reaction by stopped flow spectroscopy but even this technique was too slow and the reaction was complete within the mixing time. This has strong

implications for the reaction scheme, whereby any bromine produced will be reduced immediately to bromide whilst concurrently oxidising any oxidatively unsaturated molecules that remain. Overall, bromine oxidises RSNOs to the sulfonic acid and nitrate, equation 4.8.



Equation 4.8 Bromine oxidation of RSNOs

4.9 Reaction of bromate and SNCys at physiological pH

Two experiments were performed at pH 7.4.

Firstly to test if bromate in a 1000-fold excess would decompose SNCys. This was performed in the presence of EDTA to eliminate the copper catalysed decay. No reaction was apparent and the only observable decomposition was comparable to that expected for the photochemical/thermal decomposition pathways.

Secondly the reaction was repeated without EDTA and with buffer amounts of copper present, approximately 10^{-6} M.²⁵ A slight decrease in reaction rate was observed versus the control (without bromate) attributed to oxidation of the thiolate or Cu^+ as predicted for H_2O_2 in chapter 2. It is noteworthy that the bromate was in 1000-fold excess and as only a slight attenuation of reaction occurred this was not pursued further.

4.10 Other RSNOs

Two other RSNOs were studied, *S*-nitrosoglutathione, GSNO and *S*-nitrosopenicillamine, SNP. The reactions were performed under identical conditions with 1 mM RSNO reacting with 2 mM KBrO_3 in 0.4 M HClO_4 . The reactions were followed spectrophotometrically at 390 nm, Figure 4.18.

The red line displays the decomposition of the benchmark SNCys. GSNO (blue line) and SNP (green line) were twice as fast in the initial decay than SNCys. The rate of loss of the nitroso moiety in GSNO and SNP are comparable. The interesting section is the phase prior to bromine formation. With SNCys the onset of bromine occurs immediately after the decay of SNCys. GSNO and SNP show a phase of zero absorbance change. This is attributed to the slower oxidation of the intermediates between the RSH and the final oxidation product, RSO_3H .

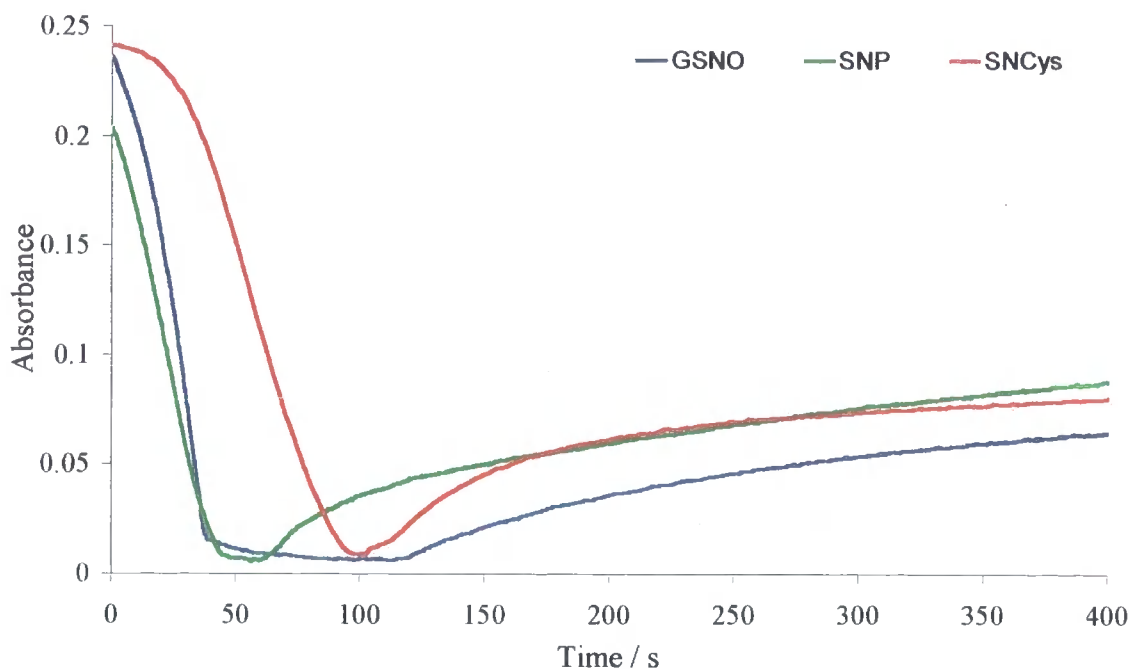


Figure 4.18 Reaction of 2 mM KBrO_3 and 1 mM RSNO in 0.4 M HClO_4

Amazingly, even though GSNO seems most susceptible to denitrosation, it is the slowest to reach the oxidatively saturated stage signified by bromine formation. Other authors have also noticed the resistance of GSH to oxidation²⁶

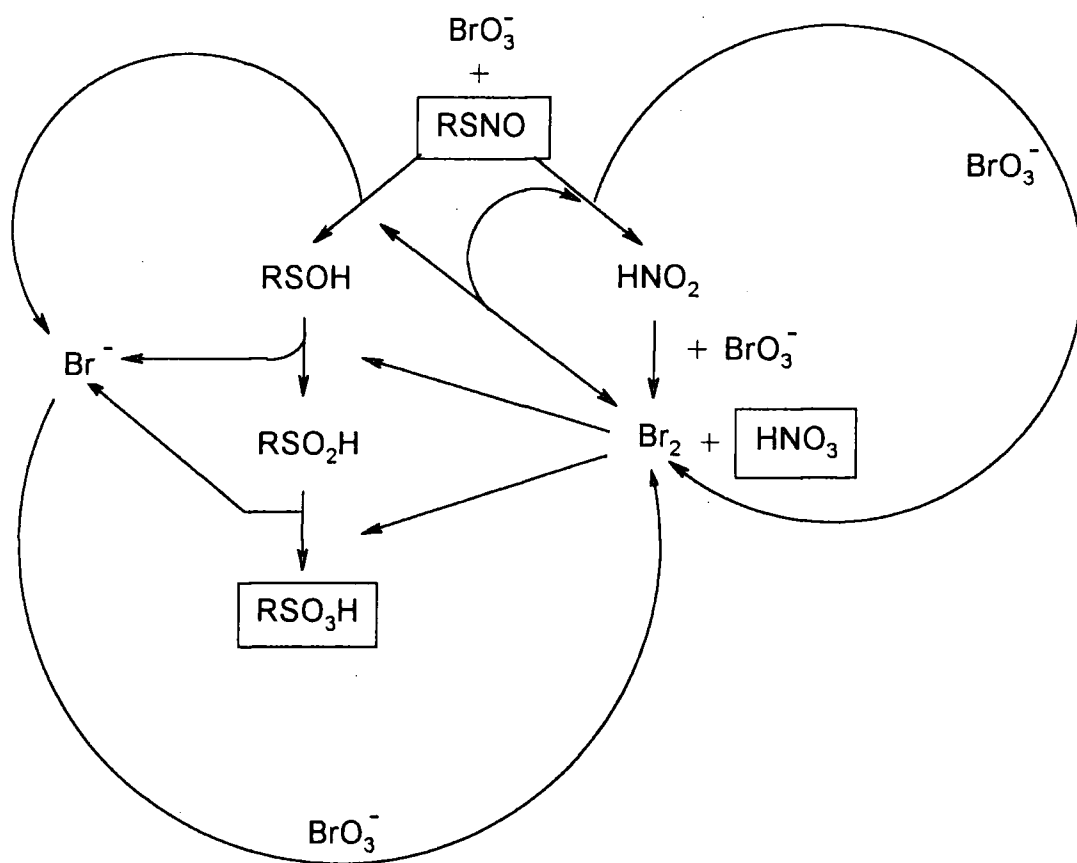
4.11 Mechanistic summary

A substantial amount of research has occurred over the past two decades in understanding the mechanisms of the reactions of acidified bromate with a number of organic substrates. In most cases non-linear behaviour is observed and in all cases complex mechanisms are uncovered. Therefore, most of the bromate-derived species

that are created in the oxidation system (see Scheme 4.2) are known and the behaviour of bromate as a pro-oxidant or initiator, is well accepted.^{8, 21, 22, 23}

Also evident is the autocatalytic behaviour, observed when bromate is in a stoichiometric excess over the substrate. This requires the presence of a “counter reagent”, which is usually some kind of reducing species, to initiate the formation of bromine from bromate.²⁷ Once bromine is formed, a cycle of reduction to bromide followed by regeneration through excess bromate is available if sufficient amounts of oxidisable species are present. And, as witnessed, when oxidative saturation is reached, free bromine will form.

Scheme 4.4 depicts a simplified version of the major steps involved in the reaction of acidified bromate with RSNOs.

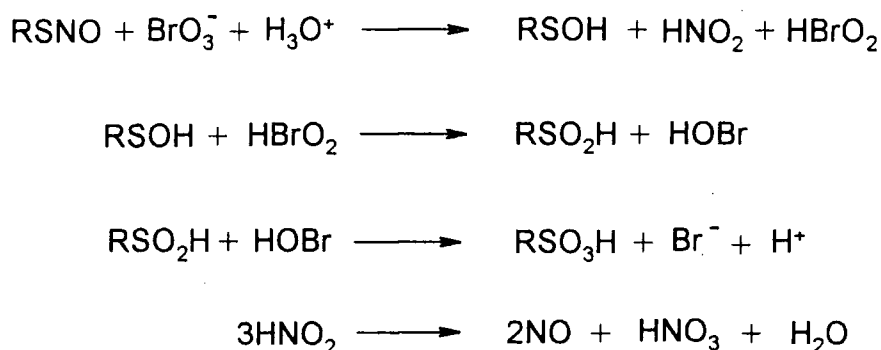


Scheme 4.4 Simplified reaction scheme for the entire reaction

The important point to note is the ability of RSNOs to react in tandem through the oxidation of the thiol and the nitroso moiety, after denitrosation.. Once the nitroso group is released it will react as nitrous acid whereas the remainder will react as a thiol yielding the detected end products of nitrate and the sulfonic acid.

4.11.1 At equimolar concentrations

At equimolar bromate and SNCys the initial stage utilises bromate. The subsequently produced oxyhalogen species could theoretically yield bromine in reaction with the formed nitrous acid. This does not occur because nitrous acid is formed in quantitative yield, confirming none has been oxidised and therefore bromine not produced. No bromine is observed at the end of the reaction, as the bromide formed will not have any bromate remaining to initiate the extraneous oxyhalogen reaction. The decay of nitrous acid is well known²⁰ and small amounts of NO were detected by a WPI MK II NO electrode but were not quantified.



Scheme 4.5 Reaction scheme for the equimolar reaction of RSNOs with acidified KBrO₃

4.11.2 Key points of the mechanism

- 1 Acidified bromate reacts with SNCys comparatively slowly in the initial decomposition phase. The initial plateau is reduced with increasing bromate concentration. Bromate behaves as a pro-oxidant.

- 2 As SNCys decomposes, nitrous acid is formed rapidly, as shown by the characteristic five fingered spectrum. The nitrous acid is formed in quantitative yield at equimolar concentrations of bromate and SNCys (determined by the known extinction coefficients).¹⁷
- 3 Nitrous acid reacts with excess bromate very quickly to yield nitrate and bromine, therefore bromine formation occurs much faster in the reaction of bromate with RSNOs than in the corresponding reaction with thiols. The production of bromine with bromate and thiols is reliant on the sequential reduction of bromate and the concomitant oxidation of thiols to yield bromide. In the thiol reaction, bromide is the precursor to bromine formation through the oxyhalogen reaction, therefore it takes longer to generate bromine than in the RSNO reaction.
- 4 The bromine formed will react with SNCys in a diffusion-controlled process, yielding bromide. It will also react with any other oxidatively unsaturated species, again yielding bromide. The bromide formed will then react with any bromate that is present to produce more bromine, thus starting the autocatalytic phase.
- 5 At low bromate concentrations, e.g. a two-fold excess of bromate over SNCys, a slower secondary formation of bromine is observed after the initial fast formation. Once all of the nitrous acid is oxidised the formation of bromine is then solely due to the extraneous oxyhalogen reaction. This process has a comparable rate with the thiol trace in Figure 4.3. The extraneous oxyhalogen reaction is only noticeable at this concentration because its rate is dramatically reduced, due to the lack of bromate present. With a larger excess of bromate the formation is much quicker and is comparable to the bromine formation resulting from the nitrous acid- bromate reaction, and is therefore unobservable.

4.12 Biological considerations

There is currently much literature discussion regarding the role of thiols and nitric oxide in bromate induced oxidations *in vivo*.

Thiols have long been advocated to protect cells and DNA sacrificially.⁶ However, recently it was shown that thiols may increase bromate induced intracellular oxidative stress, yet attenuate oxidative stress extracellularly.²⁸

It seems that this is due to the reactive species derived from reduction of bromate and the locality of the reaction determines the potential cellular damage. This was confirmed by Murata *et al.* who speculated that the reactive species created in the reduction of bromate by cysteine or glutathione are indeed the species that cause intracellular oxidative damage.²⁹

Nitric oxide has also been advocated as a potential antioxidant *in vivo* in its bound³⁰ and free forms.³¹ Also bromate is reduced *in vitro* by ligated NO^+ in metal ion complexes, yielding nitrate.³²

Interestingly nitric oxide has been shown to protect cellular glutathione levels through sacrificial oxidation by bromate.³⁰ It is difficult to extrapolate *in vitro* studies to *in vivo* systems, however, there is some correlation between the work in this chapter and the *in vivo* results obtained in reference 30, in that bromate will oxidise bound NO preferentially to thiols. It must also be noted that the work in this chapter is under acidic conditions.

4.13 Conclusion

The primary concern of this chapter was to investigate the antioxidant properties of RSNOs and compare them to thiols. The use of bromate for the oxidation of sulfur compounds is kinetically and mechanistically complex. However bromate does afford the “bromine marker” as a unique comparative tool, which, to our knowledge, has not been used this way in the literature.

Bromine is the most reactive species produced from bromate and is estimated to react with SNCys at diffusion controlled rates. The RSNO derived sulfur and nitrogen species will “mop up” all the bromate derived species as soon as they are formed until the sulfur and nitrogen products are oxidatively saturated, i.e. reach cysteic acid and nitrate, respectively. From this point the pure oxyhalogen reaction can occur and free bromine is developed.

RSNOs have been proven to be more effective antioxidants *in vitro* than their parent thiols, due the added effectiveness of the nitroso moiety in reducing reactive oxygen species.

4.14 References

- 1 C. C. Chiueh and P. Rauhala, *Free Rad. Res.*, 1999, **31**, 641; P. Rauhala, A. M. Y. Lin and C. C. Chiueh, *FASEB*, 1998, **12**, 165.
- 2 P. C. Jocelyn, "Biochemistry of the SH Group", Ch. 4, Academic Press Inc. Limited, London, 1972.
- 3 G. Rabái and M. T. Beck, *J. Chem. Soc., Dalton Trans.*, 1985, 1669.
- 4 R. H. Simoyi, *J. Phys. Chem.*, 1986, **90**, 2802.
- 5 J. S. Stamler and A. Hausladen, *Nat. Struct. Biol.*, 1998, **5**, 247.
- 6 K. Sai, T. Umemura, A. Takagi, R. Hasegawa and Y. Kurokawa, *Jpn. J. Cancer Res.*, 1992, **83**, 45.
- 7 G. R. Bernard, A. P. Wheeler, M. A. Arons, P. E. Morris, H. L. Paz, J. A. Russel and P. E. Wright, *Chest*, 1997, **112**, 164.
- 8 J. Darkwa, C. Mundoma and R. H. Simoyi, *J. Chem. Soc., Faraday Trans.*, 1998, **94**(14), 1971.
- 9 W. Fiet and K. Kubierschky, *Chem. Ztg.*, 1891, **15**, 351.
- 10 Z. E. Jolles, "Bromine and its Compounds", p. 173, Ernest Benn Limited, London, 1966.
- 11 Department of the Environment report, www.fwr.org/waterq/dwi0136.htm, 1993; West Hertfordshire Health Authority News, www.wherts-ha.nthames.nhs.uk/news/jul00/25072000.htm, 2001.
- 12 I. R. Epstein, K. Kustin and R. H. Simoyi, *J. Phys. Chem.*, 1992, **96**, 4326.
- 13 A. Vogel, "Textbook of quantitative inorganic analysis", 4th ed., p. 504, Longman, London, 1978.
- 14 "CRC Handbook of Chemistry and Physics", 63rd ed., Ed. R. C. Weast, CRC Press, Florida, 1982-1983.
- 15 K. D. Bartle, D. W. Jones and R. L'Amie, *J. Chem. Soc., Perkin Trans. 2*, 1972, **5**, 646.
- 16 B. Roy, A. du Moulinet d'Hardemare and M. Fontecave, *J. Org. Chem.*, 1994, **59**, 7019.
- 17 G. Y. Markovits, S. E. Schwartz and L. Newman, *Inorg. Chem.*, 1981, **20**, 445.
- 18 C. C. Addison and D. Sutton, *J. Chem. Soc. (A)*, 1966, 1524.
- 19 I. Lengyel, I. Nagy, G. Bazsa, *J. Phys. Chem.*, 1989, **93**, 2801.

- 20 D. L. H. Williams, "Nitrosation", Ch. 1, Cambridge University Press, Cambridge, 1988.
- 21 W. C. Bray and H. A. Liebhafsky, *J. Am. Chem. Soc.*, 1935, **57**, 51; J. P. Birk and S. G. Kozub, *Inorganic Chemistry*, 1973, **12**, 2460 and references therein.
- 22 T. X. Wang, M. D. Kelley, J. N. Cooper, R. C. Beckwith and D. W. Margerum, *Inorg. Chem.*, 1994, **33**, 5872.
- 23 S. B. Jonnalagadda and N. Musengiwa, *Int. J. Chem. Kinet.*, 1998, **30**, 111.
- 24 R. H. Simoyi and I. R. Epstein, *J. Phys. Chem.*, 1987, **91**, 5124.
- 25 D. J. Barnett, Ph. D. Thesis, University of Durham, 1994.
- 26 J. C. Deuttsch, C. R. Santhosh-Kumar and J. F. Kolhouse, *J. Chromatogr. A*, 1999, **862**, 161.
- 27 L. Metsger and S. Bittner, *Tetrahedron*, 2000, **56**, 1905.
- 28 J. L. Parsons and J. K. Chipman, *Mutagenesis*, 2000, **15**, 311.
- 29 M. Murata, Y. Bansho, S. Inoue, K. Ito, S. Ohnishi, K. Midorikawa and S. Kawanashi, *Chem. Res. Toxicol.*, 2001, **14**, 678.
- 30 A. Rahman, S. Ahmed, M. Kahn, S. Sultana-Ali and M. Athar, *Redox Report*, 1999, **4**, 263.
- 31 J. Kanner, S. Harel and R. Granit, *Arch. Biochem. Biophys.*, 1991, **289**, 130.
- 32 A. K. Jhanji and E. S. Gould, *Inorg. Chem.*, 1990, **29**, 3890.

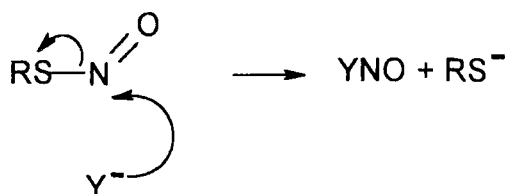
Chapter 5

5 Further reactions of *S*-nitrosothiols

The reactions of RSNOs have received much attention lately, especially after confirmation of their presence *in vivo*¹ and their applicability as NO donor drugs.² Understanding the reactions of RSNOs becomes more important with every new physiological function uncovered. This chapter investigates reactions of RSNOs with two potential *O*-nucleophiles.

5.1 Introduction

RSNOs are known to react with some nucleophiles, to effect electrophilic nitrosation, Scheme 5.1.



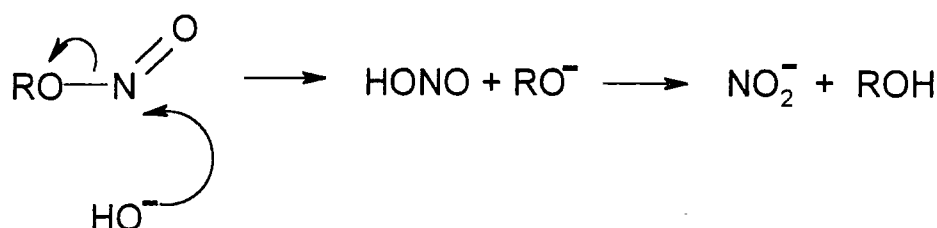
Scheme 5.1 Nucleophilic attack and denitrosation of RSNOs

A wide range of reactivity, has been observed from the extremely rapid denitrosation by some sulfur nucleophiles³ to the slow formation of the carcinogenic nitrosamines from secondary amines.⁴ Chapter 2 displayed the nucleophilic reactivity of the hydroperoxide anion which exhibited intermediate reactivity between *N*- and *S*-nucleophiles.

A number of nucleophiles have been studied in reaction with 2-ethoxyethyl nitrite, EEN, and *N*-methyl-*N*-nitrosotoluene-*p*-sulfonamide, MNTS.^{5, 6} These compounds possess *O*-nitroso group and *N*-nitroso groups, respectively. MNTS also possesses a sulfonate sulfur centre. They have been shown to react with certain *O*-nucleophiles, therefore it was anticipated that RSNOs would follow this trend.

5.2 Reaction of *S*-nitrosopenicillamine with the hydroxide anion

The acid catalysed hydrolysis of RSNOs has been studied and is the reverse of thiol nitrosation, a nitrous acid trap is required to avoid regeneration of the RSNO.⁷ The alkaline hydrolysis of RSNOs has been studied in less detail. In contrast the alkaline hydrolysis of the analogous alkyl nitrites is well studied and shown to form quantitative amounts of nitrite upon hydroxide ion attack, Scheme 5.2.⁵



Scheme 5.2 Electrophilic nitrosation of hydroxide by RONO

It was envisaged that the reaction of hydroxide ion with RSNOs would yield similar results but a study using *S*-nitrosopenicillamine, SNP, by Munro and Williams revealed only ~50% generation of nitrite,⁴ as determined by the Greiss test.⁸

A literature survey revealed no other evidence of any attempt to study the reaction of RSNOs with hydroxide ions. Consequently, a series of experiments was devised to examine further the hydroxide ion induced decomposition of a variety of structurally different RSNOs.

Most reactions were performed with sodium hydroxide in concentrations of at least 20-fold excess over the RSNO (always kept at ≤ 1 mM). Reactions were followed by recording the decrease in the characteristic absorbance of RSNOs at 340 nm over time. Where possible, rate constants were determined using the Scientist[®] computer fitting package.⁹

5.2.1 Results of the SNP and hydroxide anion reaction

Initially a pH range was investigated using a variety of buffers, Table 5.1.

Buffer	pH	In Figure 5.1
KCl	13.2	a
KCl	13.0	b
Borax	10.0	c
Borax	9.9	d
DiHydrogen Phosphate	9.4	e

Table 5.1 Buffers used for the alkaline hydrolysis of SNP, the final pH of the reaction solutions and the decay profile labels for Figure 5.1

The buffer pH was measured before and after reaction to ensure no pH change occurred during the reaction. Figure 5.1 shows the decomposition profiles for the reaction of SNP with hydroxide as in Table 5.1 and labelled accordingly.

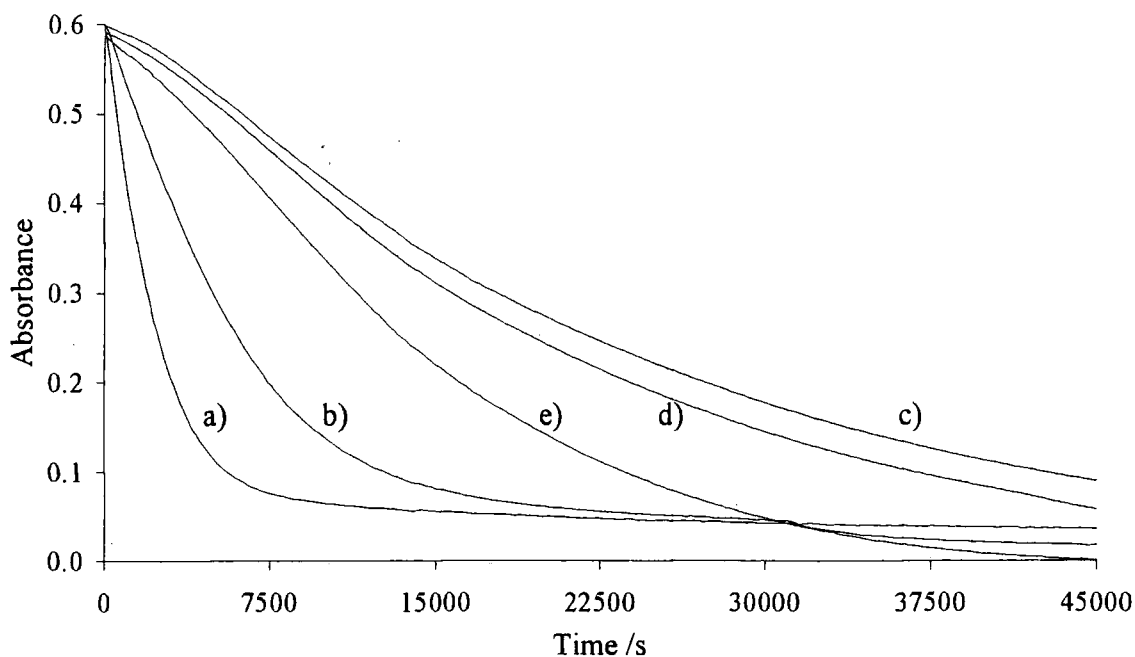


Figure 5.1 Reaction of 1 mmol dm^{-3} SNP with hydroxide at pH values in Table 5.1 with 0.1 mmol dm^{-3} EDTA.

At high pH good first order curves were obtained, but at lower pH non-exponential behaviour occurred. This was probably due to buffer interactions and effective hydroxide concentrations that were less than the concentration of SNP. The buffering system containing dihydrogen phosphate, Figure 5.1 (e), had increased reactivity over Borax buffers, Figure 5.1 d) and c), even at a lower pH. It seemed prudent therefore to use one system, as differences in buffer reactivity could not be quantified.

To obtain adequate pseudo first order conditions it was necessary to work at a $\text{pH} \geq 12.3$. Reaction solutions above this pH could be made up with NaOH alone and did not require buffering.

A study was performed on SNP to enable direct comparison with the previous work by Munro and Williams.⁴ Good first order curves were observed over a range of hydroxide concentrations, Figure 5.2.

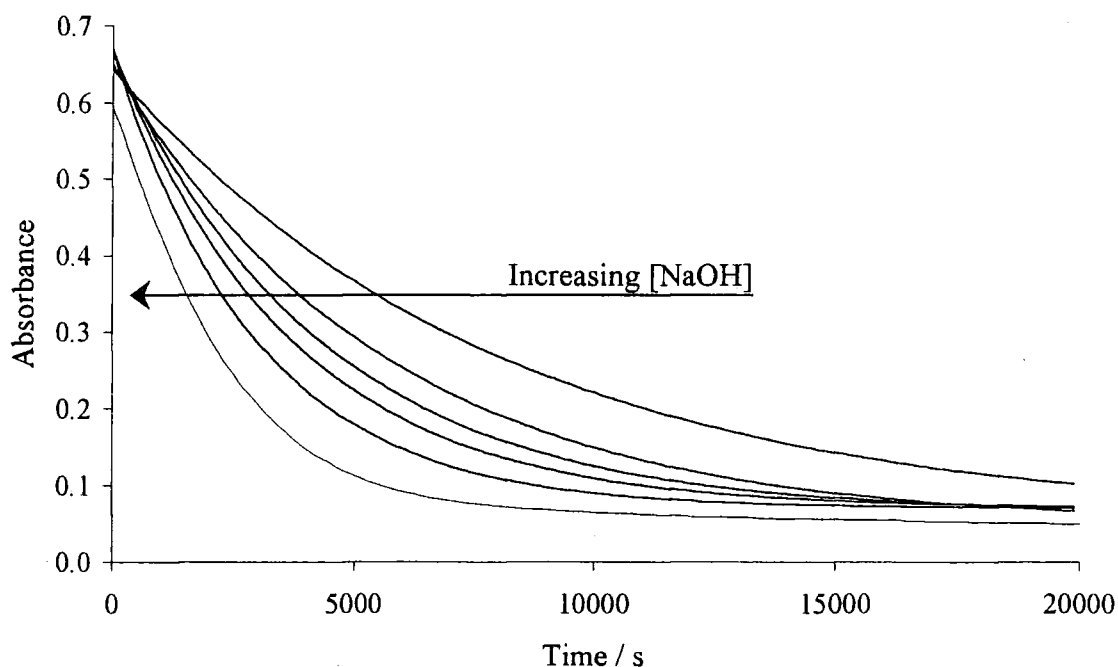


Figure 5.2 Hydroxide induced decomposition of 1 mmol dm^{-3} SNP with 0.1 mmol dm^{-3} EDTA, $[\text{NaOH}] = 40 \text{ mmol dm}^{-3}, 60 \text{ mmol dm}^{-3}, 80 \text{ mmol dm}^{-3}, 100 \text{ mmol dm}^{-3}, 130 \text{ mmol dm}^{-3}, 160 \text{ mmol dm}^{-3}$

EDTA was added as a precaution to suppress the copper catalysed decomposition reaction. However, it is doubtful that any copper catalysed decay could occur as copper hydroxide is formed readily under these conditions and should not react.

First order rate constants were obtained from the traces in Figure 5.2 using the Scientist® computer program,⁹ Table 5.2.

[NaOH] / mol dm ⁻³	$k_{\text{obs}} / 10^{-4} \text{ s}^{-1}$
0.04	1.27 ± 0.02
0.06	1.80 ± 0.02
0.08	2.30 ± 0.03
0.10	2.72 ± 0.04
0.13	3.40 ± 0.05
0.16	4.07 ± 0.04

Table 5.2 First order rate constants calculated using Scientist® from the traces in Figure 5.2

A linear relationship, with a small positive intercept, was observed between k_{obs} and [NaOH], Figure 5.3, from which the rate constant of alkaline hydrolysis k_{OH} could be determined according to the rate equation :-

$$\frac{-d[\text{RSNO}]}{dt} = k_{\text{OH}}[\text{RSNO}][\text{NaOH}] + k'[\text{RSNO}] \quad \text{Equation 5.1}$$

With $[\text{NaOH}] \gg [\text{RSNO}]$, NaOH concentration is effectively constant, thus,

$$\frac{-d[\text{RSNO}]}{dt} = k_{\text{obs}}[\text{RSNO}]$$

Where,

$$k_{\text{obs}} = k_{\text{OH}}[\text{NaOH}] + k' \quad \text{Equation 5.2}$$

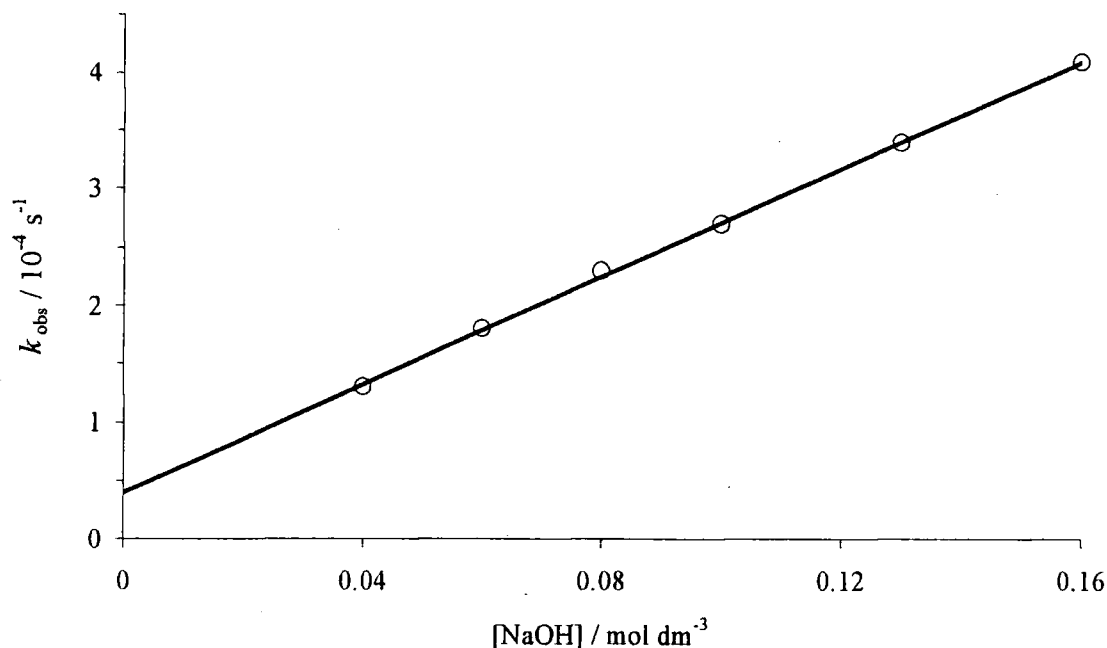


Figure 5.3 Dependence of rate constant on $[\text{NaOH}]$ from the data in Table 5.2, obtained from the reaction of SNP with varied $[\text{NaOH}]$

The value of k_{OH} was obtained from the slope of the fitted line. k' was obtained from the intercept of the y-axis and is attributed to thermal and photochemical decomposition pathways. Values for k_{OH} and k' were in very good agreement with previous work, Table 5.3.

	$k_{\text{OH}} / 10^{-3} \text{ dm}^3 \text{ mol}^{-1} \text{ s}^{-1}$	$k' / 10^{-5} \text{ s}^{-1}$
Reference 4	2.18 ± 0.04	~ 5
This work	2.31 ± 0.04	4.0 ± 0.4

Table 5.3 Summary of the rate constants obtained from Figure 5.3 and their comparison to Reference 4

5.2.2 Nitrogen product

The reaction solutions were neutralised with HClO_4 and tested for nitrite using the Greiss method, see Chapter 6.3.1.⁸ Over the $[\text{NaOH}]$ range studied, ~50% of the nitrogen yield was quantified as nitrite, Table 5.4.

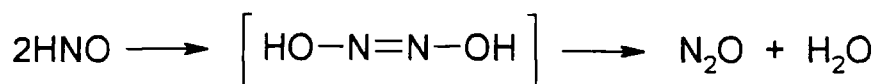
$[\text{NaOH}] / \text{mol dm}^{-3}$	% NO_2^-
0.04	47
0.06	52
0.08	48
0.13	50
0.16	51

Table 5.4 % nitrite obtained from the products of the solutions used in Figure 5.2, after neutralisation

The nitrite yield of ~50% was observed in previous studies,⁴ where it was speculated that reaction may also occur through attack at the sulfur atom of RSNOs. The remaining nitrogen yield was predicted to be nitroxyl, NO^- . However, this would require the reactivity of the hydroxide ion toward the S and N atoms to be approximately equal.

5.2.3 Attempts to detect nitroxyl.

Nitroxyl is the one-electron reduction product of nitric oxide. It is extremely reactive and is reported to form N_2O through dimerisation followed by dehydration, Scheme 5.3.



Scheme 5.3 Dimerisation of protonated nitroxyl and dehydration to N_2O

The rate constant for dimerisation is thought to be diffusion-controlled.¹⁰

The presence of nitroxyl in reaction mechanisms is mostly inferred through the detection of N_2O . This is difficult due to complexities in the detection methods required. Scheme 5.3 has been confirmed by ^{15}N tracer studies¹¹ through N_2O quantification. GC-MS is also possible but is complicated by the identical m/z value for CO_2 and difficulties using aqueous solutions.

There are some techniques based around trapping nitroxyl prior to dimerisation. These techniques can only be qualitative as they are always in competition with dimerisation. Most techniques have been adapted for the detection of nitroxyl from clean sources such as Piloty's acid ($\text{C}_6\text{H}_5\text{SO}_2\text{NHOH}$) and Angeli's salt (HN_2O_3) where the by-products during nitroxyl generation do not interfere with the trap.

For the detection of nitroxyl in the reaction between RSNOs and hydroxide, both the trap and its nitroxylated product must be stable under basic conditions. Techniques using thiol and heme groups of proteins require neutral conditions.¹²

Two techniques were utilised in an attempt to detect nitroxyl.

5.2.4 Trapping by tetracyanonickelate, TCN

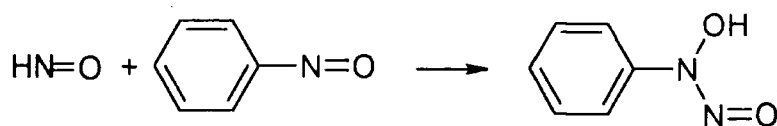
The formation of nitroxyl by Angeli's salt was detected by displacement of one of the four cyanide ligands in $[\text{Ni}(\text{CN})_4]^{2-}$, TCN.¹³ The product has a distinctive absorbance at 498 nm ($\epsilon_{498} = 427 \text{ dm}^3 \text{ mol}^{-1} \text{ cm}^{-1}$) when the reaction is performed under anaerobic conditions at alkaline pH.

A variety of conditions and concentrations were attempted in the reaction of SNP and hydroxide in the presence of the TCN complex. Unfortunately no nitroxyl was detected.

This could be a result of a number of factors including, interference from the by-products of the reaction, the decomposition of nitroxyl before trapping and ultimately the absence of nitroxyl generation in the reaction of RSNOs and hydroxide.

5.2.5 Trapping by nitrosobenzene, NB

In a solution of Angeli's salt, NB traps nitroxyl to produce cupferron (*N*-nitroso-*N*-phenylhydroxylamine), a well-known metal ion chelator that produces coloured transition metal complexes upon metal chelation, Scheme 5.3a.¹⁴



Scheme 5.3a Nitrosobenzene trapping of nitroxyl to yield cupferron

The reaction has been studied spectrophotometrically in aqueous solution following the decreasing absorbance of NB at 310 nm and the increase of cupferron at 280 nm.¹⁴

0.5 mmol dm⁻³ SNP was added to 60 mmol dm⁻³ NaOH in the presence of 1 mmol dm⁻³ NB. The repeat spectra were recorded and the solution left for 19 hours, Figure 5.4.

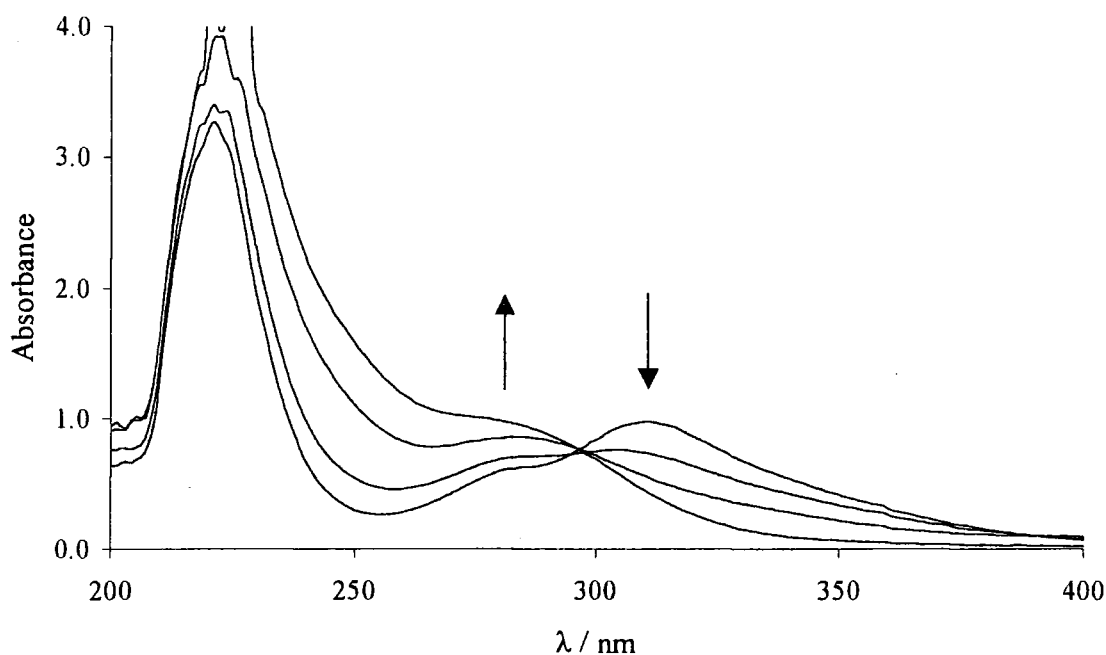
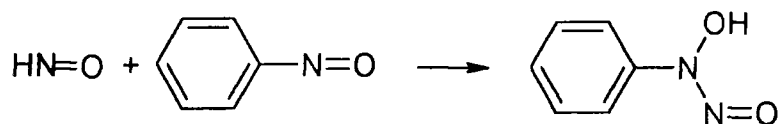


Figure 5.4 Reaction of 0.5 mmol dm⁻³ SNP with 60 mmol dm⁻³ NaOH in the presence of 1 mmol dm⁻³ NB, scans at 0, 3 and 18 minutes and 19 hrs

5.2.5 Trapping by nitrosobenzene, NB

In a solution of Angeli's salt, NB traps nitroxyl to produce cupferron (*N*-nitroso-*N*-phenylhydroxylamine), a well-known metal ion chelator that produces coloured transition metal complexes upon metal chelation, Scheme 5.3a.¹⁴



Scheme 5.3a Nitrosobenzene trapping of nitroxyl to yield cupferron

The reaction has been studied spectrophotometrically in aqueous solution following the decreasing absorbance of NB at 310 nm and the increase of cupferron at 280 nm.¹⁴

0.5 mmol dm⁻³ SNP was added to 60 mmol dm⁻³ NaOH in the presence of 1 mmol dm⁻³ NB. The repeat spectra were recorded and the solution left for 19 hours, Figure 5.4.

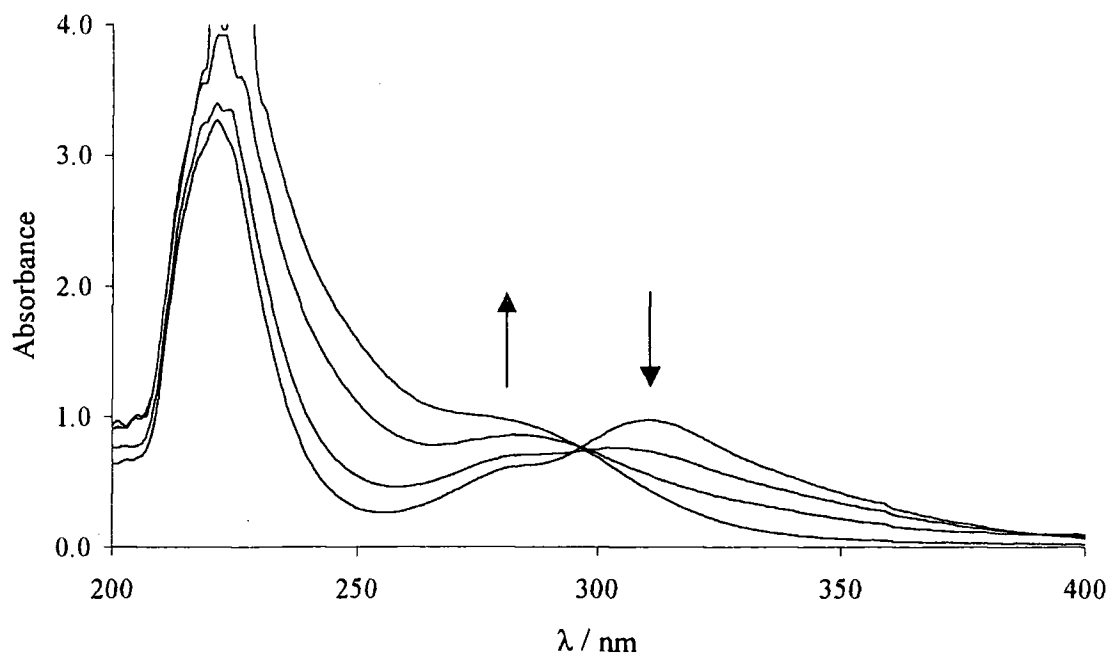


Figure 5.4 Reaction of 0.5 mmol dm⁻³ SNP with 60 mmol dm⁻³ NaOH in the presence of 1 mmol dm⁻³ NB, scans at 0, 3 and 18 minutes and 19 hrs

The characteristic peak of SNP was not initially visible due to the interfering absorbance of NB. The final absorbance centered on 280 nm was stable for at least 19 hours.

An excess of iron (III) chloride, FeCl_3 was added to form the transition metal complex of cupferron. The precipitate formed was extracted in DCM as described by reference 14. Also, authentic cupferron (1 mmol dm^{-3}) was mixed with an excess of FeCl_3 and the precipitate extracted in DCM.

The resulting spectra displayed similar absorbance maxima, Figure 5.5. They also displayed excellent correlation to the absorbencies of the authentic cupferron:Fe (III) complex and that obtained from Angeli's salt:NB:Fe (III) in reference 14 (small broad absorbance between 350 and 500 nm with a larger peak at $\sim 280 \text{ nm}$).

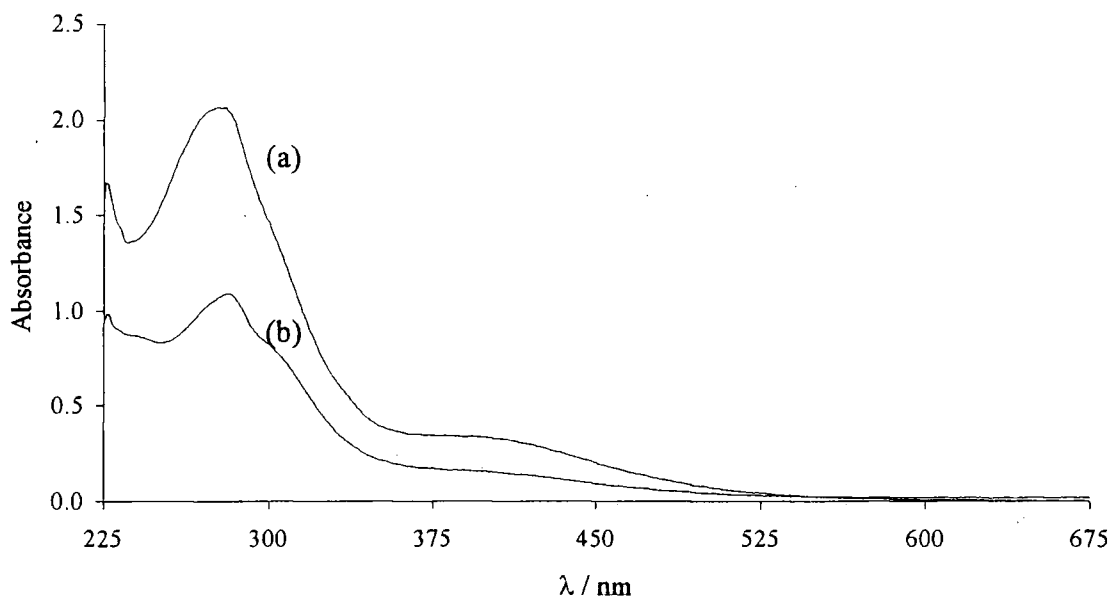


Figure 5.5 Spectra obtained from (a) authentic cupferron (b) SNP and Hydroxide with NB; both treated with excess FeCl_3 and extracted in DCM

The key peaks of the spectra were compared and it was calculated that $\sim 50\%$ of the possible cupferron:Fe (III) complex was obtained, as calculated from the initial RSNO, Table 5.5.

λ / nm	$A_{\text{Authentic}}$	A_{Sample}	% Recovered
400	0.33	0.15	47
310	1.16	0.69	59
280	2.06	1.09	53

Table 5.5 Comparisons of the spectra obtained in Figure 5.5 and % nitroxyl recovery

This suggests that ~50% of the nitrogen product was nitroxyl, trapped by NB. Other hydroxide concentrations gave similar results. Also a check of the effect of hydroxide on NB was performed. The product did not yield any detectable transition metal complexes upon iron addition and attempted extraction with DCM.

Reference 14 comments that the formation of cupferron could occur through alternative pathways not necessarily involving nitroxyl. So the possibility of transnitrosation from SNP to NB cannot be discounted. However, transnitrosation of RSNOs to nitrogen centres with SNP are known to be slow⁴ and the initial phase in Figure 5.5 is over much too quickly to account for transnitrosation.

Hence the trapping of nitroxyl is to be regarded as a qualitative technique (even though reference 14 uses it quantitatively) due to the alternative pathways to cupferron and the alternative pathways for nitroxyl removal e.g. dimerisation. However dimerisation at high pH may be subdued as the reaction occurs through the protonated form.¹⁰

It was impossible to test the direct reactivity of NB with SNP under basic conditions without the possibility of involvement from nitroxyl. Hence, nitroxyl production from SNP and hydroxide cannot be absolutely guaranteed.

5.2.6 Detection of the sulfenic acid

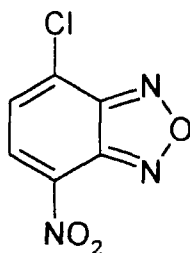
The nucleophilic attack of the hydroxide ion at the sulfur centre of an RSNO would yield a sulfenic acid, RSOH. RSOHs are postulated intermediates in many sulfur oxidations such as thiol oxidation to disulfide and the alkaline hydrolysis of disulfides, but are rarely detected or isolated.¹⁵

They are generally unstable and form a variety of products through dimerisation and self-condensation reactions, Scheme 5.4, as reviewed by Hogg.¹⁶



Scheme 5.4 Dimerisation and self-condensation decomposition pathways for RSOH

A variety of techniques were employed to detect the sulfenic acid or its products. Most techniques involve RSOH traps such as the electrophilic reagent 7-chloro-4-nitrobenzo-2-oxa-1, 3-diazole, NBD-Cl.



NBD-Cl

It forms a distinct peak at 347 nm in the UV / visible spectrum upon RSOH substitution of chloride.¹⁷ The reaction of RSNOs with hydroxide, in the presence of NBD-Cl, displayed no detectable peak at 347 nm but a large peak was observed at 460 nm. On further inspection this peak was found to form in both the presence and absence of RSNOs, suggesting interference from the hydroxide ion.

Unfortunately other methods of detection for RSOHs noted strict reaction conditions which were not viable in the study of the SNP / hydroxide reaction e.g lack of stability under the alkaline conditions used. It was therefore impossible to imply or discount the presence of a sulfenic acid.

5.3 Reactions of other RSNOs with the hydroxide anion

To obtain further understanding of the alkaline hydrolysis of RSNOs, a range of structurally different RSNOs were reacted with the hydroxide ion with the intention of creating a structure / reactivity scale.

Each RSNO generated different absorbance time plots with little correlation between them. First order and mainly sigmoidal type traces were obtained, Figure 5.6.

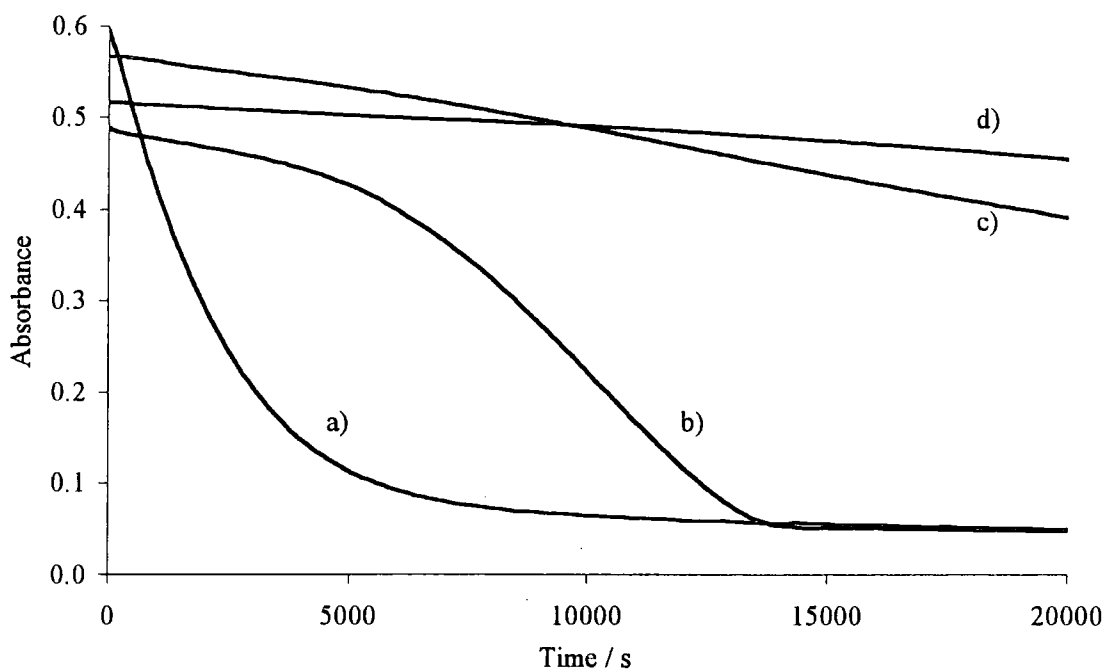


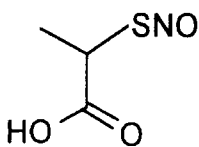
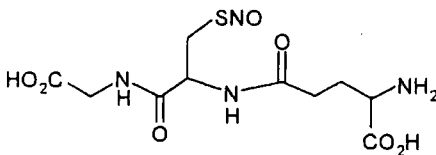
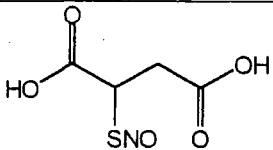
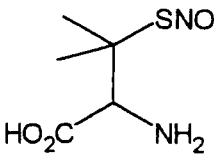
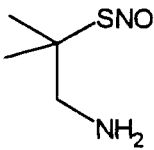
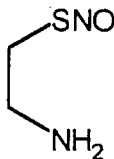
Figure 5.6 Decomposition of various RSNOs (0.5 mmol dm^{-3}) in 0.1 M NaOH .
a) SNP, b) SAE, c) S3MPA, d) SNCys.

See Table 5.6 for full names and structures

It was consistent that increasing $[\text{NaOH}]$ reduced the time taken for reaction completion, i.e. the time taken to reach zero or constant absorbance.

The time taken to decay to a constant absorbance in 0.1 M NaOH was used to construct a crude measure of reactivity, Table 5.6.

The RSOH stabilised column will be discussed in the next section.

<i>S</i> -nitrosothiol	Structure	Decay time / min	RSOH Stabilised
<i>S</i> -nitroso 2-mercaptopropionic acid S2MPA		7	Y
<i>S</i> -nitroso glutathione GSNO		30	Y
<i>S</i> -nitroso mercaptosuccinic acid SMSA		50	Y
<i>S</i> -nitroso penicillamine SNP		80	Y
<i>S</i> -nitroso 1-amino 2-methyl 2-propane thiol SAMP		80	Y
<i>S</i> -nitroso 1-amino ethane thiol SAE		330	Y/N

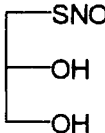
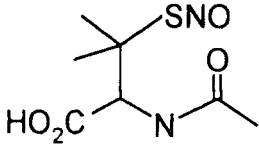
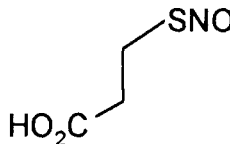
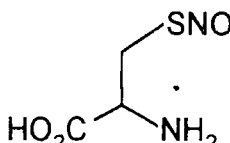
<i>S</i> -nitrosothiol	Structure	Decay Time / min	RSOH Stabilised
<i>S</i> -nitroso thioglycerol STG		415	N
<i>S</i> -nitroso <i>N</i> -acetyl penicillamine SNAP		660	N
<i>S</i> -nitroso 3-mercapto propionic acid S3MPA		70 % decayed after 16 hrs.	N
<i>S</i> -nitroso cysteine SNCys		50 % decayed after 16 hrs	N

Table 5.6 Structure reactivity scale at pH 13 for a range of RSNOs displaying the time taken to reach zero absorbance change

It is pertinent to recognise the unreactive nature of SNCys at high [NaOH]. In Chapter 2 SNCys was used at high [NaOH] in its reaction with the hydroperoxide anion. As it extremely stable at high [NaOH] we can discount any interfering reactions due to hydroxide.

5.3.1 Discussion of the reactivity of RSNOs with hydroxide

The reactivity scale bears no resemblance to the reactions of RSNOs with other nucleophiles.^{3,4,18} A wide range of reactivities are noted for the reaction of other nucleophiles with RSNOs but they all produce first order dependencies on the RSNO.

This is not the case with hydroxide and tends to suggest that there is more to the reaction mechanism than simple nucleophilic attack.

5.3.1.1 Sulfenic acids

It was hypothesised in Section 5.2.6 that RSOHs could be produced during the reaction of NaOH and RSNOs, but are unstable and rarely isolated. However, a number of RSOHs are stable with respect to dimerisation and self-condensation long enough to react through alternative pathways,^{15,16} and possibly with RSNOs. This would require certain structural features in the R group to enable stabilisation, prior to further reaction.

The presence of sterically bulky groups around the sulfur atom protect RSOHs from dimerisation and self-condensation reactions.^{15,16} Stability was increased dramatically using a bowl-shaped hydrocarbon framework around the sulfenic acid group, so much so, that a crystal structure could be obtained.¹⁹

RSOHs are also stabilised by intramolecular hydrogen bonding, preferentially adopting a 6-membered ring conformation,^{15,16} see Figure 5.6.

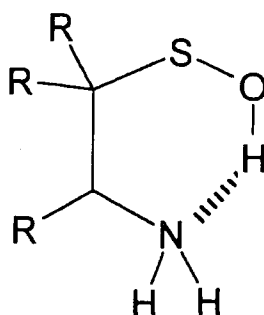
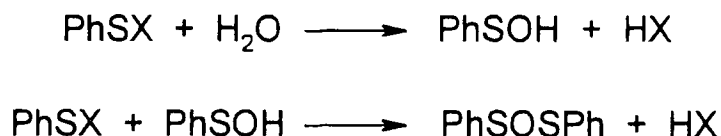


Figure 5.6 Criteria for stabilised sulfenic acids, "-----" indicates hydrogen bonding

Stability is also increased in solvents that exhibit hydrogen bonding and by alkaline conditions through stabilisation of the sulfenate ion, RSO^- .^{15,16}

RSOHs are very powerful nucleophiles, much more powerful than the hydroxide ion and once formed are known to react with the initial substrate in competition with the hydroxide ion, Scheme 5.5.²⁰



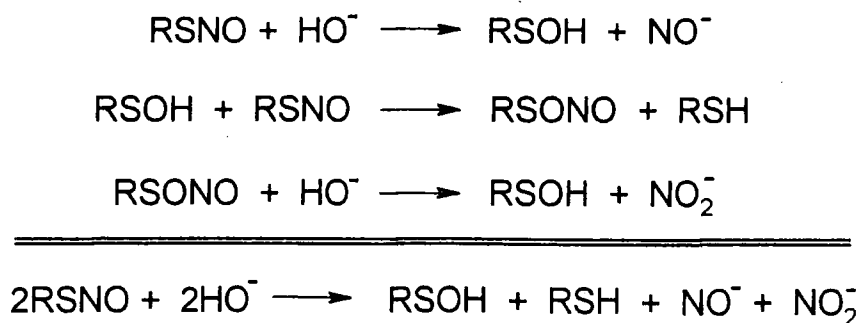
Scheme 5.5 Formation and subsequent reaction of RSOH

If the R group of the RSNO meets the criteria for the formation of a stable sulfenic acid then there is a possibility that, once formed, it will react with the more RSNO in direct competition with the hydroxide ion.

Transnitrosation from RSNOs to *O*-nucleophiles such as ascorbate¹⁸ and peroxide,²¹ occurs *via* nucleophilic attack on the nitroso nitrogen. Accordingly, RSOHs could then attack the nitroso moiety of another molecule of RSNO yielding an unstable *S*-nitrothiol (RSNO₂).

S-nitrothiols hydrolyse to RSOHs and nitrite²² or in the presence of thiolate anions yield disulfides and nitrite.²³

An overall Scheme (5.6) may then be predicted where the RSOH can be constantly regenerated. This may explain the unusual and varied absorbance time traces obtained.



Scheme 5.6 Predicted reaction scheme for RSNOs and hydroxide.

The scheme satisfies all the findings for the reaction of RSNOs with hydroxide such as 50% nitrite yield and tentatively confirms the pathway to nitroxyl. The products are then susceptible to further degradation.

The constant regeneration of the RSOH suggests an autocatalytic decomposition pathway is available, in which a sigmoidal absorbance time trace would be anticipated. Indeed this was observed with many of the RSNO tested.

The structure reactivity scale also fits Scheme 5.6. The most reactive RSNOs are those that can generate relatively stable RSOHs. This is further confirmed by analysing slight structural changes in the RSNO versus its reactivity.

There is also the possibility that reactions of the sulfenic acid may occur *via* the sulfenate anion. However, pKa values for RSOH are rarely quoted in the literature due to their unstable nature. The pKa of the sulfenic acid moiety is estimated to be ~2.2 units higher than the corresponding thiols, (thiols are ~10.5).²⁴

Aliphatic RSOHs are anticipated to be 4 - 5 pKa units smaller than their corresponding alcohols.²⁴ Hence, at pH 13 (0.1 M NaOH) RSOHs are estimated to exist in a combination of anionic and neutral forms.

5.3.2 Structural comparisons

As discussed, the presence of sterically bulky groups near to the sulfur atom stabilises RSOHs. Table 5.7 displays the effects of varied substituents on the R group of the RSNO and their effect on reactivity.

Addition of a carboxyl group has no effect on the reactivity between SAMP and SNP. Removal of the *gem*-dimethyl group decreases the relative reactivity by a factor of four as the steric protection is removed from SAMP (compared to SAE).

The most influential factor seems to be the removal of a site prone to H-bonding, by acetylation of SNP (forming SNAP), decreasing the reactivity eight-fold. This relates well to the hypothesised formation of the RSOH.

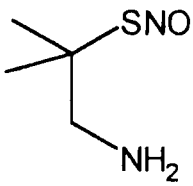
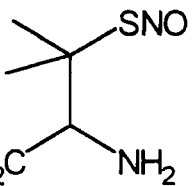
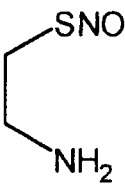
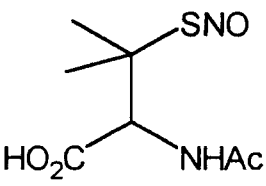
RSNO	SAMP	SNP	SAE	SNAP
Structure				
Decay time / min	80	80	330	660

Table 5.7 Change in decay time with varying substituents on the RSNO

Further confirmation is observed when considering the change in reactivity between two isomers derived from mercaptopropionic acid, Table 5.8. S2MPA is 360 times more reactive than its structural isomer S3MPA.

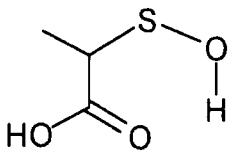
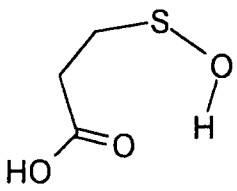
RSNO	S2MPA	S3MPA
Predicted RSOH structure		
Decay time / min	7	70% after 16 hrs.

Table 5.8 The change in reactivity with varying substituents on the RSOH

The structural change results in the removal of some steric protection of the sulfur atom and the loss of the 6-membered conformation for hydrogen bonding.

The wide variety of possible reactions suggests that a common mechanism may not be occurring. It would therefore be necessary to study of the alkaline hydrolysis of each RSNO individually.

Further work is therefore necessary to elucidate the reaction products, which have so far remained elusive.

5.4 Reaction of GSNO with the hydroxide anion

The reaction of GSNO with varying $[\text{NaOH}]$ produced some unusual decay profiles from the absorbance at 340 nm, Figure 5.4.

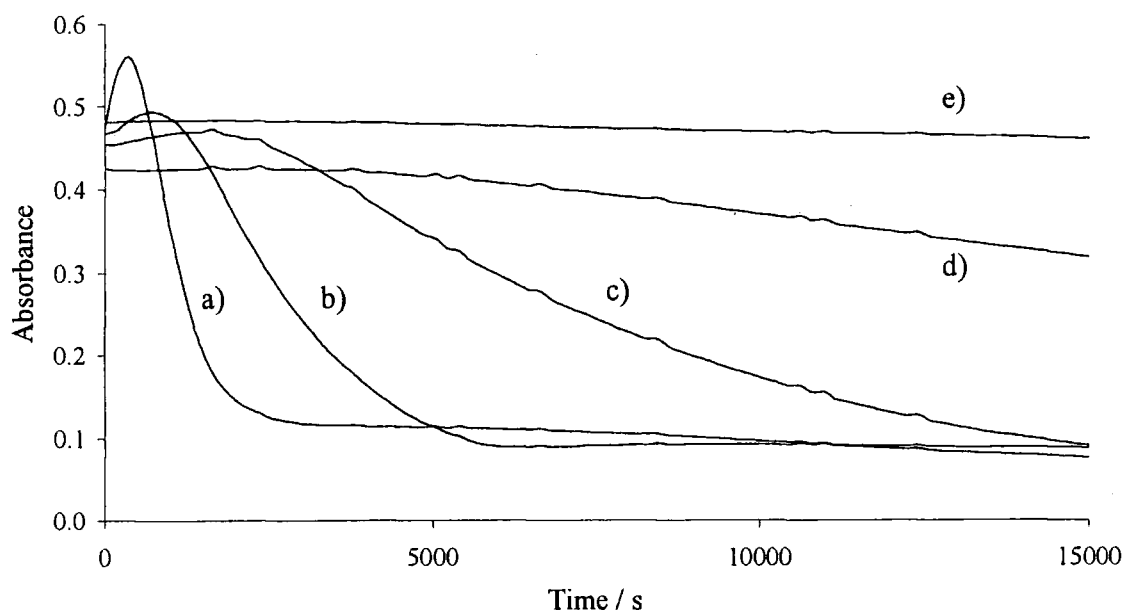


Figure 5.7 Decomposition of 0.5 mmol dm^{-3} GSNO with 0.1 mmol dm^{-3} EDTA and varying $[\text{NaOH}] =$ a) 263 mmol dm^{-3} , b) 65 mmol dm^{-3} , c) 25 mmol dm^{-3} , d) 4 mmol dm^{-3} , e) $0.17 \text{ mM mmol dm}^{-3}$

An increase in absorbance was noted prior to exponential decay at high pH. The initial absorbance increase diminished with decreasing pH. The rate of exponential decay after the initial phase was shown to be pH dependant, Table 5.9.

$[\text{NaOH}]/10^{-2} \text{ M}$	$k_{\text{exp}}/10^{-4} \text{ s}^{-1}$
26.3	17.0
6.46	4.60
2.45	1.81
0.37	0.30

Table 5.9 First order rate constants calculated from the exponential periods of the traces in Figure 5.7

The rate constants for the exponential decay period of the traces in Figure 5.7, displayed excellent first order dependence with $[\text{NaOH}]$, and allowed a value to be calculated for k_2 .

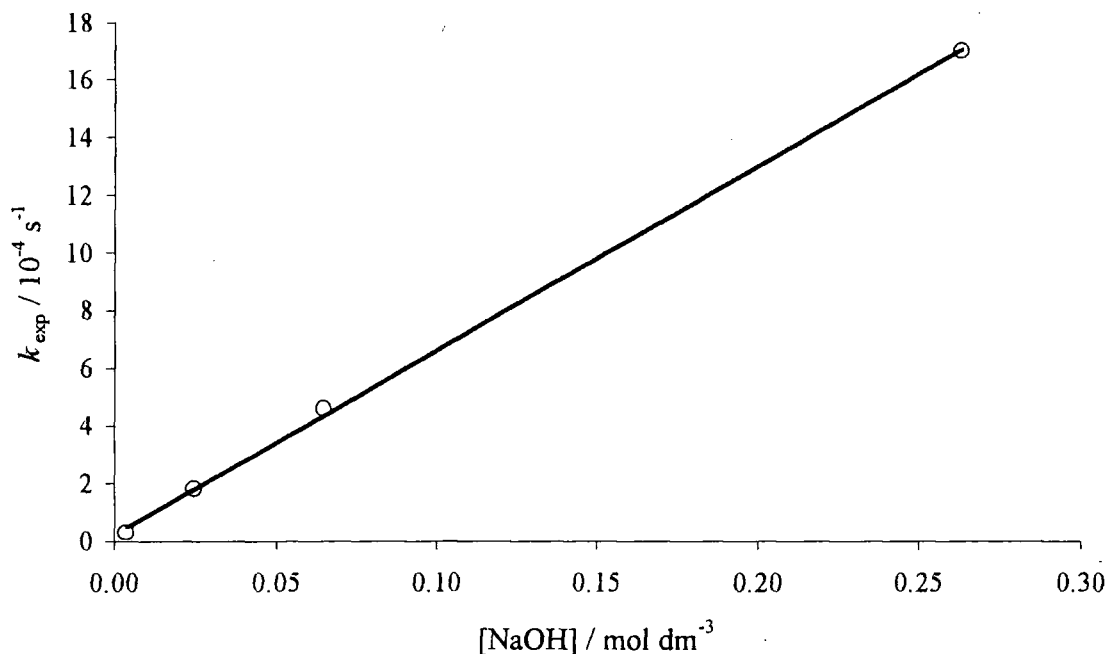


Figure 5.8 Plot k_{exp} versus $[\text{NaOH}]$ for the decay period of the traces in Figure 5.7

$$k_2 = 6.4 \times 10^{-3} \text{ dm}^3 \text{ mol}^{-1} \text{ s}^{-1}$$

The value of k_2 was tentatively assigned to the hydroxide-induced decomposition of GSNO, however, the initial increase absorbance suggested an alternative reaction was occurring.

5.4.1 Repeat scan spectra for the reaction between NaOH and GSNO

The reaction of 0.5 mM GSNO in a solution of 0.25 M NaOH was followed by repeat scans over a spectral range of 200 to 500 nm, Figure 5.9.

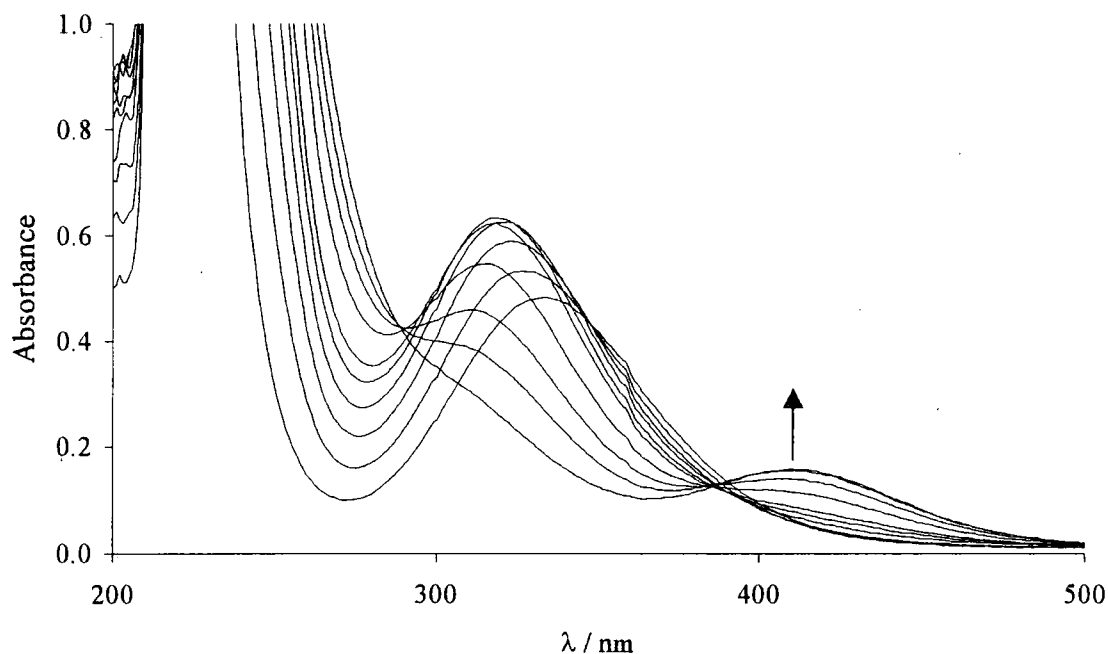


Figure 5.9 Repeat scan spectra obtained from the reaction of GSNO with 0.25 mol dm⁻³ NaOH at 2 minute time intervals

It was evident that the initial increase in absorbance at 340 nm was a result of the increase in absorbance centred around 320 nm. Accordingly the subsequent exponential decay could no longer be attributed to the hydroxide-mediated decomposition of GSNO.

Nine minutes after the initial formation, the unknown absorbing species, centred around 320 nm, began to decay. The decomposition was first order and linearly dependent on [NaOH], as observed previously, Figure 5.8. It was accompanied by the generation of a yellow species, denoted by the increase in absorbance at 410 nm, which faded over a matter of hours.

Clean isosbestic points were noted at 290 nm and 383 nm after the initial formation (9 minutes) as observed in Figure 5.10.

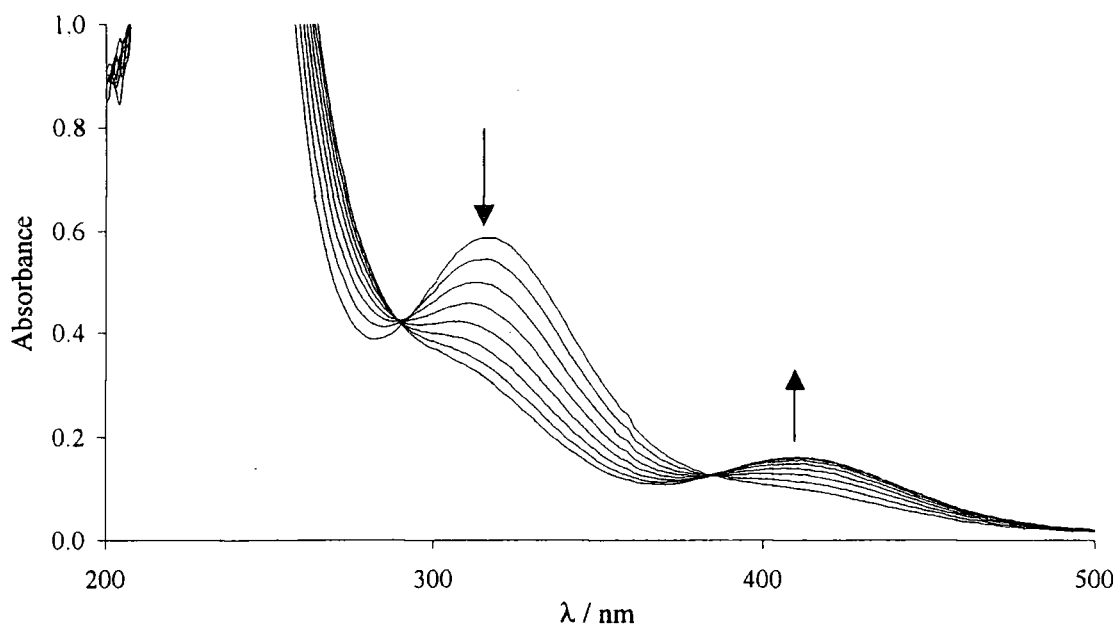


Figure 5.10 Repeat scan spectra displayed in Figure 5.9 between 10 and 18 minutes

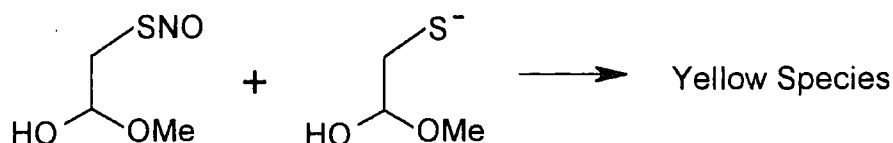
5.4.2 Identity of the yellow species

Many authors investigating the decomposition of nitroso compounds have observed the unknown yellow species.

McAninly,²⁵ used the partial nitrosation of a solution of methyl mercaptoacetate to produce, *S*-nitroso methyl mercaptoacetate, SMMA, which was stable under the acidic conditions required for nitrosation. Partial nitrosation meant that ~80% of parent thiol was still present in the solution. Upon the addition of solid NaOH, to induce a pH shift to ~10, the red coloration of the primary RSNO was replaced by deep yellow. Spectrophotometrically, the RSNO absorbance at 340 nm decreased with the concomitant formation of an absorbance at 410 nm. The species reached a maximum yield after 2 minutes and remained stable for several hours.

The yellow species was also observed after the transnitrosation from *S*-nitroso *N*-acetyl penicillamine, SNAP, to methyl mercaptoacetate at pH 10. SNAP, like all tertiary RSNOs, is green. Electrophilic nitrosation of SMAA was observed by the transient production of a red colouration, prior to the formation of the yellow product at 410 nm.

The peak intensity at 410 nm was shown to be dependent on the initial SNAP concentration. An excess of methyl mercaptoacetate was required and Scheme 5.7 was assumed.



Scheme 5.7 SMAA with an excess of methyl mercaptoacetate at pH 10 produced and unknown absorbance at 410 nm²⁵

Other thiols were tested such as 2-mercaptopropionic acid, 3-mercaptopropionic acid, cysteine and mercaptoacetic acid but no generation of the yellow species was observed.

No explanation for the nature of the absorbance was offered, however it was noted that the presence of the ester was essential, as mercaptoacetic acid did not produce the absorbance at 410 nm.

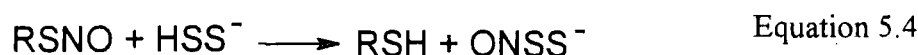
Munro and Williams observed the formation of an identical absorbance in the reaction of sulfide with RSNOs.³ The RSNO peak at 340 nm was replaced a peak at 410 nm within 1 minute with a large excess of sulfide over GSNO at pH 11.7. Clean isosbestic points were present at 293 and 379 nm and are almost identical to those observed in Figure 5.10.

An attempt to monitor the kinetics of the reaction gave “complex-absorbance time plots which were not easily interpreted”.

The yellow species was characterised as the nitrosodisulfide (or perthionitrite) which was observed previously in the reaction of NO and aqueous solutions of Na₂S, NaSH or Na₂S₂.²⁶

Alkyl nitrites³ and MNTS⁵ also slowly generated the yellow species, nitrosodisulfide, upon reaction with sulfide. Both reactions were considered too complex for kinetic analysis after repeat scan spectra revealed the occurrence of “several successive reactions with similar timescales”.⁵

Two possible routes to the nitrosodisulfide were offered in the reaction of sulfide and RSNOs.³



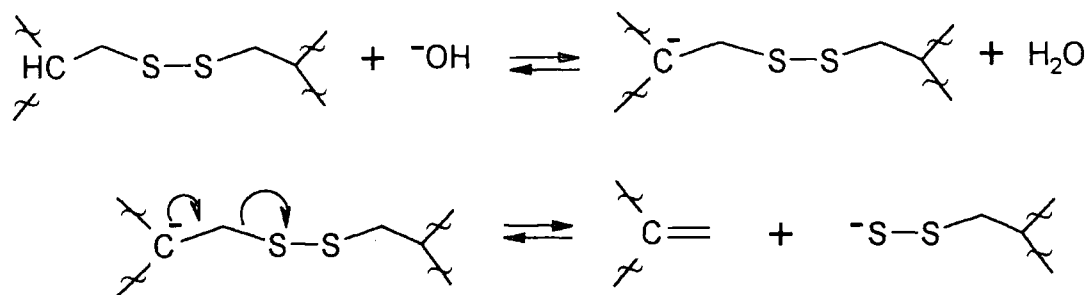
Equation 5.3 was deemed the most plausible as alkyl nitrites and MNTS both give the nitrosodisulfide. Equation 5.4 was also a strong candidate, as the production of the hydrosulfide is well known from disulfides and sulfide through perthiols.²⁷⁻²⁹ In fact, the addition of disulfide was shown to enhance the formation of the nitrosodisulfide in the reaction of sulfide and RSNOs.³

5.4.3 The reaction of hydroxide and GSNO

The formation of the yellow species from the addition of base to RSNO is only observed with GSNO. McAninly witnessed it with SMAA at pH 10, however an excess of the parent thiol was required.

GSNO must therefore possess some structural feature or unusual reactivity over other RSNOs. An extensive literature survey revealed some interesting key features regarding the reactivity of glutathione, which point to a possible mechanism, but are not conclusive.

The hydroxide attack on cystinyl residues of proteins is known to induce β -elimination.³⁰ Similarly, β -elimination is observed with cystine-based peptides including glutathione disulfide, GSSG,³¹ Scheme 5.8.



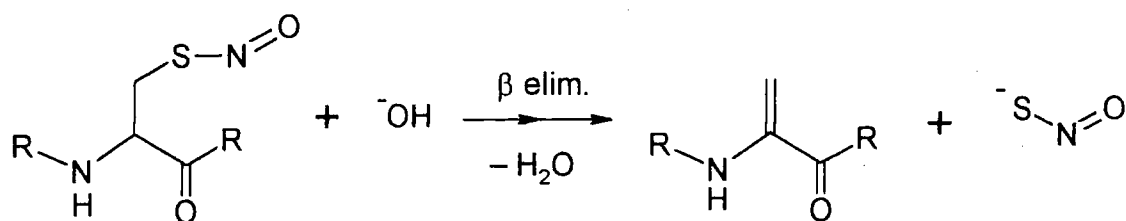
Scheme 5.8 β -elimination of cystinyl residues in proteins and peptides. Only the cystine group is displayed to simplify the scheme

The products are the corresponding dehydrogenated alanine group and a persulfide. The reaction is dependent on the acidity of the proton β to sulfur, the strength of the base and the stabilities of the leaving group and the alkene.

GSSG is much more susceptible to alkaline hydrolysis than other disulfides due its peptide links which increase the acidity of the β proton and remove the negative charge of the carboxyl group, allowing unimpeded proton abstraction.³¹

The alkene product is stabilised by conjugation with the carbonyl group of the peptide bond.

There are strong similarities if β -elimination of GSNO is compared to GSSG. The only difference is the leaving group, the thionitrite anion, Scheme 5.9.



Scheme 5.9 β -elimination of GSNO could yield the thionitrite anion.

The stability of ^-SNO in solution is unknown. Its spectral characteristics are believed to be similar to RSNOs but have not been studied in aqueous solution.³²

Hence, the peak at 320 nm in Figure 5.9 might be assigned to ^-SNO as it is proposed to react further to produce the nitrosodisulfide ion, which absorbs at 410 nm. The production of ^-SNO would then link to the observations of a yellow species obtained from alkyl nitrites and sulfide, as discussed in section 5.4.2.³

5.4.4 Conclusions on the reaction of hydroxide and GSNO

The repeat spectra obtained from the reaction of GSNO and NaOH exhibit extremely similar isosbestic points and an identical final end product spectrum, to the reaction of RSNOs and sulfide. There is a plausible argument for the nitrosodisulfide ion but its mechanism of formation from the thionitrite anion remains unknown.

Whatever the nature of the species absorbing at 320 nm, its role in the generation of the yellow species is unequivocal and the clean isosbestic points are evidence of this.

The decomposition of GSNO in alkaline solution is highlighted for the first time here. It is important to note that complex reactions may occur fairly rapidly when using GSNO at high pH.

However, as with many sulfur-based reactions, the mechanisms are complex and in this case the final assumptions are inconclusive.

5.5 Overall conclusions in the reaction of NaOH and RSNOs

The formation of sulfenic acids is well known during the oxidation of thiols. They generally exist as transient intermediates but on occasion can be stable enough to react through pathways other than dimerisation and self-condensation. When this occurs their nucleophilicity is surprisingly high and quoted as being 10^5 times that of water.^{15,16} If they become involved in the reaction mechanism it is natural that complex kinetics ensue.

For RSOHs to form during the reaction of RSNOs and the hydroxide anion, it is necessary that nucleophilic attack occurs on the sulfur atom. The nitroso group in RSNOs exhibits a small electronegativity difference between nitrogen ($N = 3.1$)^a and oxygen ($O = 3.5$).^a The group is classed as a “soft” electrophilic centre, in HSAB terms, as defined by the principles outlined by Pearson *et al.*³⁴ The sulfur atom is the “harder” centre ($S = 2.5$)^a and predicted to be the site of attack from the “hard” hydroxide anion.

This is evident in the reaction of MNTS with “hard” nucleophiles such as trifluoro ethanol and hydroxide ion. Nucleophilic attack occurs exclusively on the “hard” sulfur centre as opposed to the “soft” nitroso group.⁶

Although little is known about the stability of the nitroxyl as a leaving group its pK_a of 4.7 may suggest this to be favourable.

Once the RSOH is formed and it is sufficiently stable it may then participate in the reaction as outlined in Scheme 5.6.

Scheme 5.6 is a much more reasonable mechanism than attack on the N for the reasons mentioned and also a yield of 50 % nitrite would require identical rates of reaction at both the sulfur and nitrogen centres.

^a Electronegativity values taken from “Introduction to Organic Chemistry” 4th ed., A. Streitweiser, C. H. Heathcock and E. M. Kosower, Macmillan Publishing Company, New York, 1992.

GSNO was found to be unique amongst the other RSNOs studied in this chapter and should perhaps be removed from the reactivity scale. It conveniently highlights the diversity between reactivity and structure, and indicates the range of the reactions of sulfur compounds.

More detailed product studies may reveal or confirm further facets of the reaction but the conditions employed allow degradation of the initial products, possibly leading to erroneous mechanistic predictions.

In conclusion, the reaction of RSNOs with a simple nucleophile produces a wide range of reactivities and products. However, it was impossible to determine a common mechanism but in-roads were made towards understanding the correlation between structure and reactivity.

5.6 Reactions of *S*-nitrosothiols with phenol

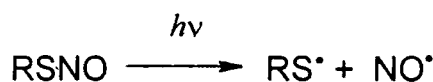
The reaction of phenol with *S*-nitroso *N*-acetylpenicillamine, SNAP, has been studied previously,³⁵ prior to the discovery of the copper catalysed decay mechanism of RSNOs³⁶.

The findings were interpreted as homolysis of the S-NO bond followed by subsequent reaction of the free NO with phenol at the *para* position, yielding *p*-nitrosophenol. *p*-Nitrosophenol is believed to exist in tautomeric equilibrium with benzoquinone monooxime, with preference for the monooxime structure in aqueous solutions, Scheme 5.10.³⁷



Scheme 5.10 Tautomerism of *p*-nitrosophenol and benzoquinone monooxime.

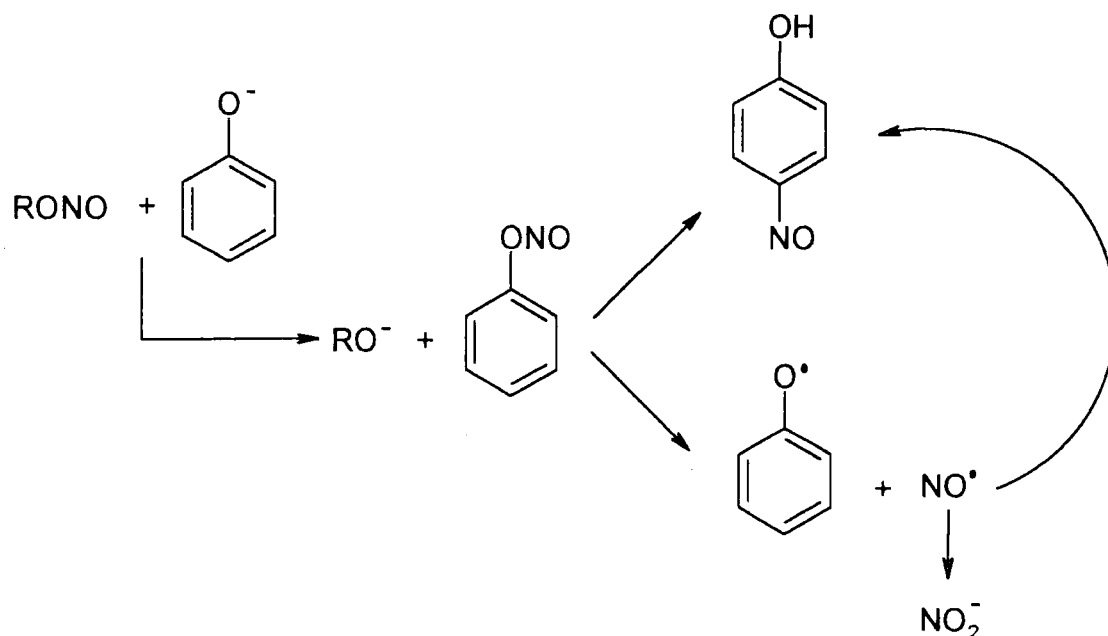
SNAP is a reasonably stable RSNO in aqueous solution due to its inability to bind copper which is known to initiate NO release.³⁶ The findings in reference 35 are consistent with a thermal or photochemical decomposition in that NO is released and thiol radicals are detected, equation 5.5.



Equation 5.5 Thermal and photochemical decomposition of RSNOs

Phenolic compounds have been shown to react with alkyl nitrites at alkaline pH. The reaction proceeds through nucleophilic attack of the phenolate anion at the nitroso group yielding a mixture of *p*-nitrosophenol and nitrite anion.⁶ The formation of the ArONO is believed to be an intermediate stage and the subsequent formation of *p*-nitrosophenol

is from internal rearrangement of the NO group, similar to the Fischer-Hepp rearrangement of aromatic *N*-nitrosamines.³⁸ The formation of nitrite is derived from homolytic cleavage of ArONO to nitric oxide followed by hydrolysis, Scheme 5.11.⁶ Some of the ArO[•] and NO may recombine to yield aromatic *C*-nitroso compounds.⁶



Scheme 5.11 Reaction of alkyl nitrites with phenol in alkaline pH

With the current understanding of the copper catalysed decay of RSNOs it is now important to reinvestigate their reactions with phenol, taking into account the fact that nucleophilic attack through the oxygen atom is a possibility.

5.6.1 Reaction of *S*-nitrosopenicillamine, SNP, and phenol at pH 7.4

S-Nitrosopenicillamine, SNP, was chosen as the RSNO to study because of its susceptibility to nucleophilic attack.^{3, 4, 18} A stock solution of phenol in methanol was prepared and then diluted to the desired concentration with phosphate buffer at pH 7.4.

The initial reaction was performed using 0.25 mmol dm⁻³ SNP as prepared in Section 6.1.1. This was added to a solution of 100 mmol dm⁻³ phenol at pH 7.4. A spectral scan between 300-500 nm was taken upon the addition of the RSNO and then again after 15 minutes. The initial spectra displayed the characteristic peak of SNP at 340 nm with the overlap of the strong absorbance due to phenol, Figure 5.11.

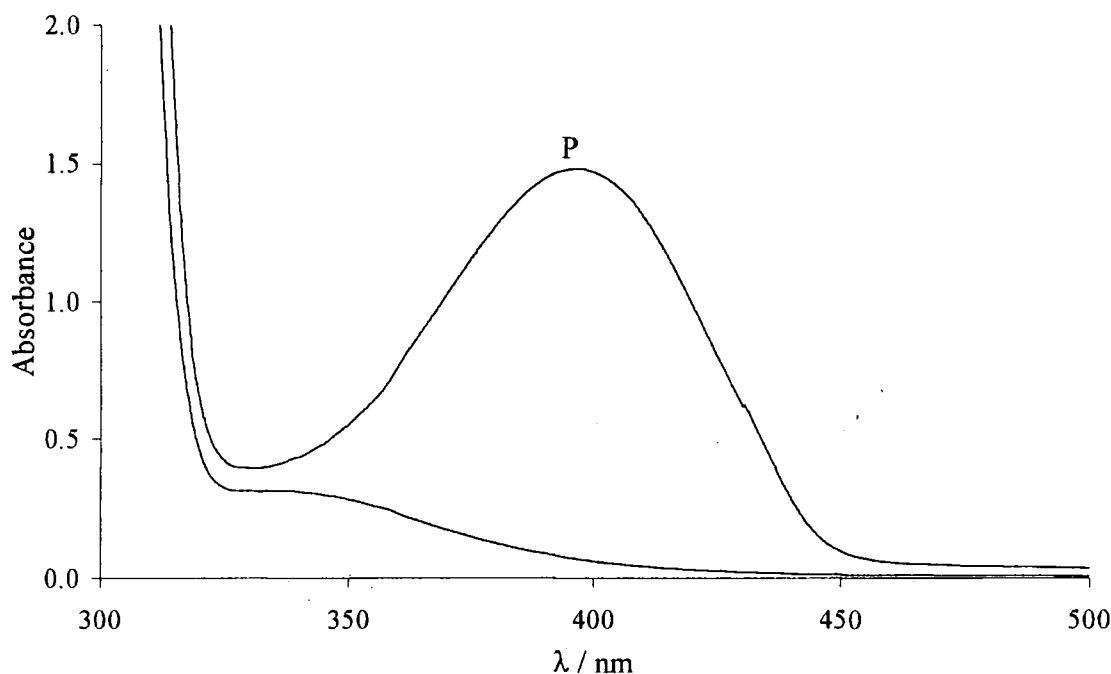


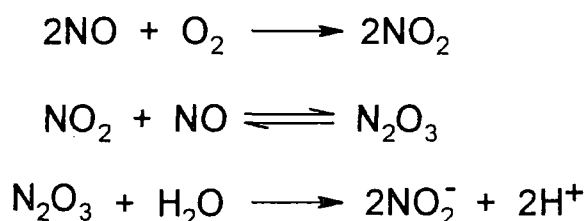
Figure 5.11 Reactant and product spectra from the reaction of SNP ($0.25 \text{ mmol dm}^{-3}$) and phenol (100 mmol dm^{-3}) at pH 7.4. Final product spectrum, P, taken after 15 minutes

After 15 minutes the reaction solution had changed from the characteristic green colour of SNP to a yellow solution. A spectral scan confirmed this with the detection of a new absorbing species centred on 400 nm.

The final product spectrum was comparable with that from the reaction of alkyl nitrites and phenol hence the product was confirmed as *p*-nitrosophenol.⁶ The product was stable and its yield was calculated as 23 % (from the initial SNP concentration) using the known extinction coefficient of *p*-nitrosophenol ($\epsilon_{400 \text{ nm}} = 27\,100 \text{ dm}^3 \text{ mol}^{-1} \text{ cm}^{-1}$).⁴⁰

At this pH it was not expected that the reaction would occur through the phenolate anion due to its $\text{p}K_{\text{a}} \sim 10$.⁶ The observations were similar to the reaction of SNAP and phenol.³⁵ However the copper present in the buffer is sufficient to effect total NO release from SNP. As the role of copper in the decomposition of RSNOs was not known at the time of the work in reference 35 we can now attribute the formation of *p*-nitrosophenol from reaction of phenol with NO or species derived from NO.

NO in the absence of oxygen is not a nitrosating agent. In solution it is widely regarded that nitrosations attributed to NO are due to nitrous acid or dinitrogen trioxide, N_2O_3 . Nitrite is the quantitative product from copper mediated RSNO decomposition through NO oxidation and hydrolysis.³⁶ If it is sufficiently protonated to nitrous acid it is capable of rapid electrophilic nitrosation. In neutral solutions the amount of nitrous acid formed is very low and nitrosations are believed to occur through N_2O_3 . N_2O_3 is formed from NO and oxygen in the aqueous phase, prior to hydrolysis to nitrite Scheme 5.11.

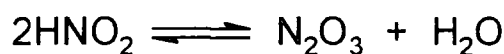


Scheme 5.11 Formation and decay of N_2O_3 from NO in aqueous solution.

In aqueous oxygenated solution the rate of NO oxidation is a third order reaction:

$$\text{Rate} = k_3[\text{NO}]^2[\text{O}_2]$$

Where $k_3 = 8 - 9 \times 10^6 \text{ M}^{-2} \text{ s}^{-1}$ at 25°C .⁴⁰ The hydrolysis of N_2O_3 is known to be very fast, with a rate constant of 3000 s^{-1} , calculated from the equilibrium constant for N_2O_3 from nitrous acid, $K = 3.0 \times 10^{-3} \text{ dm}^3 \text{ mol}^{-1}$, equation 5.6.^{41, 42}



Equation 5.6 Nitrous acid and dinitrogen trioxide equilibrium in aqueous solution

Therefore the non-quantitative yield of *p*-nitrosophenol is likely to be a result of the competing hydrolytic decomposition of N_2O_3 and the loss of NO to the headspace above the solution. In fact, the reaction of RSNOs and *N*-methylaniline, NMA, has been shown to be quantitative due to the very fast nitrosation of NMA by N_2O_3 out competing the hydrolytic pathway.³⁶

Production of NO from RSNOs may be from copper mediated, thermal or photochemical pathways and the rate of production of N_2O_3 is therefore dependent on the RSNO used and its susceptibility to decay through these three routes.

The product of N_2O_3 hydrolysis, nitrite anion, will not have any affect on phenol, as the solution pH is too high to allow sufficient nitrous acid formation.

5.6.1.1 Reaction of SNP and phenol at pH 7.4 with EDTA

In the absence of copper, brought about by the addition of 0.1 mmol dm^{-3} EDTA to the reaction solutions, only the thermal and photochemical decomposition pathways are available. As both the thermal and photochemical decomposition pathways yield NO, it was anticipated that *p*-nitrosophenol would still be formed. SNP was chosen as it is known to be one of the most thermally and photochemically unstable RSNOs.

Hence, the reaction was repeated at pH 7.4 with and without EDTA. It was followed spectrophotometrically at 400 nm (the absorbance of *p*-nitrosophenol) over time, Figure 5.12.

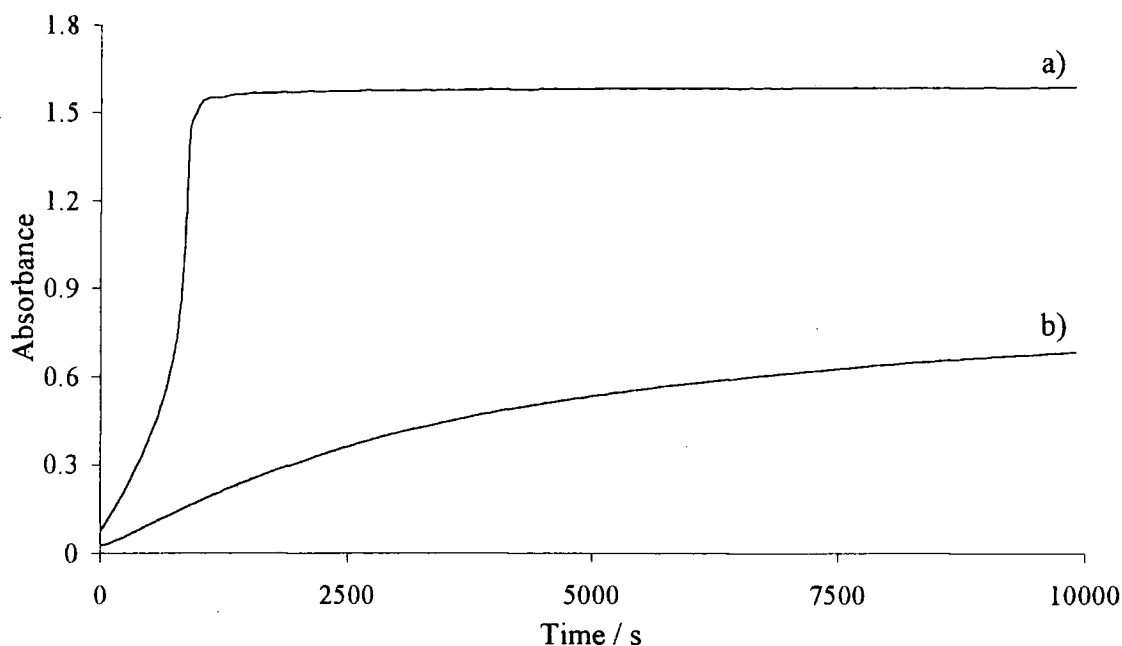


Figure 5.12 The formation of *p*-nitrosophenol from the reaction of $0.25 \text{ mmol dm}^{-3}$ SNP and 100 mmol dm^{-3} phenol at pH 7.4 with a) no EDTA and b) 0.1 mmol dm^{-3} EDTA

In the presence of EDTA *p*-nitrosophenol formation was observed to be much slower and produced a lower yield due to the slow release of NO when the copper mediated decay reaction was suppressed. The slower generation of NO leads to the slower formation of N_2O_3 hence the release of NO from SNP becomes rate limiting.

In the absence of EDTA the generation of NO is very fast and the formation of N_2O_3 and its subsequent nitrosation of phenol becomes rate limiting. This is signified by the gradual increase in rate observed when Figure 5.12 is expanded at the initial formation phase, Figure 5.13.

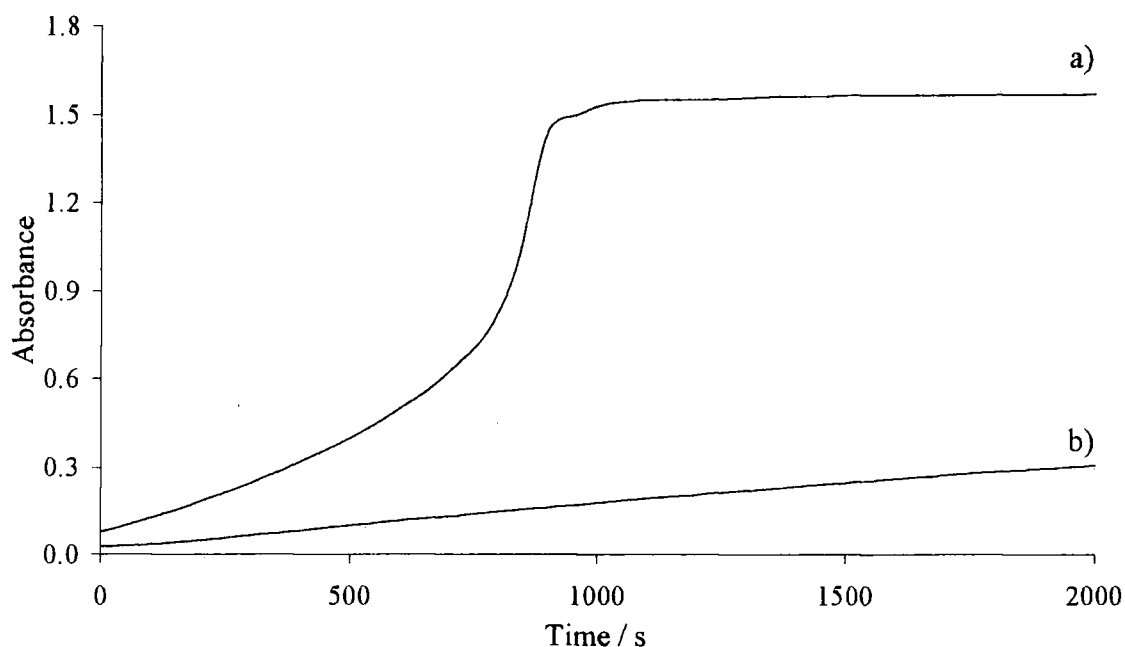
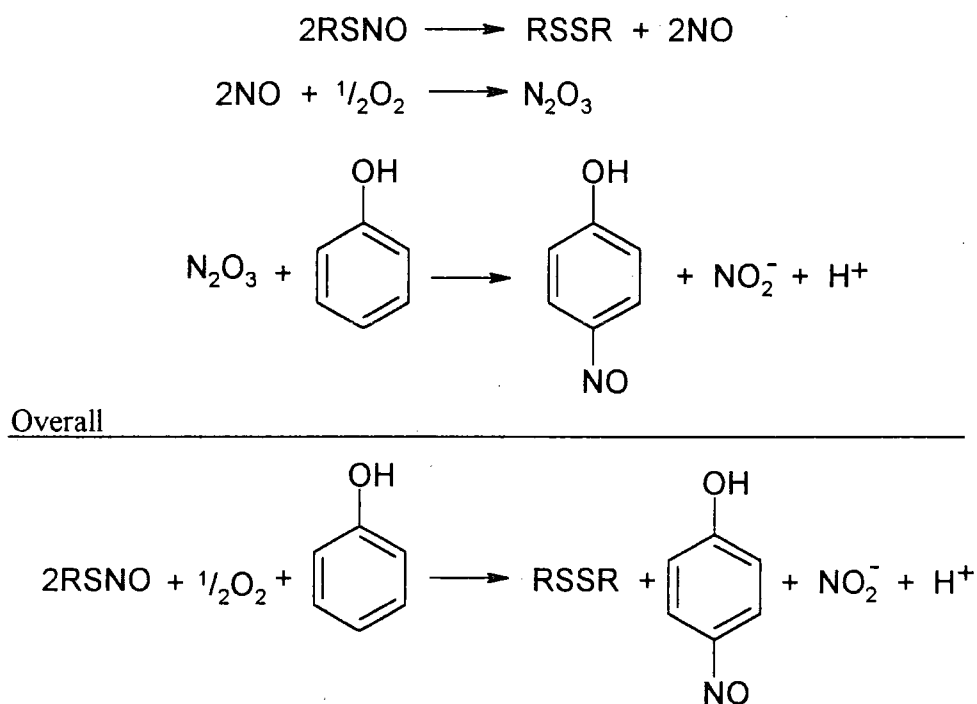


Figure 5.13 Expansion of Figure 5.12 between 0 and 2000 seconds. a) without EDTA and b) with EDTA

The prompt arrest of *p*-nitrosophenol formation is due to the exhaustion of N_2O_3 via both hydrolytic and nitrosative pathways.

5.6.1.2 Stoichiometric calculation of *p*-nitrosophenol formed

If the reaction is proceeding through N_2O_3 then the stoichiometry of the reaction is more than a simple 1:1 reaction between RSNO and phenol. The release of NO is merely an initiating stage prior to the formation of N_2O_3 , which requires 2 moles of NO . Therefore overall 2 moles of RSNO are needed to form 1 mole of *p*-nitrosophenol, Scheme 5.12.



Scheme 5.12 Overall reaction scheme for the nitrosation of phenol by RSNO s

Scheme 5.12 is analogous to a scheme proposed by Williams for the nitrosation of *N*-methylaniline.⁴³ From this the yield of *p*-nitrosophenol was recalculated as 44%.

Nitrite analysis was performed by the Griess test as described in section 6.3.1 and determined to be 48 % as calculated from the RSNO . Therefore > 90% of the nitrogen products were quantified.

5.6.2 Reaction of SNP and phenol at pH 10 with and without EDTA

The possibility of nucleophilic attack by the phenolate anion was investigated. The reaction of $0.25 \text{ mmol dm}^{-3}$ SNP and 100 mmol dm^{-3} phenol was repeated in alkaline solution at pH 10. The absorption at 400 nm was recorded spectrophotometrically over time, Figure 5.14.

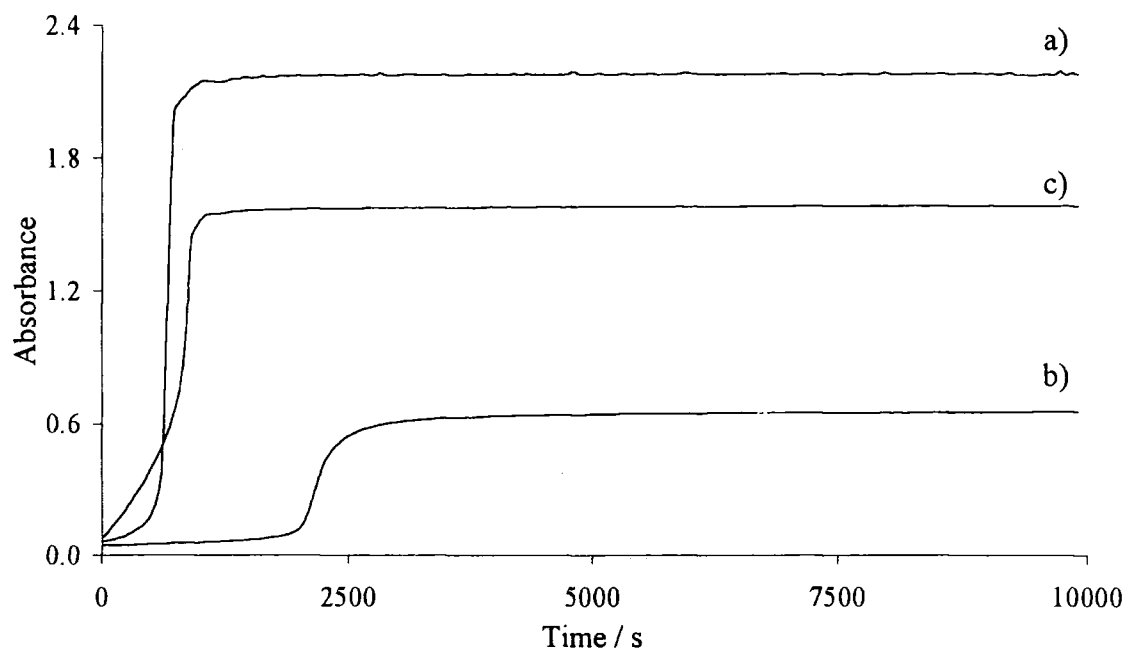


Figure 5.14 The formation of *p*-nitrosophenol from the reaction of $0.25 \text{ mmol dm}^{-3}$ SNP and 100 mmol dm^{-3} phenol at pH 10 with a) no EDTA and b) 0.1 mmol dm^{-3} EDTA c) is the reaction without EDTA at pH 7.4 for comparison

The reaction between SNP and phenol in the absence of EDTA at pH 10 bears similarities to the absorbance time data obtained at pH 7.4 without EDTA, Figure 5.14 traces a) and c) respectively. They both show an increase in rate of formation over time, which is characteristic of the build up of an intermediate species. This suggests that the phenolate anion is not involved as direct nucleophilic attack at the concentrations used should result in a first order formation trace.

Further confirmation of this is observed by the differences between the reaction with and without EDTA at pH 10. If the reaction was dependent on phenolate anion attack then the removal of the copper ions should have no effect.

The increase in *p*-nitrosophenol yield (pH 10 = 64% determined from Scheme 5.12) with an increase in pH for the reactions without EDTA may be due to N_2O_3 nitrosations being more favoured at higher pH.⁴⁴

Also the rate of production of NO from RSNOs should increase with slight increases in pH as the thiolate ion is more readily available to reduce copper (II) to copper (I). This increase is attenuated by large concentrations of hydroxide ions, which chelate copper and prevent further reaction.

The diminished yield of *p*-nitrosophenol from SNP (at pH 10 in the presence of EDTA) and the induction period is attributed to the slower release of NO through the thermal and photochemical decomposition pathways.

5.6.3 Reaction of SNP and phenol at pH 13 with and without EDTA

The reaction was repeated under strongly alkaline conditions at pH 13. No *p*-nitrosophenol was detected either with or without EDTA. This was unsurprising as under these conditions the alkaline hydrolysis of SNP would be the predominating reaction. This result also indicates that the nitrogen products of the base hydrolysis reaction are not nitrosating agents, which concurs with the mechanistic proposal outlined in Scheme 5.6.

5.6.4 Reaction of SNP and 2, 4, 6- trichlorophenol, TCP

The reaction of SNP with TCP was attempted to block the para position where nitrosation occurs. At pH 7.4 the reaction between $0.25 \text{ mmol dm}^{-3}$ and 100 mmol dm^{-3} TCP produced no measurable enhancement of SNP decomposition or any spectrophotometrically detectable products. This was expected as the para position was

blocked therefore nitrosation through the N_2O_3 pathway was unavailable. Also the solution pH of 7.4 renders the TCP ($\text{pK}_a \sim 7$)⁴⁵ partially in the protonated form, thus slowing any nucleophilic attack.

5.6.4.1 Reaction of SNP and 2, 4, 6- trichlorophenol, TCP at pH 12

Increasing the pH of the solution above the pK_a of TCP increases the proportion of unprotonated TCP anions and therefore produces conditions more favourable for nucleophilic attack. The pH increase also causes a slight shift in the absorbance of TCP but substantial enough to warrant measurement of SNP decay at 350 nm. Accordingly the concentration of SNP was increased to ease spectrophotometric detection.

1.5 mmol dm^{-3} SNP was reacted with $20 - 200 \text{ mmol dm}^{-3}$ TCP in an alkaline solution at pH 12 in the presence of 0.1 mmol dm^{-3} EDTA. The reaction medium was adjusted to pH 12 with NaOH and measured before and after to ensure no deviation from the desired pH. The absorbance of SNP at 350 nm was followed spectrophotometrically over time, Figure 5.15.

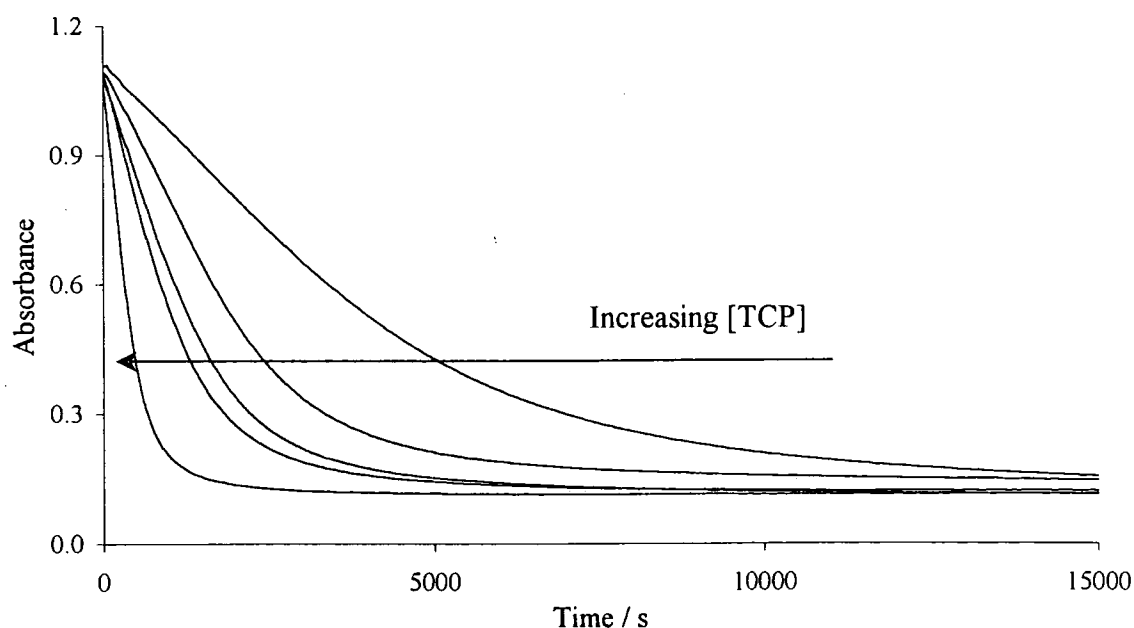


Figure 5.15 1.5 mmol dm^{-3} SNP with 20, 40, 60, 80 and 200 mmol dm^{-3} TCP at pH 12 with 0.1 mmol dm^{-3} EDTA

First order fits were obtained over the range of TCP concentrations although at lower concentrations slight induction periods were noticeable. The absorbance time traces did not tend to zero due to the residual absorbance shoulder of TCP.

First order rate constants were obtained from the traces in Figure 5.15 using the Scientist[®] computer program,⁹ Table 5.10.

[2, 4, 6- TCP] / M	$k_{\text{obs}} / 10^{-3} \text{ s}^{-1}$
0.20	2.37 ± 0.02
0.08	0.919 ± 0.005
0.06	0.732 ± 0.005
0.04	0.528 ± 0.004
0.02	0.241 ± 0.002

Table 5.10 First order rate constants obtained from the traces in Figure 5.15

A plot of the first order rate constants in Table 5.10 displayed a linear relationship between rate constant and TCP concentration from which the bimolecular rate constant, k_2 , could be obtained, Figure 5.16.

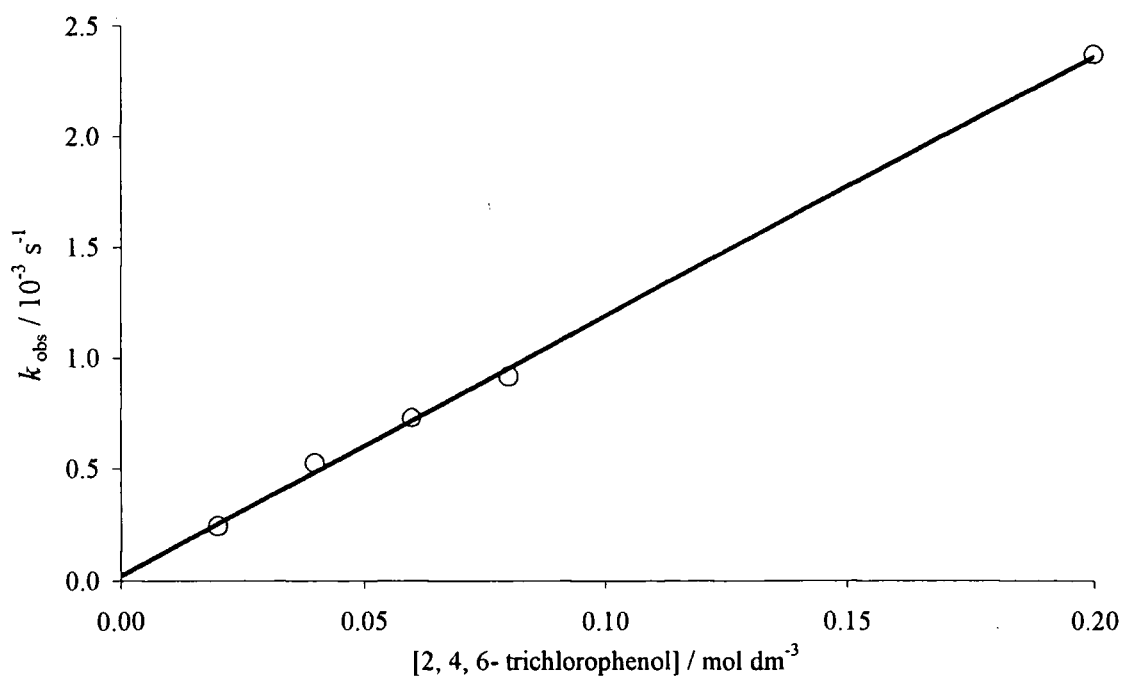


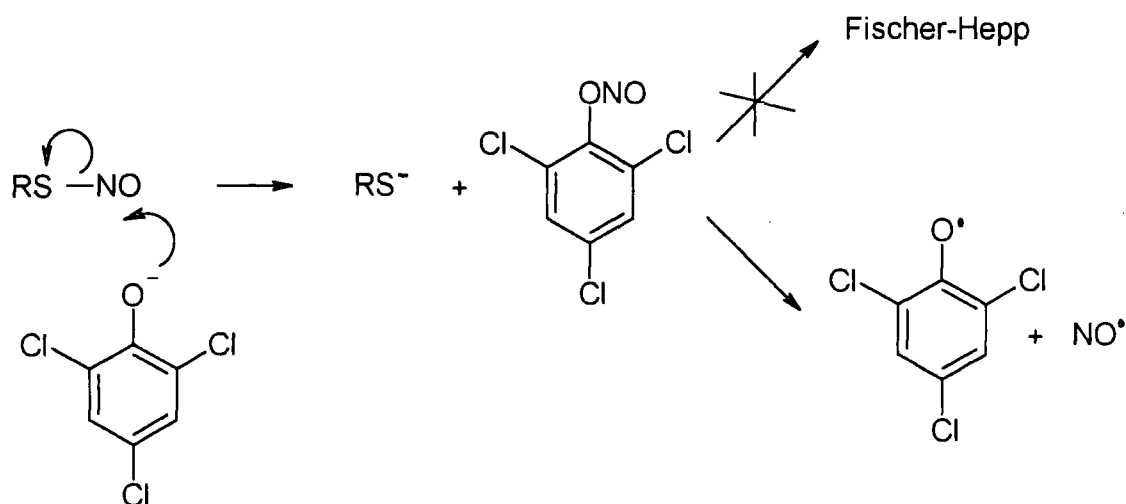
Figure 5.16 Dependence of rate constant on [TCP] from the data in Table 5.10, obtained from the reaction of SNP with varied [TCP] at pH 12

$$k_2 = (11.7 \pm 0.2) \times 10^{-3} \text{ dm}^3 \text{ mol}^{-1} \text{ s}^{-1}$$

$$k' = 2.10 \times 10^{-5} \text{ s}^{-1}$$

The intercept, k' , is due to the alkaline hydrolysis of SNP. The value of k_2 for the reaction of SNP with hydroxide anion was determined in section 5.2.1 as $2.31 \times 10^{-3} \text{ dm}^3 \text{ mol}^{-1} \text{ s}^{-1}$. Therefore the observed rate constant of reaction of SNP with hydroxide at pH 12 is calculated as $2.31 \times 10^{-5} \text{ s}^{-1}$ which shows excellent correlation with the value obtained from the intercept in Figure 5.16.

The mechanism can be assumed to be similar to reaction of *p*-halophenols and alkyl nitrites, hence, Scheme 5.13 is proposed.



Scheme 5.13 The nucleophilic attack of TCP on SNP

The nitrogen product is almost quantitative nitrite, as the Fischer-Hepp rearrangement cannot occur. The detection of radical species has been noted previously in the reaction of SNAP and a phenol with its para position blocked,³⁵ presumably due to the cleavage of the ArONO compound which has been witnessed by a number of groups.^{6, 46}

Phenolic compounds can therefore act as nucleophiles and undergo electrophilic nitrosation from RSNOs when the para position is blocked and EDTA is present to suppress the copper catalysed decomposition pathway of RSNOs.

5.6.5 Conclusion

The mechanism of reaction of RSNOs with phenolic compounds is highly dependent on the structure of the phenol, the pH of the reaction medium and the presence / absence of EDTA.

At physiological pH RSNOs undergo copper mediated denitrosation and the NO produced is oxidised to N_2O_3 in aerobic solution. N_2O_3 then nitrosates phenol but is not quantitative due to concomitant hydrolysis of N_2O_3 .

Interestingly the nitrosation of NMA from the copper initiated NO release from RSNOs is quantitative.³⁶ This reflects the greater reactivity of NMA towards nitrosation by N_2O_3 . Notably recent work has revealed that *N*-nitroso NMA formation is greatly reduced in anaerobic solutions of RSNOs.⁴⁶

In the presence of EDTA, *p*-nitrosophenol is still produced from the reaction of phenol and SNP at physiological pH. However the rate of formation is much slower and attributed to NO release from thermal and photochemical pathways. The possibility of *O*-nucleophilic attack by phenol was investigated but found to be unreactive at this pH.

At higher pH, and therefore under conditions more favourable to phenolate anion attack, absorbance time traces for the formation of *p*-nitrosophenol were strikingly similar to those obtained at pH 7.4. This suggests that the *O*-nucleophile does not play any role.

However in the reaction of alkyl nitrites and phenolic compounds it is believed that *O*-nucleophilic attack is the precursor to nitrite and N_2O_3 formation.

A similar scenario could occur in the reaction of RSNOs and phenolic compounds in that N_2O_3 formation could then effect *O*-nitrosation followed by the Fischer-Hepp rearrangement to the para nitroso conformation.

There are a number of reports to suggest this. Firstly the reaction of anisole with SNAP does not produce *p*-nitroso anisole.³⁵ Also the nitrosation of phenol by nitrous acid has been studied and is suggested to pass through the ArONO intermediate.⁴⁷

Finally *O*-nucleophilic attack was observed when the para position of the phenol was blocked. The results were in line with an analogous reaction between an alkyl nitrite and *p*-chlorophenol and a similar mechanism was suggested.

5.7 References

- 1 L. Jia, C. Bonaventura, J. Bonaventura and J. S. Stamler, *Nature*, 1996, **380**, 221; R. K. Goldman, A. A. Vlessis, D. D. Trunkey, *Anal. Biochem.* 1998, **259**, 98.
- 2 A. de Belder, C. Lees, J. Martin, S. Moncada and S. Campbell, *Lancet*, 1995, **345**, 124.
- 3 A. P. Munro and D. L. H. Williams, *J. Chem. Soc., Perkin Trans. 2*, 2000, 1794.
- 4 A. P. Munro and D. L. H. Williams, *ibid.*, 1999, 1989.
- 5 J. R. Leis, M. E. Peña and A. M. Ríos, *ibid.*, 1995, 587.
- 6 J. R. Leis, A. M. Ríos and L. Rodríguez-Sánchez, *ibid.*, 1998, 2729.
- 7 D. L. H. Williams, "Nitrosation", Ch. 7, Cambridge University Press, Cambridge, 1988.
- 8 A. Vogel, "Textbook of Quantitative Inorganic Analysis", 4th ed., p. 755, Longman, London, 1978.
- 9 Micromath[®] Scientist[®] for Windows[®], Version 2.02.
- 10 "Methods in Nitric Oxide Research", Ed. M. Feelisch and J. S. Stamler, John Wiley & Sons Ltd, Chichester, 1996.
- 11 D. N. Hendrickson and W. L. Jolly, *Inorg. Chem.*, 1969, **8**, 693.
- 12 M. P. Doyle and S. N. Mahapatro, *J. Am. Chem. Soc.*, 1988, **110**, 593.
- 13 F. T. Bonner and M. J. Akhtar, *Inorg. Chem.* 1981, **20**, 3155.
- 14 D. W. Shoeman and H. T. Nagasawa, *Nitric Oxide: Biol. Chem.*, 1998, **2**, 66.
- 15 F. A. Davis, L. A. Jenkins and R. L. Billmers, *J. Org. Chem.*, 1986, **51**, 1033.
- 16 D. R. Hogg, "The Chemistry of Sulphenic Acids and their Derivatives", Ch. 9, Ed. S. Patai, John Wiley & Sons Ltd, Chichester, 1990.
- 17 J. M. Denu and K. G. Tanner, *Biochemistry*, 1998, **37**, 5633.
- 18 A. J. Holmes and D. L. H. Williams, *J. Chem. Soc., Perkin Trans. 2*, 2000, 1639.
- 19 K. Goto, M. Holler and R. Okazaki, *J. Am. Chem. Soc.*, 1997, **119**, 1460.
- 20 J. L. Kice and T. E. Rogers, *ibid.*, 1974, **96**, 8009.
- 21 P. J. Coupe and D. L. H. Williams, *J. Chem. Soc., Perkin Trans. 2*, 2001, 1595.
- 22 M. Sokolovsky, D. Harell and J. F. Riordan, *Biochemistry*, 1969, **8**, 4740.
- 23 J. D. Artz, K. Yang, J. Lock, C. Sanchez, B. M. Bennett and G. R. J. Thatcher, *Chem. Commun.*, 1996, 927.

- 24 P. De Maria, "The Chemistry of Sulphenic Acids and their Derivatives", Ch. 7, Ed. S. Patai, John Wiley & Sons Ltd, Chichester, 1990.
- 25 J. McAninly, Ph. D. Thesis, University of Durham, 1994.
- 26 F. Seel and M. Wagner, *Z. Anorg. Allg. Chem.*, 1988, **558**, 189.
- 27 G. S. Rao and Gorin, *J. Org. Chem.*, 1959, **24**, 749.
- 28 D. J. Smith and V. Venkatraghavan, *Synth. Commun.*, 1985, **15**, 945.
- 29 D. K. Liu and S. G. Chang, *Can. J. Chem.*, 1987, **65**, 770.
- 30 Z. Bohak, *J. Biol. Chem.* 1964, **239**, 2878.
- 31 O. Gawron and G. Odstachel, *J. Am. Chem. Soc.*, 1967, **89**, 3263.
- 32 T. Chivers, A. B. F. Da Silva, O. Treu and M. Trsic, *J. Mol. Struct.*, 1987, **162**, 351.
- 33 F. A. Davis and R. L. Billmers, *J. Am. Chem. Soc.*, 1981, **103**, 7016.
- 34 R. G. Pearson and J. Songstad, *ibid.*, **89**, 1827.
- 35 S. M. N. Y. F. Oh and D. L. H. Williams, *J. Chem. Soc., Perkin Trans 2*, 1991, 685.
- 36 J. McAninly, D. L. H. Williams, S. C. Askew, A. R. Butler and C. Russell, *J. Chem. Soc., Chem. Commun.*, 1993, **23**, 1758; A. P. Dicks, H. R. Swift, D. L. H. Williams, A. R. Butler, H. H. Al -Sa'doni and B. G. Cox, *J. Chem. Soc., Perkin Trans. 2*, 1996, 481.
- 37 D. L. H. Williams, "Nitrosation", Ch. 3, Cambridge University Press, Cambridge, 1988.
- 38 Reference 37, Ch. 5.
- 39 H. Schmid, G. Muhr and P. Riedl, *Monatsh. Chem.*, 1966, **97**, 781.
- 40 M. Fontecave and J. L. Pierre, *Bull. Soc. Chim. Fr.*, 1994, **131**, 620.
- 41 Reference 37, p. 2-4.
- 42 R. Radi, J. S. Beckman, K. M. Bush and B. A. Freeman, *J. Biol. Chem.*, 1991, **266**, 4244.
- 43 D. L. H. Williams, *Nitric Oxide: Biology and Chemistry*, 1997, **1**, 522.
- 44 S. Goldstein and G. Czapski, *J. Am. Chem. Soc.*, 1996, **118**, 3419.
- 45 "CRC Handbook of Chemistry and Physics", 63rd ed., Ed. R. C. Weast, CRC Press, Florida, 1982-1983.
- 46 D. R. Noble, Unpublished results.
- 47 U. Al-Obiadi and R. B. Moodie, *J. Chem. Soc., Perkin Trans 2*, 1985, 467.

Chapter 6

6 Experimental Details

6.1 Reagents used

All reagents, unless prepared as outlined below, were supplied from Aldrich and used as purchased with no need for purification.

6.1.1 Preparation of *S*-nitrosothiols, RSNOs

The instability of many RSNOs prevents their isolation as solids. However, for the work in this thesis it was not necessary to isolate the solid. RSNOs were prepared *in situ*, resulting in ready-to-use solutions of the desired concentration. They were prepared from equimolar quantities of nitrous acid and the parent thiol by the procedure outlined below.

The parent thiol was washed into an ice cooled volumetric flask using cold 0.4 mol dm^{-3} HClO_4 and the flask was agitated, or in some cases sonicated, to aid dissolution of the thiol. An equimolar amount of sodium nitrite was dissolved in 5 mls of the cold acid to form nitrous acid. The nitrous acid solution was immediately washed into the flask with more cold acid whilst agitating the flask to ensure complete reaction. Upon addition of the nitrous acid the solution turned red or green depending on the parent thiol used.

The solution was then made up to the appropriate volume with cold water or HClO_4 depending on the final pH required. Solutions were kept in ice and away from strong light to avoid decomposition through thermal and photochemical pathways. The copper mediated decay pathway was naturally suppressed by the acidified solution, which does not allow Cu^{2+} reduction due to the absence of thiolate anions.¹

Concentrations were determined using the extinction coefficients of each RSNO at their respective absorbance maxima.

6.1.2 Preparation of peroxynitrite

Peroxynitrite was prepared from the nitrosation of H_2O_2 .² There are more elegant methods of preparation, each having differences in final yield and by-products. For the work in Chapter 3 it was necessary to generate a peroxynitrite solution that was nitrite free. The nitrosation of H_2O_2 allowed the use of excess H_2O_2 to ensure complete conversion of nitrous acid to peroxynitrite. At the rates of reaction studied, any effect of a small excess of H_2O_2 was deemed negligible.

Ice cooled solutions of $0.6 \text{ mol dm}^{-3} \text{ H}_2\text{O}_2$ in $0.7 \text{ mol dm}^{-3} \text{ HClO}_4$, $0.3 \text{ mol dm}^{-3} \text{ NaNO}_2$ in water and $1.2 \text{ mol dm}^{-3} \text{ NaOH}$, were prepared. The acidified H_2O_2 solution was placed in an ice bath and stirred using a magnetic follower. The NaNO_2 solution was then poured into the acidified H_2O_2 solution immediately followed by the NaOH solution.

Upon addition of NaNO_2 the characteristic yellow colour of peroxynitrite prevailed and was immediately quenched by NaOH to stabilise the product. Peroxynitrite solutions were kept at -10°C and were stable for weeks.

Final concentrations were determined using the extinction co-efficient for peroxynitrite at 301 nm ($\epsilon_{301} = 1\,700 \text{ dm}^3 \text{ mol}^{-1} \text{ cm}^{-1}$).³

6.1.3 Buffer preparation

Buffers were prepared using the concentrations listed in the CRC handbook⁴ and checked using a pH meter. Minor adjustments to pH were made with HCl or NaOH .

6.2 Equipment

6.2.1 Spectrophotometers

Most work was carried out using conventional UV/Visible spectrophotometers. Repeat scan spectra were measured using a Shimadzu UV-2101PC spectrophotometer. Time course runs were performed using a Perkin Elmer $\lambda 12$ or $\lambda 2$. All spectrophotometer work was performed at 25°C in stoppered quartz cuvettes with a 1 cm path-length. The reference cell contained the appropriate solvent/buffer and the spectrophotometers were zeroed against this prior to reaction. For spectral scans a baseline correction was performed using the reference cell.

An interfaced computer with the appropriate data collection software collected data. This was then translated to a format readable by Microsoft Excel[®], from which further analysis was possible.

6.2.2 Stopped-flow spectrophotometer

Reactions that were too fast to be followed by conventional UV/Visible spectrometry were studied using an Applied Photophysics Biosequential DX-17MV stopped-flow spectrophotometer.

The reaction solutions were stored in identical syringes to ensure equal volume delivery. The reaction was initiated using the computer controlled automated drive. This ensured simultaneous delivery of the reagents through the automated mixing chamber into the observation cell (1 cm path length) within 5 ms. Upon entry to the observation cell the solution causes a third syringe to load and trigger the acquisition of the absorbance time data. The drive syringes, delivery tubes and the observation cell were thermostatted by the means of a circulating water bath.

A fibre optic cable directs a beam of monochromatic light of the appropriate wavelength, into the observation cell. The light passes through the reaction solution

into a photomultiplier and the change in voltage/time is converted to absorbance change/time by the computer software. The software also allows the generation of rate constants from the recorded data.

Prior to all reactions the spectrophotometer was zeroed against the appropriate solvent/buffer.

6.2.2.1 Diode array attachment

Spectral scans were obtained on the stopped flow spectrophotometer with the use of an Applied Photophysics PD.1 Photodiode Array accessory. The procedure was identical to that set out in the previous section with the monochromator removed to allow a range of wavelengths to be studied. The accessory allowed repeat spectral scans over a range of 275 to 700 nm to be recorded with time intervals in the millisecond range.

6.2.3 pH meter

pH measurements were made on a Jenway 3020 pH meter. The meter was calibrated with standard buffers, pH 7 and pH 10 for basic measurements and pH 4 and pH 7 for acidic measurements. Calibrations and pH measurements were made at 25°C.

6.2.4 Nitric oxide electrode

The detection of NO was possible using a World Precision Instruments ISO-NO MK II nitric oxide electrode. Calibrations were performed using ascorbic acid and sodium nitrite to produce NO. Conditions were kept strictly anaerobic, to prevent aerial oxidation of NO, and at 25 °C, as NO diffusion across the electrode membrane is known to be temperature dependant. The electrode was zeroed in a solution of ascorbic acid. A calibration plot of current (nA) versus concentration of NO released ($\mu\text{mol dm}^{-3}$) was produced.

Samples were tested under identical conditions and NO quantified from the calibration plot.

6.2.5 ^1H NMR

^1H NMR spectra were obtained using a Varian Unity 300MHz spectrometer at ambient temperature. All spectra were obtained in D_2O , which was acidified to a final acid concentration of 0.4 mol dm^{-3} with HClO_4 .

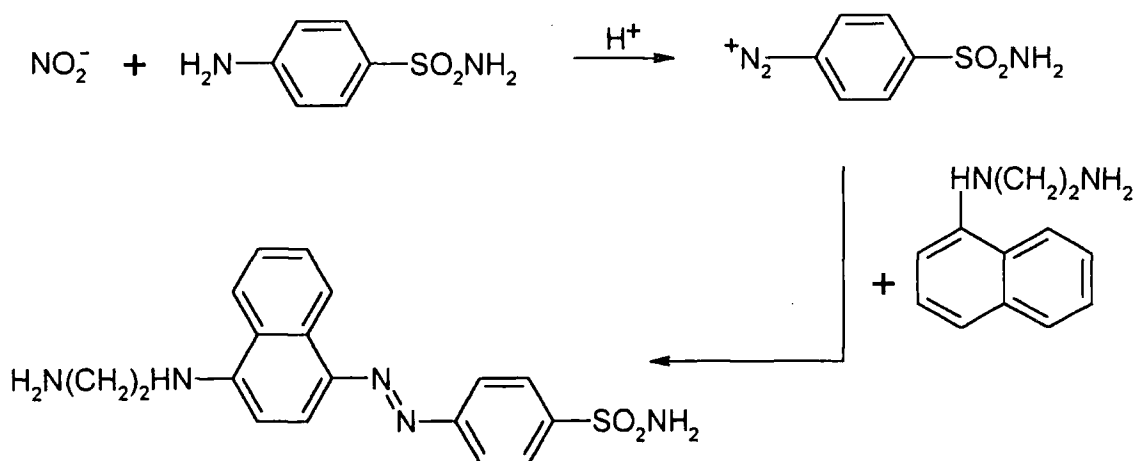
6.2.6 Scientist[®] 5

All rate constants were obtained using the Scientist[®] computer program, apart from those reactions performed on the stopped-flow spectrophotometer, which incorporated a data fitting package in the operational software.

6.3 Analytical methods

6.3.1 Griess Test

The Griess test⁶ was used to quantify nitrite in decayed reaction solutions. The test utilises the diazotisation of sulphanilamide by nitrous acid, which is generated from nitrite. The subsequent coupling of the diazonium ion to *N*-1-naphthylethylenediamine (NNED) generates a purple azo dye with an absorbance centred on 540 nm, see Scheme 6.1.



Scheme 6.1 The Griess test

1 ml of the calibration / test sample was added to 10 ml sulphanilamide (3.4 g in 100 ml 0.4 mol dm⁻³ HCl), which was ice cooled to prevent decomposition of the diazonium ion. After two minutes 14 ml NNED (0.1 g in 100 ml 0.4 mol dm⁻³) was added and the total volume made up to 50 ml with distilled water. The solution was thermostatted for ten minutes at 25 °C before its absorbance at 540 nm was measured.

Standard solutions of sodium nitrite ([NaNO₂] = 5 – 35 μmol dm⁻³) were used to construct a calibration plot from which the extinction co-efficient at 540 nm was calculated, Table 6.1.

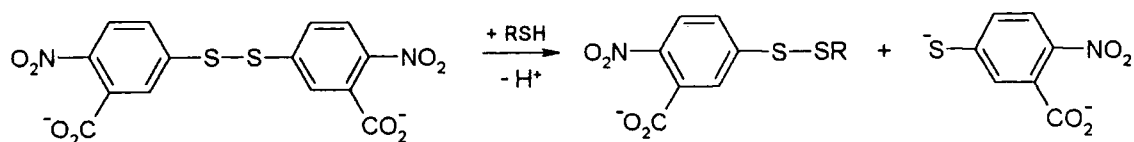
[NaNO ₂] / 10 ⁻³ M	A _{540 nm}
0.0	0.060
0.5	0.309
1.0	0.587
1.5	0.831
2.0	1.08
2.5	1.32

$$\epsilon_{540 \text{ nm}} = 50\,700 \pm 560 \text{ dm}^3 \text{ mol}^{-1} \text{ cm}^{-1}$$

Table 6.1 Calibration data for the calculation of $\epsilon_{540 \text{ nm}}$

6.3.2 Ellman's Test

The Ellman's test is a well known procedure used for the detection and quantification of thiols in solution.⁷ Thiols react with 5,5'-dithiobis(2-nitrobenzoic acid), DTNB, to form a mixed disulfide and 2-nitro-5-mercaptobenzoate, TNB²⁻, Scheme 6.2.



Scheme 6.2 Ellman's test for the quantification of thiols

TNB²⁻ exhibits an absorbance maximum at 412 nm and this is used to quantify the added thiol concentration. Authentic thiol was used to create a calibration plot from which the extinction co-efficient of TNB²⁻ at 412 nm was determined, Table 6.2.

Thiol / 10 ⁻⁵ M ⁻	A _{412 nm}
2.0	0.272
4.0	0.531
6.0	0.741
8.0	1.06
10	1.33

$$\epsilon_{412 \text{ nm}} = 13\,300 \pm 480 \text{ dm}^3 \text{ mol}^{-1} \text{ cm}^{-1}$$

Table 6.2 Calibration data for the calculation of $\epsilon_{412 \text{ nm}}$

The extinction co-efficient was in excellent agreement with the literature value of $13\,600 \text{ dm}^3 \text{ mol}^{-1} \text{ cm}^{-1}$.⁷

All thiol determinations were performed in pH 7.4 buffer and test samples were neutralised prior to analysis. 0.1 ml DTNB solution (0.05g in 10 ml methanol) was added to the test sample / authentic thiol (2.4 ml). The absorbance at 412 nm was then measured after 10 minutes at 25 °C.

6.3.3 Ammonia Test

A diagnostic kit purchased from Sigma-Aldrich Co. Ltd. was used to check reaction solutions for ammonia. The kit uses the technique created by van Anken and Schiphorst⁸ and can detect ammonia concentrations as low as $1.2 \times 10^{-5} \text{ mol dm}^{-3}$. Ammonia detection was performed on decay samples at least 12 hours after reaction initiation. The instructions supplied with the kit were followed rigorously.

6.4 Derivations

6.4.1 Spectrophotometric determination of k_{obs}

The calculation of first order rate constants, obtained under pseudo first order conditions, were based upon the following derivation.

A first order kinetic process, equation 6.1, can be followed by the rate of disappearance of X, or by the rate of formation of Y.



It may be expressed mathematically as equation 6.2, where k_{obs} is the observed first order rate constant.

$$-\frac{d[X]}{dt} = \frac{d[Y]}{dt} = k_{\text{obs}}[X] \quad \text{Equation 6.2}$$

Integration of equation 6.2 generates equation 6.3, where $[X]_0$ and $[X]_t$ are the concentrations of X at time equals zero and t respectively,

$$\ln[X]_0 - \ln[X]_t = k_{\text{obs}} t \quad \text{Equation 6.3}$$

The absorbance at time equals 0 and t can be expressed using the Beer-Lambert law ($A = \epsilon cl$, where A is the absorbance, ϵ is the molar extinction coefficient, c is the concentration and l is the path length, 1 cm), equations 6.4 and 6.5.

$$A_0 = \epsilon_X[X]_0 \quad \text{Equation 6.4}$$

$$A_t = \epsilon_X[X]_t + \epsilon_Y[Y]_t \quad \text{Equation 6.5}$$

As $[Y]_t = [X]_0 - [X]_t$, substituting for $[Y]_t$ into equation 6.5 yields :-

$$A_t = \epsilon_X[X]_t + \epsilon_Y[X]_0 - \epsilon_Y[X]_t \quad \text{Equation 6.6}$$

At the end of the reaction $t = \infty$ and $[Y]_\infty = [X]_0$, therefore :-

$$A_\infty = \epsilon_Y[X]_0 \quad \text{Equation 6.7}$$

Substitution of equation 6.7 into equation 6.6 and rearrangement produces equation 6.8.

$$[X]_t = \frac{(A_t - A_\infty)}{(\epsilon_X - \epsilon_Y)} \quad \text{Equation 6.8}$$

Similarly at time equals zero :-

$$A_0 = \epsilon_X[X]_0$$

Therefore :-

$$[X]_0 = \frac{(A_0 - A_\infty)}{(\epsilon_X - \epsilon_Y)} \quad \text{Equation 6.9}$$

Finally the substitution of equations 6.8 and 6.9 into equation 6.3 gives,

$$k_{\text{obs}} = \frac{1}{t} \ln \frac{(A_0 - A_\infty)}{(A_t - A_\infty)} \quad \text{Equation 6.10}$$

Upon rearrangement a linear equation is obtained :-

$$\ln (A_t - A_\infty) = -k_{\text{obs}} t + \ln (A_0 - A_\infty)$$

Hence, a plot of $\ln(A_t - A_\infty)$ versus time, t , should be linear with a slope equal to $-k_{\text{obs}}$.

6.4.2 Chapter 2, equation 2.6

To account for reaction through the hydroperoxide anion k_{obs} was modified to include the acid dissociation constant for H_2O_2 and the acid concentration of the solution.

$$\text{Rate} = k_D[\text{RSNO}][^-\text{OOH}] \quad \text{Equation 6.11}$$

Where k_D is the second order rate constant for the reaction between an RSNO and the dissociated H_2O_2 .

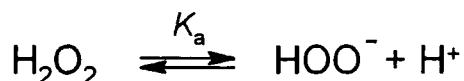
With a large excess of H_2O_2 equation 6.11 becomes equation 6.12.

$$\text{Rate} = k_{\text{obs}}[\text{RSNO}] \quad \text{Equation 6.12}$$

The pseudo first order rate constant can then be determined, equation 6.13.

$$k_{\text{obs}} = k_D[^-\text{OOH}] \quad \text{Equation 6.13}$$

The reactive species is the hydroperoxide anion,



where,

$$K_a = \frac{[^-\text{OOH}][\text{H}^+]}{[\text{H}_2\text{O}_2]} \quad \text{or} \quad [\text{H}_2\text{O}_2] = \frac{[^-\text{OOH}][\text{H}^+]}{K_a}$$

$$\text{Equation 6.14}$$

The total concentration of H_2O_2 , $[\text{H}_2\text{O}_2]_t$, is the sum of the concentrations of the neutral and deprotonated forms, equation 6.14.

$$[\text{H}_2\text{O}_2]_t = [\text{OOH}^-] + [\text{H}_2\text{O}_2] \quad \text{Equation 6.15}$$

Substituting equation 6.15 into equation 6.14 and rearranging gives equation 6.16

$$[\text{H}_2\text{O}_2]_t = [\text{OOH}^-] \left(1 + \frac{[\text{H}^+]}{K_a} \right) \quad \text{Equation 6.16}$$

Further rearrangement yields the equation for the concentration of the hydroperoxide anion, equation 6.17.

$$[\text{OOH}^-] = \frac{[\text{H}_2\text{O}_2]_t K_a}{K_a + [\text{H}^+]} \quad \text{Equation 6.17}$$

Equation 6.17 can now be substituted into equation 6.13 :-

$$k_{\text{obs}} = \frac{k_D K_a [\text{H}_2\text{O}_2]_t}{K_a + [\text{H}^+]} \quad \text{Equation 6.18}$$

Where $[\text{H}^+]$ is the acid concentration, $[\text{H}_2\text{O}_2]_t$ is the total stoichiometric concentration of H_2O_2 and K_a is the acid dissociation constant of H_2O_2 .

Therefore equation 6.18 defines the pseudo first order rate constant for the reaction through the hydroperoxide anion.

Chapter 2.8.5 includes a term to account for the reaction through the neutral form of H_2O_2 . This was easily derived using the same process as above but replacing the hydroperoxide anion term with the appropriate term for neutral H_2O_2 .

6.5 Data Fitting

Two techniques were used to fit trend lines to the experimental data obtained. The approach was dependent on the correlation being investigated.

Linear regression fitting was used to obtain the gradient and intercept from linear plots. This was performed using the data analysis function built into Microsoft Excel[®] which also calculated error values present in the gradient and intercept. Correlation coefficients were also generated by the package and used to judge the accuracy of the trendline fitted to data points, although visual inspection was the most valued guideline.

Non-linear least squares fitting was used to fit trendlines to non-linear relationships such as first order reaction profiles. This was performed by the Scientist^{®5} program, which fits experimental data to non-linear equations, plots trendlines and calculates statistics for the fit.

6.6 References

- 1 A. P. Dicks, H. R. Swift, D. L. H. Williams, A. R. Butler, H. H. Al-Sa'doni and B. G. Cox, *J. Chem. Soc., Perkin Trans. 2*, 1996, 481.
- 2 J. O. Edwards and R. C. Plumb, *Prog. Inorg. Chem.*, 1993, **41**, 599.
- 3 D. S. Bohle, B. Hansert, S. C. Paulson and B. D. Smith, *J. Am. Chem. Soc.*, 1994, **116**, 7423.
- 4 "CRC Handbook of Chemistry and Physics", 63rd ed., Ed. R. C. Weast, CRC Press, Florida, 1982-1983.
- 5 Micromath[®] Scientist[®] for Windows[®], Version 2.02.
- 6 A. Vogel, "Textbook of Quantitative Inorganic Analysis", 4th ed., p. 755, Longman, London, 1978.
- 7 G. L. Ellman, *Arch. Biochem. Biophys.*, 1959, **82**, 70.
- 8 H. C. van Anken and M. E. Schiphorst, *Clin. Chim. Acta*, 1974, **56**, 151.

Appendices

A Postgraduate Induction Course, October 1998

The induction course consisted of a series of lectures regarding:

- Safety Matters
- Manual Handling
- Electrical Appliances
- Research Resources
- Library Resources and Methods
- Computing
- Glassblowing Techniques
- High Pressure operations
- Mass spectroscopy
- NMR
- Analytical

B Conferences Attended

- RSC, Organic Reactions Mechanisms Group, Annual Seminar on Organic Reactivity, Roche Discovery Welwyn, Welwyn Garden City, September 1999.

Poster presented: Reaction of H_2O_2 with *S*-nitrosothiols – A novel source of peroxynitrite.

- European Winter School on Organic Reactivity, Bressanone, Italy, January 2000.

Poster presented: Reaction of H_2O_2 with *S*-nitrosothiols – A novel source of peroxynitrite.

- RSC, Organic Reactions Mechanisms Group, Annual Seminar on Organic Reactivity, Zeneca Agrochemicals, Bracknell, October 2000.

Oral presentation: Investigating the antioxidant properties of *S*-nitrosothiols.

- University of Durham Graduate Symposium, June 2001.

Oral presentation: Direct and indirect nitrosation by peroxynitrous acid.

- European Symposium on Organic Reactivity 8, Dubrovnik (Çavtat), September 2001.

Poster presented: Direct and indirect nitrosation by peroxynitrous acid.

Abbreviations

NO	Nitric Oxide
NO⁺	Nitrosonium Ion
NO⁻	Nitroxyl anion
GTP	Guanosine triphosphate
cGMP	3', 5-cyclic guanosine monophosphate
Ach	Acetylcholine
EDRF	Endothelium derived relaxation factor
SOD	Superoxide dismutase
NOS	Nitric oxide synthase
L-NMMA	N-monomethyl
PDE5	Phosphodiesterase type 5
RSNO	<i>S</i> -Nitrosothiol
RONO	Alkyl nitrite
SNAP	<i>S</i> -Nitroso-N-acetyl penicillamine
GSNO	<i>S</i> -Nitrosoglutathione
SNP	<i>S</i> -Nitrosopenicillamine
SNCys	<i>S</i> -Nitrosocysteine
EDTA	Ethylenediaminetetraacetic acid
GSSG	Glutathione disulfide
RSH	Thiol
RSSR	Disulfide
RSOH	Sulfenic acid
RSO₂H	Sulfinic acid
RSO₃H	Sulfonic acid
SSNO⁻	Nitrosodisulfide ion
RSeH	Selenol
DMPS	3- dimercaptopropane-1-sulfonate
MGD	<i>N</i> -methyl-D-glucamine dithiocarbamate
GTN	Glyceryl trinitrate
SIN-1	3, -morpholino-sydnomimine-hydrochloride
GC-MS	Gas chromatography – Mass spectrometry
TCN	Tetracyanonickelate

NB	Nitrosobenzene
DCM	Dichloromethane
NBD-Cl	7-chloro-4-nitrobenzo-2-oxa-1, 3-diazole
S2MPA	<i>S</i> -nitroso 2-mercaptopropionic acid
SMSA	<i>S</i> -nitroso mercaptosuccinic acid
SAMP	<i>S</i> -nitroso 1-amino 2-methyl 2-propane thiol
SAE	<i>S</i> -nitroso 1-amino ethane thiol
STG	<i>S</i> -nitroso thioglycerol
S3MPA	<i>S</i> -nitroso 3-mercapto propionic acid
RSNO₂	<i>S</i> -nitrothiol
NMA	<i>N</i> -methyl analine
TCP	2, 4, 6- Trichlorophenol
NNED	<i>N</i> -1-naphthylethylenediamine
DTNB	5,5'-dithiobis(2-nitrobenzoic acid)
TNB²⁻	2-nitro-5-mercaptobenzoate

